

**Consequences of Diurnal Variation in
Salinity on Water Relations and Yield
of Tomato**

W. van Ieperen

Promotor:

dr. ir. H. Challa
hoogleraar in de Tuinbouwplantenteelt

NN02201. 2176.

Consequences of Diurnal Variation in Salinity on Water Relations and Yield of Tomato

W. van Ieperen

Proefschrift

ter verkrijging van de graad van doctor
op gezag van de rector magnificus
van de Landbouwniversiteit Wageningen
dr. C.M. Karssen,
in het openbaar te verdedigen
op vrijdag 15 november 1996
des namiddags om vier uur in de Aula

15n931380

CIP-DATA KONINKLIJKE BIBLIOTHEEK, DEN HAAG

Ieperen, W. van

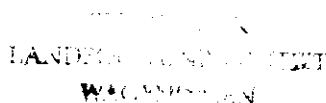
Consequences of Diurnal Variation in Salinity on Water Relations and Yield of Tomato

W. van Ieperen - [S.l. : s.n.]

Thesis Wageningen. -With ref.- With summary in Dutch

ISBN 90-5485612

Subject headings: tomato / salinity / water relations



This thesis contains results of a research project completed at the Wageningen Agricultural University, Department of Horticulture

The project was financially supported by the Ministry of Agriculture, Nature Management and Fisheries

Stellingen

PN08201, 2176.

1. De vruchten van een tomatenplant spelen een verwaarloosbare rol bij de buffering van water voor de rest van de plant.
(Dit proefschrift)
2. Bij de teelt van tomaat op watercultuur leidt een lage EC tijdens de dag, gecombineerd met een hoge EC tijdens de nacht tot een hogere produktie en minder neusrot, dan bij eenzelfde gemiddelde EC gedurende het hele etmaal.
(Dit proefschrift)
3. De uitdrukking 'meten is weten' geldt alleen dan wanneer men weet wat men meet.
4. The field of plant water relations needs good modelers and good experimenters because the system is very sensitive: plants respond very rapidly to changes in water content while measurements are limited because most available methods are destructive and necessarily disturb the system. (vrij naar: ACOCK, B. (1987). *Characterizing Physiological factors in water relations. In: Plant growth modeling for resource management. Volume II.*)
5. Integratie van hydraulisch en metabolisch georiënteerde modellen is noodzakelijk om te komen tot een goed model voor de groei van planten.
6. Het verwijderen van het vak wetenschapsfilosofie in vele academische studieprogramma's heeft tot gevolg dat steeds meer onderzoekers hun eigen vooronderstellingen niet herkennen.
7. Het lidmaatschap van een natuurbeschermingsorganisatie geldt voor vele Nederlanders als een moderne aflaat voor hun buitensporige reisgedrag.
8. Bij het verwerven van grond in eigendom staat voor een Nederlandse agrariër niet het exploitatieresultaat op de korte termijn maar het voortbestaan van het bedrijf op de lange termijn centraal.
9. Een stijgende welvaart en een duurzaam milieu zijn op de lange termijn onverenigbaar.
10. De sterke toename van het belang van het medium televisie in de internationale nieuwsvoorziening heeft er toe geleid dat velen zich verkijken op de toestand in de wereld.
11. De toename van het belang van de 'vrije' markt in de westerse samenleving leidt tot een afname van vrijheid van de zwakkeren in die samenleving.
12. Dat de stelling "Alle religies komen ten diepste op hetzelfde neer" door velen wordt onderschreven, wijst op een belangrijk gebrek aan algemene ontwikkeling in onze maatschappij.

Stellingen behorende bij het proefschrift: "Consequences of Diurnal Variation in Salinity on Water Relations and Yield of Tomato"

W. van Ieperen
Wageningen, 15 november 1996

Abstract

Ieperen, W. Van (1996). Consequences of diurnal variation in salinity on water relations and yield of tomato. Dissertation, Agricultural University, Wageningen, The Netherlands; ca. 192pp; 47 figs.; 26 tables; English and Dutch summaries

In soilless culture the EC (Electric Conductivity; mS cm^{-1}) is an important measure for the total solute concentration (salinity level) of the nutrient solution in the root environment. This study concentrates on the possibilities of short-term control of the total nutrient concentration (salinity level) in the root environment in relation to the greenhouse climate. A general assumption in this study is that the EC mainly influences plant functioning via its effect on the water relations of the plant: high salinity in the root environment osmotically decreases the availability of water to the roots of the plant. A chapter is included which deals with the current concepts, measures and methods related to the thermodynamic approach of plant water relations and the associated term water potential.

The experimental part of this study concentrates on short- and long-term responses of (changes in the) EC on plant growth and functioning. Short-term experiments were done to investigate short-term plant responses (changes in expansion growth, water status and transpiration within a day) upon changes in EC. Long-term experiments were done to investigate the effect of different day and night EC-levels on yield and quality of the fruits during a whole growth season. A simulation model was developed, which is based on the thermodynamic approach of plant water relations, to analyse and integrate the results of the short- and long-term experiments. To obtain reliable measurements of short-term changes in transpiration, water uptake and changes in plant water content (the total amount of water stored in the plant), a new method for simultaneous measurements of water uptake, transpiration and changes in plant water content on one plant was developed.

Short-term experiments were done in a growth-chamber and in a greenhouse. Changes in EC were applied in dark and in light, while transpiration, water uptake and plant water content were measured. In dark, a bipartite response was measured on expansion growth: a change in salinity initially changed expansion growth enormously, followed by partial adaptation which occurred in the light: this was interpreted as a direct hydraulic response followed by some adaptation (probably under metabolic control). Salinity changed transpiration clearly in the growth chamber but not in the greenhouse. In the growth-chamber no simple quantitative relationships were found between the changes in plant water status and changes in the rates of transpiration and expansion growth. In the greenhouse, however, the relationship between plant water deficit and transpiration over a day was influenced by salinity. A hysteresis effect over a day was observed on this relationship at low and high salinity level. At low salinity the slope of the relationship was lower than at high salinity and the hysteresis effect was less pronounced. Solute accumulation at the endodermis in the root was raised as a possible explanation for the hysteresis effect and the different slopes at low and high salinity. Simulations, however, showed that solute accumulation was not important enough to be the only cause for the different slopes. The hysteresis effect over a day was clearly simulated by the model. It was concluded that present simulation model needs some adaptation and should probably be combined with metabolic oriented models to be able to describe expansion growth.

In the long-term experiments clear positive effects were measured of the intuitive treatment (low salinity during the day and high salinity during the night) on the growth and yield of tomato: yield was increased greatly, mainly by a positive effect on average fruit size, but dry-matter distribution towards the fruits was slightly increased too. Fruit quality was influenced by the intuitive salinity treatment: dry matter percentage of the harvested fruits was decreased, while the incidence of Blossom-End-Rot was greatly decreased.

It is concluded that short-term control of the EC mainly influenced expansion growth of the fruits, and that restriction of the supply of macro-nutrients to the dark period did not influence plant growth and production negatively. Short-term control of the EC could probably be well used as a tool to choose between yield and quality in tomato culture.

Key words: salinity, EC, osmotic potential, tomato, *Lycopersicon esculentum*, transpiration, water uptake, water relations, water status, Relative Water Content, yield, quality, Blossom-End-Rot, model.

Voorwoord

Wetenschap..... Het is alweer zo'n 17 jaar geleden dat ik voor het eerst met een belangrijke facet van de wetenschap werd geconfronteerd: tijdens één van de eerste lessen in de natuur- of scheikunde aan de middelbare school presenteerde mijn toenmalige leraar een aantal uiterlijk gelijke, zwarte, vierkante dozen met in elk van die dozen een verschillend voorwerp. De dozen waren afgesloten en wij mochten "onderzoek doen" naar de aard van de voorwerpen in de dozen. Alles was toegestaan, behalve het openen van de dozen. Aan het eind van het experiment werden de "onderzoeksresultaten" vergeleken en bleken er uiteraard de nodige verschillen te zijn tussen de meningen van de "onderzoekers". Tot mijn grote frustratie bleven de dozen gesloten en kregen we ook niet te horen wat er in de dozen zat. Op deze manier werd ons de beperktheid van "het weten", maar ook de drang naar het weten bijgebracht, een les die ik niet snel zal vergeten. Ook bij het in dit proefschrift beschreven onderzoek was de drang naar "het weten" een belangrijke drijfveer voor mij. Ik heb het onderzoek mede daardoor soms met frustratie, maar verreweg het grootste deel van de tijd met veel plezier uitgevoerd. Nu ik er op terugkijk zijn verwondering en dankbaarheid goede woorden om deze periode in mijn leven te beschrijven.

Dankbaarheid is er naar al die mensen die hebben meegewerkt aan dit onderzoek. Ik denk daarbij aan het kaspersoneel zonder wiens zorg er geen planten geweest zouden zijn om onderzoek aan te doen, aan Theo wiens technische ondersteuning werkelijk onvervangbaar was, aan Menno voor de assistentie bij het modelleren en aan Henk die me wegwijst heeft gemaakt in de warboel van computers, dataloggers, vertegenwoordigers en wat al niet meer zij, en die bovendien samen met Dzetia en Remmy een groot aantal metingen t.b.v. de kasexperimenten heeft uitgevoerd. Ep, het was erg motiverend jou als collega te hebben. Je enthousiasme voor het onderzoek, en het publiceren daarvan, en je grondige kennis m.b.t. de teelt van tomaten (en andere overblijvende tuingewasjes) bleek zelfs een moeizame schrijver als ik tot het schrijven aan te kunnen zetten. Diverse studenten hebben aan het onderzoek meegeholpen. Eén ervan, Herve, heeft een grote invloed gehad op het proefschrift zoals het hier uiteindelijk ligt. Herve, mede dankzij de samenwerking met jou, je enthousiasme en je goede ideeën is het meetsysteem er in zijn huidige vorm gekomen. Zonder het meetsysteem had het proefschrift er totaal anders uitgezien.

Ik ben mijn promotor, Hugo Challa, zeer erkentelijk voor zijn begeleiding. Je hebt me veel vrijheid gegeven bij het uitkiezen van de onderzoeksonderwerpen en de uitwerking daarvan. Ik ben je dankbaar voor je geduld wanneer er weer eens een stuk wat later werd ingeleverd, en voor je snelle medewerking bij het afronden van het proefschrift. Van je grondige commentaar heb ik veel geleerd.

Ik ben mijn ouders dankbaar voor de mogelijkheid die ze mij boden om te gaan studeren. Tenslotte, lieve Karlan, bedankt voor je onontbeerlijke steun in de afgelopen jaren. Ik ben je dankbaar voor de vele dingen die je van mij hebt overgenomen omdat ik vaak 'afwezig' was. Het was niet gemakkelijk voor je omdat je alleen maar kon afwachten totdat het eindelijk af was. Nu is het dan zover. Als iemand het verdient heeft dan ben jij het. Daarom draag ik het proefschrift aan jou op.

Verwondering, dat is een belangrijk kenmerk van de wijze waarop ik de wereld om mij heen bekijk. Naast alle ellende en moeilijkheden steekt het toch wel wonderlijk mooi in elkaar. Het was een genot om een aantal jaren een groot gedeelte van mijn energie en enthousiasme in onderzoek te kunnen steken. Dit onderzoek heeft mij niet het absolute "weten" opgeleverd, maar wel enorm veel respect voor Diegene van wie ik weet dat Hij het gemaakt heeft.

Jezus heeft eens gezegd (Johannes 4:14):

"Wie gedronken heeft van het water, dat Ik hem zal geven, zal geen dorst krijgen in eeuwigheid, maar het water dat Ik hem zal geven, zal in hem worden als een fontein van water, dat springt ten eeuwigen leven".

Contents

1. General Introduction	1
1.1 General	1
1.2 Salinity and plant growth: previous research and initial assumptions	4
1.3 Aim and organisation of the thesis	6
2.Theory plant-water-relations	7
2.1 Introduction	7
2.1.1 Importance of water to plants	7
2.1.2 History plant water research	7
2.1.3 Plant Water Status; Definitions, Measures and Methods	8
2.2 Physical background theory plant-water-relations	11
2.2.1 Important properties of water	11
2.2.2 Introduction into the thermodynamic approach of plant-water-relations.	12
2.3 Cell water relations	17
2.3.1 Cell structure	17
2.3.2 Cell water potential	17
2.3.3 Cell membrane characteristics.	17
2.3.4 Cell wall characteristics	18
2.3.5 Cell growth	19
2.4 Whole plant water relations	21
2.4.1 Introduction	21
2.4.2 Long distance water transport	21
2.4.3 Transpiration; Water Uptake; Water Content	23
2.4.4 The water balance concept	23
2.4.5 Soil-Plant-Atmosphere-Continuum Concept	25
2.5 Conclusions	26
3.Short-term effects of EC on the water relations of tomato plants	27
3.1 Introduction	27
3.2 A new method to measure plant water uptake and transpiration simultaneously (J. Exp.Bot.45:51-60)	28
3.3 Short-term effects of changes in osmotic potential in the root environment on the water relations of tomato (submitted).	43
3.4 Dynamic effects of changes in electric conductivity on transpiration and growth of greenhouse-grown tomato plants (J.Hort.Sci. 71: 481-96).	60
3.5 Summary and conclusions.	79
4.Long-term effects of different day and night EC on growth and yield of tomato	81
4.1 Effects of different day and night salinity levels on vegetative growth, yield and quality of tomato (J.Hort.Sci. 71: 99-111).	82

5. Model for short-term water relations of tomato plants	98
5.1 Introduction	98
5.1.1 Introduction into crop modelling	98
5.1.2 Greenhouse crop modelling	98
5.1.3 Aim of present model study	100
5.2 Model Description	101
5.2.1 General description and assumptions	101
5.2.2 Submodel for the flow of water through the shoot and the dynamic changes in water content in tomato plants 'WRTomSim'	103
5.2.2a Description 'WRTomSim'	103
5.2.2b The xylem network	105
5.2.2c Tissues adjacent to the xylem: water potentials and water contents	106
5.2.2d Tissues adjacent to the xylem: dynamic behaviour	108
5.2.3 Submodel for water uptake by the roots 'WURoot'	109
5.2.3a Description 'WURoot'	111
5.2.3b Flow of water and solutes across endodermis	112
5.2.3c Solute distribution cortex	115
5.3 Parameters of the model	117
5.3.1 Parameters concerning the xylem network in the submodel WRTomSim	117
5.3.2 Determination of tissue related parameters in WRShoot	118
5.3.3 Parameters in the submodel 'WURoot'	123
5.4 Simulations	124
5.4.1 Simulation results root part of the model: 'WURoot'	124
5.4.2 Simulation results complete model'	134
5.4.2a Validation of the simulated water uptake at low and high salinity.	134
5.4.2b Observed and simulated changes in amount of water in the plant	135
5.4.2c Effects of different day- and night salinity levels on simulated water uptake and plant water status	139
5.5 Discussion	141
6. General Discussion	147
Summary	158
Samenvatting	162
References	166

1. General introduction

1.1 General

Crop production in greenhouses is an important specialisation of horticulture in the Netherlands. Among the vegetable crops tomato (*Lycopersicon esculentum* Mill.) is still important although its area in the Netherlands is declining, mainly due to competition from the South European countries (Table 1.1). A better marketing system and improved quality are the present responses of the Dutch greenhouse industry.

In the Netherlands, tomatoes are produced in greenhouses in which temperature, relative humidity and CO₂-concentration of the ambient air are computer controlled. Ca. 95 % of the area of tomato is grown on artificial substrates, mainly rock-wool. In these growing systems, water and dissolved nutrients are supplied by trickle irrigation, mostly controlled by a computer system. To ensure sufficient water supply to all plants in the greenhouse and to prevent increasing solute concentrations in the substrate about 20 % extra nutrient solution is usually supplied, which drains out into the soil.

Table 1.1: Greenhouse areas in the Netherlands (Anonymous, 1995)

		1990	1994
Total area	[ha]	9593	10235
area vegetables	[ha]	4453	5374
area vegetables on hydroponics	[ha]	2735 (61) ¹	3161 (59)
area tomato	[ha]	1603	1241
area tomato on hydroponics	[ha]	1293 (79)	1179 (95)

¹ percentage area hydroponics of total area between brackets

Since approximately a decade the Dutch government stimulates growers to use artificial substrates instead of soil. The aim is to reduce environmental pollution caused by discharge of chemicals (for pest management and disinfection of the soils) and nutrients into the soil and the surface water. Nowadays, in fruit-vegetable cultures biological methods for pest management, and artificial substrates disinfected using steam, are common practise, which decreased the use of chemicals enormously. To reduce the release of nutrients to the environment an increasing area is provided with recirculation systems. In these systems the drain water is collected and reused. In 1985 approximately 33 % of the tomatoes were grown in artificial substrates. In 1994 this percentage was 95 %. The high financial investments associated with this shift were compensated for by a higher production per m² greenhouse area: in 1985 average tomato production in Dutch greenhouses was 25 kg m⁻², in 1994 40 kg m⁻² (Anonymous, 1995).

Substantial contribution of this increase was due to the transition to artificial substrates utilising its better possibility for control of plant growth. However, an even larger increase in production and quality, together with a more energy-efficient production might be achieved if the technical possibilities of modern greenhouse technology are explored more thoroughly (Challa *et al.*, 1988; Challa, 1990). To achieve this, more knowledge of plant physiological and physical processes in greenhouses should be integrated in models which can be incorporated in new, and more intelligent control systems (Challa, 1993; Uding ten Cate *et al.*, 1978). This thesis investigates the possibility of a technique which is not used in horticultural practice yet: the short-term control of the total nutrient concentration (salinity-level) in the root environment in relation to the greenhouse climate.

In soilless culture the supply of nutrient solution to the plants serves different purposes: water supply and nutrient supply. The osmotic potential near the root, which depends on the nutrient concentration in the irrigation water, is used to control plant growth and development, and quality of the harvestable product. For greenhouse production of vegetable crops large amounts of water are needed: 0.5-0.9 m³ per m² greenhouse area per year (Sonneveld, 1993). Most of the water taken up by the plants is used for transpiration (>90%). This large amount of water for transpiration is necessary for leaf cooling and provides an efficient way of transport for many substances from the root to the upper parts of the plant (Boyer, 1985). Less than 10 % of the water uptake remains in the plant, of which it is the main constituent.

Nutrients are added to the irrigation water in the first place as fertilisation: in order to reach the high production level, large amounts of nutrients are necessary which results in a relatively high salinity in the irrigation water. Empirically determined long-term optima are the basis for the total amount and mutual ratios between the different elements in the nutrient solutions (Sonneveld, 1991). In horticultural practise the total concentration of solutes in the irrigation water is characterised by the electric conductivity (EC, mS cm⁻¹) of the solution, and ranges roughly between 2 and 5 mS cm⁻¹, dependent on e.g. the production system, the crop, the status of the crop, and the desired quality of the harvestable product. Nutrient supply in a way conflicts with the supply of water: the high salinity of the nutrient solution decreases the availability of water to the roots of the plant and therefore decreases the "water status" (water potentials, relative water content, turgor-pressure) and related physiological functioning of the plant (Table 1.2): For instance, due to the high salinity-level accompanied with the optimal high concentration of nutrients, water potentials in the plant may decrease severely during the day, restricting CO₂-assimilation and cell expansion growth rate. Consequently maximal growth rate is not achieved.

Table 1.2: Generalised Sensitivity to Water Stress of Plant Processes or Parameters (after Hsiao, 1973)

	Sensitivity to Stress →		
	very sensitive		in-sensitive
	Reduction in tissue water potential required to affect the process →		
	0 MPa	1 MPa	2 MPa
Cell Growth	████████████████████		
Wall synthesis	████████████████		
ABA Accumulation	████████████████████████████		
Stomatal Opening	██		
CO ₂ -assimilation	██		
Respiration	████████████████████████████		
Proline Accumulation	████████████████████████████████		
Sugar Accumulation	████████████████████████████████████		

On the other hand, maximal growth rate does not necessarily lead to optimal growth for long term production. In horticultural practise a high salinity-level is sometimes supplied on purpose, to influence plant development or to influence the quality of the harvestable product. For instance to force young tomato plants into the generative stage, a nutrient solution with a high salinity-level is usually supplied during a short period. To increase the quality of the fruits on a tomato plant sometimes a higher salinity level than the long-term "optimal" level is supplied to increase the dry matter percentage of the fruits (Ehret and Ho, 1986a). In that case the associated production loss is accepted in order to obtain a better fruit quality.

The salinity level in the root environment is not the only factor that influences the water status of the plant. The rate of transpiration, which depends mainly on the climate and irradiance level in the greenhouse, is another important factor that influences the water status of the plant on the short-term: high transpiration by the shoot decreases the water status and related physiological functioning of the plant in the same manner as high salinity in the root environment. It was mentioned by Bruggink *et al.*, (1987) that it should be possible to improve plant growth by adapting the salinity level in relation to the rate of transpiration, thus diminishing water deficits in the plant at high transpiration. In soilless culture the salinity-level in the root environment can be adjusted quickly. Bruggink *et al.* (1987) showed that the growth of young tomato plants was improved by lowering the salinity level of the nutrient solution during the day (at high transpiration) and increasing it during the night (low transpiration). In their experiments the effect of fluctuating salinity levels in older generative plants was

not investigated, and the role of the water status of the plant was not clear. In this thesis the principle of fluctuating salinity is extended to a study with respect to fruit production and plant growth of mature tomato plants, as well as the role of the water status of the plant in determining the effects.

1.2 Salinity and plant growth: previous research and initial assumptions present research

Numerous reports about the effects of constant salinity on greenhouse grown tomato plants are available. Results obtained at fluctuating salinity levels within a day on the other hand, are rare. Most important responses are in short: High salinity clearly decreases plant growth (Hayward and Long, 1943; Sanchez Conde and Azura, 1979) including leaf area (Bruggink *et al.*, 1987) and fruit yield (Ehret and Ho, 1986a; Ho and Adams, 1989). During early production the decline in yield was mainly due to a decline in fruit size, later on fruit number was decreased too (Adams and Ho, 1989).

Ehret and Ho (1986a) reported that dry matter partitioning between roots, stems, leaves and fruits was not changed by salinity level, except for a very high salinity (17 mS cm^{-1}) when the dry matter partitioning towards the fruits was reduced. Charbonneau *et al.*, (1988) in contrary reported a decrease in shoot/root ratio at moderate salinity (6 mS cm^{-1}), which agrees with findings in cucumber seedlings (Van den Sanden and Veen, 1992).

High salinity increased dry matter, sugar and acid contents of the fruits (Massey *et al.*, 1984; Rudich *et al.*, 1977). The Ca^{2+} content of the fruits on the other hand, was decreased, which caused a higher incidence of blossom-end-rot in the fruits (Adams and El-Gizawy, 1988; Ehret and Ho, 1986; Van Goor, 1968). High salinity applied during the night had a similar effect, but high salinity applied during the day did not reduce the Ca^{2+} content in the fruits (Bradfield and Guttridge, 1984). According to Ho (1989) there is a diurnal pattern in the uptake of Ca^{2+} by the fruit: a higher proportion of the absorbed Ca^{2+} moves into the fruit at night than during the day. Water uptake was reduced at high salinity level (Ho and Ehret, 1984; Papadopoulos and Rendig, 1984)

Many of these long-term responses are explained through the effect of salinity on the water status of the plant: Salinity influences the availability of water to the roots of the plant which causes a decrease in water potentials in the xylem of the plant. As a result tissue water content decreases and in response turgor pressure declines. Due to this reduced turgor pressure, tissue expansion ceases and stomata close to conserve water. On the long-term root growth is promoted (at the expense of shoot growth) to assure that water uptake can meet the demand for transpiration (e.g. Hsiao, 1973).

Adaptation may occur due to accumulation of osmotically active materials in the plant (Morgan, 1984). The relationships are summarised in Figure 1.1.

In Figure 1.1 the internal water status of the plant is represented by a single plant water content. In reality the water status of organs and tissues varies throughout the plant. The position of the organs on the plant and the connection with the “long-distance” water transport path of the xylem are important properties that influence the local water status (Nobel, 1983). The variation in water potentials in the plant may cause variation in physiological responses throughout the plant.

Nevertheless this simplified system is still rather complex, especially when one realises that the greenhouse climate itself is usually a quickly changing boundary of the system. Moreover, short-term observations of transient responses of the water status of a plant in response to changes in salinity or the greenhouse climate are rare and difficult to gather. Therefore interpretation of the observed long-term responses is a difficult task. The use of appropriate models concerning plant water relations may help to integrate the interacting processes and so understand plant responses upon short-term changes in salinity and greenhouse climate.

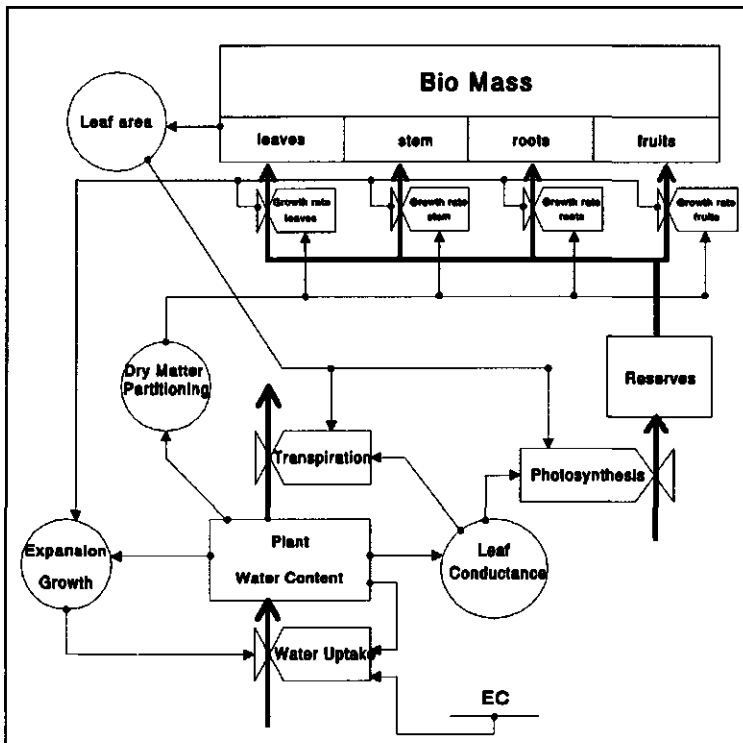


Figure 1.1: Simplified relational diagram of the influence the EC on the water relations of a greenhouse crop.

1.3 Aim and organistaion of the thesis

The aim of this thesis is to explore the possibilities for short-term control of the EC in the root-environment in relation to the aerial environmental conditions to improve growth and production of greenhouse-grown tomato. It is assumed that the responses of the plant to changes in salinity level are mediated by the water relations of the plant, in particular the turgor-pressure or Relative Water Content of the plant (RWC^p). Research was done on different integration levels and time scales. To define a clear theoretical framework of plant water relations, physical aspects and general concepts concerning the current view of plant water relations are summarised in Chapter 2. Because an important role is assumed for the plant water relations in determining effects on plant growth and production (Figure 1.1), and because present methods to measure plant water relations on the short-term are difficult to use for several reasons (see 2.1.3), a new method was developed to measure short-term rates of transpiration, water uptake and variations in plant water content and expansion growth simultaneously (Chapter 3.2). This method was used to gather experimental data concerning diurnal changes in the rates of transpiration, water uptake and expansion growth of a plant upon changes in salinity in the root environment. Experiments were conducted in a growth chamber with a stable climate to quantify the effect of changes in salinity-level on expansion growth, transpiration and plant water deficits and their interrelationships (Chapter 3.3). The constant climate and low radiation level in the growth chamber are not representative for the usual climate in the greenhouse while they are known to influence plant water relations greatly. Therefore comparable experiments were conducted in a greenhouse to check whether responses found in the growth chamber were qualitatively comparable with responses observed in the greenhouse (Chapter 3.4). In the greenhouse experiments it is also investigated whether plants adapt to the short-term to salinity level. To investigate whether the positive effects of fluctuating salinity on the growth of young tomato plants (Bruggink *et al.*, 1987) were maintained during the production phase, extensive greenhouse experiments were done during several growth seasons. Effects of day/night salinity treatments on dry matter production, dry matter distribution, as well as on expansion growth of fruits and of whole plant were investigated. (Chapter 4). A simulation model was developed and used as a tool to help understand the effects of changes in salinity on internal plant water relations and in particular on the dynamics of water uptake by the roots and the changes in water content in the shoot (Chapter 5). In the general discussion (Chapter 6) a synthesis is presented of results obtained in the short-term experiments on single plants in growth chambers and greenhouses, and obtained in the long-term experiments on a whole crop with the aid of the simulation model. Finally, the possibilities of short-term salinity control in horticultural practise are discussed.

2. Theory plant-water-relations

It is generally assumed that, at least for a large part, effects of salinity on plant growth are mediated via plant water relations. This chapter briefly describes the role of water in plants, as well as current techniques to measure it. It also gives a brief description of the theory necessary to understand properly the current concepts, measures and methods related to the thermodynamic approach of plant water relations, and associated term water potential (ψ_w). Over the last few decades, this approach has been widely accepted by plant physiologists, and has been used as the basis of many models concerning plant-water-relations. Knowledge about the physical background, and assumptions made to make this theory applicable in plant water relations, is necessary for responsible use of the approach and term ψ_w .

2.1 Introduction

2.1.1 Importance of water to plants

Water is of major importance to plant life. For herbaceous plants it is the predominant constituent, sometimes accounting for up to 95% of the total weight of the plant. It is an essential component of the cytoplasm and vital for the structural integrity of biological molecules participating either directly or indirectly in all metabolic activities of plants (Baker, 1985). Water is also involved in many other, non-metabolic processes, such as transpiration, providing indispensable leaf cooling at high irradiance, and the transport of solutes, assimilates and phytohormones through the whole plant. Furthermore, water is essential to maintain cell turgidity on which plant structure and plant expansion growth depends.

2.1.2 History of plant water research

It may be clear that plant water relations interested scientists for a long time: First observations were recorded between 300 and 400 BC, when Aristotle discussed plant food and Theophrastus the importance of the weather for plant growth. More recent is the work of Hales (18th century), who made quantitative observations of transpiration, water absorption and root pressure on grapevine, and the work of Sachs (19th century), who found that water flow through the plant is related to transpiration and that root pressure is an osmotic process. Subsequently, it became clear that water deficits in plants control plant water transport as well as plant physiological activity. Therefore many scientists started to search for suitable parameters and methods to measure the hydration level of plant tissues. As a result much of the knowledge and theories concerning plant water relations were already known at the beginning of this century. However, a general concept and related parameter for plant water status with respect to water transport and plant physiological activity, was still lacking.

During the second decade of the 20th century progressive scientists started to treat plant water relations in terms of free energy status and chemical potential of water, thus introducing thermodynamics into plant physiology (Renner, 1912; Ursprung and Blum 1916; Thoday, 1918; see Kramer, 1988a). Full acceptance of the use of thermodynamics, applied on plant water relations, was achieved after Slatyer and Taylor (1960) explained the advantages of this theory and the attended measure water potential (ψ_w), which is equally applicable in soil, plant and atmosphere.

Through the years especially the thermodynamic approach proved to be useful in understanding water transport phenomena in plants and between plants and their environment. During last decade, the value of ψ_w as a measure of plant water status in relation to physiological processes became discussed again (Kramer, 1988b; Passioura, 1988; Schulze et al., 1988; Boyer, 1989). Sinclair and Ludlow (1985) claimed that many metabolic processes are better correlated with the relative water content (RWC: actual water content/water content at saturation) of a plant than with ψ_w . Many authors found that stomatal closure and cell expansion were influenced by physical or physiological (osmotic) drought in the root environment while ψ_w of the leaf remained unchanged. Field experiments (Bates and Hall, 1981), split-root experiments (Blackman and Davies, 1985; Gollan et al., 1992) and experiments where pressure was applied on the soil root system confirmed these results. (Gollan et al., 1986; Davies and Zhang, 1991). The existence of non-hydraulic root-shoot communication, probably by changed concentrations of ions or phytohormones in the xylem sap, were proposed (Davies and Jeffcoat, 1990).

Nevertheless the ψ_w concept remains important since ψ_w and its components are the driving forces for water transport and therefore affect many metabolic processes indirectly (Boyer, 1989)

2.1.3 Plant Water Status; Definitions, Measures and Methods

The term water status applied to a plant is qualitative term, which refers to the general state of a plant in relation to water. It has no units and can only be used in a relative sense. A plant with a "low" water status refers to a plant which suffers shortage of water, while a "high" water status refers to a plant without water deficits. Plant water status often refers to other, commonly used quantitative terms. Two types of quantitative terms are employed: intrinsic and extrinsic terms. Intrinsic terms are based on essential characteristics of water, which are not dependent on the amount of water. For instance: temperature, density and concentration. Water potential is an example of an intrinsic term, describing the plant water status quantitatively as the free energy status of water. Extrinsic terms are in some way based on the total amount of water in the plant. Water Content (WC), Specific water content (WC_s), Relative Water Content (RWC) and Water Saturation Deficit (WSD) are examples of extrinsic terms (Taylor,

1968). WC, which equals the difference between fresh and dry weight (FW-DW), is the most direct measure for the amount of water in a plant or plant part. However, WC of a plant changes enormously over plant life due to growth, making it is too variable to be a proper measure for water status. RWC and WSD are WC alike measures, but relative to the WC at full turgor (WC_{max}). These terms meet the requirements of a general applicable term for water status better than WC or WC_s , although, according to Acock (1987), the determination of WC_{max} depends as much on timing and technique as it does on plant properties. The term RWC as a measure for plant water status, is widely used by plant physiologists.

According to Schulte (1992), intrinsic variables, in contrary to extrinsic variables, can be sensed directly by the plant, presuming a remote sensing ability is lacking. However, it is possible that a plant senses changes in extrinsic variables via intrinsic variables: for instance cell volume changes via changes in cell pressure or cell wall tension. Important advantages of an intrinsic over an extrinsic variable are the independence of the intrinsic variable of the circumstances it is measured in, and the capability of free exchange with other situations.

Through the years a lot of techniques and methods are developed to study plant water relations by measuring one of the mentioned variables (Slavik, 1974). Most important methods are described briefly below. Which method is used, depends on the measure of interest, the integration level on which measurements are desired (cell, tissue, plant or plant community level) and the desired resolution in time. Commonly used methods for measuring the water potential are:

- Visual examination or detection by weighing of swelling, shrinking or constant weight of samples of tissue in graded series of osmotic solutions. The tissue water potential is equivalent to the osmotic potential of the solution that causes no change of weight or volume (Slavik, 1974).
- Pressure Chamber: a branch or leaf is cut and sealed into a pressure chamber with its cut end outside. Pressure is slowly raised in the chamber until sap emerges from the xylem vessels at the cut end. The positive pressure that is needed to force out sap from the cut end is equal to the negative water potential that was present in the sample before it was severed (Scholander, 1965).
- Thermocouple Psychrometry: Psychrometric methods are based on the existence of an equilibrium between the water potential of plant tissue enclosed in a small chamber and the water potential of the air in the chamber. Vapour pressure in the chamber is measured as a small wet-bulb temperature depression using thermocouples. The water potential is calculated from the measured vapour pressure. Measurements have to be done in isothermal conditions after a suitable period of equilibration which may be hours (Spanner, 1951).

-Pressure Probe: A micro capillary is inserted into a cell and measures the intracellular pressure (Turgor, ψ_p , ψ_p) directly. If cell osmotic potential is also measured cell water potential can be calculated (Steudle and Zimmermann, 1974).

Most of the methods described above are destructive and therefore not applicable to monitor fast changes in plant water status in relation to a fast changing environment such as a greenhouse climate. Psychrometric methods allow in situ determination of plant water potential. However, this type of measurements is not very reliable due to some theoretical and experimental errors (Shackel, 1984). The methods are very sensitive for changes in temperature, and usually need long equilibrium periods between subsequent measurements. The pressure probe technique is an invasive technique able to monitor pressure in single cells. It is a very sensitive technique and therefore hardly suitable for use outside laboratory circumstances. There are several methods to measure the absolute water content of plants or parts of plants, and variations in water content of plants or parts of plants:

-Determination of water content: Measuring fresh weight (FW) and dry weight (DW) after oven-drying. Water Content (WC) equals FW-DW. Specific Water Content (WC_s) equals WC/DW. Comparable but more advanced are the methods determining the water saturation deficit (WSD) or related term Relative Water Content (RWC) which was proposed by Weatherly (1950) as "relative turgidity". It is the water content of a tissue relative to the water content of the same tissue at full turgor. Determination is done by weighting the sample before and after saturation to full turgidity and correcting for dry weight.

-Measuring short-term changes in thickness or length of plant parts (stems, leaves) by mechanical devices. (Klepper, 1971; Acevedo *et al.*, 1971)

-Measuring short-term changes in thickness of a water layer between a radiation source and receiver through absorption characteristics of β -particles or microwaves (Nakayama and Ehler, 1964).

-Pulsed NMR method: movement of water molecules and water content is monitored using nuclear magnetic resonance techniques. The method is non-destructive and non-invasive (Reinders, 1987).

Some of the mentioned methods to measure plant water content are able to monitor changes in water content of plant parts on the short term and in a non-destructive manner. However, application of these methods in greenhouses is often difficult, due to the relative unstable environment, the expenses (NMR) or regulations associated with the use of these methods (radioactive techniques).

2.2 Physical background theory plant-water-relations

2.2.1 Important properties of water

Water has some distinct properties which make it very suitable for its purpose in plant life. On earth, water is available in relative large quantities. It is commonly found in all three phases (solid, liquid and vapour), due to its favourable boiling (100 °C) and freezing (0 °C) point. For most plants that are important to agricultural production, especially the liquid and vapour phase of water are important.

For its purpose as transport- and reaction medium in the plant, the dipole moment and the hydrogen bonding potential of water molecules are extremely important. Due to these properties water is the best known universal solvent. It is also involved in many reactions as a component (e.g. photolysis). The structure of water around ions and colloidal particles favours the reactivity of enzyme-catalysed reactions (Meidner and Sherrif, 1976)

Between water molecules strong attracting forces exist which are due to the tendency of each water molecule to associate with others via hydrogen bonds. These, so called cohesion forces, permit high negative pressures along a water column without breaking it (tensile strength of water columns). In the liquid phase, water has a very high surface tension or surface free energy (0.0782 J m^{-2} at 20 °C), due to the orientation of the water molecules at surfaces. Capillary rise, the tendency of water to fill capillary spaces, is the result of the surface tension in combination with strong adhesion forces between water molecules and the walls of a small capillary. It appears that these adhesion forces are substantially greater than the intermolecular cohesion forces between water molecules. The combination of the high tensile strength of water in the tracheids and vessels of the xylem, together with capillary rise, provide a reliable system to transmit tensions along the water conducting system of a plant, with as a result the flow of water over relative long distances.

To prevent overheating and large temperature variations in the plant, the high vaporisation energy ($H_{\text{vap}} = 2454 \text{ J g}^{-1}$ at 20 °C), together with the high specific heat of water ($C_p^{\text{water}} : 4.175 \text{ MJ m}^{-3} \text{ }^\circ\text{C}^{-1}$ at 20 °C) are other important properties of water. The vaporisation energy (H_{vap}) is the energy which is necessary to break the bonds between water molecules at the transition from the liquid to the vapour phase. The specific heat (C_p^{water}) indicates the energy change of a unit volume water associated with a temperature change of one degree. In a plant vaporisation takes place before water leaves the plant through transpiration. As a result the plant loses a considerable amount of 'latent' energy, which partially counterbalances the gain in energy by radiation absorbance. The high C_p^{water} prevents the plant from extreme temperature fluctuations, since water is the predominant constituent of a plant.

2.2.2 Introduction into the thermodynamic approach of plant-water-relations.

The thermodynamic approach has been widely accepted as a tool to understand plant water relations (Dainty, 1976; Tyree and Jarvis, 1986). This approach is based upon the treatment of water in terms of energy, and the application of the laws of thermodynamics to plant water relations. The associated measure of the water status of a plant or part of a plant is the water potential (ψ_w) (Slatyer, 1967; Taylor, 1968)

The water potential (liquid phase)

ψ_w has been derived from the chemical potential of water, μ_w , which indicates the free energy, associated with, and available for conducting work. μ_w consists of different components which all alter the free energy status of water:

$$\mu_w - \mu_w^{\circ} = RT \ln(a_w) + \overline{V}_w P + m_w gh \quad (2.2)$$

in which:

μ_w	: chemical potential of water	J mol^{-1}
μ_w°	: reference chemical potential of water (free, at reference height and temperature)	J mol^{-1}
R	: gas constant (8.3143)	$\text{J mol}^{-1} \text{K}^{-1}$
T	: absolute temperature	K
a_w	: activity of water	-
\overline{V}_w	: partial molal volume of water	$\text{m}^3 \text{mol}^{-1}$
P	: pressure	$\text{J m}^{-3} = \text{Pa}$
m_w	: molar mass of water (18.016)	g mol^{-1}
g	: gravitational acceleration	m s^{-2}
h	: height	m

Before introduction in plant physiology, the quantity water potential was already commonly used by soil physicists. To be comparable with the pressure dimensions of their water potential, μ_w was converted to the quantity ψ_w with dimensions J m^{-3} (= Pa) (Eq. 2.3). Using ψ_w instead of μ_w Eq. 2.2 may be rewritten into Eq. 2.4:

$$\psi_w = \frac{(\mu_w - \mu_w^{\circ})}{\overline{V}_w} \quad (2.3)$$

$$\psi_w = \frac{RT}{\overline{V}_w} \ln(a_w) + P + \frac{m_w gh}{\overline{V}_w} \quad (2.4)$$

The three terms on the right side of Eq. 2.4 are known as the osmotic, pressure and gravitational component of ψ_w .

The osmotic component

The first term of Eq. 2.2, $RT\ln(a_w)/\bar{V}_w$, represents the effect of solutes in an aqueous solution on the water potential. This osmotic term is usually negative ($a_w < 1$). a_w equals $N_w \times \gamma_w$, the mol fraction of water multiplied by the activity coefficient of water (γ_w) in the solution. The presence of solutes in water decreases N_w (mol H_2O /mol[H_2O +solute]), and the mobility of water molecules due to interacting forces between water and the solute molecules. Changes in N_w , and in the mobility of water molecules alter the energy status of water. The mobility of water molecules is described by γ_w , which equals unity for an ideal solution with no interaction between water and solute molecules. The activity coefficient (γ_w) decreases with an increasing amount of solutes in the solution. The activity (a_w) may be regarded as a concentration quantity for water, corrected for interaction between water and solute molecules (Slatyer, 1967). The presence of solutes in a solution increases the osmotic pressure (π) of that solution (π is a positive quantity). π and a_w are related via \bar{V}_w , the molar volume of water, according to Eq. 2.5 (Nobel, 1983):

$$\pi = -\frac{RT\ln(a_w)}{\bar{V}_w} = -\frac{RT\ln(\gamma_w \times N_w)}{\bar{V}_w} \quad (2.5)$$

in which:

a_w	: the activity coefficient	-
N_w	: mol fraction of water in a solution	-
π	: osmotic pressure	MPa

Osmotic pressure has often been related to the concentrations of dissolved solutes instead of to the activity of water. Assuming biological solutions ideal ($\gamma_w = 1$), the van 't Hoff relation may be derived (Eq. 2.6), which describes the relation between total solute concentration in a solution and the osmotic pressure of that medium π . (Nobel 1983):

$$\pi = \frac{RT}{\bar{V}_w} \ln(\gamma_w \times N_w) \cong RT \sum_j C_j \quad (2.6)$$

in which:

$\sum_j C_j$: total solute concentration	mol m^{-3}
--------------	------------------------------	--------------

The osmotic pressure (π) is always positive or zero. Potentials in plants are usually negative due to the presence of solutes in water in the plant.

The pressure component (hydrostatic pressure)

The term P in Eq. 2.2 represents the effect of hydrostatic pressure (in excess to atmospheric pressure) on the water potential. Due to pressure, water molecules are brought slightly closer together, making water more concentrated and therefore increasing the chemical potential of water. Through the years plant physiologists used various units for expressing pressures in plants. In this thesis the SI unit for pressure is used: Pa (or MPa due to the magnitude of pressures commonly found in plants). In plants positive pressures (turgor in cells) as well as negative pressures (in xylem vessels and cell walls) are found.

The gravitational component

The term $m_w gh / \bar{V}_w$ represents the gravitational component of the water potential (ψ_h). It influences the energy status of water due to keeping water at a certain height h above reference level. ψ_h , which is often omitted by plant physiologists, is only $0.0098 \text{ MPa}\cdot\text{m}^{-1}$. In high trees, however, it may be important. In small plants the gravitational component is unimportant and may therefore be omitted.

The matric component

Some authors add an additional component to Eq. 2.2, called the matric potential (ψ_m). This term deals with the interaction forces between water and other molecules at interfaces. Strict thermodynamically, these forces are already represented in the osmotic and pressure components of the water potential (Passioura, 1980). Therefore, the matric potential is further omitted.

The presence of solutes, and the usually negative hydrostatic pressure in the xylem, decrease the free energy of water in the plant. Therefore, at reference water potential μ_w / \bar{V}_w is zero and the water potential in plants is usually negative.

Knowledge from different backgrounds and many authors contributed to the thermodynamic approach of plant water relations. As a result various conventions to describe the different components of the water potential are in use (Eq. 2.7 and 2.8).

$$\psi_w = P - \pi + \rho_w gh \quad (2.7)$$

$$\psi_w = \psi_\pi + \psi_p + \psi_h \quad (2.8)$$

in which:

ρ_w	: density of water (998.2 at 20 °C)	kg m ⁻³
ψ_p	: (= P) the hydrostatic pressure potential	MPa
ψ_π	: (= - π) the osmotic potential	MPa
ψ_h	: (= $\rho_w g h$) the gravitational potential	MPa

In this thesis the notation and terminology of Eq. 2.8 is used.

The water potential in the vapour phase

Until here, only water in the liquid phase was considered. However, the energy status of water may also be expressed in terms of water potential in the vapour phase. According to the theory of thermodynamics, vapour and liquid of the same temperature in equilibrium, have equal water potentials. Substituting Raoult's law (Eq. 2.9) into Eq. 2.2, Eq. 2.10 results (at atmospheric pressure). The term e^a/e_s^a is also known as the relative humidity of the air (RH):

$$N_w = \frac{e^a}{e_s^a} \quad (2.9)$$

$$\psi_w^{liq} = \psi_w^{vap} = \frac{RT}{V_w} \ln \left(\frac{e^a}{e_s^a} \right) = \frac{RT}{V_w} \ln(RH) \quad (2.10)$$

in which:

ψ_w^{liq}	: water potential liquid phase	MPa
ψ_w^{vap}	: water potential vapour phase	MPa
e^a	: partial water vapour pressure in air	kPa
e_s^a	: saturation water vapour pressure in air	kPa
RH	: relative humidity of the air	-

The thermodynamic description of the energy status of water and the quantity ψ_w , being equally applicable for water in the liquid and vapour phase, and therefore in soil, plant and atmosphere, are of great advantage to the research of internal plant water relations and the water relations between plant and environment (Cowan, 1965; Kramer, 1988b).

Water transport according to the thermodynamic approach

The thermodynamic approach provides, besides the quantity water potential, an attractive theoretical basis for water transport through a plant. According to this ap-

proach, water always flows from an area with a high free energy status to an area with a lower free energy status. In terms of water potential: water flows along a gradient in decreasing water potential. In general water transport may be described using the general transport equation (Eq. 2.11), analogous to Ohm's Law (van den Honert, 1948; Cowan, 1965):

$$J_v = \frac{(\Delta\psi_w)}{R} \quad (2.11)$$

in which:

J_v	: flow of water	$\text{m}^3 \cdot \text{s}^{-1}$
$\Delta\psi_w$: gradient in water potential	MPa
R	: hydraulic resistance against the flow of water	$\text{m}^{-3} \cdot \text{s}^1 \cdot \text{MPa}$

However, not in all plant parts, where water transport occurs, all components of the water potential add to this flow. For instance, within the apoplastic xylem differences in osmotic potential may exist, but do not cause the flow of xylem sap. Instead solutes diffuse from areas with a high solute concentration to areas with a low concentration, and consequently force some water molecules to diffuse in opposite direction. However, resulting net flow of the xylem sap will be zero. Gradients in pressure potential, and in large trees also in gravitational potential, induce the flow of water in the apoplastic xylem.

With water transport across the endodermis of a root, or between apoplast and symplastic tissue anywhere in the plant, osmotic potential differences may add to the flow of water. When semi-permeable membranes are involved in the transport part, free diffusion of solutes is blocked, and consequently net transport of water occurs.

With transpiration, defined as the transport of water vapour between leaf interior and ambient air, pressure potentials and gravitational potentials are not involved. Instead the vapour transport is driven by a vapour concentration difference.

2.3 Cell water relations

2.3.1 Cell structure

Most of the plant cells involved in plant water status are mature. They contain a large central vacuole which holds the major part of the total cell water. The vacuole is surrounded by a membrane (tonoplast) and a thin layer of cytoplasm and associated cell membrane (plasmalemma). Both membranes are semi-permeable and separate the cell content from the external medium. The cells are constrained by a tough, although flexible, polymeric cell wall.

2.3.2 Cell water potential

The water potential inside the cell mainly results from the positive ψ_p and negative ψ_π of the solution inside the vacuole (Dale and Sutcliffe, 1986). The ψ_π of the cell may vary between 0 to -2.0 MPa, due to different concentrations of solutes (salts, sugars, organic acids and amino acids) in the vacuole. The actual value of ψ_π depends besides upon species and plant part, also on the water status of the cell: Active accumulation of solutes in the vacuole may occur to counterbalance low water potentials in the cell environment. (Morgan, 1984)

The ψ_p in the cell is mainly the result of the cell wall applying pressure on the cell content. If ψ_w outside the cell is higher (less negative) than inside, the cell tends to absorb water. This absorption of water results in an increased cell volume which extends the cell wall. The cell wall, in turn, applies compressing forces on the cell water. As a result the hydrostatic pressure in the cell increases (ψ_p becomes more positive). When water enters the cell and the amount of solutes remains constant, solute concentration in the vacuole decreases, and consequently ψ_π becomes less negative. Since ψ_p and ψ_π in the cell increase, total cell water potential increases. When cell water potential reaches the outside water potential, water absorption ceases and cell volume becomes stable. A convenient way to present the relations between cell volume and the different components of the water potential graphically, is in a Höfler diagram (Fig. 2.1) (Höfler, 1920).

2.3.3 Cell membrane characteristics.

Two types of water exchange between a cell and its environment may occur: Transport to adjacent cells via plasmodesmata, and transport across the cell membrane to the surrounding apoplast. Analogous to the general transport equation (Eq. 2.11), the flow of water (J_w) across the cell membrane may be described, proportional to the water potential difference ($\psi_w^{env} - \psi_w^{cell}$) between cell and surrounding apoplast (Eq. 2.12)

$$J_w = L_p (\psi_w^{env} - \psi_w^{cell}) \quad (2.12)$$

in which:

J_w	: Water flow rate per m^2 membrane area	$m^3 \cdot m^{-2} \cdot s^{-1} = m \cdot s^{-1}$
L_p	: Hydraulic conductance=inverse hydraulic resistance	$m^3 \cdot m^{-2} \cdot s^{-1} \text{ MPa}^{-1}$
ψ_w^{env}	: Water potential environment	MPa
ψ_w^{cell}	: Water potential cell	MPa

The proportional factor L_p , the hydraulic conductance, is a measure for the permeability of the cell membrane to water. So far, the assumption was made that only water moves across the membrane. Usually, solutes are also transported across the membranes: by mass flow, diffusion or by active transport mechanisms (Katchalski and Curran, 1965). As a result, the gradient in ψ_π between cell and environment alters, and consequently the rate of water transport. Therefore instead of J_w , J_v is introduced: the volume flux of water and solutes across a cell membrane per unit area (Eq. 2.13):

$$J_v = L_p \left[(\psi_p^{env} - \psi_p^{cell}) + \sigma (\psi_\pi^{env} - \psi_\pi^{cell}) \right] = \quad (2.13)$$

$$J_v = L_p (\Delta \psi_p + \sigma \Delta \psi_\pi)$$

in which:

J_v	: Volume flow of water and solutes	$m \cdot s^{-1}$
σ	: reflection coefficient	-

The reflection coefficient σ may be regarded as a dimensionless measure of the degree at which the solute is reflected by the membrane. It is a combined characteristic for all solutes that are transported across a membrane. When the membrane is impermeable to solutes, σ is unity: in that case Eq. 2.13 equals Eq. 2.12. When the membrane is permeable to water and to some extent also permeable to solutes, σ has a value between zero and one.

2.3.4 Cell wall characteristics

Important characteristics of the cell wall are wall elasticity and plasticity. When pressure is applied to the cell wall (stress) a deformation of shape, strain, results. This deformation can be either elastic or plastic. Totally plastic deformation is defined as the deformation that retains completely when the pressure on the wall is released. A totally elastic deformation occurs when the cell wall returns to its original shape after the pressure is released. Normally a plant cell wall has both elastic and plastic properties.

The elastic characteristic causes the positive inner pressure in a plant cell: when cell volume increases it is accompanied with elastic deformation of the cell wall, inner pressure increase is completely due to the volume increase of cell water. The modulus of elasticity, ϵ , describes the relation between changes in internal pressure and cell volume (Eq. 2.14): the more elastic the cell wall, the smaller ϵ .

$$\epsilon = \frac{d\psi_p}{dV} \cdot V \quad (2.14)$$

in which

ϵ	: Modulus of elasticity	MPa
ψ_p	: pressure potential (turgor) inside cell	MPa
V	: cell volume	m ³

Using the pressure probe it was found that ϵ is not a constant but varies with turgor (Zimmermann and Steudle, 1974): ϵ is small when P is low and high when P is large. ϵ also varies with cell "volume" or stage: small and immature growing cells have a lower ϵ than big mature cells (Steudle *et al.*, 1977).

For multi-cellular tissues the bulk modulus of elasticity, $\bar{\epsilon}$ has been introduced:

$$\bar{\epsilon} = \frac{d\bar{\psi}_p}{dW} \cdot W \quad (2.15)$$

in which:

$\bar{\epsilon}$: Bulk modulus of elasticity	MPa
\bar{V}	: Average turgor of cells in tissue	MPa
W	: Weight of symplastic water	g

The bulk modulus of elasticity was also found to be pressure and volume dependent, and has generally a lower value than ϵ of comparable single cells (Tyree and Jarvis, 1986).

2.3.5 Cell growth

Plastic deformation of cell walls is more important in young, fast expanding cells than in mature cells, but even in mature cells plastic deformation may occur. Contrary to elastic deformation, plastic deformation allows a permanent volume increase of a cell, at constant inner pressure. In growing cells, internal cell water potential never reaches an equilibrium with external water potential because the cell wall relaxes continuously. As a result ψ_p tends to decrease, lowering ψ_w and establishing a water potential gradient between cell and environment. Consequently, water is ab-

sorbed simultaneously, extending cell volume and restoring ψ_p , assuming ψ_π remains about stable. The water potential, ψ_w , being lowered in growing cells inducing a so-called 'growth induced water potential gradient', has been shown experimentally by Nonami and Boyer (1993).

Cell wall relaxation is a combination of cell wall loosening and hardening processes which are partially mediated by metabolism (Cosgrove, 1993). Irreversible cell expansion takes place when there is a certain positive ψ_p in the cell, which forces the cell walls to deform plastically. According to Lockhart (1965) the cell expansion rate is proportional to the difference between internal ψ_p and a threshold value for ψ_p (p'). Below p' no growth takes place (Eq. 2.16).

$$\frac{dV}{dt} = m(\psi_p - p') \quad (2.16)$$

in which:

V	: cell water volume	m ³
ψ_p	: cell pressure potential	MPa
p'	: cell threshold pressure potential	MPa
m	: plastic cell wall extensibility	m ³ s MPa ⁻¹

However, controversy exists about the role of ψ_p regulating cell expansion rate. The difference between ψ_p and p' is usually small (0.01-0.03 MPa; Frensch and Hsiao, 1994), and many studies have shown that p' and m are variables, which change in response to changes in ψ_p at a time scale of about 10 min (Passioura and Fry, 1992).

Others questioned the Lockhart concept (e.g. Zhu and Boyer, 1992). They restricted the role of ψ_p to placing the cell wall under strain enough to let growth occur, but the growth rate being dependent on other, metabolic regulated factors. Nevertheless, the water potential and its components are important for cell expansion (reviews: Taiz, 1984; Boyer, 1985; Cosgrove, 1986).

2.4 Whole plant water relations

2.4.1 Introduction

A plant may be considered as a single hydraulic system: All functioning parts are coupled together by a continuous water connection. This water connection is important because it is the transport channel for many substances throughout the plant, whereas it also provides for a conducting system for hydraulic signals. Due to this continuous water connection plants are able to react sufficiently to water deficits in the root and shoot environment, thus preventing damage by huge water loss.

Transpiration is the most important cause for the transport of water in a plant: More than 90 % of the water absorbed by the roots passes through the plant directly to the atmosphere. Less than 10 % of the water taken up is used for expansion growth. Short-term changes in relative water content of tissues all over the plant, i.e. de- or rehydration, are another, small cause for water transport which may influence water uptake. Boyer (1985) combined the different types of water flow in a plant in the water balance equation:

$$U - E = G + H \quad (2.17)$$

in which

U	: water uptake rate	$\text{m}^3 \cdot \text{s}^{-1}$
E	: transpiration rate	$\text{m}^3 \cdot \text{s}^{-1}$
G	: expansion growth rate	$\text{m}^3 \cdot \text{s}^{-1}$
H	: water flow due to de- or rehydration	$\text{m}^3 \cdot \text{s}^{-1}$

Although the latter flow is less important in a quantitative sense, it is essential for the understanding of the dynamics of internal plant water status upon changes of environmental conditions.

In this chapter long and short distance water transport in a plant, as well as transpiration and water uptake are briefly discussed to set up a general framework of thinking concerning whole plant water relations.

2.4.2 Long distance water transport

Water transport in vascular plants may be distinguished into apoplastic and symplastic transport. Apoplastic transport refers to transport via the non-living part of the plant, mainly conducting via cell walls, intercellular spaces, tracheids and xylem vessels. Apoplastic transport takes place external to the cell membranes (plasmalemma). Long distance water transport in the apoplast flows via the xylem. The vessels and tracheids of the xylem provide for a continuous, apoplastic, water connec-

tion between plant roots and transpiring leaves. Vessels are long tubes of joined vessel members, elongated cells that have rigid secondary cell walls, and at maturity, lack protoplasts. The end walls, the place where individual vessel members are connected, are either perforated (the perforation plates) or absent. The lateral cell walls of the vessels have also porous characteristics: the pitted areas. Transpiration is the predominant driving force for xylem water flow. The bulk water flow is through the xylem of the plant. Slavik (1974) gave an indication of the average maximum velocities of water transport in the xylem of herbs: $10\text{--}60 \text{ m}^3 \cdot \text{m}^{-2} \cdot \text{h}^{-1}$.

The flow of water through xylem vessels is often considered to be laminar, linear and comparable with flow through ideal capillaries (Dimond, 1966; Nobel, 1983). Therefore it may be described using Poiseuille's law (Eq. 2.18).

$$J_v = -\frac{r^2}{8\eta} \cdot \frac{\partial P}{\partial x} \quad (2.18)$$

in which

J_v	: volume flow through a cylinder	$\text{m}^3 \cdot \text{m}^{-2} \cdot \text{s}^{-1}$
r	: radius of cylinder	m
η	: viscosity of the solution	Pa.s
$\frac{\partial P}{\partial x}$: hydrostatic pressure gradient	$\text{Pa} \cdot \text{m}^{-1}$

The acceptance Poiseuille's law is based on the assumption that xylem vessels are comparable to long continuous ideal tubes, although xylem vessels consists of different vessel elements with perforation plates and rough lateral cell walls which are perforated. Therefore, deviations from laminar flow and the consequent analogy with Poiseuille's law are likely (Zimmermann, 1984). According to Poiseuille's law, the pressure gradient is linearly related with the volume flow by the vessel hydraulic conductivity $L_p = \pi r^4 / 8\eta$. Dimond (1966) found that Poiseuille's law was a good approximation for the flow of water through the vessels of tomato xylem. Wolterbeek (1986), on the other hand, argued that for tomato pressure-flow relations in xylem vessels are defined largely by vessel wall characteristics, rather than by the analogy with ideal capillaries.

Symplastic transport refers to transport via the living part of the plant: transport within a cell, transport from cell to cell via plasmodesmata. Symplastic transport is bounded by a continuous plasmalemma. Long distance water transport via the symplast flows via the sieve-tube system of the phloem. The phloem mainly transports photosynthetic products (sucrose) dissolved in water from the photosynthetic active sites of the plant (leaves) and storage organs to all other parts of the plant where they are needed. Supplying (sources) and receiving organs (sinks) in a plant play an important role in phloem transport. The flow rate in the phloem is relative low: $0.06\text{--}6.6 \text{ m}^3 \cdot \text{m}^{-2} \cdot \text{h}^{-1}$

¹. The direction is from sources to sinks. Phloem transport is probably driven by an osmotic induced pressure gradient between source and sink (Canny, 1985). In this thesis, phloem water transport is not taken into account.

2.4.3 Short-distance water transport

Besides transport of water over long distances through the xylem, water is also transported between the xylem and the surrounding tissues. Contrary to the apoplastic transport in the xylem, the water transport between xylem and adjacent tissues is between apoplast and symplast. Consequently water has to cross membranes with relative low hydraulic conductance's. While transport of water through the xylem is driven by gradients in pressure potential entirely, with water transport between xylem and adjacent tissues the gradient in osmotic potential adds also to this driving force. Water exchange between xylem and adjacent tissues may be caused by growth lowering the pressure potential in the symplast of the adjacent tissue, by water loss of the tissue to the environment, or by changes in RWC due to alterations in xylem pressure potential.

2.4.4 Transpiration and water uptake

Quantitatively, the transpiration stream is the most important water flow in vascular plants. Transpiration mainly occurs in leaves. The usual pathway for water through the leaf is via xylem vessels and cell walls to the water-air interfaces at the intercellular spaces in the leaf. At the water-air interfaces, water transfers from the liquid phase into the vapour phase, dissipating energy as latent heat. Normally, the air in the intercellular spaces is saturated, causing a high, temperature dependent, vapour concentration in the leaf. The water vapour concentration gradient between intercellular spaces and ambient air provides the driving force for diffusion of water molecules from the inner leaf to the outside air. The diffusion pathway consists of two phases with different resistance's. In the first phase, water moves from the inner leaf either via the stomata or via the waxy cuticle to the surface of the leaf. The resistance of the cuticular path is relative high (2500 to 10000 $s\ m^{-1}$; Nobel, 1983 pp 393), while the resistance of the stomatal path is variable due to active control of stomatal aperture (50 to $\infty\ s\ m^{-1}$ for herbs). In the second phase, water moves across the boundary air layer adjacent to the leaf. The resistance of the boundary layer (r_b) depends on the thickness of the layer which in turn depends on leaf shape and windspeed (De Wit, 1978). The boundary layer resistance, r_b , may vary between 13 $s\ m^{-1}$ for a thin layer and 130 $s\ m^{-1}$ for a thick layer (Nobel, 1983). Total resistance for transport of water vapour can be calculated using Eq. 2.19, transpiration is given by Eq. 2.20:

$$r_{\text{tot}} = \left(\frac{1}{r_c} + \frac{1}{r_s} \right)^{-1} + r_b \quad (2.19)$$

in which

r_{tot}	: total diffusion transport resistance	s.m^{-1}
r_c	: cuticular resistance	s.m^{-1}
r_s	: stomatal resistance	s.m^{-1}
r_b	: boundary layer resistance	s.m^{-1}

$$E = \frac{1}{r_{\text{tot}}} \times \frac{\rho C_p^{\text{water}} \times (e_s^{\text{leaf}} - e^{\text{ambient air}})}{H_{\text{vap}} \gamma} \quad (2.20)$$

in which

E	: transpiration rate per m^2 leaf area	$\text{m}^3 \cdot \text{m}^{-2} \cdot \text{s}^{-1}$
ρC_p	: volumetric heat capacity of the air	$\text{J} \cdot \text{m}^{-3} \cdot \text{K}^{-1}$
γ	: psychometric constant	$\text{Pa} \cdot \text{K}^{-1}$

Transpiration causes leaf water potential to lower and thus induces a water potential gradient between root environment and leaf. This water potential gradient is generally regarded to be the driving force for long distance water transport through the xylem.

Closely coupled to transpiration is the uptake of water by the roots. Normally, more than 90% of the water absorbed by the roots is lost by transpiration. Usually transpiration is the main factor causing low pressure potentials in the root xylem. It greatly influences the water potential gradient between root environment and root xylem, the main driving force for water uptake.

The cell differentiation zone of the root, where the root surface is still permeable by the lack of a cuticle, is the region where most of the water and solute uptake occurs. This region normally extends from 2 to 50 mm from the root tip. At the cell differentiation zone radially inwards, root epidermis, cortex, endodermis with casparian strips, pericycle and vascular tissue are found. Water and solutes traverse the single layer epidermis easily. In the cortex the pathway of water is either symplastic or apoplastic. Although the symplast in the cortex is continuous through plasmodesmata, it has a much lower hydraulic conductivity than the apoplastic pathway via the cell walls. It is therefore generally assumed that most of the water enters the symplast of the root at the endodermis, where the apoplastic pathway is blocked by the casparian strip. The main hydraulic resistance of the roots is assumed to be located at endodermis level. After crossing the endodermis water enters the xylem vessels in the inner circle. Because membranes are involved in this pathway, pressure and osmotic compo-

nents add to the water potential gradient between root environment and root xylem (the driving force for water uptake by the root).

2.4.5 Soil-Plant-Atmosphere-Continuum Concept

Steady-state flow of water from the root environment to the transpiring leaves and finally the ambient air, is often considered in terms of a simple resistance model (van den Honert, 1948). The pathway for water is called the soil-plant-atmosphere continuum (SPAC)(Cowan, 1965). Analogous to the flow of current in a electric resistance network, water flow through the SPAC occurs along a water potential gradient. Using Ohm's law analogy steady state flow through the SPAC may be described using Eq. 2.21:

$$J_v = \frac{\Delta\psi_w}{r} = \frac{\psi_w^{rc} - \psi_w^r}{r_s} = \frac{\psi_w^r - \psi_w^l}{r_p} = \frac{\psi_w^l - \psi_w^a}{r_a} \quad (2.21)$$

in which:

J_v	: water volume flow	$m^3 m^{-2} s^{-1}$
ψ_w^{rc}	: water potential of the root environment	MPa
ψ_w^r	: water potential of the root	MPa
ψ_w^l	: water potential of the leaf	MPa
ψ_w^a	: water potential of the bulk air	MPa
r_s	: resistance of the soil pathway	$MPa m^{-1} s$
r_p	: resistance of the plant pathway	$MPa m^{-1} s$
r_a	: resistance of the vapour pathway	$MPa m^{-1} s$

Although the introduction of Eq. 2.21 was undoubtedly an important step forwards, using it in models has to be done carefully for several reasons: In Eq. 2.21 different types of water transport are apparent: Mass flow in the liquid phase, and diffusion of water molecules in the vapour phase. Normally, the drop in water potential over the compartments in the liquid phase (soil and plant) is much lower than the drop in the vapour phase (max. 3 MPa vs. 100 MPa). Therefore according to Eq. 2.21, r_s and r_p differ largely from r_a . It is better to separate flow of water through the soil, plant and atmosphere continuum (SPAC) into two coupled systems: flow in the liquid phase, through soil and plant, and flow in the vapour phase from the plant to the atmosphere. The first type of flow may be considered as mass flow and is therefore proportional to a water potential gradient. The second type of flow (vapour) results from diffusion and is therefore proportional to a concentration gradient or vapour pressure gradient. The second remark concerning Eq. 2.21 is that it is only valid with steady state water flow, thus at stable environmental conditions and constant plant properties. It may be clear that in real life such a situation is rare: Due to fluctuating environmental conditions plant transpiration alters in time, which in turn causes changes in water potential in the xylem. Consequently water potential gradients between xylem and tissues adjacent to

the xylem develop, with as a result short-distance water exchange between xylem and adjacent tissues. In addition the change in water content in the adjacent tissues causes a change of tissue water potential due to altered pressure and osmotic properties, which in turn influences the water potential gradient between xylem and adjacent tissues, and therefore the water exchange rate. To overcome this problem more sophisticated models than Eq. 2.21 were developed. In these models the behaviour of tissues adjacent to the xylem were included in the resistance network by adding resistance-capacitance combinations to the network (Nobel, 1983). One of the shortcomings of interpreting whole plant water relations in terms of resistance-capacitance networks is the absence of growth: Resistance-capacitance networks are able to describe the dynamic changes in plant water content due to water potential alterations, but are not able to describe the continuous gain in water content due to expansion growth.

To add growth to these models plastic properties of cell walls have to be taken into account: The rate of cell wall relaxation determines the maximal rate at which cell expansion (volume increase) may occur. As a result of this relaxation, water uptake into growing tissues occurs at stable water potential. Turgor may vary or restrict cell wall relaxation, while metabolic factors are also important. These factors complicate the introduction of growth into models concerning plant water relations seriously.

Other problems using simple equations based on water potentials and resistances may arise since the soil-plant-atmosphere system is seldom isothermal and transport of solutes and heat may contradict the thermodynamics assumptions (Passioura, 1988a).

2.5 Conclusion

Last decades important research has been done on water relations in plants at several integration levels: Single cell, Tissue, Plant, and Plant-Environment combinations. The thermodynamic approach has proved to be very useful because it may be applied at all integration levels, provided that it is used in a correct way: The simple use of the term water potential in explaining effects of salinity on important aspects of plant water relations may introduce serious misunderstandings. It depends on the nature of the system investigated which parts of the water potential are important. For instance, with long distance water transport through the apoplastic xylem the far most important part is the pressure potential; with water uptake by the root, on the other hand, pressure and osmotic potentials are important. Dynamics of volume changes of single cells are the basis for dynamics in volume changes in tissues and in the whole plant. Knowledge of principles of water relations of single cells and tissues may be extrapolated to the whole plant, aiming to explain effects of salinity on temporary (RWC^p) and permanent (growth) volume changes.

3. Short-term effect of EC on the water relations of tomato

3.1 Introduction

Water deficits in a plant (expressed in water potential or Relative Water Content, RWC) are expected to influence expansion growth (by influencing cell expansion) and transpiration (by influencing stomatal conductance). Normally, these water deficits vary during a day due to changes in the greenhouse climate (irradiance). The salinity-level in the root environment (EC) also influences the water deficits in a plant. Interaction may be expected between the greenhouse climate and the EC in the root environment in influencing water deficits in the plant over a day.

To properly investigate relations between changes in EC, greenhouse climate and plant water deficits, short-term observations of measures concerning plant water deficits are necessary. Commonly, discrete methods of measuring plant water deficits are used: samples of leaves or whole leaves are collected over a day for determination of the courses of water potentials (using the pressure bomb or psychrometric methods) or relative water contents (weighing method). However, the accuracy of these methods in greenhouses and the resolution in time is rather low while the destructive character of the measurements influences the results. Therefore, these methods are not suitable for short-term research, and another way of measuring plant water deficits was searched for.

In this chapter a new method is presented that enables short-term simultaneous determination of the rates of transpiration and water uptake of a single plant (Chapter 3.2; Van Ieperen and Madery, 1994). The diurnal course of the amount of water in the plant (including the increase due to growth) may be calculated from these measures. Using this method changes in the amount of water in the plant may be measured almost instantaneous upon changes in the EC or greenhouse climate.

Short-term effects of changes in EC on diurnal transpiration, water uptake and plant growth rate were investigated in a controlled environment (Chapter 3.3) and in a greenhouse environment (Chapter 3.4; Van Ieperen, 1996).

3.2 A New Method to Measure Plant Water Uptake and Transpiration Simultaneously.

W. VAN IEPEREN and H. MADERY, 1994. *A New Method to Measure Plant Water Uptake and Transpiration Simultaneously. Journal of Experimental Botany* 45: 51-60.

Abstract

A new weighing lysimeter system is described measuring transpiration and water uptake simultaneously on one plant, growing in water culture. The measurements may be made for short time intervals (minutes) making it possible to monitor quick responses to changing environmental conditions. Fresh weight change, a combination of growth and water status alterations in the plant, may be calculated from transpiration and water uptake. The system consists of two communicating vessels, filled with nutrient solution; each placed on an electronic balance. One of these vessels carries the plant and is connected to the other by a flexible tube. Water uptake will cause an equal decrease of the solution-level in each vessel. The weight decrease of the vessel with no plant provides a measure of water uptake, the total weight decrease on both balances represents transpiration.

Test observations showed that measurements of transpiration and water uptake in a greenhouse can be made to an accuracy of about $0.5 \text{ mg}\cdot\text{s}^{-1}\cdot\text{plant}^{-1}$. With fluctuating radiation, a clearly radiation dependent transpiration was measured on a tomato plant in a greenhouse. These measurements showed a delay between transpiration and water uptake. Consequently fresh weight also fluctuated with radiation. An immediate decrease in transpiration was measured upon closure of a screen in the greenhouse, accompanied by an increase in fresh weight. From late afternoon until sun-rise a constant fresh weight increase was measured; first at a relatively high rate probably due to growth and recovering from water deficits, thereafter at a constant rate probably only due to growth.

Introduction

According to the widespread concept of the Soil Plant Atmosphere Continuum, developed by van den Honert (1948), water uptake and water flow through a plant are driven by a water potential gradient that results from a water deficit in the leaves. This water deficit is generated by a difference between the extent of water uptake and transpiration. Moreover, the water balance of a whole plant depends upon water uptake

and transpiration. Consequently, factors controlling the rates of transpiration and of water uptake are of vital importance to the plant.

The water balance of a plant may be characterised by Eq. 3.2.1, where U and E are the transpiration and water uptake fluxes, and G and H are the storage fluxes for growth and re-hydration (or de-hydration), respectively (Boyer, 1985).

$$U-E=G+H \quad (3.2.1)$$

During the night when the water status of the plant is usually constant, the growth rate (G) will be the difference between U and E. During the day the situation is more complex: De- or re-hydration of plant tissues will occur due to changing environmental conditions that influence transpiration and water uptake, such as radiation, relative humidity, temperature, CO₂-concentration, and temperature and water potential in the root environment. The difference between U and E will be a combination of growth and de- or re-hydration (G+H). Water potentials of plant tissues will change as a result of de- and re-hydration. Since water potentials influence cell expansion by turgor (Cosgrove, 1986) growth is coupled to de- and re-hydration: G and H are dependent variables.

Obviously the water deficit of plants depends upon a dynamic interaction between environmental conditions and plant factors. Therefore, along with measurements of the environmental conditions, accurate determination of the dynamics of transpiration and water uptake are important. Measuring rates of water uptake and transpiration simultaneously on a short-term basis (minutes) can provide information about the dynamics of the water content of the plant in relation to its environment. On a longer term basis (days) these measurements can provide information on fresh weight growth of the plant.

Accurate methods for measuring transpiration rate (gasometric and gravimetric method) and water uptake rate (potometer) have been developed previously (Slavik, 1974). Important disadvantages of the gasometric method are the disturbance of the immediate surroundings of the plant by the measurements and the relatively expensive equipment that is necessary. The main disadvantages of using a potometer for long-term water uptake measurements in situ centre around difficulties involving the effect of aeration of the nutrient solution on the measurements and problems automating the potometer (McDonald, Jordan and Ford, 1981).

This paper describes a new, relatively simple and inexpensive method to measure simultaneously the rates of transpiration and water uptake on one plant with a high

resolution, based on gravimetric principles. Tests of the system and some preliminary results on tomato plants are presented.

Materials and methods

Measurement system

The measurements were based upon continuous weight records of two communicating vessels filled with nutrient solution. The vessels were cylindrical and of identical dimensions. The test plant was placed in vessel 1 and was supported by a rigid construction of 3 PVC-poles (diameter 1 cm) with some small PVC cross-links, that was fixed to this vessel (Figure 3.2.1).

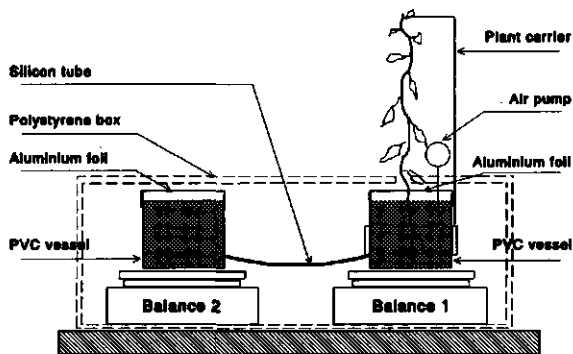


Figure 3.2.1: Apparatus to measure the rates of transpiration and water uptake on one plant simultaneously.

The roots of the plant were placed in nutrient solution in this vessel, and aerated with an air pump. Vessel 1, with plant, was placed on balance 1, vessel 2 on balance 2. The vessels were connected to each other by means of a silicon tube so that there was no drag between the balances. Both vessels were sealed with a sheet of aluminium foil to prevent evaporation from the vessels. The whole system, except the PVC-construction and plant, was placed in a polystyrene box to minimise effects of the environment on the weight measurements.

Theory

The average rate of transpiration of a plant over an interval t is given by Eq. 3.2.2. Water uptake (and transport to the parts of the plant above the water level) lowers the level of the nutrient solution in both communicating vessels. The distribution ratio over the two vessels of the weight of water that has entered the plant, depends upon the water surface areas of both vessels. The average rate of water uptake over an

interval t is given by Eq. 3.2.3. The vessel factor in Eq.3.2.3 depends on the water surface areas of both vessels according to Eq. 3.2.4. In the case of two equal vessels the vessel factor will be equal to 2.

$$E = \frac{\Delta W_1 - \Delta W_2}{\Delta t} \quad (3.2.2)$$

$$U = \frac{\Delta W_2 \times V_f}{\Delta t} \quad (3.2.3)$$

$$V_f = \frac{A_1}{A_2} + 1 \quad (3.2.4)$$

In which:

E	: rate of transpiration	[mg.s ⁻¹]
U	: rate of water uptake	[mg.s ⁻¹]
W _{1,2}	: weight on balance 1 and 2, respectively	[g]
t	: time	[s]
V _f	: vessel factor	[-]
A _{1,2}	: area vessel on balance 1 and 2, respectively	[m ²]

Tests of the method

Apart from plant transpiration, water can leave the system by evaporation directly from the vessels. The extent of these losses was established experimentally as follows: The vessels were filled with nutrient solution and covered with perforated aluminium foil as normal. No plant was placed in the system; the air pump was on. The system was operated over several days in a greenhouse and surrounded by a canopy. Weight changes on both balances were measured and analysed. Finally measurements were made on empty vessels on the balances to check how dependent results obtained with an empty system were on the greenhouse climate.

The vessel factor in Eq. 3.2.4 was established experimentally. Water was added to vessel 1 at a rate of about 58 mg.s⁻¹ using a dispensing pump (Watson Marlow 505DI) over a period of 24 hours. The weight increase on both balances was measured at time intervals of 60 s. The distribution of weight over the two vessels was checked by comparing the weight increase on both balances over the whole 24 hour period as well as at 60 s time intervals.

The time coefficient for transport of water from one vessel to the other defines the resolution in time at which two successive weight measurements may be made. The time coefficient was determined by adding 1.4 ml of water several times to vessel 1 and measuring the subsequent change of weight in both vessels. The weight change in vessel 2 was fitted to Eq. 3.2.5 to estimate the time coefficient.

$$W_2 = W_{\text{end}} \times (1 - e^{-\frac{t}{\tau}}) \quad (3.2.5)$$

In which:

W_2	: Weight on balance 2	g
t	: Time	s
W_{end}	: Final weight in equilibrium	g
τ	: Time constant (coefficient)	s

The effect of the diameter of the connecting tube was tested by repeating the described procedure with two tubes of the same length (20 cm) but with different inside diameters (5 mm and 6.5 mm).

Equipment and data-acquisition

For the tests and experiments with plants described in this paper two PVC vessels (inside diameter 21 cm, volume 6.5 dm³) connected by a silicon tube (inside diameter 5 mm, length 20 cm) were used. The vessels were placed on two Mettler PE11 balances. Analogue outputs of the two balances were measured using a HP 44702A/B High-Speed Voltmeter in a HP3852A Data-Acquisition and Control Unit (Hewlett Packard). The output signals were sampled at a rate of approximately 300 samples per balance per 60 s.

With the short term measurements to determine the time coefficient of the system, average values were calculated every second. With the test measurements and with the measurements on plants over longer periods, average values were calculated every 60 s. For the experiments carried out in the greenhouse, running averages over 540 s (9 minutes) were calculated to reduce the noise on the output signals of the balances. The rate of transpiration and of water uptake were calculated from these 'noise'-filtered values using Eq. 3.2.2 to 3.2.4.

Measurements on tomato plants in a greenhouse

To demonstrate the performance of the system the results of two diurnal cycles of water uptake and transpiration measurements, obtained with two different plants under different environmental conditions, are presented in this paper. The measurements were made Spring 1992 in one of the greenhouses of the Department of Horticulture, Agricultural University Wageningen.

Plant material

Tomato plants (*Lycopersicon esculentum* Mill. cv. Counter) were grown on water culture on a circulating nutrient solution in a greenhouse under natural light and a minimum temperature regime of 18°C night and 20°C day. The plants were transferred to the measurement system several days before the start of the measurements.

The plant morphological characteristics are shown in Table 3.2.1. Although the number of trusses and leaves of the two plants differed, the leaf areas of the two plants, the main characteristic affecting transpiration rate, were comparable. The differences between the plants were the result of differences (mainly light) in their growing conditions.

Table 3.2.1: Characteristics of the tomato plant used for *E* and *U* measurements

Plant	Fresh weight	Dry weight		
14/03	[g]	[g]		
Roots	84.19	4.76		
Stem	169.98	13.95	Leaf area [cm ²]	7317
Leaves	259.30	25.80	Length [cm]	213
Fruit	296.64	21.05	Nr Leaves [-]	32
Total	810.11	65.76	Nr Clusters [-]	9
Plant				
16-05				
Roots	232.40	10.76		
Stem	168.10	14.84	Leaf area [cm ²]	7822
Leaves	391.20	40.26	Length [cm]	188
Fruit	31.60	2.75	Nr Leaves [-]	20
Total	823.30	68.61	Nr Clusters [-]	5

Experimental Conditions

Experiments were carried out in a multispan Venlo-type greenhouse covered with single glass, with a tomato crop, consisting of plants of the same dimensions and age as the plant placed on the experimental device. The tomato plants were placed in rows, 2 plants per m². The measurement system, including balances and vessels, was placed in a polystyrene box, located in a pit in the ground so that the top of the plant to be measured was at the same height as the other plants in the greenhouse, a little aside of a row of plants.

The composition of the nutrient solution (Graves, 1983) in the circulating water culture during growth before use in the experiments and during the measurements in the vessels is shown in Table 3.2.2. During an experiment the EC of the nutrient solution in the vessel containing a plant rose slowly. The EC was kept within 0.5 mS.cm⁻¹ from the desired 3.5 mS.cm⁻¹ by measuring it about every 3 hour and adding tap water when necessary.

Global radiation outside the greenhouse, air temperature and relative humidity inside the greenhouse were measured during the experiments. Air temperature and relative humidity are not presented in this paper.

The first experiment, on 14-15 March 1992, was carried out on a day with fluctuating radiation. The second experiment, on 16-17 May 1992, was on a sunny, cloudless day. During that day the screen in the greenhouse was operated according to

the amount of radiation. It closed above 600 W.m^{-2} of global radiation outside the greenhouse and opened below that value.

Table 3.2.2: Composition of the nutrient solution used during growth before use in the experiments and in the vessels during measurements on plants.

	MMol.l ⁻¹		μMol.l ⁻¹		
NO ₃ ⁻	21.68	Fe ³⁺	45		
NH ₄ ⁺	1.90	Mn ²⁺	10		
Ca ²⁺	5.00	Zn ²⁺	5		
K ⁺	13.32	B ⁻	30		
Mg ²⁺	3.04	Cu ²⁺	0.75		
H ₂ PO ₄ ⁻	1.90	Mo ⁺	0.50	EC	3.5 mS.cm ⁻¹
SO ₄ ²⁻	5.71			pH	6.0

Results

Errors on the weight readings

When no plant was present on the system equal rates of weight change were observed on both balances, probably as a result of direct evaporation from the vessels: $-0.02 \pm 0.45 \text{ mg.s}^{-1}$ on balance 1 and $-0.02 \pm 0.27 \text{ mg.s}^{-1}$ on balance 2 (Figure 3.2.2), calculated over 1440 time intervals of 60 s). Long-term fluctuations of these rates are neither noticeable on balance 1 nor on balance 2. With empty vessels the weight on balance 1 showed a daily course with a maximum of about 0.8 g around 15:00 pm and a minimum of -0.2 g around 02:00 am. The weight reading of balance 2 was about stable. The average rates of weight change were 0.00 ± 0.42 and $0.00 \pm 0.27 \text{ mg.s}^{-1}$ on balance 1 and 2 respectively ($n=1440$, results not shown in figures).

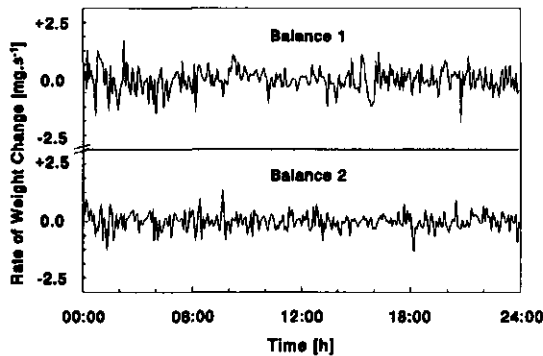


Figure 3.2.2: Courses of calculated rates of weight change of the vessels with nutrient solution on both balances.

Short-term fluctuations of the rate of weight change were more pronounced on balance 1 than on balance 2. It is likely that air movement had more effect on vessel 1 since the latter was carrying the PVC-system outside the polystyrene box. With a plant on balance 1 short-term fluctuations increased and 'noise' reduction became necessary. To reduce 'noise' on the readings of both balances a running average over 540 s (9 minutes) was calculated with the experiments shown in this paper.

It is difficult to give a correct estimation of the accuracy of the water uptake and transpiration measurements using noise reduction, since both are far from constant during day-time. The accuracy of the measurements however, can be estimated from night measurements when water uptake and transpiration are approximately constant. It has to be taken into account that air movement was normally lower during the night compared to the day since the greenhouse was not ventilated at night. From several night measurements (results not shown) an accuracy of about $0.5 \text{ mg}\cdot\text{s}^{-1}$ was estimated.

Vessel factor

A water addition rate to vessel 1, that varied between 57 and $59 \text{ mg}\cdot\text{s}^{-1}$, caused an about equal rate of weight increase on both balances that varied between 28.5 and $29.5 \text{ mg}\cdot\text{s}^{-1}$ (Figure 3.2.3). The distribution ratio between the vessels, calculated from these three rates at every time interval of 60 s , fluctuated between 0.98 and 1.02 (Figure 3.2.3). The average distribution ratio was 0.999 ± 0.004 ($n=1440$) and thus the vessel factor 1.999 . The error for the calculated water uptake rate, due to fluctuations of distribution ratio, is about 0.2% of the calculated water uptake rate. This means a maximum error of about $0.13 \text{ mg}\cdot\text{s}^{-1}$ which is much lower than the 'noise' on the readings.

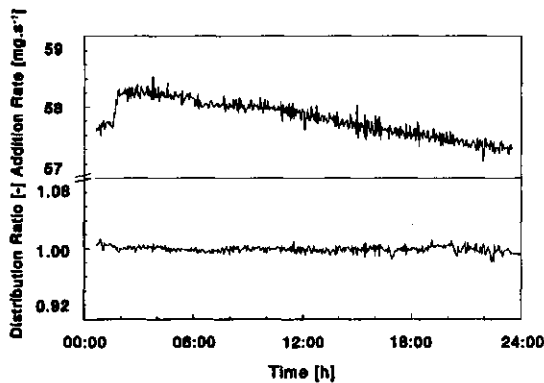


Figure 3.2.3: Measured distribution ratio of water between vessel 1 and 2 at a water addition rate of approximately $58 \text{ mg}\cdot\text{s}^{-1}$ to vessel 1.

Time coefficient

The output of both balances immediately after the addition of 1.4 ml water in vessel 1 is shown in Figure 3.2.4 for two tube diameters. The time course of weight

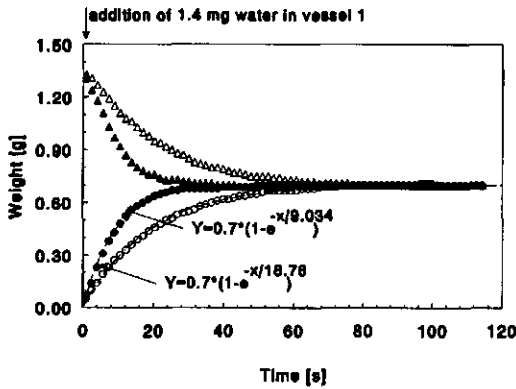


Figure 3.2.4: The effect of the addition of 1.4 ml water to vessel 1 on the weights of the two vessels for two tube diameters and the estimation of the time coefficient for water flow between the vessels for two tube diameters. Δ : Vessel 1; \circ : Vessel 2 (open: tube-diameter = 5 mm; closed tube-diameter = 6,5 mm.)

showed the same pattern for both tube diameters, but the time till equilibrium was longer for the smaller tube. The dashed curves in Figure 3.2.4 were obtained by fitting the values of vessel 2 to Eq. 3.2.5. The estimated time coefficient (τ) for the system using a tube with inside diameter 6.5 mm was 9.03 s ($R^2=0.996$) and for the tube with inside diameter 5 mm 18.73 s ($R^2=0.996$).

Measurements on plants:

Day 1 (14-15 March 1992)

There was, as may be expected (Nobel, 1985; Slatyer, 1967), a close relationship between measured transpiration rate and global radiation: almost all the dynamics of the radiation level are reflected in the measured transpiration rate (Figure 3.2.5A).

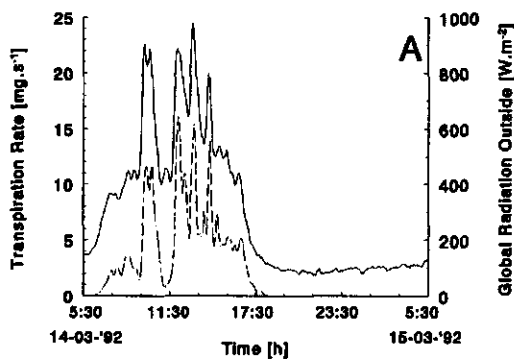


Figure 3.2.5A: Relationship between global radiation outside the greenhouse (---) and measured diurnal transpiration (—) at day 1 (14-15 March 1992).

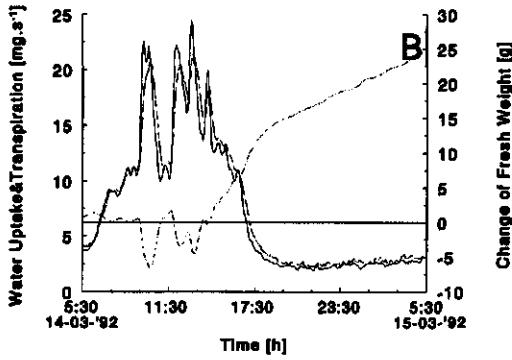


Figure 3.2.5B: Relationship between simultaneously measured transpiration (—; see Figure 3.2.5A) and water uptake (---), and the calculated course of fresh weight change of the plant (- - -) on day 1 (14-15 March 1992).

The measured rate of water uptake tailed the transpiration rate after a time (Figure 3.2.5B). Over the day fresh weight gain was reduced with increasing radiation and increased with decreasing radiation.

Over 24 hours the rate of transpiration was, on average, lower than the rate of water uptake, resulting in an increase in fresh weight (Figure 3.2.5B). During the night period relatively constant rates of transpiration and water uptake were measured. The resulting stable rate of fresh weight increase was about 0.28 mg.s^{-1} .

Day 2 (16-17 May 1992)

When global radiation reached 600 W.m^{-2} (10:30 am) the screen in the greenhouse closed by 95 percent (Figure 3.2.6A). With increasing radiation, water uptake

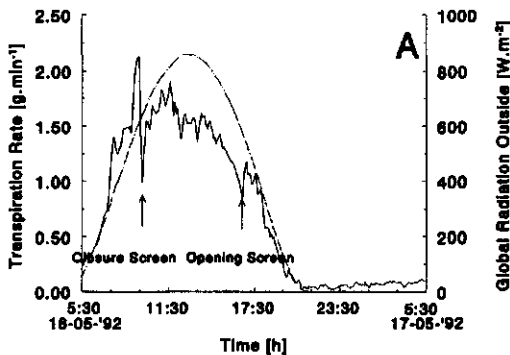


Figure 3.2.6A: Effect of closure of the greenhouse screen above 600 W.m^{-2} global radiation (---) outside the greenhouse on the diurnal course of transpiration (—) on day 2 (16-17 May 1992).

rate followed transpiration rate with some delay resulting in a loss of weight (Figure 3.2.6B).

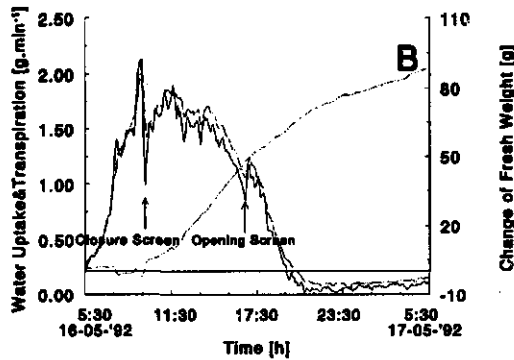


Figure 3.2.6B: Relationship between simultaneously measured transpiration (—; see also Figure 3.2.6A) and water uptake (---), and the calculated course of fresh weight change (· · ·) of the plant on day 2 (16-17 May 1992).

The immediate effects on the rates of transpiration and water uptake were obvious: transpiration rate dropped at once to a much lower value followed after some time by a drop in water uptake rate. During the period of screen closure water uptake was always higher than transpiration resulting in a continuous increase of fresh weight. After the screen opened again, sudden increases of transpiration rate and subsequent water uptake rate were measured. During the following dark period a stable rate of fresh weight increase of about $0.65 \text{ mg} \cdot \text{s}^{-1}$ was measured.

Discussion

Measurements on plants

As observed by others (de Graaf and van den Ende, 1981; Stanghellini, 1987; Aikman and Houter, 1990), transpiration rate was largely dependent upon the global radiation (Figure 3.2.5A and Figure 3.2.6A). The effect of fluctuating radiation on transpiration rate probably resulted from a direct effect of radiation on stomata resistance (Schultze, and Hall, 1982) combined with a changed vapour pressure deficit between leaf and surrounding air, due to changed leaf temperature by altered radiation absorption.

The time lag between the rates of water uptake and transpiration (Figure 3.2.5B and Figure 3.2.6B) was observed by Slatyer (1967), Cowan (1965) and Aston and Lawlor (1979). It may be due to buffering by the plant through a combination of resistance's to water flow through the plant and capacitance for water storage in the

plant and is the main cause of water status alterations in the plant (Boyer, 1985; Nobel 1985).

From the course of fresh weight (Figure 3.2.5B and Figure 3.2.6B) two characteristics are apparent: an overall gain of fresh weight, at constant rate during the second half of the night, and a fluctuating fresh weight during the day. Although this method is not able to separate G and H, some remarks can be made. It is likely that during the dark period, after some time water content reaches an equilibrium value ($H=0$) due to stable environmental conditions. Consequently the stable rate of fresh weight increase must be predominantly due to growth (G). Differences between the measured night growth rate in May (Figure 3.2.6B) and March (Figure 3.2.5B) are probably due to the availability of more assimilates in May due to higher daily radiation.

During the day and the start of the night period, alterations in both water status and growth contributed to the dynamics. Remarkable variations in the courses of fresh weight of both plants were observed during daytime. Water status alterations (H), which corresponded to a changing rate of transpiration, clearly contributed to the dynamics of fresh weight in Figure 3.2.5B due to variations in radiation, and in Figure 3.2.6B due to screening in the greenhouse. In particular during the day it was difficult to distinguish between H and G since the water status of the plant, which is changed by H, influences the growth rate of the plant (Cosgrove, 1986). After a sudden fresh weight increase of about 7 g directly after screen closure, fresh weight increased at a higher rate than during the following night (Figure 3.2.6B). This was probably as a result of the plant growing faster during the daytime than at night which was also seen in for tomato fruits by others (Kamoto and Naita, 1975; Ehret and Ho, 1986c; Pearce, Grange, and Hardwick, 1993). It is also possible that the smaller increase of fresh weight of the plant in March during daytime compared to the following night was caused by more pronounced water deficits in the plant. Perhaps the relatively small root system of this plant contributed to the development of a water deficit (Table 3.2.1).

Accuracy of the measurement system

The reliability of the measurements depended largely on the accuracy of the balances that were used. Long and short-term fluctuations of the reading of the balances, caused both by the instability of the equipment and influences of the environment, may have affected the accuracy of the measurements.

Long-term fluctuations are not important to the calculated rates of transpiration and water uptake because their influence on short time intervals is normally much smaller than that of short-term fluctuations. However, long-term fluctuations may influence the daily course of fresh weight noticeably. The long-term fluctuation of the

reading on balance 1 was probably caused by temperature dependency of this balance. Since the error was only small no correction was made.

Short term fluctuations only disturb the calculated rates of transpiration and water uptake. Their reduction, using a running average, causes a loss of resolution in time. Normally, an optimal time-span over which the running average has to be calculated, has to be searched for, depending on the reduction of noise that is necessary and the loss of resolution in time that is allowed.

Direct evaporation from the vessels causes a small over-estimation of about 0.033 mg.s^{-1} of the calculated rates of water uptake and transpiration. This error is much lower than the one caused by short-term fluctuations and thus negligible with short-term measurements. With long-term measurements it may become important and should be taken into account. The vessels have to be covered to limit direct evaporation. However, some leakage of the cover is necessary to prevent pressure gradients between the vessels when the water level in the vessels lowers. These pressure gradients obstruct free flow of water between the vessels.

Vessel Factor

The calculated water uptake is proportional to the vessel factor (Eq. 3.2.4). Since transpiration equals about 90 percent of the water uptake (Boyer, 1985), the effect of these deviations on calculated fresh weight change may be more than 10 percent. It may be clear that a distinct and constant vessel factor is important for correct measurements on water uptake rate and fresh weight change. The distribution ratio of water between the vessels (Figure 3.2.3) shows no systematic differences in time indicating equal cross-areas of the vessels at different depths. The cross-area of the stem of the tomato plant, which decreases A_1 (Eq. 3.2.4), lowered the vessel factor by about 0.3 percent to 1.994: the diameters of the vessels of the system therefore have to be chosen much higher than that of the stem and a correction is required on the vessel factor.

Time Coefficient

The time coefficient of the system depends mainly upon the dimensions of the vessels and tube. Resistance to water transport through the tube influences the rate of water flow between the vessels and consequently the time coefficient of the system. A small tube diameter (Figure 3.2.4) or a longer tube (results not shown) increases the resistance resulting in a higher time coefficient. The dimensions of the vessels also affect the time coefficient of the system. They define, together with the amount of water absorbed by the plant, the initial driving forces that lead to water transport between the vessels: With the same amount of water absorbed, the water level difference between both vessels and the subsequent initial driving force for water transport through the

tube are higher with a small vessel diameter compared to that of a large vessel diameter: A small vessel diameter results in a small time coefficient.

With the determination of the time coefficient for the system (about 10 seconds), rates of water uptake and transpiration may be calculated on weight measurements at a resolution of 60 s.

Inherent errors

Three other types of errors, inherent to the use of this method, have to be taken into account: an error due to density changes of the nutrient solutions during a measurement, an error due to dry weight increase of the plant and an error due to changes of root volume.

During an experiment the concentration of nutrients in the solution in vessel 1 may change as a result of a disproportion between water and nutrient uptake. Consequently, the density of the solution in vessel 2 alters because of diffusive flow of nutrients between the vessels. The calculated transpiration rate is not affected but the calculated water uptake rate is. During the experiments, the maximum EC rise in vessel 1 was 0.5 mS.cm^{-1} in about 24 hours, which equals a density increase of about $0.0013 \text{ kg.dm}^{-3}$, while no EC change was measured in vessel 2. This was probably due to the relatively slow diffusion rate of nutrients through the tube between the vessels. Thus no error appeared on the calculated water uptake rate due to density changes. EC alterations in vessel 1 may also influence the water uptake rate of a plant directly by osmotic effects (Aston and Lawlor, 1979, Slatyer, 1961). The extent of this effect depends on the sensitivity of the plant and may be far more important than the error through density changes. To avoid these errors the volume of the vessels has to be large enough to prevent quick EC changes. With long-term measurements the EC of the nutrient solution in both vessels has to be controlled.

The second inherent error is caused by the increase in dry weight of the plant which takes place simultaneously with transpiration and water uptake. The dry weight accumulation of a plant results from nutrient uptake and CO_2 -fixation. No error results from nutrient uptake because the nutrients that are absorbed by the roots remain on balance 1. The maximum increase in weight for tomato due to net photosynthesis is about $0.75 \text{ mg CO}_2.\text{s}^{-1}.\text{plant}^{-1}$ (Acock *et al.*, 1978). This causes an underestimation of the calculated transpiration rate during the day. At night when net photosynthesis is negative due to respiration, transpiration is a little overestimated. The calculated water uptake rate is not influenced since the weight change, discussed above, is located as a whole on balance 1. High photosynthetic rates are normally accompanied by high transpiration rates: with an estimated transpiration rate of 50 mg.s^{-1} per plant the percentage error in the calculated transpiration rate is about 1.5 percent at maximum net

photosynthesis rate. In short-term experiments this error is unimportant, but in long-term experiments it should be taken into account.

The third inherent error is caused by changes in fresh weight of the roots in vessel 1. These changes are the result of root growth and re- or dehydration of root tissues due to water status changes of the plant. Variations of root volume induce water flow between the vessels resulting in an errant calculation of the water uptake rate. Since the capacitance of the roots for water storage is relatively small (Nobel, 1985), volume changes due to re- or dehydration of root tissues will also be small. The subsequent error on the water uptake rate will therefore be negligible. The increase in root volume due to root growth is unimportant in short-term measurements. On long-term growth measurements root growth has to be taken into account.

Conclusions

The results obtained with tomato clearly demonstrate that simultaneous measurement of transpiration and water uptake, using the presented method, proved to work quite well, even under greenhouse conditions. Consequently this relatively simple and cheap method is an interesting tool to investigate relationships between environment, water relations of the plant and the diurnal course of fresh weight accumulation. Monitoring short-term changes of plant water status together with long-term growth may be of great interest in understanding more of the dynamic behaviour of plants in relation to their environment.

Measuring transpiration and water uptake using this method of communicating vessels is associated with several errors. A fundamental understanding and analysis of these errors is necessary to be sure that the system is usable for the purpose desired. The analysis of errors and time coefficients of the system used in this paper shows that when balances and material and dimensions of vessels and tube used are chosen dependent on the requirements of the research, the system is able to measure the rates of water uptake and transpiration with a high accuracy and at a resolution of a few minutes.

3.3 Short Term Effects of changes in Osmotic Potential in the Root Environment on the Water Relations of Tomato.

W. VAN IEPEREN, 1996. *Short term effects of changes in osmotic potential in the root environment on the water relations of tomato.*

Abstract

The short-term effects of daily changes in salinity (osmotic potential in the root environment; ψ_n^o) on the rates of transpiration (E), water uptake (U), expansion growth (G) and changes in relative water content (ΔRWC^p) of a young tomato plant (*Lycopersicon esculentum* Mill. cv Counter) were investigated in relation to alternating light and dark periods in the shoot environment (16 h at an irradiance of 45 W m^{-2} , and 8 h in dark). Diurnal courses of the rates of E and U were measured in a controlled environment (stable climate) using a new method for integrated E and U measurements. Rates of E and U were accurately measured at a resolution of 60 s. Changes in the amount of water in the plant were calculated from U-E. Growth and ΔRWC of the plant were derived from the course of the amount of water in the plant during a day.

E was not zero in dark. In dark and light, E and G were clearly decreased by salinity on the short-term. ΔRWC^p at the two light transitions (dark-light and light-dark) increased with increasing salinity (decreasing ψ_n^o). Differences in E between salinity levels were predominantly due to differences in leaf conductance, according to calculations made with a model based on the heat balance of a leaf. ΔE at light transitions were approximately similar at all salinity levels: no straightforward relationship was found between ΔRWC^p and ΔE (leaf conductance), and also not between ΔRWC^p and changes in G.

Although it was demonstrated very clearly that salinity changes transpiration and expansion growth on the short-term, simple straightforward relationships between salinity and E and G, mediated via short term changes in RWC^p , were not found.

Introduction

In modern greenhouses, plant growth is regulated by controlling the greenhouse climate: temperature and relative humidity of the air (T_{air} , RH_{air}) and sometimes light-level. The salinity level in the root environment (osmotic potential, ψ_n^o) is a factor which considerably influences plant growth, especially when the transpiration rate of the plant is high (e.g. Van Ieperen, 1996). With the introduction of modern hydroponic growth systems, short-term control of ψ_n^o has become technical possible. Applied in relation with the greenhouse climate, it may be used to control plant growth and qual-

ity of the harvestable product (Adams and Ho, 1989; Bruggink, *et al.*, 1987). Until now, short-term control of salinity is not incorporated in the control system in greenhouses, partly because little is known about short-term responses of plants upon alterations in ψ_{π}^n .

It is well known that salinity decreases the water status of a plant (expressed in water potential (ψ_w^p) or relative water content (RWC^p)), as well as its transpiration (E) and expansion growth (G) (e.g. review of Hsiao (1973)). Causal relationships between the water status and changes in the rates of transpiration and growth of a plant are often assumed. Changes in important physiological processes, such as stomata opening (CO_2 -assimilation and transpiration) and cell expansion (growth), are correlated with changes in RWC^p (Hsiao, 1973; Boyer, 1985; Cosgrove, 1986): a low RWC^p is often correlated with a small stomata opening, and with a low cell expansion rate.

During a day the amount of water in a plant (Water Content Plant, WC^p) changes almost continuously: Usually it increases due to irreversible cell expansion, while at the same time varying due to reversible changes in RWC^p . These reversible alterations in RWC^p are often considered as a hydraulic capacitance effect: the RWC and associated water potential in the symplast of tissues adjacent to the xylem change in response to alterations in water potential in the apoplastic xylem vessels (ψ_w^x) (Nobel, 1983). Alterations in ψ_w^x are primary due to changes in the rate of transpiration and to changes in the availability of water in the root environment of the plant, but are also influenced by the water potentials in the tissues adjacent to the xylem (Jarvis *et al.*, 1981; Boyer, 1985; Nobel, 1983). The availability of water in the root environment for uptake by the roots is, besides by physical shortage of water, also influenced by the salinity level in the root environment.

The rates of transpiration (E) and water uptake (U), and RWC^p are influenced by shoot and root environmental conditions. E is mainly influenced by the climate around the shoot. In water culture growing systems, such as hydroponics in greenhouses, ψ_{π}^n influences U. E and U together influence RWC^p . It is generally assumed that RWC^p influences E via stomatal opening, and U via an effect of RWC^p on expansion growth and on re- and dehydration processes.

The aim of present study was to investigate short-term effects of changes in salinity (ψ_{π}^n) on the water status (RWC^p) and growth of young tomato plants in relation to their transpirational water loss. The aim was to find out whether on the short-term, clear relationships exist between RWC^p and E and between RWC^p and G, measured on a plant in situ, while ψ_{π}^n was daily changed

To enable controllable changes in the shoot environment, the experiments were done in a growth chamber where predefined environmental conditions were enabled: changes in transpiration rate were induced by alternating light and dark periods at a

further stable climate. Measuring alterations in plant water status variables and expansion growth on the short-term is difficult: most of the common methods are destructive (pressure bomb; psychrometric methods; RWC by weighing) and not accurate with short-term measurements in situ. Therefore, in present study a relative new method for short-term simultaneous measurements of E and U on the same plant was used (Van Ieperen and Madery (1994), which provides values for E and U that are accurate enough to draw a closed water balance per plant (3.3.1; Boyer, 1985).

$$U - E = G + H \quad (3.3.1)$$

where G is the water flow rate due to irreversible cell expansion and H is the flow rate accompanied with rehydration or dehydration of cells; the reversible elastic volume changes. H is the flow of water that causes changes in RWC^p. These different types of flow may occur simultaneously (Boyer, 1985). When E and U are measured accurately and simultaneously on the same plant, any change in the amount of water in the plant (G+H) is known. Consequently, the course of the amount of water in the plant can be calculated.

On the short-term it is normally not possible to distinguish between G and H. However, when E has been constant for some time the water status of a plant (RWC^p) may be considered stable (Nobel, 1983). In that case, H will be close to zero and thus U minus E equal to G. To establish such circumstances, present experiments were carried out under controlled environmental conditions where the light level was the only external factor influencing E. The plant was growing under alternating light (constant level) and dark periods. Growth rate was derived from U and E during steady state light and dark periods. Transitions between light and dark were used to obtain information about the effects of ψ_{π}^{rs} on changes in transpiration level (ΔE) and plant water status (ΔRWC). Additional continuous measurements on stem diameter were done because it may be expected that stem diameter measurements give information closely related to the change in amount of water in the plant.

Material and methods

Plant material and growth conditions

Tomato plants (*Lycopersicon esculentum* Mill. cv Counter) were germinated in sand repeatedly, and 10-13 d after sowing transplanted to a water culture growth system in a greenhouse (T_{air} : 25 °C; RH: 70%, natural light conditions in summer-autumn). Nine weeks after transplanting, the plants were transferred to a growth chamber (length \times width \times height = 4 x 4 x 2.2 m) of the phytotron of the Department of Horticulture, Wageningen Agricultural University to adapt to the constant climate (T_{air} 25 \pm 0.5 °C, RH 60 \pm 10 %) and to the 16 h light period (Irradiance 45 W m⁻² by Phillips fluorescent tubes HF 83). One plant was placed on the measurement system for

simultaneous determination of E and U, in the middle of the growth chamber. Eight other plants served as borders and were placed on gullies with circulating nutrient solution around the measurement system. In all experiments, the border plants were subjected to the same ψ_{π}^{re} -treatment as the plant on the measurement system. During the 5 d adaptation phase, ψ_{π}^{re} was kept constant at -0.18 MPa by replacing the nutrient solution once a day. The nutrient solution contained (in (conc.) mM): 30.98 NO_3^- , 2.73 NH_4^+ , 7.15 Ca^{2+} , 19.03 K^+ , 4.35 Mg^{2+} , 2.73 PO_4^{3-} , 8.15 SO_4^{2-} , 0.026 Fe^{3+} , 0.006 Mn^{2+} , 0.003 Zn^{2+} , 0.017 B^- , 0.0004 Cu^{2+} , 0.0003 Mo^+ , pH was 6.0. All nutrient solutions were aerated. To change ψ_{π}^{re} , the nutrient solution (in the measurement system as well as in the gullies) was replaced by another one with a proportional in- or decreased concentration of macro elements. Repetitions per experiment were made after each other (with different plants), because there was only one system for E and U measurements available.

Experimental setup and method to determine G and $\Delta\text{RWC}^{\text{p}}$

Simultaneous measurements of E and U were made on a the tomato plant in the growth chamber using the method of integrated measurements of E and U on a single plant (Van Ieperen and Madery, 1994; described briefly below). Short-term changes in the amount of water in the plant were calculated from U and E (Eq. 3.3.1) at three salinity levels (-0.01 MPa, -0.18 MPa and -0.36 MPa). At each salinity level the plant was exposed to two light levels (dark and light, 45 W m^{-2}) at a further stable climate (T_{air} , RH_{air}) to impose two levels of transpiration rate. Within a dark or light period the driving force for transpiration was kept stable, aiming to induce a stable transpiration rate and therefore a stable plant water status within some time after a light transition. Figure 3.3.1 shows the expected diurnal courses of E and U (Figure 3.3.1A), and the course of the amount of water in the plant (WC^{p}) (Figure 3.3.1B). Nobel (1983) mentioned a time constant of approximately 60 s for changes in stem diameter of a tomato plant after changes in water supply or transpiration rate. It was assumed that this time constant is closely related to the time constant for changes in WC^{p} . It was therefore assumed that changes in WC^{p} after a light transition should be completed within 1 h after a light transition. Thus, besides during the 1 h transition phases, H was assumed to be close to zero and the slope of the course of WC^{p} equal to G. It is assumed that during each transition phase (after a change in light-level, Figure 3.3.1B) the water status of the plant changes ($\Delta\text{RWC}^{\text{p}} \approx \Delta\text{WC}^{\text{p}} / \text{WC}^{\text{p}}$ at saturation), due to the capacitance effect.

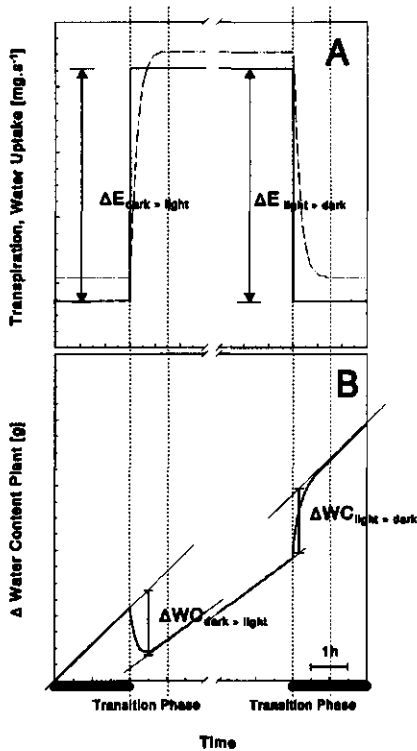


Figure 3.3.1: Expected courses of the rates of transpiration (—, A), water uptake (---, A) and plant water content (WC^p , B) during a transition from dark to light and opposite. ΔWC : change in plant water status due to a light transition, and ΔE : change in transpiration level due to a light transition.

Before the start of each 3 d period of measurements, all nine plants (border and on the system) were weighted. At the end of each experiment, they were weighted again to obtain the overall gain in fresh weight per plant.

After each period of measurements, all plants were placed on tap water ($\psi_{\pi}^c = -0.01$ MPa), and allowed to rehydrate during one night. After the night period, the lights remained off until the following plant characteristics were measured: fresh weights of root system, stem, leaves and whole plant, and plant height and leaf area (LI-COR Model 3100 Area Meter, Lincoln, USA).

Leaf temperature and leaf conductance before and after each light transition were estimated from measured T_{air} , RH_{air} , Irradiance and E using the Penman-Monteith equation for latent heat loss, and the heat balance of a leaf (Appendix 3.3.I)

Measurements were done to investigate the effect of daily changes in ψ_{π}^c on E , G and $\Delta(R)WC^p$ at two light transitions (between light and dark and opposite). After the adaptation phase was finished, ψ_{π}^c was altered daily during three following days at 3 h after the light was switched on. The order in ψ_{π}^c was: -0.18 , -0.36 and -0.01 MPa. The measurements were repeated three times ($n=3$ plants; Table 3.3.1).

Besides the E and U measurements, stem diameter variation was measured on one of the border plants (LVDT, Linear Variable Differential Transformer, HBM W1/E5, Höttinger Baldwin Meßtechnik, Germany).

Table 3.3.1: Characteristics of the tomato plants on which simultaneous transpiration and water uptake measurements were conducted^a (Means \pm SE, $n=3$).

Number of Leaves	Cluster	Stem Length	Fresh Weight				Leaf Area
			Leaves	Stem	Roots	Plant	
[-]	[-]	[cm]	[g]	[g]	[g]	[g]	[m ²]
20 \pm 1.2	4 \pm 0.2	105 \pm 7.8	211 \pm 2.5	110 \pm 1.6	75 \pm 6.7	425 \pm 10.4	0.68

^aDetermined after the experiments were finished.

Simultaneous measurements of transpiration and water uptake:

Simultaneous, short-term (min) measurements of E and U were made using the method of Van Ieperen and Madery (1994): Two similar vessels (PVC, diameter 20 cm, volume 3 l, connected to each other by a 1 cm diameter, 15 cm length silicon tube) were filled with nutrient solution and placed on two electronic balances (Sartorius MP 4800 P+, Goettingen, Germany) (Figure 3.3.1). The vessels were sealed with slightly perforated aluminium foil to prevent direct evaporation as much as possible. The plant was placed on balance one. Balances with vessels were placed in a polystyrene box to reduce the effect of air movement on the weight measurements. Weight on each balance was measured each second using a personal computer. Averages were calculated over 1 min, and stored. To reduce background noise a moving average was applied over 7 min. E was calculated from the total weight loss on both balances. U was calculated from the weight loss on balance two (slave balance), multiplied by a factor, which was always close to 2.00, since the water taken up by the plant originated half

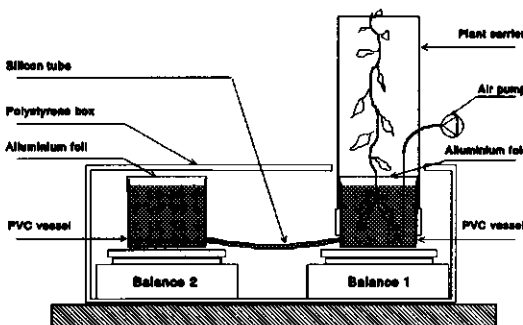


Figure 3.3.2: Apparatus to measure the rates of transpiration and water uptake simultaneously on one plant.

from vessel one, and half from vessel two. The stem of the plant crossing the surface area of the water in vessel one, causes a low deviation from 2.00. This deviation was calculated and determined experimentally for each plant (Van Ieperen and Madery, 1994).

Before the measurements on plants were started, test measurements were done using vessels filled with nutrient solution, but without a transpiring plant on the system. Instead an artificial 'plant' was placed on vessel 1 to simulate the effect of air movement on the weight measurements. Artificial transpiration was induced by removing nutrient solution from vessel 1 at a rate of 1.0 mg s⁻¹ using an accurate dispensing pump (Watson-Marlow 505DI). Test measurements were conducted during one week in an

empty growth chamber with an equal climate regime as with the measurements on plants.

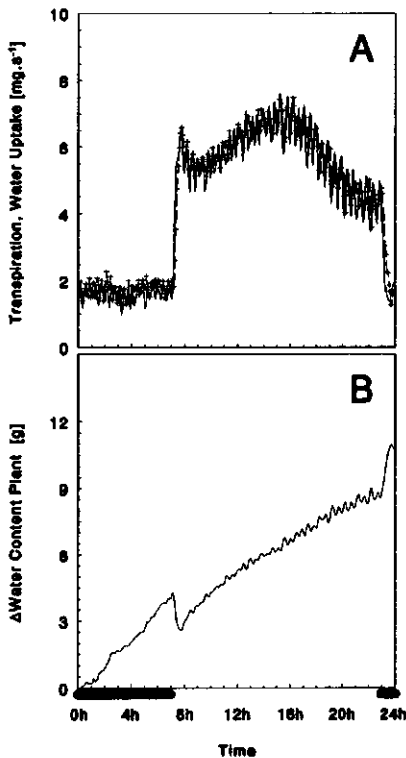
Climate measurements

T_{air} and RH_{air} were measured between the plants in the growth chamber at one minute time intervals (Rotronic Hygrometer Series I 200, Basserdorf, Switzerland). The Vapour Pressure Deficit ($e_s - e_a$) was calculated from these measures according to Monteith and Unsworth (1990). The same procedure of data handling was used as with E and U and stem diameter measurements. Wind speed at leaf level in the growth chamber was measured using a hand-held anemometer.

Results

Test measurements on the system for simultaneous determination of E and U.

Measured E and U during the test measurements in the growth chamber agreed



with the rate of water loss from vessel one induced by the dispensing pump ($1.0 \pm 0.02 \text{ mg.s}^{-1}$, and $1.0 \pm 0.01 \text{ mg.s}^{-1}$ for E and U respectively, values calculated per minute \pm maximal deviation, after noise reduction by a running average over 7 minutes). The deviations of E and U were normally distributed and independent of the light/dark periods. The deviations are assumed to be due to the effect of air movement on the reading of the balances. At all salinity levels the overall calculated increase in amount of water in the plant on the system (calculated from measured E and U), agreed with the additional weight measurements on the plant before and after a measurement period. No differences in total weight increase between the plant on the measurement system and the border plants were observed (results not shown).

Figure 3.3.3: Diurnal courses of simultaneously measured transpiration (—), water uptake (— + —, A) and amount of water in the plant (—, B).

General characteristics of the diurnal course of transpiration.

E, irrespective of the ψ_n^{re} -treatment, showed a clear diurnal pattern (Figure 3.3.3A). E was always lower during the dark than during the light. E was about constant during the dark but showed a distinct long-term pattern during the light, in spite of the constant climate and light level. Consequently, during the light the assumed steady state situation was not achieved: RWC^{p} was most likely not constant during the day. However, since the sudden changes in E were large at light transitions while the time constant for changes in RWC^{p} were assumed to be short (minutes), most of the sudden changes in WC^{p} at light transitions could be attributed to the change in RWC^{p} .

Upon the diurnal pattern of E, small and relatively quick fluctuations were observed (Figure 3.3.3A, Figure 3.3.4A and C). These were most likely the result of fluctuations of the vapour pressure deficit of the air (Figure 3.3.4B and D) caused by the climate controller.

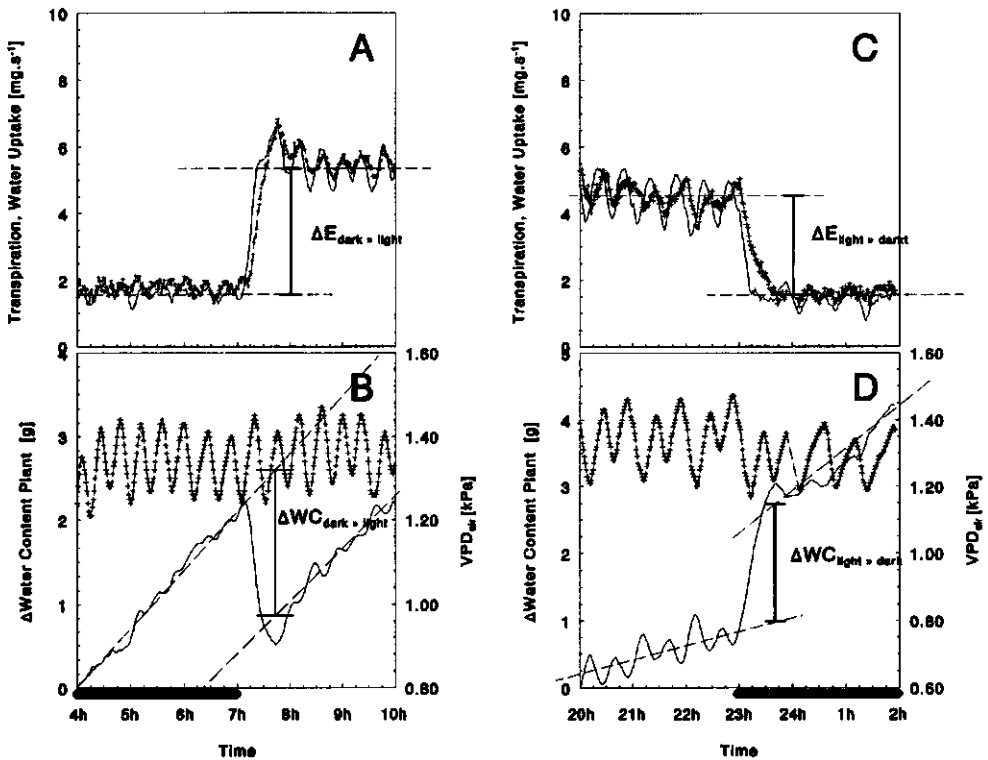


Figure 3.3.4A-D: Effect of a sudden changes in light level on the courses of transpiration (—, A and C), water uptake (— + —, A and C), and amount of water in the plant (—, B and D). The course of vapour pressure deficit of the growth chamber air is presented in B and D (— + —).

General characteristics of the diurnal pattern of water uptake and plant fresh-weight change.

All measurements exhibited the same general characteristics for the pattern of water uptake and of fresh weight change. The pattern of U was almost equal to that of E. U was usually a little higher than E. For short periods following the light transitions, U was clearly lagging behind E (Figure 3.3.4B and D). The amount of water in the plant (WC^p) increased steadily during dark and light, except for short periods following light transitions. Immediately after the light transitions, large changes in WC^p were observed: a loss of water at the start of the light period and an increase of water in the plant at the start of the dark period (Figure 3.3.4B and D). These sudden changes in WC^p were related to sudden changes in water flow through the plant, and were therefore interpreted as changes in RWC^p , due to the capacitance effect

Superimposed over the long-term dynamics of WC^p , small variations were evident. Because these fluctuations were not observed during the test measurements without a plant, they were related to behaviour of the plant. The small variations closely matched the small fluctuations in E and related U (Figure 3.3.4A-D), which in turn were closely related to variations in VPD_{air} .

Table 3.3.2: Effect of the osmotic potential in the root environment (ψ_n^r) on the rates of transpiration (E) and growth (G) of young tomato plants during four periods of a day: 1.5h - 0h before each light transition (End Light Period and End Dark Period), and 1.5h - 3h after each light transition (Start Light Period and Start Dark Period). Means \pm SE, n=3

ψ_n^r MPa	End light period		Start Dark Period		End Dark Period		Start Light Period	
	E $mg \cdot s^{-1}$	G $\mu g \cdot s^{-1}$	E $mg \cdot s^{-1}$	G $\mu g \cdot s^{-1}$	E $mg \cdot s^{-1}$	G $\mu g \cdot s^{-1}$	E $mg \cdot s^{-1}$	G $\mu g \cdot s^{-1}$
-0.01	7.7 \pm 0.82	427 \pm 21	3.8 \pm 0.19	534 \pm 31	4.4 \pm 0.34	497 \pm 14	10.4 \pm 0.99	521 \pm 69
-0.18	6.1 \pm 0.58	271 \pm 62	2.3 \pm 0.25	440 \pm 59	2.7 \pm 0.31	378 \pm 52	7.7 \pm 0.98	413 \pm 75
-0.36	5.8 \pm 0.57	157 \pm 0	2.0 \pm 0.22	311 \pm 38	2.1 \pm 0.27	213 \pm 22	7.0 \pm 1.02	382 \pm 55

The effect of ψ_n^r on ΔRWC^p and G

Salinity level (ψ_n^r) clearly affected the courses of E and WC^p (Figure 3.3.5). For clarity in figures only the results of the lowest and highest ψ_n^r -treatments are presented. The intermediate treatment always gave intermediate results. The severe drops of E (marked with an O, Figure 3.3.5A) were correlated with human presence in the growth chamber (to check the system and to prepare the next change in ψ_n^r), which influenced the vapour pressure deficit and CO_2 -concentration in the air clearly (results not shown).

Average E, and estimated G during the 1.5 h periods before and after light transitions are given in Table 3.3.2. E decreased with decreasing ψ_n^r . Within salinity

level, E was higher at the start of the light period than at the end of the light period. At the start of the dark period E was a little lower than at the end of the dark period.

Measured E and climate (Irradiance, T_{air} and RH) were used to calculate leaf temperature (T_{leaf}) and leaf conductance (g_L) (see Appendix 3.3.I, Table 3.3.3). Calculated differences in T_{leaf} at light transitions were below 1 °C. As a result, 60 to 70 % of the measured differences in E could be attributed to differences in g_L .

G was always lower at lower ψ_x^e (Table 3.3.2). Within each ψ_x^e -treatment, G decreased clearly during the dark period, and at the start of the light period, G was higher than at the end of the light period (Table 3.3.2). However, G at the start of the light period must be interpreted carefully since the courses of WC^p were not linear within 1.5 h after the lights were switched on (Figure 3.3.5B). Steady state was not

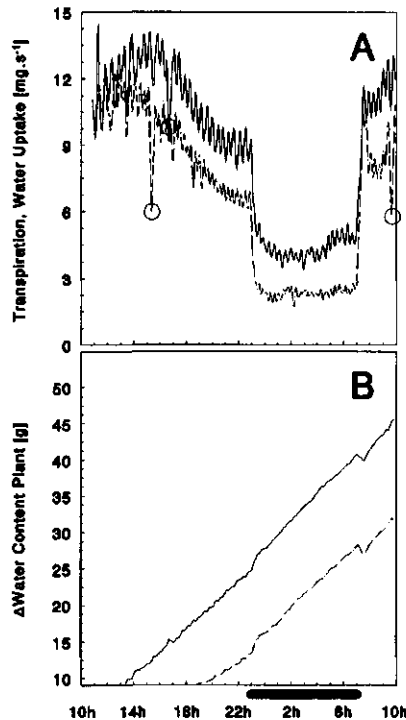


Figure 3.3.5: Effect of salinity on the diurnal courses of transpiration (A), water uptake (A) and amount of water in the plant (B) at low (—) and high (---) salinity. The peaks indicated by the circles (A) are caused by human presence in the growth chamber.

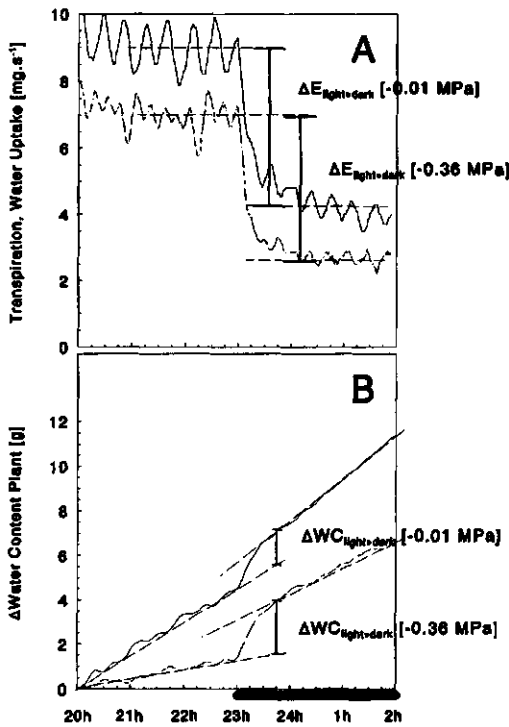


Figure 3.3.6: Courses of transpiration (A) and amount of water in the plant (B) at low (—) and high (---) salinity, measured during a transition from light to dark.

achieved and changes in RWC^P and G might still have occurred. Therefore, estimated values for G during the start of the light period are further omitted.

To investigate relations between changes in E and G and changes in plant water status (ΔWC^P), changes in E and G were derived at light transitions using average E and G immediately before and after a light transition (Figure 3.3.6; Table 3.3.3). The absolute change in E between light and dark was larger when the light was switched on than when the light was switched off ($|\Delta E_{\text{dark-light}}| > |\Delta E_{\text{light-dark}}|$). $|\Delta E_{\text{dark-light}}|$ did not differ between the salinity treatments. $|\Delta E_{\text{light-dark}}|$ on the other hand, decreased with decreasing ψ_n^e . At all ψ_n^e -treatments, G increased after the lights were turned off. The change in G ($|\Delta G_{\text{light-dark}}|$)

was lower when ψ_n^e was -0.01 MPa as compared to the lower ψ_n^e -levels.

Changes in WC^P were estimated after the lights were turned off ($|\Delta WC^P_{\text{light-dark}}|$, Figure 3.3.6B) and after the lights were turned on ($|\Delta WC^P_{\text{dark-light}}|$) (Table 3.3.4). ΔWC^P was larger at lower ψ_n^e . The changes in RWC^P were low: assuming the total plant weight (Table 3.3.1) close to saturated WC^P , RWC^P changed only 0.2 to 0.5 % at light transitions. No direct comparison between absolute RWC^P at different ψ_n^e -treatments could be made, since measuring E and U was stopped during each change in ψ_n^e .

Generally, stem diameter showed the same characteristics and reactions on the ψ_n^e -treatments and light regime as WC^P (Figure 3.3.7).

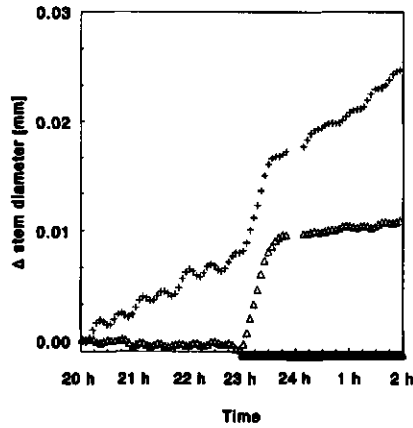


Figure 3.3.7: Course of stem diameter at low (+) and high (Δ) salinity during a transition from light to dark.

Table 3.3.3: Effect of ψ_n^{re} on calculated leaf temperature (T_{leaf}) and leaf conductance for water vapour (g_L) during four periods of a day: 1.5h - 0h before each light transition (End Light Period and End Dark Period), and 1.5h - 3h after each light transition (Start Light Period and Start Dark Period).

ψ_n^{re} MPa	End light period		Start Dark Period		End Dark Period		Start Light Period	
	T_{leaf} $^{\circ}C$	g_L $mm\ s^{-1}$	T_{leaf} $^{\circ}C$	g_L $mm\ s^{-1}$	T_{leaf} $^{\circ}C$	g_L $mm\ s^{-1}$	T_{leaf} $^{\circ}C$	g_L $mm\ s^{-1}$
-0.01	25.4	1.14	24.7	0.61	24.7	0.71	25.2	1.59
-0.18	25.5	0.87	24.8	0.36	24.8	0.42	25.4	1.14
-0.36	25.5	0.83	24.8	0.31	24.8	0.33	25.4	1.02

Calculations were made using measured transpiration rates (Table 3.3.2), estimated net radiation absorbance (R_N) and boundary layer resistance for vapour (R_{bv}), and the Penman-Monteith equation for latent heat loss and heat balance of a leaf (Appendix 3.I): R_{bv} : $26.3\ m.s^{-1}$, R^N : $45\ W.m^{-2}$, A_L : $0.68\ m^2$

Table 3.3.4: Effect of ψ_n^{re} on changes in transpiration rate (ΔE), in growth rate (ΔG) and in water status (ΔWC^p) of a tomato plant at transitions from light to dark (lights turned off) and from dark to light (lights turned on). Means \pm SE, $n=3$

ψ_n^{re} MPa	lights turned off			lights turned on		
	$\Delta E_{light-dark}$ $mg\ s^{-1}$	$\Delta G_{light-dark}$ $\mu g\ s^{-1}$	$\Delta WC^p_{light-dark}$ g	$\Delta E_{dark-light}$ $mg\ s^{-1}$	$\Delta G_{dark-light}$ $\mu g\ s^{-1}$	$\Delta WC^p_{dark-light}$ g
-0.01	-3.9 ± 0.63	107 ± 10.1	1.0 ± 0.09	6.0 ± 0.65	24 ± 55	-0.8 ± 0.27
-0.18	-3.7 ± 0.33	169 ± 13.5	1.4 ± 0.15	5.1 ± 0.67	35 ± 23	-1.2 ± 0.02
-0.36	-3.8 ± 0.35	154 ± 38.3	2.0 ± 0.06	4.9 ± 0.75	169 ± 34	-1.9 ± 0.29

Discussion

Transpiration and leaf conductance (g_L)

Generally, on the short-term, E may only change due to a change in driving force for water vapour diffusion ($e_s^{\text{leaf}} - e_s^{\text{air}}$), or due to a change in conductance of the diffusion pathway (Eq. A.3.1). In present experiments e_s^{air} was approximately constant, ignoring the relative small and quick fluctuations in $\text{VPD}_{\text{air}} (= e_s^{\text{air}} - e_s^{\text{air}})$ caused by the climate controller (Figure 3.3.4B and D). Within a light or dark period e_s^{leaf} was not changed by an external factor. This does not mean that e_s^{leaf} was constant because changes in E alter T_{leaf} through variation in latent heat loss. T_{leaf} is closely related to e_s^{leaf} (Eq. A.3.2).

Within a dark period E was approximately constant. Consequently, T_{leaf} and g_L were constant too (Table 3.3.3). Within the light periods, however, E followed a clear diurnal pattern (Figure 3.3.3A). This pattern was not induced by an external factor in the shoot- or root-environment of the plant: temperature of the root medium, as well as e_s^{air} were constant. T_{leaf} was not altered by another factor than the changing transpiration rate. Consequently it must have been a slowly changing conductance of one or more of the parts of the diffusion pathway that initially caused the diurnal pattern in E during the light. In principle, conductance's of the stomata, cuticula and boundary layer could have changed, but most likely some kind of endogeneous rhythm caused a diurnal pattern in stomata opening during the light (Martin and Meidner, 1971, 1972; Mansfield and Snaith, 1989).

At the light transitions, the situation is more complex. Irradiance is an external factor that changes the opening status of the stomata (Raschke, 1975) and T_{leaf} at the same time. Consequently, driving force and conductance for transpiration are changed (g_L and e_s^{leaf}). The change in T_{leaf} is tempered by the change in latent heat loss accompanied with a change in E (thermal feed-back). The simulated changes in T_{leaf} between dark and light were small (Table 3.3.3) and accounted for only 30 - 40 % of the change in E . The change in E at light transitions was mainly due to a direct effect of light on g_L . Figure 3.3.4A shows clearly that g_L increased during the first 5 to 10 minutes after the lights were switched on. E increased gradually, even though the increase in net radiation was nearly instantaneous. The salinity level in the root environment clearly influenced E in dark (Table 3.3.2).

The measured diurnal pattern of E during the light was not the result of slowly changing external factors, since the environmental conditions were constant. Therefore it must have resulted from a diurnal pattern of g_L , which was even more pronounced than the pattern of E since changes in E caused by changes in g_L are tempered by a thermal feedback (an increase of E lowers T_{leaf} and therefore the driving force for E). It is unlikely that a slowly changing RWC^{p} caused the pattern of g_L and thus of E , be-

cause there was no other cause that could have changed RWC^p during the light period than the change in E itself.

With the present experiments, three factors seem to influence g_L : light, and an endogenous rhythm. g_L increased strongly with increasing light intensity, which is a well known effect (Raschke, 1975). At each salinity-level, the change in g_L was different between the two light transitions while the change in light level was the same. This was probably the result of g_L already being decreased by the endogenous rhythm at the end of the light period.

No clear relation could be found between changes in RWC^p and changes in E. While $|\Delta WC^p_{light-dark}|$ and $|\Delta WC^p_{dark-light}|$ were about equal within each salinity-level, $|\Delta E_{light-dark}|$ was lower than $|\Delta E_{dark-light}|$. At the light transition from light to dark $|\Delta E|$ was about the same at all salinity-levels, while $|\Delta WC^p|$ clearly changed (Table 3.3.4).

Interpreting these results in terms of effects of RWC^p is difficult, since we are dealing with changes in E and changes in WC^p upon an unknown absolute levels of RWC^p which probably differed considerably between ψ_{π}^e -treatments. Moreover, the absolute changes in RWC^p at light-transitions, estimated from total fresh weight of the plant and ΔWC^p , never exceeded the 1 %. It is very well possible that these small changes in RWC^p are too low to induce any effect on stomatal conductance.

Stomatal closure under drought, such as induced by low ψ_{π}^e , has been reported widely (e.g. Gollan *et al.*, 1986; Tardieu *et al.*, 1993). Last two decades there has been much discussion about factors regulating responses of stomata to drought (Raschke, 1975; Schulze, 1986; Tardieu and Davies, 1993). Some authors obtained correlations between g_L and leaf water status (Hsiao, 1973; Bradford and Hsiao, 1982), others reported g_L -changes which were not related to water status changes in the leaves (Aston and Lawlor, 1979; Gollan *et al.*, 1986; Munns and King, 1988; Jensen *et al.*, 1989; Zhang and Davies, 1990). Several authors suggested that changes in phytohormones generated by the roots play a role in stomatal closure (Tardieu *et al.*, 1992; Tardieu and Davies, 1993). With our experiments marked changes in E, even during the dark, were observed when roots were subjected to a uniform osmotic stress of relatively mild level in a solution. Changes in g_L are the result of a combination of changes in light level, an endogenous rhythm and ψ_{π}^e .

Water status

Although the measured changes in WC^p at light-transitions were rather low, clear differences were found between salinity treatments. The larger change in WC^p and thus in RWC^p at high salinity at further comparable changes in E and water flow rate through the plant was probably the result of a larger hydraulic capacitance of the plant at lower RWC^p and related water potential. The volumetric modulus of elasticity

of cells or tissues is lower (cell walls more elastic) at lower water content (Tyree and Jarvis, 1982).

Growth

Irreversible cell expansion (G) results from two interdependent processes: water absorption and cell wall growth (Cosgrove, 1986). RWC^P may influence both processes by altering the water potential difference between growing tissue and xylem, and by influencing cell turgor (Lockhart, 1965). Although steady state was not achieved in the light period, it can be concluded that ψ_n^e influenced G (Table 3.3.2). How ψ_n^e influenced G is less clear. While $|\Delta WC^P|$ was clearly larger at lower ψ_n^e , no such relation was found between $\Delta G_{\text{light} \rightarrow \text{dark}}$ and ψ_n^e (Table 3.3.4). If the hydraulic capacitance was larger at low ψ_n^e , the larger $|\Delta WC^P|$ could have been associated with a similar shift in turgor. Instead there seems to be an optimal ψ_n^e for $\Delta G_{\text{light} \rightarrow \text{dark}}$ somewhere between -0.01 and -0.36 MPa (Table 3.3.4). Therefore, a unique relation between RWC^P and G seems unlikely.

Assimilate concentration in the growing tissues could also have been a factor influencing G (Tyree and Jarvis, 1982). Cell wall growth is under metabolic control and requires a constant supply of assimilates. Assimilate concentration in the growing tissues could also influence the rate of water absorption through osmotic effects on the water potential difference between xylem and growing tissue (Frensch and Hsiao, 1994). It is very likely that with present experiments assimilate concentration was different at the light transitions at different ψ_n^e . E during the light period before the light-dark transitions, and, as was concluded before, g_L differed between the ψ_n^e -treatments. With g_L , the CO₂-assimilation differed between the ψ_n^e -treatments. However, not only the current ψ -level but also the ψ -levels in the recent history of the plant influence the assimilate level. Therefore no conclusions can be drawn about relations between assimilate-level, plant water status and fresh-weight growth rate. During the dark G decreased clearly (Table 3.3.2), while the plant water status may be assumed constant or at most slowly increasing. The decline of G during the dark could have been the result of depletion of assimilates due to growth and maintenance, which must have occurred during the dark.

ABA is another factor that may have caused the effect of ψ_n^e on G: Increased endogenous ABA may influence both water absorption and cell wall growth through decreased tissue conductance and cell wall extensibility (Bensen *et al.*, 1988). A clear relation between ABA-concentration in the xylem and leaf growth rate of drought stressed maize and sunflower plants was found before (Davies and Zhang, 1991; Zhang and Davies, 1990).

The presented results showed that simultaneous E and U measurements and the calculated course of fresh weight together may give a great deal of information about

the complex effect of the environment on plant water relations, and their link with short-term fresh-weight growth rate. The method has the advantage of being relative simple and inexpensive. Furthermore, all derived characteristics originate from simultaneous measurements on the same plant. ψ_n^{re} clearly influenced g_L , G and ΔRWC^P at light-transitions. Interpreting the role of RWC^P on changes in g_L and G is difficult since several factors seem to interact, including an endogeneous rhythm.

Present results show that a simple straightforward approach of stomatal conductance and plant growth, based on only the physics of water relations in the plant may give, already on short-term (within a day), large problems interpreting effects of shoot and root environment.

Appendix 3.3.1

Transpiration involves diffusion of water vapour from the leaf interior to the bulk air, and may be described by (Monteith and Unsworth, 1990):

$$E = \frac{1}{r_l + r_{bv}} \times \frac{\rho C_p (e_s^{leaf} - e_a^{air})}{\lambda \gamma} \quad A.3.1$$

$$e_s^{leaf} = 611 \times e^{\frac{17.4 T_{leaf}}{(T_{leaf} + 239)}} \quad A.3.2$$

in which

E	Transpiration rate per m ² leaf area	kg H ₂ O m ⁻² s ⁻¹
ρC_p	Volumetric heat capacity of the air	J m ⁻³ K ⁻¹
e_s^{leaf}	Saturated water vapour pressure inside leaf	Pa
e_a^{air}	Actual water vapour pressure in ambient air	Pa
T_{leaf}	Leaf temperature	°C
r_l	Resistance of the leaf for water vapour	s m ⁻¹
r_{bv}	Resistance of the boundary layer for water vapour	s m ⁻¹
γ	Psychometric constant	Pa K ⁻¹
λ	Latent heat vaporisation of water	J kg ⁻¹ H ₂ O

Equation A.3.1 may be separated into two parts: the first part, with the resistance's in the denominator, represents the overall conductivity of the diffusion path. The second part represents the water vapour concentration gradient between leaf interior and ambient air which is the driving force for the diffusion process and thus for transpiration.

At light transitions, overall conductivity and driving force change due to changes in leaf conductance and in leaf temperature. The relative importance of the two factors to the change in transpiration may be calculated. Leaf temperature may be calculated from the equations for convective heat transfer between leaf and bulk air (A.3.3), the steady

state heat balance for a leaf (A.3.4), the estimated net radiation flux density (R_n) and the resistance of the boundary layer for heat transfer (A.3.5):

$$T_{\text{leaf}} = \frac{C \times r_{\text{bh}}}{\rho C_p} + T_{\text{air}} \quad \text{A.3.3}$$

in which

C	flux of convective heat loss	W m^{-2}
r_{bh}	boundary layer resistance for heat	s m^{-1}

$$C = R_n - \lambda E \quad \text{A.3.4}$$

in which

λE	flux of latent heat loss	W m^{-2}
R_n	net radiation flux density	W m^{-2}

$$R_{\text{bh}} = 200 \times \sqrt{\frac{w}{u}} \quad \text{A.3.5a}$$

in which

w	average leaf width	m
u	windspeed	m s^{-1}

$$r_{\text{bv}} = 0.93 \times r_{\text{bh}} \quad \text{A.3.5b}$$

Omitting long wave radiation exchange between leaf and surroundings, R_n during the dark may be assumed zero. Treating the plant as a cone and irradiance 100 % diffusive, R_n during the light was assumed to be between 70 and 100 % of the measured irradiance in the growth chamber and therefore between 31 and 45 W m^{-2} (Monteith and Unsworth, 1990). R_{bh} , calculated as a function of measured wind speed at leaf level ($u = \pm 5 \text{ m s}^{-1}$) and average leaf width ($w = \pm 0.1 \text{ m}$) was estimated to be about 28,3 s m^{-1} (Goudriaan, 1977). The driving force for transpiration was calculated using calculated T_{leaf} and measured e_a^{air} ($T_{\text{air}}, \text{RH}_{\text{air}}$). From this driving force and measured rates of transpiration the overall conductivity was calculated (Eq. A.3.1).

Leaf conductivity results of the conductivity of the stomata ($g_s = 1/r_s$) and cuticula ($g_c = 1/r_c$) in parallel. g_c is usually low ($\pm 0.5 \text{ mm s}^{-1}$, Goudriaan, 1977) and approximately constant. g_s in contrary may vary (0.0001 to 0.1 m s^{-1}). Since r_{bv} and g_c were constant during the growth chamber experiments, all changes in overall conductivity at light transitions may be attributed to changes in g_s . The relative importance of changes in overall conductivity and driving force are calculated at all light transitions: g_s accounted for 60-70 % of the change in transpiration rate at all light transitions.

3.4 Dynamic effects of changes in Electric Conductivity on transpiration and growth of greenhouse-grown tomato plants.

W. VAN IEPEREN, 1996. *Dynamic effects of changes in Electric Conductivity on transpiration and growth of greenhouse-grown tomato plants. Journal of Horticultural Science* 71 (3) 481-496.

Abstract

The dynamic responses of the rates of growth and transpiration of greenhouse grown tomato plants (*Lycopersicon esculentum* Mill. cv. Counter) were investigated upon changes in the osmotic potential in the root environment (ψ_{π}^{re}). Once a day, ψ_{π}^{re} was alternated between -0.01 (high) and -0.36 MPa (low). Changes in ψ_{π}^{re} were conducted in light or dark. Rates of water uptake (U) and transpiration (E) were simultaneously measured on the same plant, growing on water culture under natural light conditions. The accuracy of measured E and U was sufficient to calculate changes in plant water content (WC^p) on minute base. Courses of WC^p were analysed, and changes in WC^p attributed to growth and alterations in plant water deficits. During large parts of the dark the course of WC^p was linear and changes in WC^p were completely attributed to irreversible growth. During the light, WC^p fluctuated upon the courses of global radiation and associated E, while increasing. These fluctuations in WC^p, as well as transient changes in WC^p immediately after ψ_{π}^{re} -changes in dark were attributed to changes in plant water deficit. At low ψ_{π}^{re} , growth rate was lower and plant water deficits were higher than at high ψ_{π}^{re} . Growth rate changed almost immediately upon changes in ψ_{π}^{re} . Changes in growth rate were initially larger when a change in ψ_{π}^{re} was conducted in dark than when it was conducted in light. These initially larger responses were partially counterbalanced during the following light period, indicating adaptation of the plant during the light. E during the light was hardly influenced by the applied ψ_{π}^{re} -levels. In dark, E decreased after a change in ψ_{π}^{re} from high to low, while it increased after the opposite ψ_{π}^{re} -change. However, the differences in E-level were minimal. At low ψ_{π}^{re} , plant water deficits increased more with increasing E than at high ψ_{π}^{re} . Within both ψ_{π}^{re} -levels, hysteresis was observed on the relation between E and plant water deficit over a day: At similar transpiration rate, plant water deficit was higher in the afternoon than in the morning. The hysteresis effect was more pronounced at low ψ_{π}^{re} .

Introduction

Salinity can influence plant growth in several ways. One of the well known long-term responses is a reduction in plant size and leaf area, which limits plant transpi-

ration and CO₂-assimilation and therefore plant growth. Short-term responses (minutes-days), such as the reduction of cell expansion and stomatal closure (Hsiao, 1973), are primarily responsible for this long-term effect. These short-term responses induced by salinity seem to be similar to responses caused by water stress induced by the shoot environment (Munns, 1993). However, the mechanisms behind them may be different (Davies and Zhang, 1991; Gollan *et al.*, 1986; Passioura and Gardner, 1990). In the longer term, plants may adapt to salinity by osmotic adjustment (Morgan, 1984).

Effects of salinity do not only occur in saline soils, but also in artificial growth systems, such as soilless cultures in greenhouses. Due to the combination of a relatively high fertilisation level in the irrigation water and high transpiration rates, salt levels in the root environment may increase as a result of a disproportion between water and solute uptake by the roots (Fiscus, 1977; Gardner, 1965). This can be measured as high EC (Electric Conductivity) or low osmotic potential in the root environment (ψ_n^{rc}), and decreases the availability of water to the roots. In combination with the usually high transpiration rates in greenhouses, this may cause significant water deficits in the plant, and influence plant functioning significantly (Bradford and Hsiao, 1982; Hsiao, 1973). Especially for many horticultural crops which have harvestable parts with relatively low dry matter concentration, these effects of ψ_n^{rc} might be important. Knowledge of the effects of changing salt levels and the greenhouse climate on short-term plant water relations is necessary for short-term control of irrigation and of the EC of the nutrient solutions applied.

Much of the research on this field is done using discrete methods to measure plant water deficits. Well known measures are the water potential and the relative water content of a plant or plant part. The techniques to obtain values for these variables are mostly destructive and are often conducted on plant parts (mostly leaves or leaf discs). They may therefore introduce interaction between the measurements and obtained results, especially when the sample frequency is high. In greenhouses, the accuracy of the values obtained for these measures is generally low, due to spatial differences in water deficits within a plant and crop, and due to rapidly changing ambient conditions. The applied techniques and methods are often not without theoretical objections (Slavik, 1974; Shackel, 1984; Zimmermann *et al.*, 1993).

Continuous measurements of elongation on leaves, stems, fruits and roots using Linear Variable Displacement Transducers (LVDT's) have given valuable information about short-term responses to salinity and drought stress (e.g. Acevedo *et al.*, 1971; Cramer and Bowman, 1991; Frensch and Hsiao, 1994; Pearce *et al.*, 1993ab). However, these types of measurements were unidirectional, and conducted on single plant parts and could therefore only give qualitative indications of whole plant responses. Moreover, most experiments were conducted in growth chambers in a relatively con-

stant environment and low light levels. Simply applying the results obtained to greenhouse-grown plants is suspect since an interaction may be expected between high radiation and salinity affecting plant water relations.

Recently a new, integrated method has been described to measure the rates of water uptake and transpiration simultaneously on a single plant (van Ieperen and Madery, 1994). This method provides short-term measurements of the rates of plant transpiration (E) and water uptake (U), which are accurate enough for calculation of changes in plant water content (WC^P) at minute intervals (Eq. 3.4.1):

$$U-E = dWC^P/dt \quad (3.4.1)$$

Using this equation the course of WC^P may be calculated by integration in time. Changes in WC^P may be due partially to plant growth and partially to changes in plant water deficit (Boyer, 1985). To distinguish between these two types of changes in WC^P , growth was defined as the irreversible increase in maximal water content in the plant. Consequently, growth rate must be larger than or equal to zero. Growth is related to the plastic, irreversible extension of cell walls. The plant water deficit (the difference between maximal water content and actual water content of the plant) is related to the relative water content of the plant, and is a measure of the water status of the plant. Changes in plant water deficit are reversible and usually change upon alterations in environmental conditions. Changes in plant water deficit are related to the elastic properties of cell walls (Cosgrove, 1993). Growth and changes in plant water deficit may occur simultaneously. However, under certain conditions, one or other of these two processes may be negligible or lacking. For instance: growth may be inhibited by a low water status (high water deficit), and stable environmental conditions may cause a constant plant water deficit.

In order to investigate short-term growth and transpiration responses of tomato plants to changes in ψ_n^{rc} , E and U measurements were made on plants which were subjected to alternating low and high ψ_n^{rc} -levels. Changes in ψ_n^{rc} were imposed in the light and in the dark to allow separation between growth and changes in plant water deficits. Short-term adaptation of the plant to ψ_n^{rc} was investigated by measuring growth during subsequent dark periods after a change in ψ_n^{rc} in dark.

Materials and methods

Plant material and growth conditions

Seeds of tomato (*Lycopersicon esculentum* Mill. cv Counter) were germinated in sand and raised on water culture in a greenhouse. After the first truss started to

flower, the plants were transferred to a special NFT-system in a nearby greenhouse compartment (12×12.8 m) with the possibility of changing ψ_{π}^{rc} in the short term (van Ieperen, 1995). All plants were grown with alternating ψ_{π}^{rc} -levels (-0.01 and -0.36 MPa). Changes in ψ_{π}^{rc} were made once a day: for half of the plants in light (at 10.00 hours) and for half of the plants in dark (at 22.00 hours). The plants on the NFT-system served on the one hand as a supply of measurement plants, and on the other hand as a border, providing a normal greenhouse climate and radiation profile around the measurement system for E and U (see below). Mature, fruit-carrying tomato plants were used for the E and U measurements.

Temperature (T_{air}) and relative humidity (RH) setpoints were 20/18 °C (day/night) and 80%, respectively. All measurements were made in the autumn (October-November 1993). Normal crop management and a standard nutrient solution (EC = 2.5 mS cm⁻¹; ψ_{π}^{rc} = -0.09 MPa) were used to raise the tomato plants (see: van Ieperen, 1995). The concentration of macro-elements was increased proportionally to obtain the low ψ_{π}^{rc} (EC = 10 mS cm⁻¹; ψ_{π}^{rc} = -0.36 MPa). All macro-elements were removed from the solution to obtain the high ψ_{π}^{rc} (EC = 0 mS cm⁻¹; ψ_{π}^{rc} = -0.01 MPa).

Simultaneous measurement of E and U

The method of van Ieperen and Madery (1994) was used to measure E and U simultaneously on the same plant. The measurement system (Figure 3.4.1) was located in the middle of the greenhouse compartment (12×12.8 m).

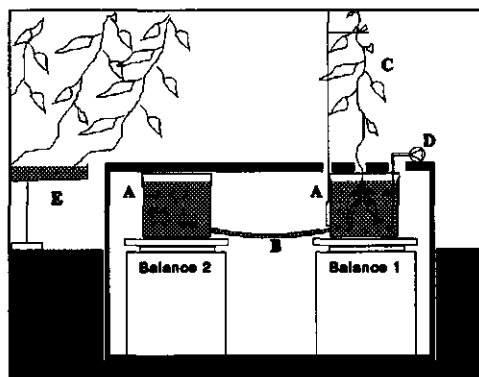


Figure 3.4.1: Apparatus to measure the rates of transpiration and water uptake simultaneously on one plant. A: Communicating PVC-vessels filled with nutrient solution; B: connecting silicon tube between the vessels; C: Plant; D: Air pump; E: NFT-system with border plants around the measurement system.

Two similar, communicating vessels (diameter 21 cm, volume 6.5 l, connected by a 6.5 mm diameter, 20 cm length silicon tube, filled with nutrient solution) were placed on two Mettler PE11 balances. The plant was placed on balance one, with its roots below the water surface in the vessel. The nutrient solution in that vessel was aerated con-

tinuously. The vessels were sealed with slightly perforated aluminium foil to prevent direct evaporation. Vessels and balances were placed in a polystyrene box in a pit in the ground, so that the height of the measurement plant was similar to that of the border plants around it. The temperature of the nutrient solution in the vessels was roughly constant (20 ± 2 °C). Analogue output of the balances were measured using a HP 44702A/B High-Speed Voltmeter in a HP3852A Data-Acquisition and Control Unit (Hewlett Packard, USA). Each balance was sampled about 300 times per minute. Averages were calculated per minute and stored on the hard-drive of a Personal Computer (HP-Vectra, Hewlett Packard, USA). To reduce the background noise on the weight measurements moving averages were calculated over 7 min.

E was calculated as the cumulative weight loss on both balances per minute. U was calculated as the weight loss on the slave balance (balance two) per minute, multiplied by a factor which was about 1.98. This factor represents the ratio between the cross-sectional areas of the water surfaces in vessel one to that of one plus two, corrected for the cross sectional area of the stem of the tomato plant. The factor is close to 2, because about half of the solution taken up by the plant originates from vessel one and about half originates from vessel two (van Ieperen and Madery, 1994). From the E and U measurements dWC^p/dt was calculated (Eq.3.4.1) and used to construct the courses of WC^p during periods of 24 h. These courses of WC^p were used to obtain information about the effects of ψ_n^{rs} on plant growth rate during periods when the water deficit of the plant could be assumed to be constant (mainly in dark), and on plant water deficits when growth rate could be assumed constant or was easily estimated.

Before using the system for measurements on plants, tests measurements were conducted to check for environmental effects on the weight readings: during one week weight measurements were done on the system in the greenhouse, which was fully operational except for the plant, which was lacking. Instead an artificial, non-transpiring plastic plant was placed on balance one. E and U were simulated by removing nutrient solution from vessel one using an accurate dispensing pump (Watson Marlow 505DI, UK) at a rate of 10 g h^{-1} during 120 h (day and night).

Measurements of E and U on plants were tested by measuring E and U during periods of 24h on several plants at a constant ψ_n^{rs} (-0.09 MPa). These measurements started in the dark. Growth of the plants was determined separately from the E and U measurements by weighing before and after. Growth over 24 h was also determined by calculating the course of WC^p from the E and U measurements. The total increase in WC^p was compared to the measured growth by before and after weighing.

In addition to E and U, once a minute, measurements were made of global radiation at 3 m above the greenhouse (solarimeter; Kipp, The Netherlands), T_{air} and RH

in the greenhouse at plant height (Rotronic Hygrometers Series I 200, Basserdorf, Switzerland) using the HP3852A Data-Acquisition and Control Unit.

Experimental setup

In the first experiment the effects of changes in ψ_x^{so} made in light on the courses of E, U and the resulting WC^{p} were investigated. Just before the change in ψ_x^{so} at 10 h a plant was taken from the border plants, which were then being subjected to a ψ_x^{so} of -0.01 MPa. That plant was carefully placed on the measurement system at a ψ_x^{so} of -0.36 MPa, following the normal ψ_x^{so} schedule. The first 10 h of the E and U measurements were ignored to allow the plant to recover from the transfer to the measurement system. Over the following two days E and U were measured, and ψ_x^{so} was changed at 10 h from -0.36 to -0.01 MPa on the first day, and from -0.01 to -0.36 MPa at 10 h on the second day. This procedure was repeated on four plants of about similar size.

In the second experiment changes in ψ_x^{so} were made in the dark. The plant was chosen from the border plants at -0.36 MPa, which were subjected to daily changes in ψ_x^{so} at 22 h. The plant was placed on the measurement system at 10 h, and the next change in ψ_x^{so} was made at 22 h and E and U were measured: On the first day, ψ_x^{so} was changed from -0.36 to -0.01 MPa, and on the second day from -0.01 to -0.36 MPa. The second experiment was also repeated on four plants of similar size.

After each measurement, the plant was removed from the system, the number of leaves (>2 cm) and trusses were counted. Leaf area (LICOR 3100 area meter, Lincoln, USA) and the fresh weights of leaves, stem, fruits and root system (after carefully drying with tissue paper) were measured. Dry weights were measured after the plant had been dried for at least one week in a ventilated oven (65 °C).

Results

Test measurements

E and U, measured on the system without a plant, were 10 ± 1.2 and 10 ± 0.7 $\text{g}\cdot\text{h}^{-1}$, respectively (averages, calculated over one minute intervals after a 7 min moving average \pm maximal deviation from average). The deviation on U being lower than on E, was probably due to the lower effect of air movement on the weight measurements on balance two. The deviation from the average was normally distributed over the 120 h period, indicating that there was no dependence of the weight measurements on the greenhouse climate. The total loss of water from the system, which was not caused by the dispensing pump, was about 5 g (over 120 h). This loss of water is assumed to be due to the direct evaporation from the system, and was low: 0.04 g h^{-1} , which was below the noise level.

Test measurements on plants resulted in roughly similar estimates of growth over 24 h, measured by weighing before and after, and by E and U measurements (integration of dWC^p/dt in time). Differences between these two methods were within 4% (results not shown).

Diurnal courses of plant transpiration, water uptake and plant water content

Characteristics of the plants used for the E and U measurements, and of the greenhouse climate during the periods of measurements are given in Table 3.4.1 and Table 3.4.2. Measured diurnal courses of global radiation, transpiration (E), water uptake (U) and water content of the plant (WC^p) are presented in several figures, representing the characteristic situations that occurred in experiments 1 and 2.

Table 3.4.1: Characteristics of the plants used for simultaneous determination of E and U in experiment 1 and 2.

	Exp.	Roots	Stem	Leaves	Fruits	Total
Fresh weight	1	103 ± 15.2	218 ± 31.1	442 ± 27.3	461 ± 83.5	1224 ± 56.3
[g]	2	110 ± 17.2	291 ± 35.9	537 ± 35.3	585 ± 103.2	1523 ± 76.4
Dry weight	1	9.2 ± 2.74	20.2 ± 0.75	53.4 ± 1.73	41.5 ± 9.61	123.3 ± 3.45
[g]	2	9.1 ± 3.01	26.2 ± 1.21	53.8 ± 3.54	47.8 ± 10.54	136.9 ± 4.52
	Exp.				Exp.	
Leaf area	1	1.12 ± 0.092		Plant length	1	1.83 ± 6.4
[m ²]	2	1.39 ± 0.069		[m]	2	2.22 ± 8.4
No Leaves	1	30 ± 2.1		No Trusses	1	8 ± 0.2
[-]	2	30 ± 2.3		[-]	2	9 ± 0.4

Means ± SE, determined on four plants per experiment.

Table 3.4.2: Average temperature (T_{air}) and relative humidity (RH) of the greenhouse air during subsequent day and night periods in experiment 1 and 2, and the daily solar radiation integrals.

ψ_n^{rc} [MPa]	Exp.	Radiation integral [MJ.m ⁻² .d ⁻¹]		T_{air} [°C]		RH %	
		day (7h-18h)	night (18h-7h)	day (7h-18h)	night (18h-7h)	day (7h-18h)	night (18h-7h)
-0.01	1	4.7 ± 1.18	19.8 ± 0.62	17.6 ± 0.23	86 ± 0.4	81 ± 0.7	
-0.36	1	6.5 ± 0.64	21.7 ± 0.96	17.8 ± 0.34	84 ± 0.2	81 ± 0.3	
-0.01	2	3.0 ± 0.37	19.2 ± 0.11	17.6 ± 0.28	88 ± 0.4	81 ± 0.5	
-0.36	2	5.1 ± 0.74	21.1 ± 0.39	17.9 ± 0.35	86 ± 0.2	81 ± 0.4	

Means ± SE over four days. *In experiment 1 changes in ψ_n^{rc} were conducted at 10 h. Values for experiment 1 are related to the ψ_n^{rc} after the change in ψ_n^{rc} at 10 h. In experiment 2 changes in ψ_n^{rc} were conducted at 22h. Values for experiment 2 are related to the ψ_n^{rc} before the change in ψ_n^{rc} at 22h.

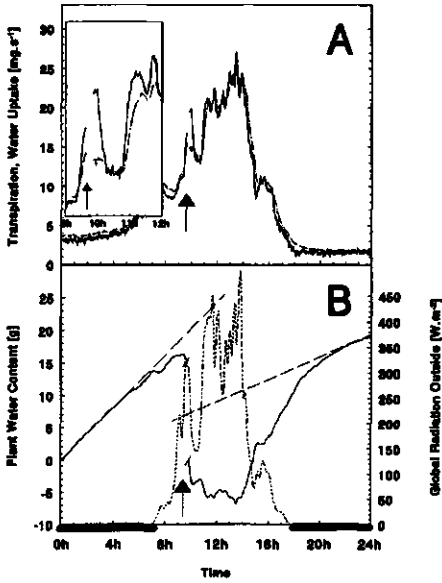


Figure 3.4.2: Measured rates of water uptake (— — —) and transpiration (——) (A), and the courses of plant water content (WC^p) (——) and global radiation (— - —) (B) during a day that the osmotic potential in the root environment (ψ_r^e) was changed from -0.01 MPa to -0.36 MPa at 10.00 hours. (marked by an arrow). The inset in A displays a closer view on the courses of water uptake and transpiration just before and after the change in ψ_r^e . The dashed lines in B are the regression lines on the WC^p -curve that were used to calculate the growth rate of the plant in subsequent dark periods.

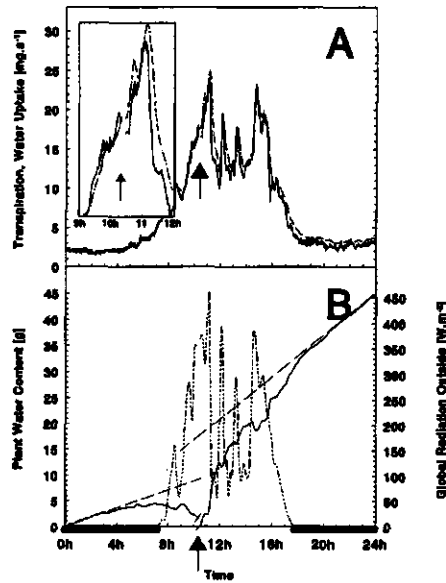


Figure 3.4.3: As in Figure 3.4.2 except that the changes in the root environment were from -0.36 to -0.01 MPa.

Changes in ψ_r^e (marked by an arrow) were conducted in the light (experiment 1; Figure 3.4.2 and Figure 3.4.3), and in the dark (experiment 2; Figure 3.4.4 and Figure 3.4.5). ψ_r^e was changed from -0.01 to -0.36 MPa (Figure 3.4.2 and Figure 3.4.4) and in opposite direction (Figure 3.4.3 and Figure 3.4.5). Figure 3.4.6 present detailed views on the courses of E, U and WC^p before and after the changes in ψ_r^e in dark, as shown in Figure 3.4.4 and Figure 3.4.5 respectively. The insets in Figure 3.4.2 and Figure 3.4.3 display a close view of the courses of E and U during the changes in ψ_r^e in light.

In Figure 3.4.2 and Figure 3.4.3 the courses of E, U and WC^p were broken due to the application of changes in ψ_r^e at about 10 h. WC^p was reset to zero at the restart of the E and U measurements after the changes in ψ_r^e . This was done because E and U

were not measured for several minutes during the change in ψ_{π}^c . For a similar reason the curves in Figure 3.4.4 to Figure 3.4.6 were broken at 22 h.

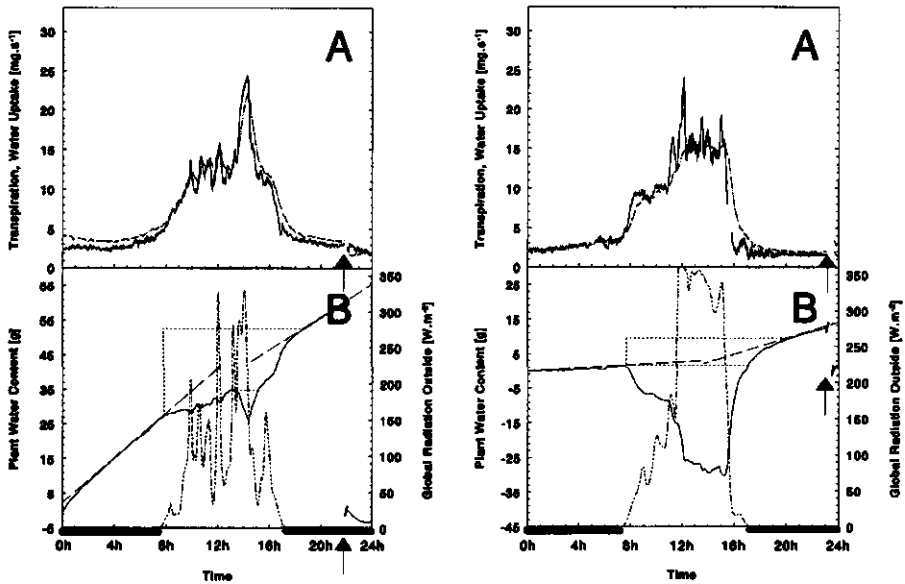


Figure 3.4.4: As in Figure 3.4.2 except that the changes in the root environment were made in dark at 2200 hours. The dotted curves during the light period (B) represent the theoretical limitations of the WC^p curve corrected for variations due to reversible changes in WC^p .

Figure 3.4.5: As in Figure 3.4.4 except that the changes in the root environment were from -0.36 to -0.01 MPa and were made in dark at 2200 hours. The dotted curves during the light period (B) represent the theoretical limitations of the WC^p curve corrected for variations due to reversible changes in WC^p .

The characteristics of the courses presented were representative of all repetitions. Courses of repetitions during the light periods were not exactly similar, since they were conducted over time and thus under different environmental circumstances (global radiation).

Generally, E was closely related to global radiation (Figure 3.4.2 to Figure 3.4.5). U followed E with a time delay of about half an hour, as is clearly visible in the peaks in global radiation (i.e. Figure 3.4.3 and Figure 3.4.4). On average, U was a little higher than E. As a result WC^p increased in time. During the light period, fluctuations in WC^p were measured in this course of increasing WC^p , which were related to the courses of global radiation and E.

Analysis of the WC^p -curves

During long periods in the dark, WC^p increased at a constant rate (Figure 3.4.2B - Figure 3.4.5B). Assuming that re- and dehydration processes of tissues in the

plant were completed at that time, the change in WC^P was attributed to irreversible growth. Growth rates during these dark periods were calculated from the slope of a first order fit on the WC^P -curves during these periods.

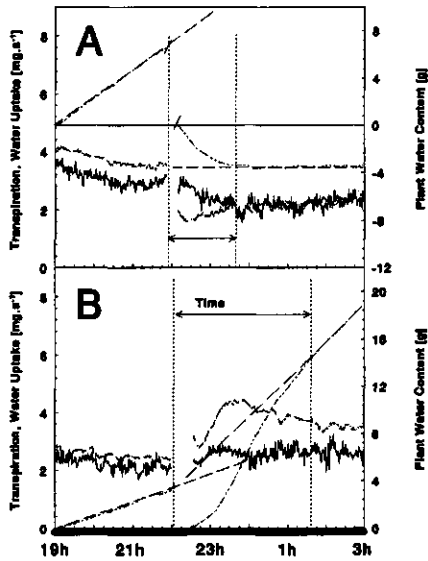


Figure 3.4.6: More detailed views of the courses of water uptake (---) and transpiration (—) and plant water content (WC^P) (---) during the changes in the root environment in the dark alterations when ψ_n^{rc} was changed from -0.01 to -0.36 MPa in the dark (Figure 3.4.6A) and when ψ_n^{rc} was changed from -0.36 to -0.01 MPa in the dark (Figure 3.4.6B). The courses of WC^P were reset to zero after the change in ψ_n^{rc} . The dashed lines are the regression lines on the WC^P -curve, which were used to calculate the growth rate of the plant before and after the ψ_n^{rc} -change.

With an unbroken WC^P -curve during the light period (Figure 3.4.4 and Figure 3.4.5; experiment 2), average growth rate in light could be derived from the WC^P curves. The relative water content of the plant before and after the light period may be assumed equal, due to similar environmental conditions, ψ_n^{rc} and E. Therefore, changes in WC^P due to alterations in plant water deficits were on average zero over the light period, and the total increase in WC^P in light could be attributed to growth. Average growth rate during the light period was calculated as the increase in WC^P over the period between 7h and 19h divided by time.

In contrary to the estimated growth rate during dark periods, the average growth rate during the light was not similar to the actual growth rate: Actual growth rate may have changed due to temporary changes in plant water deficit or other environmental factors (e.g. T_{air}).

Changes in ψ_n^{rc} conducted in light (experiment 1)

Plant growth rate during the dark was considerably lower when ψ_n^{rc} was -0.36 MPa than when ψ_n^{rc} was -0.01 MPa (Regression lines Figure 3.4.2 and Figure 3.4.3; Table 3.4.3). With all plants, transpiration rate in the dark was lower when ψ_n^{rc} was -0.36 than when ψ_n^{rc} was -0.01 MPa. However, averaged over all repetitions this difference was not statistically significant (Table 3.4.3). Expressing transpiration rate per m^2 leaf area increased the difference between the ψ_n^{rc} -treatments slightly, but it remained statistically non-significant (results not shown). T_{air} and RH were roughly similar on

the subsequent nights when measurements were made (results not shown). It is possible however, that the temperature of the heating pipes and the distance between the plant and pipes differed between repetitions. This may have caused transpiration differences by influencing the energy balance of the leaves, without changing the surrounding climate.

Table 3.4.3: Effects of a daily alternating osmotic potential in the root environment (ψ_n^{rc}) on the growth rate (dWC^p/dt) and transpiration rate (E) of a tomato plant^a in dark^b. The change in ψ_n^{rc} was conducted in light at 10 h (experiment 1).

ψ_n^{rc}	dWC^p/dt	E
[MPa]	[mg.s ⁻¹]	[mg.s ⁻¹]
-0.01	0.61 ± 0.027	1.63 ± 0.320
-0.36	0.21 ± 0.017	1.26 ± 0.144

Means ± standard errors, determined on four plants; ^aPlant characteristics see Table 3.4.1; ^b dWC^p/dt was calculated as the slope of the linear regression on the WC^p -curve in dark (between 20h - 5h; $R^2 > 0.99$).

Immediately after the change in ψ_n^{rc} from -0.01 to -0.36 MPa in light, E rose appreciably more than U (Inset Figure 3.4.2). As a consequence WC^p decreased considerably. Immediately after the change in ψ_n^{rc} from -0.36 to -0.01 MPa in light, the opposite responses of U and WC^p were measured (Inset Figure 3.4.3): ψ_n^{rc} influenced WC^p by a clear effect on U .

Changes in ψ_n^{rc} conducted in dark (experiment 2).

E during the dark was influenced by ψ_n^{rc} -level (Table 3.4.4), however the differences were statistically non-significant. When transpiration rates of a single plant before and after a ψ_n^{rc} -change in the dark were compared, a small, but consequent effect was found: E decreased after a decline in ψ_n^{rc} from -0.01 to -0.36 MPa (Figure 3.4.6A) and increased after a raise in ψ_n^{rc} from -0.36 to -0.01 MPa (Figure 3.4.6B).

Plant growth rate differed clearly between the ψ_n^{rc} -levels (Table 3.4.5). After a change in ψ_n^{rc} from -0.01 to -0.36 MPa (Figure 3.4.6A) growth rate ceased almost

Table 3.4.4: Effects of a daily alternating osmotic potential in the root environment (ψ_n^{rc}) on the transpiration rate (E) of a tomato plant^a in dark. The change in ψ_n^{rc} was conducted at 22 h in dark (experiment 2). E was calculated during the dark period after the change in ψ_n^{rc} (2 h-5 h) and during the dark period before the next change in ψ_n^{rc} (19 h - 22 h).

ψ_n^{rc}	E [mg.s ⁻¹]	
	dark (2 h - 5 h)	dark (19 h - 22 h)
[MPa]		
-0.01	2.36 ± 0.313	2.17 ± 0.333
-0.36	1.67 ± 0.251	1.87 ± 0.333

Means ± standard errors, determined on four plants; ^aplant characteristics: see Table 3.4.1.

completely, while it increased by a factor three after the opposite ψ_x^{re} -change (Figure 3.4.6B). During the light period following the ψ_x^{re} -change from -0.36 to -0.01 MPa, growth rate decreased, resulting in a lower growth rate during the dark period before the next ψ_x^{re} -change (Figure 3.4.4B and Table 3.4.5). The opposite was measured at -0.36 MPa: after the light period following the change in ψ_x^{re} from -0.01 to -0.36 MPa, growth rate in dark was partially recovered (Figure 3.4.5B and Table 3.4.5).

The transient responses of U and WC^p after a change in ψ_x^{re} in dark differed between changes from -0.01 to -0.36 MPa (Figure 3.4.6A) and opposite (Figure

Table 3.4.5: Effects of a daily alternating osmotic potential in the root environment (ψ_x^{re}) on the growth rate (dWC^p/dt) of a tomato plant^a in dark and light^b. The change in ψ_x^{re} was conducted in dark at 22 h (experiment 2).

ψ_x^{re} [MPa]	dWC^p/dt [$mg \cdot s^{-1}$]		
	dark (2 h - 5 h)	light (5 h - 19 h)	dark (19 h - 22 h)
-0.01	1.06 ± 0.148	0.65 ± 0.009	0.69 ± 0.005
-0.36	0.08 ± 0.026	0.06 ± 0.019	0.36 ± 0.015

Means ± standard errors, determined on four plants; ^aplant characteristics: see Table 3.4.1. ^bThe dark period has been separated into a period after (2 h - 5 h) and a period before the next change in ψ_x^{re} (19 h - 22 h); In dark dWC^p/dt was calculated as the slope of the linear regression on the WC^p -curve. dWC^p/dt during the light was calculated as the difference between WC^p at 5 h and at 19 h, divided by the length of time period (14 hours).

3.4.6B): A relative short transient time (time until the course of WC^p became linear again) of about 1.5 h was found after the change from high to low ψ_x^{re} , due to an almost immediate decrease in U, followed by a slow partial recovering of U together with a slow decrease in E (Figure 3.4.6A). The transient time after the opposite change in ψ_x^{re} was much longer: about 3.5 h. After this change in ψ_x^{re} , U did not change immediately to a new value, but recovered slowly to a relatively high value during about 1 h, followed by a slower decrease during a period of about 2.5h (Figure 3.4.6B). These different responses were clearly visible during all repetitions.

Assuming that the transient courses of WC^p after a change in ψ_x^{re} in the dark are partially due to growth and partially due to changes in plant water deficit, the change in plant water deficit was estimated using the following procedure: The linear regression line on the WC^p curve after the change in ψ_x^{re} was extrapolated back to the time the change in ψ_x^{re} was imposed, and the difference between this line and the measured WC^p was estimated as the change in plant water deficit. The changes in plant water deficit, calculated in this way, were small (about 4 g at both changes in ψ_x^{re}), which was less than 1% of the total plant water content.

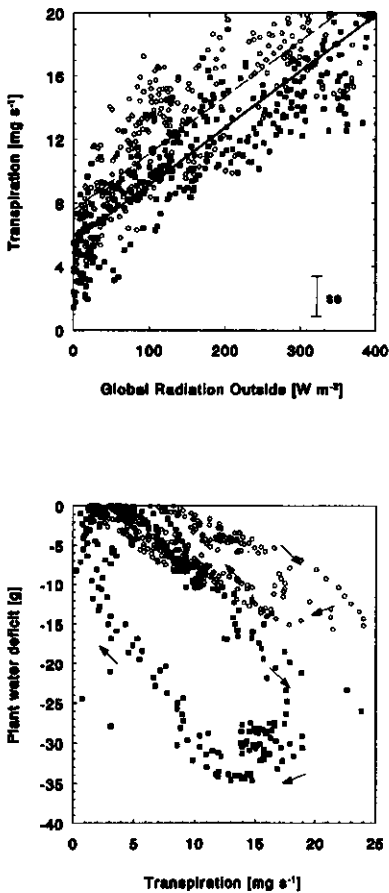


Figure 3.4.7: (A) The relation between global radiation outside the greenhouse and measured transpiration at two levels of osmotic potential in the root environment. $\psi_{\pi}^{\text{rc}} = -0.01$ MPa (O) and -0.36 MPa (■). (B) The relation between measured transpiration and estimated plant water deficits (relative to the night plant water deficits) at two levels of osmotic potential in the root environment (·). The arrows indicate the sequence of measurements over a day. $\psi_{\pi}^{\text{rc}} = -0.01$ MPa (O) and -0.36 MPa (■).

than at high ψ_{π}^{rc} . Hysteresis on this relation was found within a day. The hysteresis effect was more pronounced at low than at high ψ_{π}^{rc} .

In order to estimate plant water deficits during the light period an similar procedure was conducted: The course of WC^p due to growth was estimated, and the difference between this course and the measured course of WC^p was used as an estimate of plant water deficit. When ψ_{π}^{rc} was low (-0.36 MPa) during the light (e.g. Figure 3.4.5), this was not difficult, since growth rate during the light was about zero and consequently measured dWC^p/dt could be attributed as a whole to changes in plant water deficit. However, when ψ_{π}^{rc} was high (-0.01 MPa) during the light, growth during the light was substantial (e.g. Figure 3.4.4) and could have changed considerably during the light. To estimate plant water deficits at high ψ_{π}^{rc} during the light, a growth curve was assumed for the light period. Within the constraint of growth rate \geq zero, all growth curves between the dotted borders (Figure 3.4.4) are possible. However, not all curves are likely. For a rough estimation of plant water deficits during the light, the growth curve representing a constant growth rate during the light was chosen.

Plant water deficits (relative to the night value), plotted against measured E (Figure 3.4.7B), were clearly effected by ψ_{π}^{rc} . At low ψ_{π}^{rc} , plant water deficit increased more with increasing E

To find out if there was any effect of ψ_{π}^{rc} on E during the light period, measured E was plotted against global radiation at both ψ_{π}^{rc} -levels (data of experiment 2; Figure 3.4.7A). E at high ψ_{π}^{rc} tended to be somewhat higher than E at low ψ_{π}^{rc} . However, the differences obtained were not significant.

Discussion

Method for measuring E and U

The idea to use simultaneous E and U measurements for research in plant water relations was not new. Several researchers presented dynamic courses of E and U to show delayed responses between E and U upon changes in environmental conditions (e.g. Slayter, 1967; Aston and Lawlor, 1979). However, most of these measurements were not accurate enough to combine them in a closed water balance for a plant, as is possible with E and U measurements obtained by the system of van Ieperen and Madery (1994). The strength of this method is the combination of its simplicity, its high accuracy and high resolution in time, and its insensitivity to environmental conditions. These qualities make it very applicable for research in greenhouses with relative fast changing environmental conditions. To be used for calculation of dWC^p/dt , E and U have to be measured very accurately, because usually a relative high percentage (often > 90%) of the water taken up by the plant is used for transpiration (Boyer, 1985). This results in almost equal values for E and U, while the small difference between E and U determines dWC^p/dt (Eq. 3.4.1). Consequently small errors in the determination of E and U could lead to large errors on the course of WC^p . The test measurements conducted on the system without and with a plant showed that the system worked quite well under greenhouse conditions and that the accuracy of the measurements was high. E and U being equal during the whole test period without a plant, showed that the calculation of U was correct, at least for the removal of the first 600 g of nutrient solution from both vessels, that the climate in the greenhouse did not influence the weight measurements, and that both vessels were constant in diameter. The total removal of nutrient solutions from the vessels was during all experiments lower than 600 ml per vessel. The test measurements on plants showed that fresh weight accumulation over 24 h was measured correctly. This means that there was no systematic error in the calculation of U from the weight measurements on balance 2. Tests concerning the resolution in time are described and conducted before by van Ieperen and Madery (1994) and showed that E and U could be well measured within 40 seconds using present configuration of vessels and connecting tube.

Interpreting the course of WC^p in terms of irreversible growth and reversible changes in plant water deficit, as is presented in this paper, is basically similar to the interpretation of elongation measurements on single cells (e.g. Zhu and Boyer, 1992),

leaves (e.g. Cramer and Bowman, 1991) and roots (Frensch and Hsiao, 1994) using LVDT's (Linear Variable Displacement Transducers). However, instead of these one dimensional elongation measurements at fixed places on the plant, in current method the whole water content of the plant is subject to the measurements. This implies on the one hand, that based upon results obtained using present method conclusions can be drawn concerning whole plant responses to changes in environmental conditions, but on the other hand, that different responses of individual organs and tissues in time or position on the plant are averaged over the whole plant. While present method is very well suited for research on dynamic responses of a whole plant to changes in environmental conditions, it is less useful for dedicated research on for instance the relation between turgor and growth, because the latter is position and tissue specific.

The course of WC^p being linear during large parts of the dark has been interpreted as irreversible growth of the plant being sustained at undiminished rates during the whole dark period (up to 9 h, experiment 1). This linearity implies that assimilate supply did not limit plant growth rate on the short-term. This was in agreement with the findings of Pearce *et al.* (1993a) on tomato fruits, and of Christ (1978) on wheat leaves. Pearce *et al.*, (1993a) reported that the mean fruit growth rate during the night only decreased when the daily radiation integral became below $6 \text{ MJ m}^{-2} \text{ d}^{-1}$. During most of our experiments the daily radiation integral was below this value (Table 3.4.2). Nevertheless, in most cases plant growth rate remained constant during the whole dark period, showing that in our experiments enough assimilates were produced during the light to maintain stable growth during the night. Probably, the relative low night temperature in present experiments (Table 3.4.2) caused relative low plant growth rates by influencing metabolic activity, resulting in an associated lower depletion rate of assimilates. One exception was found during experiment 1: After a day with a radiation integral of $1.8 \text{ MJ m}^{-2} \text{ d}^{-1}$ (lowest measured) the course of WC^p started to deviate from linearity at the end of the dark period (Figure 3.4.3B), which could have been due to shortage of assimilates limiting growth. Prolonged WC^p measurements during several days at low irradiance after a period of high irradiance, showed a time delay of more than 24 h before plant growth rate started to lower (unpublished data). These results suggest that in present experiments other factors than assimilate supply limited plant growth. Temperature might have been such a factor, since it is well known that growth is a temperature dependent process due to its dependence on metabolic activity. However, in present experiments temperature was not a variable. Although it differed between day and night, temperature regime was similar in all ψ_x^e -treatments. Another important factor establishing growth rates is the plant water status.

ψ_x^e clearly influenced plant growth rate in the dark (Table 3.4.3 and Table 3.4.5). The immediate inhibition of growth after a change in ψ_x^e from -0.01 to -0.36 MPa in dark

(Figure 3.4.6A) suggests a role for plant water status. To maintain the about similar transpiration rates before and after the alterations in ψ_n^{rc} in dark (Figure 3.4.6), the flow of water and water potential gradients between root environment and leaves must have been about similar before and after the change ψ_n^{rc} . This means that the water potential in the xylem must have decreased by about 0.35 MPa after changing ψ_n^{rc} from -0.01 to -0.36 MPa. To establish growth (such as before the change in ψ_n^{rc}), the water potential in the expanding cells must have been lower than in the adjacent xylem. This gradient in water potential is called the growth-induced water potential (Nonami and Boyer, 1993). The existence of such a water potential gradient associated with growth has been demonstrated recently by measuring single cell water potentials in a growing soybean stem (Nonami and Boyer, 1993). Determination of these growth-induced water potentials in leaves and stems of tomato plants, showed that the magnitude was small: water potential was lowered by only 0-0.25 MPa, being positively related to the relative growth rates (Okatani, *et al.*, 1995). A sudden decrease of the water potential in the xylem of the plant of -0.35 MPa exceeds this growth induced water potential. As a result water flow from the xylem to the growing cells ceases, and growth rate became about zero. After the following light period, growth was partially recovered (Table 3.4.5). This might have been due to osmoregulation: the active accumulation of solutes in cells to decrease their osmotic potentials, thus restoring the water potential gradient and related water flow between xylem and cells (e.g. Morgan, 1984; Bernstein, 1963). When in the next dark period ψ_n^{rc} was changed back to -0.01 MPa, a large increase in growth rate was measured (Table 3.4.5): growth rate being considerably larger than measured at the same ψ_n^{rc} -level before the first change in ψ_n^{rc} (-0.01 to -0.36 MPa; Table 3.4.5). This could have been due to effect of the extra solutes in the cells. After the following light period growth rate was lowered to a much lower value again.

The non-linearities in the WC^p -curves were interpreted as alterations in plant water deficit, related to the reversible elastic properties of cell walls all over the plant (Cosgrove, 1993). These non-linearities were clearly apparent in relation to the fluctuations in global radiation during the light (e.g. Figure 3.4.4), and at the beginning of all dark periods as a general recovering from plant water deficits which had developed during the day (Figure 3.4.2B-Figure 3.4.5B). Other reasons for non-linearity's on the course of WC^p were the changes in ψ_n^{rc} conducted in light and in dark. Especially the ψ_n^{rc} -alterations in dark showed clear responses on the course of WC^p (Figure 3.4.6). According to the definition of growth rate used (being ≥ 0), the decrease in WC^p after the change in ψ_n^{rc} from -0.01 to -0.36 MPa (Figure 3.4.6A) could undoubtedly be attributed to an increase in plant water deficit. This decrease was small: about 4 g (Figure 3.4.6A). The total decrease was probably somewhat larger since the first 15 min after the change in ψ_n^{rc} the measurements were halted. Assuming the extreme case

of E being constant at 3.5 mg s^{-1} and U being zero during these 15 min, the decrease in WC^P would increase by another 3-4 g. The total decrease in plant water deficit after a change in ψ_{π}^e from -0.01 to -0.36 MPa was between 4 and 8 g. The total water content of the plant involved was about 1350 g (Table 3.4.3). This means that the relative water content of the plant was lowered by only 0.3 to 0.6%. Nevertheless plant expansion growth was inhibited completely. The measured change in relative water content is quite reliable: similar changes in plant water deficit were measured during all repetitions, and the opposite changes in ψ_{π}^e showed comparable small changes in plant water deficit (Figure 3.4.6B), assuming a growth rate during the transient phase which was between the growth rates before and after the change in ψ_{π}^e .

The main cause for the delay between E and U was the hydraulic capacitance effect of tissues adjacent to xylem upon changes in xylem water potential (Nobel, 1983): Changes in E induce water potential alterations in the xylem of the plant. As a result tissues around the xylem start to exchange water with the xylem to obtain a new water potential equilibrium with the xylem. For instance: when E lowers, water potentials in the xylem increase and water flows from the xylem to the tissues. This causes an extra source for water, increasing U relative to E . As a result U decreases at a lower rate than E , which is measured as a delay. This delay between E and U caused the fluctuating component on the course of WC^P during the light period.

In present experiments we tried to quantify the changes in plant water deficit during the light by estimating a course of WC^P corrected for changes in plant water deficit (the growth course), and calculating the difference between this growth course and the actual measured course of WC^P . It may be clear that the accuracy of calculated plant water deficit depends to a large extent on the accuracy of the estimated growth course. While expansion growth during the dark was rather easily estimated, expansion growth during the day was complex, and not easily deduced from the course of WC^P : during the day. T_{air} was higher (Table 3.4.2) and more variable (not shown), and plant water deficits fluctuated upon the course of radiation, while both probably influenced expansion growth. The total growth over a light period is known, assuming plant water deficit in the dark periods before and after the light period similar. This, in combination with the restriction of growth rate being \geq zero caused the error on the estimated growth course and associated plant water deficits to be low at low ψ_{π}^e . At high ψ_{π}^e on the other hand, the error on estimated plant water deficits might have been significant.

Effects of ψ_{π}^e on E

The rate of plant transpiration (E) in a greenhouse environment depends upon several factors of which global radiation is the most important one, as it provides the energy necessary for transpiration. E increased about linear with global radiation at both ψ_{π}^e -levels (Figure 3.4.7A). E was somewhat higher at low ψ_{π}^e , although the differ-

ence was not significant. Several saturation type functions were tried to fit on the measured data, but best fits were found to be linear, although especially at low E, the relation differed from linearity. This was probably due to light induced changes in stomatal conductance between 0 and 100 W m⁻² (Behboudian, 1977; Hicklenton and Jolliffe, 1980). At high global radiation the relation with E is complex due to interactions between plants and greenhouse climate: changes in crop transpiration may significantly change greenhouse climate (RH) and leaf temperature, thus changing the driving force for transpiration being the vapour pressure deficit between stomatal cavities and greenhouse air (Burrows and Milthorpe, 1976; Jarvis and McNaughton, 1986). The reducing effect of stomatal closure on E may have been counterbalanced by an increased leaf temperature and by a decreased vapour pressure in the air both due to reduced transpiration. Therefore, it is possible that the effect of ψ_n^{re} on stomatal conductance was significant, although this was not measured on E. However, since no measurements were conducted on leaf temperature nor on stomatal conductance this could not be concluded from present experiments.

E measured in dark was consequently lower at high ψ_n^{re} as compared to at low ψ_n^{re} (Table 3.4.3 and Table 3.4.4). However, the obtained differences were marginal, and in most cases not significantly different.

Non-linear relations between E and plant water deficits (Figure 3.4.7B) have often been explained by changing hydraulic conductance's for water transport through the plant. A change in hydraulic resistance due to ψ_n^{re} could explain the difference in slopes between the relationships at low and high ψ_n^{re} , but it can not explain the hysteresis effect over a day. No hysteresis was measured on the relations between global radiation and transpiration (Figure 3.4.7A).

The hysteresis could have been the result of de- and re-hydration processes developing slowly over a day, thus indicating high time constants. However, based on the small delay times between E and U after sudden radiation changes (Figure 3.4.2A-Figure 3.4.5A), which are also due to re- and dehydration processes (Nobel, 1983), this seems not very likely, unless different tissues are involved with different time constants for changes in water content. Changes in stem and leaf thickness measured on herbaceous plants are normally closely related to E and consequently have low time constants (Nobel, 1983; Plodowska *et al.*, 1989). It is possible that the fruits, of which is known that the xylem connection with the stem is poor (Lee, 1989), change their relative water content with these high time constants. However, interaction with phloem water transport which is very important to fruit growth may not be neglected.

Another explanation for the hysteresis effect over a day might have been a slowly changing solute concentration in the cortex of the roots, changing the availability of water to the plant over a day. Due to a disproportion between solute and water

uptake over the endodermis in the roots, the solute concentration at the outside of the endodermis may rise, the concentration largely being dependent upon the water flow rate through the roots and the solute concentration in the root medium. This might have caused the different slopes in Figure 3.4.7B at low and high ψ_n^e . However to cause the hysteresis effect, the course of solute concentration in the root cortex must have been delayed after the course of E, which seems unlikely since the solute concentration at endodermis level depends, besides on mass flow with the water uptake and solute uptake by the plant, also on diffusion of solutes between cortex and root medium. The latter is a relative rapid process due to a small diffusion distance and a high diffusion coefficient (Newman, 1971) and will therefore not allow a significant delay time between the course of E and the course of solute concentration in the cortex.

The courses of water uptake after changes in ψ_n^e in dark (Figure 3.4.6) may also point to changing solute concentrations in the root cortex. U after a change from a high to a low solute concentration (-0.36 to -0.01 MPa) did not increase immediately (Figure 3.4.6B), in contrary to the direct decrease after the opposite change in ψ_n^e (Figure 3.4.6A). It is possible that immediately after this change in ψ_n^e the solute concentration in the cortex was not changed, since the roots were not rinsed with the new solution. Due to the uptake of solutes over the endodermis, and to the diffusion back to the nutrient solution, the solute concentration in the cortex slowly lowers and consequently water uptake increases as a result of a more favourable osmotic potential gradient across the endodermis. The slow decrease in U, which follows the initial increase, might have been due to dilution of the xylem sap, since solute uptake ceases and solutes are transferred to the shoot. Another reason for the secondary decrease in U might have been re-hydration processes in the plant getting completed.

From the present results it can be concluded that the method for simultaneous E and U measurements is a valuable addition to methods for research on short-term plant-water-relations in response to variations in the greenhouse climate and root environment. It was shown that although the effect of ψ_n^e on E was low (at moderate radiation levels), expansion growth was influenced considerably, and that adaptation to a ψ_n^e -level occurs during the light period.

3.5 Summary and conclusions

The new method to measure the rates of transpiration and water uptake simultaneously on one plant with a high resolution in time (Chapter 3.2) is used as a tool to investigate relationships between environment, water status of the plant, short-term expansion growth and transpiration. Measured diurnal courses of transpiration and water uptake were used to calculate transients of plant water content (WC^P). These transients were discussed in terms of expansion growth and alterations in plant water deficit. The effect of changes in salinity on the observed transients of whole plant water content were comparable with the effect of salinity on elongation transients of single cells (Zhu and Boyer, 1992) and leaves and roots (e.g. Frensch and Hsiao, 1994; Serpe and Matthews, 1992).

In this thesis the term "plant water content" is further used for the obtained property calculated from simultaneously measured water uptake and transpiration. It would have been more precise to call it "water content of the shoot". However, this small misconception is not very important because variations in root volume are expected to be negligible compared to variations in shoot water content.

According to the growth-chamber experiments (Chapter 3.3), the rate of transpiration depends highly on the salinity level in the root environment. Measurements in the greenhouse (Chapter 3.4), however, demonstrated that the effect of the salinity level on transpiration rate was at the most small. Probably, the differences in climate conditions (global radiation, T_{air} , RH and windspeed) between growth-chamber and greenhouse caused these different responses. It is possible that the effect of salinity on stomatal conductance was more pronounced than the observed effect on transpiration rate, because thermal (and hydraulic) feed-back mechanisms exist in a greenhouse. For the time being it is plausible to conclude that changes in salinity in the range 0-10 mS cm^{-1} do not significantly influence plant transpiration in a greenhouse on the short-term.

Measurements in the growth-chamber and greenhouse (Chapter 3.3 and 3.4) demonstrated that expansion growth was influenced significantly by the salinity level in the root environment, and that expansion growth altered almost immediately upon a change in salinity in light (Chapter 3.4; Figure 3.4.2 and 3.4.3) and in dark (Chapter 3.4.4; Figure 3.4.5). In the greenhouse experiments a clear bipartite response was measured after a change in salinity in dark: a firm initial response appeared almost immediately after a change in salinity level, followed by a partial reversed response after 12-24 h. After a change in salinity in light the initial response was less firm: adaptation to the new salinity level appeared already during the same light period.

In the growth-chamber and greenhouse experiments alterations in plant water deficit, induced by the climate (transpiration), were more pronounced at high salinity (± 35 g water loss at high (15 mg s^{-1}) transpiration) than at low salinity (± 15 g water loss at high transpiration). Changes in plant water deficit caused by a change in salinity in dark on the other hand, were relatively small: approximately 8 g (-0.01 and -0.36 MPa) on a total plant weight of ± 1200 g. Thus, plant water deficit at low salinity during the light exceeded the water deficit in the plant caused by a change in salinity from low to high salinity. Even so, plant growth rate during the dark was completely ceased after a change from low to high salinity, while at low salinity and a substantial larger plant water deficit during most of the light, average plant growth rate was much larger. No clear quantitative relationships were found between changes in plant water deficit and changes in transpiration and expansion growth.

Short-term control of the EC may very well be used to influence expansion growth on the short-term. Only partial adaptation to the EC level occurs after several hours, probably mediated by metabolic activity. Short-term control of the EC to influence plant transpiration in a greenhouse is not effective, although its effect on stomatal opening is .

4. Long-term effects of different day and night EC on growth and yield of tomato.

In previous chapter it was clearly shown that changes in EC almost immediately influenced the rate of water uptake, the development of water deficits and expansion growth in the tomato plant. Previous experiments lasted only a few days and were done on single plants. Especially in the greenhouse experiments clear responses were measured on single plants. However, it remains uncertain whether the short-term positive effects sustain on the long-term when a whole canopy is involved. It is also uncertain whether the short-term effect on expansion growth leads to a positive effect on the yield and the quality of the produced tomatoes.

In this chapter long-term effects of different day- and night salinity treatments were investigated on a greenhouse grown tomato crop. It was investigated whether already reported positive effects of fluctuating salinity on the growth of young tomato plants (Bruggink *et al.*, 1987) were maintained during the production phase. Effects of fluctuating salinity on dry matter production, dry matter distribution, plant growth and yield as well as some aspects of fruit quality were investigated.

4.1 Effects of different day and night salinity levels on vegetative growth, yield and quality of tomato.

W.VAN IEPEREN, 1996. *Effects of different day and night salinity levels on vegetative growth, yield and quality of tomato. Journal of Horticultural Science* 75: 99-111.

Abstract

Tomato plants were grown in nutrient film technique at constant, and different day and night salinity levels to investigate whether salinity could be used to control vegetative growth, fruit yield and quality (size, dry-matter percentage, and incidence of blossom-end rot (BER)). Greenhouse experiments were conducted with the following salinity treatments: 5/5, 9/9, 1/9 and 9/1 (day/night salinity levels in mS.cm^{-1}). The salinity treatments influenced fruit yield clearly: Yield was increased greatly at 1/9. It was decreased at 9/1, although not as much as at 9/9. Yield differences were mainly due to differences in average fruit size, except at 9/9, where after 12 weeks of harvesting the number of harvested fruits was decreased too. Considering the number of unripe fruits on the plants, in near future a lower the number of harvested fruits was expected at 9/1, and a slightly higher number at 1/9 as compared with 5/5. These differences in the numbers of harvested fruits were partially due to differences in plant development, and partially to differences in fruit setting and fruit abortion between the EC-treatments. Before the fruit harvesting phase was reached, vegetative growth of young tomato plants was decreased at 9/9, and at lower extent also at 9/1 as compared with 5/5. It was not altered by the 1/9 treatment. Similar results were found for leaf area. Plant development and dry-matter distribution in the young plants were not influenced. After 12 weeks of fruit harvesting, comparable responses of the salinity treatments were observed on vegetative growth and leaf area. The number of trusses was slightly decreased at 9/9 and 9/1, and within the vegetative plant parts dry-matter distribution towards the roots increased to the disadvantage of the leaves. Dry-matter distribution towards the fruits was increased at 1/9 and decreased at 9/9 as compared with 5/5.

Fruit quality was influenced considerably by the salinity treatments: Dry-matter percentage of the harvested fruits was higher at 9/9 and slightly lower at 1/9 as compared with 5/5, whereas at 9/1 it was intermediate between 5/5 and 9/9. Differences in yield were not only due to differences in fruit water content: dry weight per fruit was also changed. These changes were comparable to changes in fresh weight yield, but less pronounced. The incidence of BER was influenced greatly by the salinity treatments: it was almost absent at 1/9, while it was increased at 9/1 and 9/9 as compared with 5/5.

Introduction

Nutrient solutions used for growing tomato plants commercially in nutrient film culture (NFT) or in artificial substrates, usually have a constant salinity level in the range 30-75 mM total ion concentration (equivalent to 0.07-0.18 MPa osmotic pressure (π), and to 2-5 mS.cm⁻¹ electric conductivity (EC)). This salinity range resulted from empirically determined long-term optima for the concentrations of all nutrients in the solution. Lower concentrations restrict plant growth due to nutrition being the limiting factor for growth or, in extreme cases, due to deficiency effects (Winsor and Adams, 1987). Higher ion concentrations may reduce plant growth due to osmotic effects (Ho and Adams, 1989): A high osmotic pressure in the root environment lowers the availability of water to the roots. In combination with a high transpiration rate, high osmotic pressure may lower water potentials in the plant. Low water potentials are correlated with low turgor, which is commonly associated with reduced cell expansion and thus reduced plant growth (Hsiao, 1973). A high π in the root environment may also cause growth reductions by stomata closure, induced by either low turgor in the leaves or by signals originating from the roots (Davies and Zhang, 1991). Stomata closure lowers plant growth rate by decreasing CO₂-assimilation rate and related dry-matter production.

A high salinity level decreases the growth and yield of tomato plants clearly (Bruggink *et al.*, 1987; Sánchez Conde and Azuara, 1979). It reduces the amount of dry-matter distributed towards the fruits (Ehret and Ho, 1986a), the size of the fruits (Adams and Ho, 1989; Ehret and Ho, 1986a) and improves the dry-matter content of the fruits (Massey *et al.*, 1984). High salinity increases the incidence of blossom-end rot (BER), a physiological disorder due to a local lack of calcium in the fruits (Ehret and Ho, 1986b): High salinity decreases the Ca²⁺-uptake by the roots, and Ca²⁺-transport via the xylem towards the fruits (Ho *et al.*, 1993).

A change in salinity level will not alter the nutrition status of the plant in the short-term to such an extent that it influences plant growth immediately. Water potentials, related cell expansion rates and transport processes, on the other hand, change almost immediately upon a change in π in the root environment (Munns, 1993). Several researchers realised that short-term control of salinity level in relation to the greenhouse climate could be used to improve plant growth, production and quality of tomato fruits. Bruggink *et al.* (1987) found a positive effect of a low salinity level (l) during the day combined with a high salinity level (h) during the night (l/h treatment) on the vegetative growth of young tomato plants. Ho and Adams (1989) investigated a reversed strategy (h/l treatment) to improve fruit quality. They tried to improve fruit dry-matter content by a high salinity during the day, arguing that it should be possible to overcome the negative effect of high salinity on Ca²⁺ uptake and transport through

the plant by applying a low salinity level during the night. However, they were still confronted with Ca^{2+} deficiency and a considerable yield loss, and concluded that applying fluctuating salinity levels would not be advantageous to commercial tomato production.

It is possible that the opposite salinity-treatment (l/h), used by Bruggink *et al.*, (1987) on young tomato plants, is also advantageous in the fruit producing phase. Low salinity during the day, when transpiration is relative high, probably improves the average plant water status and related growth rate by influencing dry-matter production and cell expansion rate. It could therefore also increase fruit expansion growth substantially. It probably has no negative effect on the incidence of BER: low salinity during the day enhances the Ca^{2+} -uptake by the roots (Ho, 1989) and, due to less negative water potentials in the stem xylem, Ca^{2+} -transport via the xylem towards the fruits. A negative effect of a l/h treatment on fruit dry-matter content, on the other hand, may also be expected. However, this negative effect is probably low, since it might be counterbalanced by enhanced dry-matter production during the day, and reduced cell expansion rates during the night.

The aim of the present work was to investigate whether short-term control of salinity level could be used to control fruit production and quality, and to what extent effects on plant growth, development and dry-matter partitioning during all growth phases add to differences in fruit yield and fruit quality. Experiments were conducted with plants with their fruit-producing phase in summer and autumn to investigate the importance of the climate conditions upon the effects of the salinity treatments.

Material and Methods

General

Seeds of tomato (*Lycopersicon esculentum* Mill. cv. Counter) were germinated in sand. The seedlings were transferred to a water culture system after they had reached a height of about 15 cm. The growing system, a 9×1.5×0.15 m (l×w×h) bench, was filled with circulating nutrient solution and covered by perforated polystyrene plates. It was placed in a compartment of the multispan Venlotype greenhouse at the department Horticulture of the Wageningen Agricultural University. The plants were mounted on polystyrene plates to allow the development of a root system, appropriate for plant growth in a NFT-system. They were maintained on this growing system until the first truss started to flower. Then, the plants were transferred to another compartment (12 × 12.8 m) of the greenhouse with a special NFT-system (described below). Plants were grown according to the high-wire system (Van de Vooren *et al.*, 1986). Each time the top of the plants reached the wire (2.4 m above plant base), the four

oldest leaves were removed and the plants were lowered. Flowers were pollinated three times a week with the aid of an 'electric bee', and axillary shoots were removed once a week. Temperature setpoint was 20°C (day and night), and relative humidity setpoint was 70%. Greenhouse climate was controlled by a commercial climate control computer system (DAKO, Hoogendoorn, 's Gravenzande, The Netherlands).

The first week after transplanting, the nutrient solution in the NFT-system had the same composition, pH and EC as the nutrient solution in the other water culture growing system: It contained (mol m⁻³): K⁺, 9.5; Ca²⁺, 3.6; Mg²⁺, 2.2; NH₄⁺, 1.4; NO₃³⁻, 15; PO₄³⁻, 1.4; SO₄²⁻, 4.1; Fe³⁺, 0.026; Mn²⁺, 0.006; Zn²⁺, 0.003; B⁻, 0.017; Cu²⁺, 0.0004; Mo⁺, 0.0003. pH was maintained between 6.0 and 6.5, and EC between 2.0 and 2.5 mS cm⁻¹.

The EC-treatments started one week after transplanting. Four EC-treatments were applied, two treatments with an equal EC during day and night: 5/5 mS cm⁻¹ and 9/9 mS cm⁻¹ (day/night), and two treatments with different day and night EC's, but an 24h average EC of 5 mS cm⁻¹ (1/9 mS cm⁻¹ and 9/1 mS cm⁻¹). A day or night period lasted 12h, and started at 0600 hours and 1800 hours, respectively. EC levels were changed by a proportional increase or decrease of the concentration of macro-elements in the nutrient solution.

NFT-system:

32 gullies (length 4 m, width 0.15 m, slope 1:50) were distributed in 16 rows of 2 gullies (tail to tail) over a greenhouse area of 9 x 12.8 m. Plants were grown at a density of 2.1 per m². The greenhouse was separated into four square blocks in which the four EC-treatments were distributed randomly (four replicates in a randomised block design). Consequently there were 16 plots; each plot consisted of two adjacent (length to length) gullies of 4 m with seven plants on each gully. The plants on the outside edges of the gullies served as guard plants. Depending upon the experiment, one or more plants from the other six plants were chosen randomly for measurements. Results within a plot were averaged.

Nutrient solution was supplied over the whole length of each gully by a perforated tube (diameter 1 cm). The tube was mounted 5 cm above the water level in the gullies, to ensure sufficient aeration of the nutrient solution near to the roots. The total rate of supply per gully was about 0.12 m³ h⁻¹. All gullies were covered with plastic foil, black coloured on the underside, white on the upperside. Nutrient solution was supplied to each plot separately from one of four two-vessel-systems (volume 0.35 m³ vessel⁻¹), a two-vessel-system for each EC-treatment. Depending upon the EC-treatment, the vessels were filled with nutrient solutions with equal, or different EC's. At the start of a day or night period, the supply of nutrient solution of all four systems was halted for 30 min to allow complete drain of the solution from the system. After

rinsing with the new solutions for about 20 min, all systems switched over to the other vessels. EC and pH were monitored in the return tubes, once per 15 min. The solutions were adjusted for EC and pH when they differed more than 0.5 mS cm^{-1} from the EC setpoint. Depending upon the water use of the crop, the solutions were renewed 1-4 times per week.

Experimental setup:

Four experiments were conducted over a period of about 2 years (Table 4.1). Experiment 1 investigated the effect of the EC-treatments on plant growth before the fruit harvesting phase was reached. Just before the first fruits were ripe enough to be picked, the experiment was ended and four plants per plot (two per gully) were measured destructively. Fresh and dry (ventilated oven for at least one week at 60°C) weights of leaves, stem, fruits and roots (after carefully drying with tissue paper) were determined. Leaf area was measured (LICOR 3100 area meter, Lincoln, USA), and the number of leaves ($>2 \text{ cm}$), trusses, and individual fruits were counted.

Table 4.1: Some basic information on the four greenhouse experiments: Sowing, transplanting, first harvesting and ending dates. Average outside daily global radiation (I_{global}) and average greenhouse air temperature (T_{air}) measured between planting date and the ending date of an experiment.

Experiment	Sowing date	Planting date	First harvesting	Ending date	I_{global} [MJ m ⁻² day ⁻¹]	T_{air} [°C]
1	29 Nov 1991	15 Jan 1992	-	11 Mar 1992	4.5	19.9
2	28 Feb 1992	15 Apr 1992	18 Jun 1992	21 Jul 1992	17.5	23.8
3	24 Jul 1992	7 Sep 1992	29 Oct 1992	4 Dec 1992	6.0	19.8
4	1 Dec 1992	22 Jan 1993	24 Mar 1993	18 Jun 1993	11.4	21.0

Experiment 2 started as experiment 1: Just before first fruit harvest, 2 plants per plot were measured destructively, and the same plant variables were determined as in experiment 1. Removed plants were replaced by spare ones. Experiment 2 was extended in the fruit producing phase. On two plants per plot, measurements concerning yield and quality aspects of harvested fruits were conducted during a five weeks harvesting period to investigate the effect of the EC-treatments on early production. Each harvest time (three times a week) the number and total fresh and dry weights of harvested fruits were determined per plant, as well as the number of harvested fruits with BER. At the end of experiment 2, two plants per plot were measured destructively, and the same plant variables as in experiment 1 were determined.

Experiment 3 was a repetition of a part of experiment 2, but carried out in the autumn. The number, fresh and dry weights of harvested fruits as well as the incidence of BER were determined during the first five weeks of harvesting. Three times a week, dates of flowering of individual flowers of the first seven trusses were measured.

Experiment 4 was a repetition of experiment 2. However, no destructive measurements on whole plants were conducted until the end of the experiment, and the harvesting phase was extended to 12 weeks. Dates of flowering of the first seven trusses were measured as in experiment 3. Yield and quality aspects of harvested fruits were determined. At the end of the experiment, two plants per plot were measured destructively, and the same plant parameters were measured as in experiment 1 and 2. In experiment 1 and 2 no fruit pruning was applied, in experiment 3 and 4 all trusses were pruned to seven flowers after the seventh flower started to flower. Analysis of variance was performed on the data reported.

Results

Effects of constant and fluctuating EC levels on yield

Tomato fruit production was clearly influenced by the salinity treatments and the time of the year (Table 4.2). After the first 5 weeks of fruit harvesting, yield was lower in autumn than in spring. This was due to a lower number of harvested fruits, as well as to smaller fruits in autumn (Table 4.2). The lower autumn production was correlated with a lower daily radiation integral (Table 4.1). Differences between salinity treatments were less pronounced in the autumn experiment than in the spring and summer experiments.

In spring, summer and autumn, a constant high EC-treatment (9/9) reduced yield compared with the other treatments with a lower 24h average EC (5/5, 1/9 and 9/1; Table 4.2). During the first 5 weeks of harvesting, this reduction in yield was due to reduced fruit size only. After 12 weeks of fruit harvesting, however, the number of harvested fruits per plant also declined (Table 4.2).

Applying fluctuating EC-treatments caused remarkable effects on yield in spring and summer, but not in autumn. In spring and summer, a low EC during the day (1/9) increased yield more than 20%. A high EC during the day, on the other hand (9/1), reduced yield by 14%. Similar tendencies, although for the greater part not statistically significant, were found for harvested dry weights per plant (results not shown). Yield differences between the 1/9, 9/1 and 5/5-treatments were mainly due to differences in fruit size, which was considerably higher at 1/9 than at 9/1, and intermediate at 5/5 (Table 4.2). The number of harvested fruits was not influenced by the fluctuating EC-treatments.

Table 4.2: Effects of constant and different day and night EC-levels on yield and quality aspects of harvested tomatoes. The results are from different experiments (see Table 4.1). Values are cumulative over the harvesting periods of given length (in weeks).

	Experiment Information			light/dark EC (mS cm ⁻¹)				Significance P
	No.	Season	Weeks	9/1	1/9	5/5	9/9	
Fresh weight yield [kg plant ⁻¹]	2	spring	5	2.76b	3.90c	3.19b	2.07a	0.01
	3	autumn	5	1.09b	1.15b	1.05b	0.85a	0.01
	4	spring/summer	12	4.65b	6.58c	5.40b	2.32a	0.01
Number of harvested fruits [plant ⁻¹]	2	spring	5	46.6	55.3	49.1	48.6	n.s.
	3	autumn	5	24.8	25.4	24.8	23.5	n.s.
	4	spring/summer	12	90.7b	93.1b	87.4b	79.2a	0.05
Average fresh weight per fruit [g fruit ⁻¹]	2	spring	5	57.7b	70.5c	65.0c	42.7a	0.02
	3	autumn	5	43.9b	45.2b	42.2b	36.2a	0.02
	4	spring/summer	12	53.5b	70.6c	62.6bc	31.9a	0.05
Dry-matter Percentage [%]	2	spring	5	6.6b	5.7a	6.0a	7.6c	0.01
	3	autumn	5	5.6b	5.1a	5.4ab	6.5c	0.05
	4	spring/summer	12	6.2b	5.2a	5.8b	9.0c	0.01
Percentage of fruits with BER [%]	2	spring	5	4.2b	0.6a	2.5b	25.1c	0.02
	3	autumn	5	3.7b	0.5a	2.2b	8.7c	0.02
	4	spring/summer	12	14.8c	0.4a	3.0b	55.6d	0.05

Means within a row that are followed by the same letter are not significantly different ($P=0.05$) according to Student's t-test.

¹ BER Blossom-end rot, analysed after logit transformation of the data.

Quality of harvested fruits

Dry-matter percentage, fruit size and the incidence of BER were clearly influenced by the EC treatments (Table 4.2). At the constant high EC-treatment the dry-matter percentage of the fruits was higher, and the average fruit size considerably lower than at the other EC-treatments. The incidence of BER was increased greatly by a constant high EC (up to 56% of the harvested fruits at 9/9 in the spring/summer experiment).

Applying fluctuating EC's influenced the dry-matter percentage of harvested fruits clearly in all experiments (Table 4.2): a low EC during the day decreased, and a high EC during the day increased the dry-matter percentage of the harvested fruits (1/9 and 9/1 versus 5/5). In autumn, the differences in dry-matter percentage were mainly due to differences in fruit fresh weight: the average dry weight per fruit (2.33 g) was not influenced by the EC-treatments in the autumn. In spring and summer, fruit dry-matter percentage was changed by alterations in both fruit fresh and fruit dry weight. Although in both spring/summer experiments fruit dry weight was higher at 1/9, and lower at 9/1 than at 5/5, the obtained differences were not statistically significant different (results not shown). Changes in fruit dry weight only partially counterbalanced the effect of changes in fruit fresh weight on dry-matter percentage.

The effect of fluctuating EC's on the incidence of BER was obvious: BER was almost absent at low EC during the day, and increased considerably at high EC during the day. This effect was measured in all seasons (Table 4.2).

In spring and summer, average dry weight per fruit was decreased at 9/9 compared with the other EC-treatments: In experiment 2: 3.23 versus 3.93 g fruit⁻¹, and in experiment 3: 2.84 versus 3.53 g fruit⁻¹. Such differences were not measured in the autumn experiment (2.33 versus 2.34 g fruit⁻¹). It is possible that the relative high incidence of BER at 9/9 reduced the dry-matter import per fruit by shortening the growing period of the individual fruits due to early ripening. To find out whether BER influenced the average dry weight per fruit, average dry weight per fruit was calculated separately for fruits with BER and for fruits without BER at the constant high EC-treatment (Table 4.3): Dry (and fresh) weight per fruit were lower in fruits with BER than in fruits without BER. However, the fruits without BER at 9/9 also showed a lower dry weight than the fruits at the other treatments (1/9, 9/1 and 5/5): Therefore, the lower dry weight per fruit at high EC was not exclusively an effect of the presence of BER.

Table 4.3: Effect of BER¹ on fresh and dry weights per fruit² at 9/9 mS cm⁻¹.

Experiment	Incidence of BER within a harvest	Fresh weight per fruit g fruit ⁻¹	Dry weight per fruit g fruit ⁻¹	N (fruits)	N (harvests)
2	no BER	46.1 ± 1.46	3.39 ± 0.087	388	79
2	100% BER	32.8 ± 4.50	2.54 ± 0.320	45	17
2	0-100% BER	39.4 ± 1.65	3.00 ± 0.117	395	68
4	no BER	35.1 ± 0.76	3.05 ± 0.055	246	101
4	100% BER	30.5 ± 0.54	2.73 ± 0.080	305	97
4	0-100% BER	30.7 ± 0.25	2.77 ± 0.045	716	134

Means and standard errors; ¹BER: Blossom-end rot; ²No weight measurements on individual fruits were available, because harvested fruits were pooled per plant. Each harvest time, the average fresh and dry weights per fruit (Table 4.2) were calculated from the ratio between harvested fresh or dry weight and number of harvested fruits per plant. The number of fruits with BER were counted per plant. To determine the effect of BER on fresh and dry weights per fruit, all harvests of the 9/9 treatment were assigned to one of the following three groups: A group in which none of the harvested fruits had BER (0%), a group in which all fruits had BER (100%), and a group of harvests with both types of fruits (0-100%). Average fresh and dry weight per fruit were calculated for each group. The number of harvests and fruits per group are given.

Effects of the EC treatments on growth and development of young plants

The salinity treatments influenced the growth of young tomato plants clearly (Table 4.4): Increasing the 24h average EC from 5 to 9 mS cm⁻¹ reduced plant fresh weight by 20-30%, plant dry weight by 15-20%, and leaf area by 20-30%. Growth reductions were found on vegetative and generative (unripe fruits) plant parts.

Applying fluctuating EC levels also affected the growth of young tomato plants (Table 4.4): The 9/1 treatment (high EC during the day) decreased plant fresh weight by 8-19%, plant dry weight by 9-13%, and leaf area by 17-21% compared with the 5/5 treatment.

Table 4.4: Effects of constant and different day and night EC-levels on the growth and development of tomato plants before the harvesting stage was reached.

Property	Experiment		light/dark EC (mS cm ⁻¹)				Significance P
	No.	Plant part	9/1	1/9	5/5	9/9	
Fresh Weight [kg plant ⁻¹]	1	veg. ¹ parts	0.65ab	0.86c	0.81bc	0.59a	0.01
	1	gen. ² parts	0.42a	0.52b	0.49ab	0.34a	0.05
	1	whole plant	1.07ab	1.38c	1.30bc	0.93a	0.05
	2	veg. Parts	1.27	1.32	1.34	1.13	n.s
	2	gen. Parts	0.53ab	0.71b	0.63b	0.41a	0.05
	2	whole plant	1.80ab	2.03b	1.97b	1.54a	0.03
Dry Weight [g plant ⁻¹]	1	veg. Parts	57a	73b	67ab	56a	0.01
	1	gen. Parts	32	36	33	30	n.s
	1	whole plant	89a	109c	100ac	86a	0.05
	2	veg. Parts	114ab	122b	123b	101a	0.04
	2	gen. Parts	39	49	45	35	n.s
	2	whole plant	153ab	171a	168a	136b	0.05
Dry-matter Percentage [%]	1	veg. Parts	8.76a	8.52a	8.26a	9.46b	0.01
	1	gen. Parts	7.61b	6.65a	6.72a	8.82c	0.02
	1	whole plant	8.41a	7.94a	7.81a	9.19b	0.02
	2	veg. Parts	9.03	9.28	9.26	9.00	n.s
	2	gen. Parts	7.37b	6.83a	7.18ab	8.53c	0.01
	2	whole plant	8.58a	8.43a	8.59a	8.88b	0.02
Leaf area [m ² plant ⁻¹]	1		1.09a	1.38b	1.34b	0.96a	0.03
	2		1.00a	1.22b	1.21b	0.97a	0.02

Means within a row that are followed by the same letter are not significantly different (P=0.05) according to Student's t-test.

¹ Vegetative plant parts; ² Generative plant parts.

The 1/9 treatment (low EC during the day) increased plant fresh and dry weights slightly, but did not affect leaf area. Generally, both vegetative and generative (unripe fruits on the plant) plant parts were affected. The dry-matter percentages (dry weight/fresh weight) of the vegetative plant parts did not differ between the 1/9, 9/1 and 5/5 treatments. The dry-matter percentage of the unripe fruits, on the other hand, was affected considerably: it was increased by a high EC during the day and decreased by a low EC during the day (Table 4.4). Cumulative proportional distribution of dry-matter in the young plants was not affected by the EC-treatments: about 30% of the dry-matter was distributed to the fruits, 42% to the leaves, 18% to the stem and 10% to the roots. The development rate of the young plants was not affected by the EC-treatments either: The numbers of leaves, trusses and fruits per plant did not differ

between the EC-treatments (results not shown). Average flowering dates of individual flowers of the first seven trusses were similar in all EC-treatments (results not shown).

Growth and development of the plants after a period of fruit harvesting

The effect of the EC-treatments on total plant growth increased with plant age, predominantly due to the effect on the generative plant parts (Table 4.5). Cumulative fresh and dry weights of the plants (including weights of picked leaves and harvested fruits) decreased in the following order: 1/9, 5/5, 9/1, and 9/9 mS cm⁻¹. Overall dry-matter percentage followed the same pattern (Table 4.5).

Table 4.5: Effects of constant and different day and night EC-levels on growth and development of tomato plants including harvested fruits and picked leaves. The presented results are cumulative values over whole growth periods of two experiments.

Property	Experiment		light/dark EC (mS cm ⁻¹)				Significance P
	No.	Plant part	9/1	1/9	5/5	9/9	
Fresh Weight [kg plant ⁻¹]	2	veg. ¹ parts	1.81	2.00	1.94	1.87	n.s
	2	gen. ² parts	3.97ab	5.09c	4.55bc	3.46a	0.02
	2	whole plant	5.97ab	7.09c	6.49bc	5.32a	0.02
	4	veg. Parts	1.68a	2.27c	2.11bc	1.87ab	0.03
	4	gen. Parts	5.13b	8.27d	6.57c	2.91a	0.04
	4	whole plant	6.81b	10.55d	8.68c	4.78a	0.05
Dry Weight [g plant ⁻¹]	2	veg. Parts	222	248	243	242	n.s
	2	gen. Parts	279	312	297	287	n.s
	2	whole plant	501	559	545	528	n.s
	4	veg. Parts	222a	269b	277b	259ab	0.04
	4	gen. Parts	327b	456c	414c	243a	0.04
	4	whole plant	548a	726c	691c	501b	0.05
Dry-matter Percentage [%]	2	veg. Parts	12.28	12.38	12.55	12.97	n.s.
	2	gen. Parts	7.03c	6.12a	6.52b	8.28d	0.04
	2	whole plant	8.65a	7.88a	8.40a	9.90b	0.02
	4	veg. Parts	13.17b	11.88a	13.15b	13.85b	0.01
	4	gen. Parts	6.39b	5.52a	6.30b	8.33c	0.01
	4	whole plant	8.05b	6.88a	7.96b	10.48c	0.01
Leaf area [m ² plant ⁻¹]	2		1.63	1.88	1.81	1.65	n.s.
	4		1.90a	2.57b	2.50b	1.86a	0.05
Trusses [plant ⁻¹]	2		14.4	14.8	14.8	14.6	n.s.
	4		19.3	20.7	20.7	18.4	0.06

Means within a row that are followed by the same letter are not significantly different (P=0.05) according to Student's t-test.

¹ Vegetative plant parts including removed leaves; ² Generative plant parts, including harvested fruits.

The effect of the EC-treatments on the generative plant parts (fruits) was especially obvious: cumulative fresh and dry weights of the fruits were considerably decreased at constant high EC (9/9), and at a somewhat lower extent at the fluctuating EC treatment with a high EC during the day (9/1). Applying a low EC-during the day

(1/9) increased the cumulative fresh and dry weights of the fruits (Table 4.5). Dry-matter percentage of the generative plant parts increased in the following order: 1/9, 5/5, 9/1, and 9/9 mS cm⁻¹.

The effect of the salinity treatments on the vegetative growth of the producing plants was somewhat different from the effect measured on the young plants: While with young plants cumulative fresh weight of the vegetative plant parts was lowest at 9/9, with fruit producing plants vegetative growth was found to be lowest at 9/1.

As with the young plants, applying a low EC during the day (1/9) did not change the vegetative growth during the fruit producing phase notably: neither the vegetative fresh and dry weights, nor the leaf area differed from the 5/5 treatment.

In contrast to the results with young plants, the proportional dry-matter distribution over the plant was changed by the EC-treatments during the fruit harvesting phase (Table 4.6):

Table 4.6: Effects of constant and fluctuating EC-levels on the proportional dry-matter distribution between vegetative and generative parts of the plant, and on the dry-matter distribution within the vegetative plant parts. Measured after 5 weeks (experiment 2) and after 12 weeks (experiment 4) of fruit harvesting

	Experiment	Light/dark EC (mS cm ⁻¹)				Significance, P
		9/1	1/9	5/5	9/9	
% Vegetative parts	2	44.4a	44.3a	45.0a	45.7b	0.05
% Generative parts	2	55.6a	55.7a	55.0a	54.3b	0.05
<i>Within the vegetative parts of the plant</i>						
% Roots	2	14.3b	12.2a	12.4ab	15.3b	0.05
% Stem	2	30.1	29.3	31.1	30.6	n.s.
% Leaves	2	55.5a	58.5b	56.4ab	54.1a	0.05
<i>Within the vegetative parts of the plant</i>						
% Vegetative parts	4	40.6b	37.1a	40.2b	51.5c	0.05
% Generative parts	4	59.6b	62.9c	59.8b	48.5a	0.05
% Roots	4	10.4b	8.1a	8.0a	13.6c	0.01
% Stem	4	32.1	32.3	31.6	33.0	n.s.
% Leaves	4	57.5b	59.6c	60.4c	53.4a	0.05

Means within a row that are followed by the same letter are not significantly different ($P=0.05$) according to Student's t-test.

At 9/9 the percentage of dry-matter distributed to the fruits was reduced in favour of the vegetative plant parts. At 1/9 a significant higher proportion of dry-matter was distributed towards the fruits. The proportional distribution of dry-matter among the vegetative organs was also affected by the EC treatments (Table 4.6): At a constant high EC or a high EC during the day, less dry-matter was distributed to the leaves in favour of the roots. Applying a low EC during the day (1/9) did not change the proportional dry-matter distribution between the vegetative organs.

After 12 weeks of harvesting, plant development was slightly affected by the EC-treatments: the number of trusses was slightly (not-statistically significant) reduced at 9/9 and 9/1 as compared with 5/5 and 1/9 (Table 4.5). Similar responses were found on the number of leaves (results not shown). In all other experiments, with young tomato plants, as well as after 5 weeks of fruit harvesting, similar tendencies (not statistically significant) were found on the numbers of trusses and leaves.

Table 4.7: Effects of constant and fluctuating EC-levels on the total number of harvested fruits per plant, and fruit load per plant after 12 weeks of fruit harvesting in experiment 4.

	Light/dark EC (mS cm ⁻¹)				Significance P
	9/1	1/9	5/5	9/9	
Number of harvested fruits	90.0 a	93.1 a	87.4 a	79.2 b	0.05
Fruit load per plant ¹ (Number)	18.0 a	38.5 b	35.1 b	19.3 a	0.02
Fruit load per plant ¹ (kg)	0.48 c	1.69 a	1.17 b	0.59 c	0.02
Total number of fruits	108.0 a	131.6 b	122.5 b	98.5 a	0.03
Number of trusses	19.3	20.7	20.7	18.4	n.s.

Means within a row that are followed by the same letter are not significantly different ($P=0.05$) according to Student' t-test.

¹ Number and fresh weight of fruits on the plant at the end of experiment 4.

After 12 weeks of harvesting, the number of unripe fruits on the plant was twice as high at 1/9 and 5/5 as at 9/1 and 9/9 (Table 4.7). Moreover, not only the number of unripe fruits on the plant was higher at 1/9 and 5/5, but also the average fresh and dry weights per fruit. (results not shown).

Discussion

It is not surprising that in present experiments a higher 24h average EC-level decreased fresh and dry weights of greenhouse grown tomato plants; It was observed before in rockwool (Adams, 1991), NFT-systems (Ehret and Ho, 1986a) and in water culture (Shannon *et al.*, 1987). When experiments were extended into the fruit harvesting phase, reductions in harvested fruit fresh and dry weight were also observed (Adams, 1991; Ehret and Ho, 1986a). Remarkable, however are the result of fluctuating EC-treatments on fruit yield, fruit quality and plant characteristics (i.e. plant size and dry-matter partitioning)

Fruit yield and quality

Most remarkable are the clear effects of fluctuating EC-treatments on fruit yield and on the incidence of BER. The EC-treatment with the low salinity during the day (1/9), especially, enhanced fruit yield considerably as compared with the EC-

treatment with similar 24h average, but constant salinity level (5/5) (Table 4.2). This increase in yield was measured in spring and summer, but not in autumn. Probably the higher global radiation and temperature in spring and summer (Table 4.1) enhanced the contrasts between the EC-treatments: High radiation usually increases dry-matter production and therefore the potential growth rate of individual fruits. It has also been reported that higher temperature increase the import of assimilates into the fruits (Walker and Ho, 1977) and the rate of fruit expansion (Pearce *et al.*, 1993; 1993a). The summer climate causes lower water potentials in the plant by inducing a higher transpiration rate. Low stem water potentials have an immediate effect on phloem turgor, reducing the driving force for water flow into the fruit and therefore the rate of fruit expansion (Johnson *et al.*, 1992). Besides high transpiration, high salinity level also lowers water potentials in the plant (Bruggink *et al.*, 1987). Fruit expansion growth was therefore probably more susceptible to changes in salinity level at high radiation than at low radiation.

Differences in yield between the EC-treatments were mainly due to differences in average fruit size (Table 4.2), although also a slight reduction in the number of harvested fruits was measured at EC 9/9 after the first 12 weeks of harvesting were finished. In the later cropping stage changes in average fruit size accounted for about 65-85% of the differences in yield among the EC-treatments. Since the dry-matter percentage of tomato fruits is low (5-10%), these different fruit sizes were correlated with significant alterations in accumulated water in the fruits. From the fluctuating EC-treatments it can be concluded that the EC-level during the day influences fruit expansion rate more than the EC-level during the night. This might have been due to the diurnal pattern in fruit growth rate being higher during the day than during the night, as was reported by Ehret and Ho (1986c). However, this type of diurnal pattern in fruit growth rate was not found by Johnson *et al.* (1992), who found a strong correlation between the apoplastic water potential gradient between stem and fruit, and fruit expansion rate. This may explain the enhanced effect of fluctuating EC-treatments on fruit size: High salinity in combination with high transpiration lowers stem water potentials more than low salinity in combination with high transpiration.

Different numbers of harvested fruits among EC-treatments contributed also to the obtained differences in yield (Table 4.2). More pronounced differences in the number of harvested fruits were expected if the experiment would have been continued, since the numbers and average size of the unripe fruits on the plants (Table 4.7) were lower at 9/9 and 9/1 as compared with the other treatments. These results are consistent with the findings of Adams and Ho (1989), who observed a depression in number and size of harvested tomato fruits by increasing salinity after 26 weeks of harvesting. The lower number of fruits (fruit load at the end of experiment 4) on the plant at 9/9

and 9/1 (Table 4.7) could only partially be attributed to a lower numbers of trusses per plant (Table 4.5): It could only account for 10-16 fruits, while the measured difference was 22-23 fruits per plant. Consequently, the average number of fruits per truss was lower at 9/9 and 9/1 than at 1/9 and 5/5. A constant high EC, or a high EC during the day must have reduced fruit setting or increased fruit abortion. Especially the salinity level during the day influenced fruit setting or fruit abortion. These effects on fruit setting and fruit abortion seemed to appear especially on the later trusses, since after 12 weeks of harvesting only minor differences in the number of harvested fruits were found, and relative large differences in the number of unripe fruits (Table 4.7).

Quality of the harvested fruits was affected clearly by the EC-treatments: Increased dry-matter percentages at constant high EC, or at high EC during the day (Table 4.2) is well known (e.g., Ehret and Ho, 1986a; Adams and Ho, 1989). However, in contrary to their findings, this response was not due solely to a reduction in water content of the fruits; average dry weight per fruit was reduced too, which agreed with the observations of Gough and Hobson (1990) and Adams (1991). Upon their results, Adams and Ho (1989) concluded that the supply of assimilates to the fruit is not affected by water relations of the plant, and that the effect of salinity on fruit yield is purely an osmotic effect reducing water accumulation in the fruits. He attributed the reduction in total fruit dry weight, which was observed in all studies, completely to the retarding effect of salinity on the number of fruits that set. Our data do not support these conclusions; The lower number of harvested fruits at high EC accounted for not more than 30 % of the decline in harvested fruit dry weight. The decrease in dry weight per individual fruit due to high EC was much more important. There was one important difference between our experiments and those of Ehret and Ho (1986a) and Adams and Ho (1989), which might have caused these different findings: In contrary to the present study, in which all fruits were included in dry weight determinations, Ehret and Ho 1986a) and Adams and Ho (1989) determined fruit dry weights on a limited number of fruits from fixed places on the plant. It is possible that these fruits were not representative for all fruits on the plant.

Another important effect on harvested fruit quality was the incidence of BER. The observed increased in incidence of BER at high salinity level is well known (e.g., Ehret and Ho, 1986b). Although the used cultivar used, Counter, is only little susceptible to BER (Ho *et al.*, 1993), important differences in the incidence of BER were observed between the EC-treatments (Table 4.2). BER is caused by loss of selective permeability of cell membranes due to a local Ca^{2+} deficiency (van Goor, 1968). Therefore problems with Ca^{2+} uptake and distribution towards the fruit were identified as the main causes for BER (Ehret and Ho, 1986b). It is well known that BER in tomato fruit

can be induced by high salinity in the root environment; high salinity reduces the uptake of Ca^{2+} by tomato plants, and decreases the distribution of Ca^{2+} towards the distal tissue of the fruits. In addition, Adams and Ho (1992) suggested that BER might be caused by an imbalance between the rate of fruit growth and the rate of Ca^{2+} movement towards the fruit: acceleration in cell expansion requires extra Ca^{2+} for cell membrane synthesis, and therefore extra Ca^{2+} import in the fruit. It is therefore remarkable that at the 1/9-treatment BER almost diminished; Although fruit expansion rate increased, no deficiency of Ca^{2+} in the fruit occurred. The import of Ca^{2+} in the fruit must have been increased to meet the higher demand.

The most important factor responsible for Ca^{2+} import into tomato fruit is the water flow via the xylem, because Ca^{2+} movement is restricted to the xylem. The xylem connection in the pedicel is poor (Lee, 1989) and consequently 90% of the water imported by the fruit flows via the phloem (Ehret and Ho, 1986c). Water potentials in the stem xylem are relatively low during the day, and xylem water flow and associated Ca^{2+} movement towards the fruit may be zero or reversed during large periods of the day (Johnson *et al.*, 1992). A low EC during the day probably enhanced Ca^{2+} import in the fruit by increasing the water potential in the stem xylem, and thus the xylem water flow towards the fruit. The EC-level during the night was probably less important, since in general stem water potentials are higher during the night than during the day. Probably the Ca^{2+} uptake by the roots being higher during the day than at night (Ho and Adams, 1989), increases the effect of daytime EC as compared with the EC during the night.

Plant growth, development and dry-matter partitioning

Plant responses (growth, development and dry-matter distribution) were influenced by the EC-treatments (Table 4.4-Table 4.6). Positive changes in dry-matter production as well as in proportional dry-matter distribution contributed to the increased dry weight yield at 1/9. Negative changes in dry-matter production and proportional dry-matter distribution caused the lower dry weight yield at 9/9.

The differences in total plant dry weight between the EC-treatments (Table 4.4 Table 4.5) were related to the differences in leaf area; the higher the leaf area, the higher the total plant dry weight. An eventual additional effect of the EC-treatments on stomatal opening could not be concluded from present results. Leaf area was reduced equally at 9/9 and 9/1. This indicates that the EC during the day, especially, was important to leaf expansion, probably by lowering turgor in the growing leaf cells (Munns, 1993). The positive effects of fluctuating EC with a low EC during the day on vegetative growth and leaf area of young plants, as reported by Bruggink *et al.* (1989), was not confirmed by our observations. However, our experiments with young plants

were conducted in the spring, while their experiments were conducted in mid-summer and the plants at high EC suffered severe water stress during the day.

The EC-effect on proportional dry-matter distribution towards the fruits increased in time: while no effect was measured on young tomato plants, with fruit producing plants it was decreased at high EC by about 1% after 5 weeks of harvesting, and by about 11% after 12 weeks of harvesting (Table 4.6). The reduction at high EC was in accordance with the observations of Ehret and Ho (1986a). These effects on the proportional distribution of dry-matter towards the fruits were not necessarily due to a direct effect of salinity on the distribution of assimilates within the plant. Differences in fruit load per plant (number of fruits on the plant) between the EC-treatments may also have influenced the dry-matter partitioning towards the fruits (Heuvelink and Buiskool, 1995). A high incidence of BER, may have reduced average dry weight per fruit at high salinity by inducing a shorter growing period of the fruits.

Present results provide some interesting information on growth responses of tomato to diurnal salinity in the root environment, as well as further insight into the cause of BER. In contrary to Adams and Ho (1989) who concluded upon experiments with a h/l EC-treatment that fluctuating salinity would not be advantageous in tomato production, we conclude that a l/h EC-treatment can be advantageous as a tool to reduce BER and to enhance yield. Although most present growing systems (rockwool) do not allow EC-fluctuations on the short-term, it might be possible make use of it in future, since there is a tendency to growing systems with less substrate volume and recirculation possibilities.

5. Model for short-term water relations of tomato plants.

5.1 Introduction

In the previous chapter it was shown that different day and night salinity-levels caused clear effects on plant growth, fruit production and the incidence of Blossom End Rot (BER) in the fruits. It was assumed that various aspects of plant water, such as flow of water, water potentials and turgor are involved in determining these effects.

Because water relations of greenhouse crops make part of a complicated system involving greenhouse climate, plants and root environment, experimental proof for the role of plant water relations can only be obtained via numerous, complicated experiments. Only a limited amount of experimental results is available (Chapter 3 and 4).

In this chapter a simulation model of the water relations in a plant is described. This model was developed as a tool to analyse the experimental results, to facilitate understanding and generalisation.

5.1.1 Introduction into crop modelling

Since the late sixties various crop models have been introduced in agricultural research. Most of these models have been developed for field crops, and are able to describe crop growth under various conditions. In these models plant processes such as photosynthesis and respiration are usually described as functions of light intensity, CO₂-concentration, temperature and crop parameters, and are used to calculate dry matter production and availability for growth. Distribution functions, dependent on time or plant development, are often used to calculate the partitioning of dry matter among plant organs (Spitters *et al.*, 1989). Dry matter production and distribution determine the growth in dry weight of harvestable parts of the plant (Challa and Schapendonk, 1986). Growth in fresh weight of plant part is obtained by multiplying with the dry matter fraction of that plant part (e.g. de Koning, 1994). Most of the models for field crops work with time steps of one or more days, using average values for climate variables.

5.1.2 Greenhouse crop modelling

Production in greenhouses differs in important aspects from the production of field crops: Important environmental conditions for plant growth, such as temperature, relative humidity, CO₂-concentration of the air and (to some extent) irradiance, can be influenced. In most modern greenhouses these factors are controlled by a climate control system. Since the crop/greenhouse system is rather complex, modelling of the system may provide new opportunities for optimising production.

Most horticultural products are produced for the fresh market, where quality of the fresh product is a major factor influencing its value. Therefore not only the dry matter production but also fresh weight is of major importance, since the dry matter content influences the quality of the harvestable product greatly. Both, production and quality of the product depend to a large extent upon the greenhouse climate. For instance, irradiance does not only influence dry matter production by influencing photosynthesis, it also influences plant transpiration by a combined effect on plant properties and greenhouse environment. Plant transpiration affects the water status of the plant (e.g. relative water content; water potentials) on the short-term (minutes), which in turn affects the flow of water and solutes through the plant, as well as expansion growth of the plant.

Crop growth in greenhouses is strongly influenced by the greenhouse climate, which in turn depends highly on the outside weather and the operation of the greenhouses climate control. Therefore, to model production in greenhouses, integrated knowledge on plant physiology, greenhouse climate and control systems is necessary (Uding ten Cate *et al.*, 1978). Concerning the greenhouse climate, important progress was made by modelling it in terms of coupled energy and water vapour balances (Bot, 1983). Much of the effort on the modelling of plant growth in greenhouses was made on dry matter production in response to greenhouse climate factors, such as radiation inside the greenhouse (Heuvelink, 1996) and elevated CO₂-concentrations in the greenhouse air (Nederhof, 1994). Special attention was paid to the effects of periodical harvests and fruit load on dry matter distribution within a plant (Heuvelink, 1996; de Koning, 1994). Stanghellini (1987) investigated plant transpiration primarily in relation to greenhouse climate rather than on the basis of internal plant water relations. In greenhouse research in general little attention has been paid to internal plant water relations, because it is assumed that water is not a limiting factor for crop growth. This assumption, however, is not very strong, since it is well known that especially with high radiation in the summer the water potentials in greenhouse-grown plants decrease significantly, which influences important plant physiological processes such as stomatal opening, cell expansion and the transport of water and solutes to growing tissues in the plant negatively. The usually high salt concentration in the root environment of the plants, due to a high nutrition level, increases these effects further.

Several models have been introduced to simulate internal water relations of greenhouse-grown plants. The model of Marcelis (1989) for instance, predicted the diurnal course of the transpiration of tomato plants well. However, it did not describe internal plant water status adequately because only one lumped plant water potential (and related water content) was used, while for the simulation of the flow of water between different plant parts gradients in water potentials between these plant parts are

essential. The model of Bruggink (1988) assumed separate water potentials (and associated water contents) for a leaf compartment and a stem/root compartment. In these compartments xylem and adjacent symplast were not distinguished, although it is well known that hydraulic resistance's in the xylem are much lower than hydraulic resistance's between the xylem and the symplast around it (Boyer, 1985). Consequently, this model is not able to simulate short-term variations of local water potentials throughout the plant adequately.

In order to analyse diurnal cycles of transpiration rates and plant water potentials c.q. water contents of some desert perennials, Nobel and Jordan (1983) used electric circuit analogues that included hydraulic resistances representing the xylem in the plant and resistance-capacitance (RC) combinations representing the tissues adjacent to the xylem in leaves, stems and roots. Roughly, the hydraulic resistances in the xylem cause the water potential distribution through the plant in steady state conditions (stable transpiration), while the RC-combinations cause the dynamic behaviour of the system after a change in transpiration rate. This technique was also used by Landsberg *et al.* (1976) to describe water flow and changes in water potentials/ water contents in apple trees.

One of the difficulties of modelling water uptake by a plant is the interaction between the water and solute flow into the plant at low water uptake rates: Both, water and solute uptake influence the osmotic component of the driving force for the water uptake (the water potential gradient between the root xylem and the root environment). Fiscus (1975) and Dalton *et al.* (1975) independently developed about similar models to describe the water uptake. The uptake of water in the model of Marcelis (1989) was based on the model of Fiscus *et al.* (1983), while the model of Bruggink (1988) ignored the interaction between solute and water uptake. Another aspect which may influence the water uptake is the accumulation of solutes in the cortex of the root, caused by the filtering out of solutes from the water stream at the endodermis (Fiscus, 1977). None of the mentioned models took into account this aspect of water uptake.

5.1.3 Aim of present model study

The aim of the present model study is to use present knowledge about water relations for a adequate analysis of the observed short-term dynamics of internal water relations in tomato plants (Chapter 3.4) in relation to their transpiration and the salt concentration in the root environment. The model should deal with the long distance water flow via the xylem, as well as with the short distance water flow between xylem and adjacent tissues and related changes in water content at different locations in the plant. The model should further facilitate the future incorporation of processes such as expansion growth, solute flow via the xylem and stomatal movements and related variations in stomatal conductance.

5.2 Model Description

5.2.1 General description and assumptions

The model for short-term water relations in tomato growing in water culture has been separated into two sub models: a sub model for the water relations in the plant (*WRTomSim*), and a sub model for the radial water uptake by the roots (*WURoot*). An electric analogon of the model is given in Figure 5.2.1.

WRTomSim describes the internal water relations in the root and shoot of a single plant. This sub model describes the flow of water through the apoplastic xylem

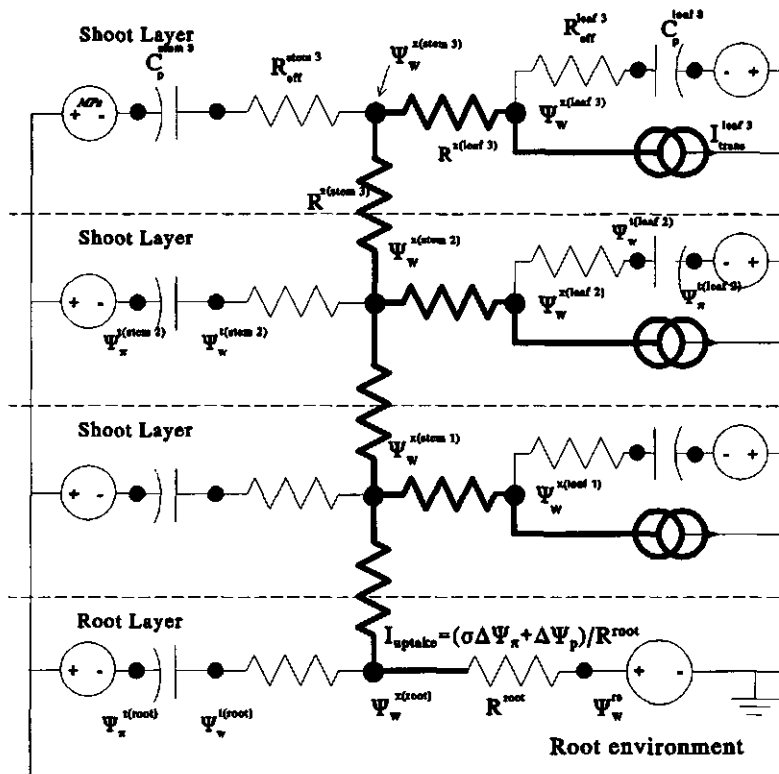


Figure 5.2.1: A network model for the pathways of water in a plant. Water flows from the root environment, along a gradient in water potential via the xylem ($\Psi_w^{x(-)}$) of the root, stem and leaves (bold components) to the shoot environment due to transpiration at three plant heights (I_{trans}^{leaf} , represented by the double circles). Along the xylem network capacitors (C_p) are connected to the xylem via hydraulic tissue resistances (R_{eff} , thin components), representing storage of water in the tissues adjacent to the xylem. In non-steady state situations water may flow between the xylem and adjacent tissues, causing variations in water contents of the storage components. The osmotic potentials in the tissues and the root environment are represented by potential sources (single circles), which are not constants but depend on osmotic potentials at saturation and actual relative water contents of the tissues.

transport system, and the dynamics of the water content of tissues adjacent to the xylem in the root system, stem and leaves. The standard sub model does not include the fruits, since the major water connection between fruits and stem is via the symplastic phloem (Lee, 1989), and consequently the water relations of the fruits are mostly dependent upon water transport through the phloem. The sub model does also not include growth. The sub model *WURroot* describes the radial water flow between the root environment and the root xylem, and the variations in solute concentrations in cortex and xylem of the root system. The latter since it may influence the radial water flow through the root (the water uptake of the plant) substantially.

The most important driving force for water transport through the plant is transpiration: Transpiration is an important sink for water in the plant. Expansion growth (not included in standard model) may also act as a sink for water, while the tissues adjacent to the xylem may act alternately as sinks and sources for water, dependent upon their momentaneous water status in relation to that of the local xylem. In general, over 24 h, transpiration is the major sink for water (>90%), while 0-10% of the overall water uptake is stored in plant tissue (growth). On average changes in relative plant water content are zero over 24 h.

The system described by the model is the water related part of the plant. The boundaries of the system are the input and output sites for water (liquid phase) of the plant. Therefore the boundaries of the whole model are the evaporating surfaces inside the leaves (the cell walls in the stomatal cavities), where water leaves the system, and the epidermis of the root, where water enters the system. Input variables, associated with the boundaries of the model, are the plant transpiration (I_{trans} , $m^3 \cdot s^{-1}$), and the water potential in the root environment (ψ_w^{re} , MPa). Since the model concerns a plant growing in water culture, the pressure potential (ψ_p^{re} , MPa) in the root environment may be assumed zero, and consequently ψ_w^{re} equals the osmotic potential in the root environment (ψ_π^{re} , MPa) which may be related to the concentration of solutes in the solution around the roots according to Van't Hoff's law (see Eq. 2.6).

Important output variables of the model are the dynamics of the rate of water uptake by the plant, water flow rates in the xylem and between xylem and surrounding tissue, and water contents and water potentials in tissues in the root system, stem and leaves. The simulation time step is in the order of seconds since some of the processes incorporated have rather short time constants.

It is assumed that long distance transport of water via the xylem vessels takes place along gradients in water potential. Strictly, the flow of water through the xylem is not driven by a gradient in water potential, but by a gradient in the pressure potential, a component of the water potential. However, it is assumed that the osmotic potential of the xylem sap is uniform throughout the xylem, and therefore does not add

to gradients in water potential in the xylem. Consequently the water potential may be used as well.

Water uptake by the roots is assumed to be driven by a combination of gradients in pressure potential and in osmotic potential. In steady state situations no transport of water takes place between the xylem and adjacent tissue; In non steady state situations, water transport between the apoplastic xylem and adjacent tissues (symplast) may occur all along the xylem pathway. This type of water transport between apoplast and symplast is driven by a combination of gradients in pressure and osmotic potential. Active accumulation of solutes in the symplast, the so-called osmoregulation (Morgan, 1984), is ignored.

Relative strengths and the positions of sinks and sources for water in the plant, together with the resistances of the conducting xylem vessels, result in a water potential distribution in the xylem network in the plant. Local changes in xylem water potential induce dynamic changes in water content and related water potentials in the tissues adjacent to the xylem.

Implicit assumptions of the present model are: isothermal conditions to enable the use of the thermodynamic approach, and a continuous water column in the xylem vessels to enable free conductance of pressures and water. The resistance of water conducting vessels is assumed to be constant, due to their rigid construction. Some of these assumptions are not completely valid: for instance serious temperature gradients may exist in a greenhouse grown tomato crop, due to net radiation differences between the top and bottom of the crop or local heating, and cavitation in the xylem vessels may be significant during 'drought' (Zimmerman *et al.*, 1993).

The model is restricted to thermodynamic properties: it does not account for any metabolic mediated effect or for effects of phytohormones.

5.2.2 Sub-model 'WRTomSim' for the flow of water through the shoot and the dynamic changes in water content and water potentials in tomato plants.

5.2.2a Description 'WRTomSim'

In the sub-model *WRTomSim* the shoot has been separated into three shoot layers and one root layer (Figure 5.2.1). Three shoot layers are distinguished to account roughly for plant architecture, and to enable transpiration at different plant heights in the model. Several structures are recurring in Figure 5.2.1; the structure of shoot layers are similar. Each shoot layer consists of a stem and a leaf component. Each stem and leaf component include an apoplastic component, representing mainly the xylem transport pathway (bold), and a symplastic component, representing the symplast of the tissue adjacent to the xylem (thin). The shoot-layers are interconnected

by 'hydraulic stem resistances' ($R^{x(stem)}$, $\text{MPa}\cdot\text{m}^{-3}\cdot\text{s}$), representing the total hydraulic resistance of the xylem in the stem internodia between the midpoint of shoot-layer and one layer below or above. In each shoot-layer the leaf component is connected to the midpoint of the stem component by a 'hydraulic leaf resistance' ($R^{x(leaf)}$, $\text{MPa}\cdot\text{m}^{-3}\cdot\text{s}$), which is a substitute resistance for the hydraulic resistances of the xylem in all petioles and leaves in a shoot-layer. All hydraulic xylem resistances together form the apoplastic xylem network.

The symplastic components of each root, stem or leaf compartment (the thin marked capacitance voltage-source combinations) represent the volume of water bound within the cells in a lumped compartment. The symplastic component of each compartment is connected to the xylem of that compartment by means of an 'effective hydraulic resistance' (R_{eff}^t , $\text{MPa}\cdot\text{m}^{-3}\cdot\text{s}$). The effective hydraulic resistances between apo- and symplast are mainly determined by the hydraulic resistances of the membranes in the transport path.

The apoplastic xylem network enables long distance transport of water and the propagation of pressure potentials through the plant. It is responsible for the relative distribution of water potentials within a plant at steady state. The symplastic tissues are responsible for the dynamic behaviour of water potentials and associated water contents in the plant on changes in root and shoot environmental conditions.

The boundaries of the sub-model *WRTomSim* are the evaporating sites inside the stomatal cavities and the root xylem. The associated input variables of this sub-model are the measured transpiration rates per leaf layer ($I_{trans}^{leaf\ n}$, $\text{m}^3\cdot\text{s}^{-1}$), and the water potential in the root xylem ($\psi_w^{x(root)}$, MPa). Using the measured transpiration rate as an input variable instead of simulating it as a function of climate and plant properties, reduces uncertainty in the simulation results; it eliminates the errors associated with estimating the micro-climate, the boundary layer resistance and stomatal resistances. The other input variable, the water potential in the root xylem, is an output variable of the other sub-model *WURoot*. In Figure 5.2.1 the transpiration rates are presented as current sources (double circles). It is assumed that the transpiration rate (transport of water vapour between leaf interior and surrounding air) equals the flow of water across the upper boundary of the model (the transition of water from the liquid to the vapour phase inside the leaf). This assumption is a simplification, since the vapour pressure and therefore the amount of water inside the stomatal cavities may differ, for instance by changes in leaf temperature. The effect of temperature is probably small.

The output of the sub-model includes water contents, water-, pressure- and osmotic-potentials in the tissues of all seven compartments (3 stem, 3 leaf and 1 root

compartment). The water potential distribution in the xylem network as well as the associated water flow rates in the xylem and between the xylem and the adjacent tissues are also output of the model.

5.2.2b The xylem network

To avoid duplications only the structures and associated equations are discussed: in these equations the superscript x means that the parameter or variable is associated with the xylem, the superscript t means that it is associated with the adjacent tissue. In the model long distance transport of water via the xylem is described analogous to Ohm's Law (van den Honert, 1948; Cowan, 1965):

$$J_v = \frac{\Delta\psi_w^x}{R^x} \tag{5.2.1}$$

where ψ_w^x (water potential, MPa) corresponds to the electric potential, R^x (hydraulic resistance, $\text{MPa}\cdot\text{m}^3\cdot\text{s}$), to electrical resistance, and J_v (water flow rate, $\text{m}^3\cdot\text{s}^{-1}$) to electrical current. The xylem of the plant is a branched system, in which each branch has its own hydraulic resistance. The water content of the xylem is assumed to be constant because the xylem consists of rigid non-elastic vessels. Therefore, the xylem system in Figure 5.2.1 may be treated analogous to an electric resistor network where Fick's law can be applied. The sum of all flows into and out of a xylem junction is zero:

$$\sum J_v = 0 \tag{5.2.2}$$

Based upon this analogue, for each xylem junction (black filled circle in Figure 5.2.1) an algebraic equation may be derived by substituting Eq. 5.2.1) for each branch. For instance, for the junction associated with the water potential $\psi_w^{x(\text{stem}2)}$, Eq. 5.2.3 can be derived:

$$\frac{\psi_w^{x(\text{stem}2)} - \psi_w^{x(\text{stem}1)}}{R^{x(\text{stem}1)}} + \frac{\psi_w^{x(\text{stem}2)} - \psi_w^{x(\text{stem}3)}}{R^{x(\text{stem}2)}} + \frac{\psi_w^{x(\text{stem}2)} - \psi_w^{x(\text{leaf}2)}}{R^{x(\text{leaf}2)}} + \frac{\psi_w^{x(\text{stem}2)} - \psi_w^{t(\text{stem}2)}}{R_{\text{eff}}^{t(\text{stem}2)}} = 0 \tag{5.2.3}$$

which may be rewritten as:

$$a\psi_w^{x(\text{stem}1)} + b\psi_w^{x(\text{stem}2)} + c\psi_w^{x(\text{stem}3)} + d = 0 \tag{5.2.4}$$

where a,b,c and d are constants that depend on the parameters $R^{x(\text{stem}1)}$, $R^{x(\text{stem}1)}$, $R^{x(\text{stem}1)}$ and $R_{\text{eff}}^{t(\text{stem}2)}$ and on the tissue water potential $\psi_w^{t(\text{stem}2)}$. (Each time the water potential distribution in the xylem is calculated, water potentials in all adjacent tissues are treated as constants). In each of the seven xylem junctions in Figure 5.2.1 equations

analogous to Eq. 5.2.4 are derived, resulting in a set of seven equations with six unknown variables. In the model, these equations are solved using the substitution method.

5.2.2c Tissues adjacent to the xylem: water potentials and water contents

In the model the total water content of a compartment n (leaf, stem or root) (WC^n , m^3) has been separated into a symplastic (WC_{sym}^n) and an apoplastic part (WC_{apo}^n). The apoplastic part represents the xylem, intercellular spaces and cell walls in the compartment; the symplastic part represents the volume of water bounded within cell membranes in the tissues. The ratio between WC_{apo}^n and WC_{sym}^n is assumed to be constant at saturation, defining the fraction symplastic water at saturation as:

$$WC^{(n,sat)} = WC_{apo}^{(n,sat)} + WC_{sym}^{(n,sat)} \quad (5.2.5a)$$

$$f_{sym}^n = \frac{WC_{sym}^{(n,sat)}}{WC^{(n,sat)}} \quad (5.2.5b)$$

The apoplast is assumed to be saturated continuously due to its rigid structure. The actual water content of the symplast may alter upon changes in water potential in the adjacent xylem. The relative water content of an organ ($RWC^{(n)}$, -) is a commonly used variable in plant water relations. It is defined as the ratio between the actual water content ($WC^{(n)}$) and the water content at saturation ($WC^{(n,sat)}$), and includes the water contents of apoplast and symplast:

$$RWC^{(n)} = \frac{WC^{(n)}}{WC^{(n,sat)}} \quad (5.2.6)$$

In the model it is assumed that alterations in tissue water content are completely due to changes in water content in the symplast, because the apoplast is assumed to be saturated continuously. Therefore, besides $RWC^{(n)}$ the relative water content of the symplast ($RWC_{sym}^{(n)}$) is defined, which equals the ratio between $WC_{sym}^{(n)}$ and $WC_{sym}^{(n,sat)}$:

$$RWC_{sym}^{(n)} = \frac{WC_{sym}^{(n)}}{WC_{sym}^{(n,sat)}} \quad (5.2.7)$$

When in a compartment water potentials in xylem and adjacent tissue differ, water flows between xylem and tissue. The direction and magnitude of the flow depend upon the direction and magnitude of the water potential difference between tissue and xylem. Eq. 5.2.8 yields the rate equation for the absolute water content of the symplast

in the tissue (which equals the rate equation for the total water content because the water content of the apoplast is assumed to be constant):

$$\frac{dWC_{sym}^{(n)}}{dt} = \frac{\psi_w^{x(n)} - \psi_w^{t(n)}}{R_{eff}^{(n)}} \quad (5.2.8)$$

where $R_{eff}^{(n)}$ ($m^{-3} s^{-1} MPa$) is the effective hydraulic resistance for water transport between apoplast and symplast. This type of resistance is generally much larger than the resistances in the xylem because water transport across membranes (cell membrane and tonoplast) is involved.

Changes in $WC_{sym}^{(n)}$ are due to the principle that tissues adjacent to the xylem aim to become in a water potential equilibrium with the xylem (Nobel, 1983). These changes in $WC_{sym}^{(n)}$ correspond to a capacitance effect superimposed on the xylem network for water flow through the plant. The dynamic behaviour and magnitude of this type of water exchange is determined by the absolute capacitance for water storage in the symplast of the tissue ($C^{t(n)}$, $m^3.MPa^{-1}$) and the resistance $R_{eff}^{(n)}$. Analogous to a capacitor in electric circuits, $C^{t(n)}$ of a tissue has been defined as the net amount of water accumulated in the symplast of the tissue ($\Delta WC_{sym}^{t(n)}$) that leads to an increase in water potential in that symplast of $\Delta \psi_w^{t(n)}$ (Nobel, 1983; Davies, 1986).

In principle two components of the water potential in the symplast contribute to this capacitance effect: The pressure potential ($\psi_p^{t(n)}$) because cell walls apply increasing pressure on the water in the symplast with increasing (relative) water content, and the osmotic potential ($\psi_\pi^{t(n)}$) because volume changes induce solute concentration changes and therefore alterations in $\psi_\pi^{t(n)}$ in the symplast. Therefore in the present model the capacitance has been divided into a pressure and an osmotic part: the osmotic part is represented by a variable voltage source, positioned in series with the pressure-based hydraulic capacitance $C_p^{t(n)}$ (5.2.9a). To normalise $C_p^{t(n)}$, it can be related to the water content of the symplast at saturation ($C_p^{t(n)^*}$, 5.2.9b).

$$C_p^{t(n)} = \frac{\Delta WC_{sym}^{t(n)}}{\Delta \psi_p^{t(n)}} \quad (5.2.9a)$$

$$C_p^{t(n)^*} = \frac{\Delta R WC_{sym}^{t(n)}}{\Delta \psi_p^{t(n)}} \quad (5.2.9b)$$

$C_p^{t(n)^*}$ is related to the bulk modulus of elasticity of a tissue (see 2.3.4), and therefore pressure dependent. In the model however, $C_p^{t(n)^*}$ was treated as a constant. When $WC_{sym}^{t(n)}$ decreases while the total amount of solutes in the symplast remains constant, solute concentration increases, and consequently $\psi_\pi^{t(n)}$ decreases. In the electric analogon (Figure 5.2.1.) the osmotic potentials in the symplast of the tissues are

represented by voltage sources (single circles), which are positioned in series with the pressure-based hydraulic capacitances. The actual osmotic potential is a function of $RWC_{sym}^{i(n)}$, and the osmotic potential at saturation ($\Psi_n^{i(n, sat)}$):

$$\Psi_n^{i(n)} = \frac{\Psi_n^{i(n, sat)}}{RWC_{sym}^{i(n)}} \quad (5.2.10)$$

5.2.2d Tissues adjacent to the xylem: dynamic behaviour

Combining Eq. 5.2.8 with Eq. 5.2.9a yields the rate equation for the pressure potential in the symplast of the tissue (Eq. 5.2.11):

$$\frac{d\psi_p^{i(n)}}{dt} = \frac{\Psi_w^{x(n)} - \Psi_w^{i(n)}}{R_{eff}^{i(n)} \times C_p^{i(n)}} \quad (5.2.11)$$

The dynamic behaviour of the model depends mainly on the various $R_{eff}^i C^i$ -combinations in tissues representing parts of the model (Figure 5.2.1): Analogous to RC-combinations in electrical circuits the dynamic behaviour of each $R_{eff}^i C^i$ -combination may be characterised by a time-constant (τ^i , Eq. 5.2.12).

$$\tau^i = C^i \times R_{eff}^i \quad (5.2.12)$$

The time-course of ψ_w^i (and WC^i), after a sudden change in water potential in the adjacent xylem (at $t = 0$), may be taken analogous to the dynamics of the change in charge of a capacitor in an electrical RC-circuit upon a change in potential:

$$\psi_w^i(t) = \left(\psi_w^i(0) - \psi_w^i(\infty) \right) \times e^{\left(\frac{-t}{\tau} \right)} + \psi_w^i(\infty) \quad (5.2.13)$$

This principle is used to determine values for the parameters R_{eff}^i (see further 5.3.1).

State variables

The dynamics of the main state variables in the sub-model are described by the differential equations 5.2.8 and 5.2.11. They include the water contents of the symplastic tissues of the three stem and leaf layers (Figure 5.2.1), and the associated pressure potentials in the stem and leaf tissues. Osmotic potentials and water potentials in the tissues, as well as the water potential distribution in the xylem network and relative water contents of different plant parts are derived from these state variables.

5.2.3 Sub-model 'WURoot' for water uptake by the roots.

Following the work of van den Honert (1948), plant physiologists often treat the flow of water through root systems (J_v) analogous to the law of Ohm: a difference in water potential between root xylem and root medium ($\Delta\psi_w$) drives water at a steady rate (J_v) through a constant hydraulic resistance (R^{root}). This simple approach is often used in models concerning water transport through plants (e.g. Nobel and Jordan (1983); Landsberg *et al.*, 1976; Bruggink *et al.*, 1988). In many studies, however, R^{root} was found to be not a constant, but dependent on the rate of water uptake and external factors such as the salt concentration in the root environment (see Passioura, 1984). Because in this thesis especially changes in total salt concentration in the root environment are the matter of interest, the simple approach is not suitable in our model for water transport through the tomato plant. The second reason to reject this simple approach follows from usually observed J_v - $\Delta\psi_p$ relationship during determination of R^{root} (e.g. Lopushinsky, 1964; Shalhevet *et al.*, 1976): to determine R^{root} experimentally, usually a detached root system is placed in a pressure chamber with the cut-end outside the chamber and its roots in a nutrient solution inside the chamber. Applying pressure in the chamber induces flow through the root system which can be measured by collecting the expressed sap at the cut-end. At high flow rates generally a linear relation between pressure ($\Delta\psi_p$) and flow is found (Figure 5.2.2). The slope of this relationship equals the hydraulic conductance of the root system (i.e. $1/R^{\text{root}}$). At low flow rates however commonly non-linearities are observed which according to Ohm's Law are explained by a changing R^{root} . However, the curvature of Figure 5.2.2 does not necessarily imply that R^{root} varies because water flow across the endodermis is not only

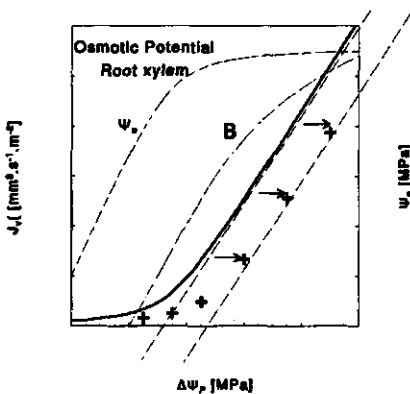


Figure 5.2.2: Differences between simulated (—) and measured (+) (J_v - $\Delta\psi_p$)-relationships (with a model including coupled solute and water flow). Curve B (---) represents the expected (J_v - $\Delta\psi_p$) relationship by Passioura (1988) when solute accumulation at the endodermis occurs.

driven by $\Delta\psi_p$ but also by other components of the water potential.

The difference in water potential ($\Delta\psi_w$) results from differences in pressure potential ($\Delta\psi_p$) and osmotic potential ($\Delta\psi_\pi$), which both contribute to water flow. In Figure 5.2.2 the relation between pressure and flow is curved at low flow rate with a positive intercept on the flow axis at zero pressure ($\Delta\psi_p = 0$). The osmotic potential of the expressed xylem sap ($\psi_\pi^{x(\text{root})}$) increases considerably with increasing flow rate and is normally found to be close to zero and about constant at high flow rates because $\psi_\pi^{x(\text{root})}$ mainly depends on the ra-

tio between the import of solutes and water in the xylem. Consequently, at high water flow, $\Delta\psi_{\pi}$ approaches the osmotic potential in the root environment (ψ_{π}^r). At high flow rates $\Delta\psi_{\pi}$ becomes less important compared to $\Delta\psi_p$. This implies that the non-linearity at low flow rate results from shifting the importance of $\Delta\psi_p$ and $\Delta\psi_{\pi}$ while R^{root} remains constant (Mees and Weatherley, 1957; Lopushinski, 1961; 1964; Passioura, 1988).

Fiscus (1975) and Dalton *et al.* (1975) independently developed similar models which were able to describe coupled water and solute flow through plant roots. Both models simulate the above described non-linearity well. The models are based on transport equations for water and solutes across an individual semi-permeable membrane. According to these models, at low flow rates active transport of solutes into the xylem decreases the xylem osmotic potential, which induces water flow into the xylem even when there is no pressure difference. At higher flow rates, due to increasing pressure differences, xylem sap becomes more and more diluted, and the contribution of the osmotically induced water flow reduces resulting in an asymptotically linear relation between pressure and flow.

Although these models simulate the qualitative aspects of water uptake well, sometimes quantitative discrepancies were found between simulation results and measured data: The simulated ($\Delta\psi_p$ - J_v)-curve was shifted along the $\Delta\psi_p$ -axis compared to the measured data (Figure 5.2.2) in a manner which could not be explained by a simple change in parameter values. Newman (1976) criticised the models for that. Fiscus (1977) responded that in experiments the effective ψ_{π} outside the endodermis might have been lower than the actual ψ_{π} in the root environment (ψ_{π}^r), due to accumulation of solutes at the semi-permeable endodermis. He argued that, since at high J_v the xylem sap is usually more diluted than the solution around the roots, solutes must be filtered out by the endodermis. When solutes arrive at the endodermis faster than they are taken up, they will tend to accumulate, causing a higher solute concentration and thus a lower ψ_{π} at endodermis level. As the concentration builds up, diffusion back increases, and an equilibrium solute concentration at endodermis level results which will be higher than the solute concentration in the root medium. Passioura (1984) made some rough calculations based on these suggestions of Fiscus (1977), and presented a modified ($\Delta\psi_p$ - J_v)-relationship (Curve B in Figure 5.2.2). Since this curve did not meet the measured data at all, Passioura (1984) rejected the solution provided by Fiscus (1977).

Based on the suggestions of Fiscus (1977) concerning solute accumulation at the endodermis, in this chapter a new model is described which is based on the models of Fiscus (1975) and Dalton *et al.* (1975) and extended with the solute mass balance in the cortex of the root. Pressure and osmotically driven water transport, and the dy-

dynamic behaviour of the solute concentration at the endodermis are incorporated, as well as the concentration dependent solute transport across the endodermis. Because the solute concentration at the endodermis is a dynamic property, it probably influences the relation between $\Delta\psi_p$ and J_v over a day.

The aim of the present model study is to describe the water uptake of a tomato plant grown on water culture as a function of changing solute concentration in the root environment and of changing water flow driven by transpiration, and the effect of solute accumulation at the endodermis on the apparent R^{root} . The submodel is used to find out whether solute accumulation in the cortex significantly changes the relation between pressure and water flow through the root, and whether dynamic aspects of the solute accumulation dynamically changes the apparent R^{root} during a day.

5.2.3a Description 'WURoot'

The sub-model *WURoot* describes the radial water uptake by a root system of tomato, including the effects of coupled solute and water flow. The solute distribution in the cortex of the root, based upon solute mass flow and diffusion in the cortex and epidermis, is incorporated in the submodel to describe the actual ψ_π just outside the endodermis.

The boundaries of the model are the root xylem on the one hand, and the epidermis layer of the root on the other hand. Input variables associated with these boundaries are the pressure potential in the root xylem ($\psi_p^{\text{x(root)}}$), and the osmotic potential in the root environment (ψ_π^{e}). The root environment is assumed to be well stirred. Important output variables are the rate of water uptake by the root system and the osmotic potential in the root xylem. Distribution of the solute concentration in the root cortex is output as well. The parameters of the submodel include parameters that describe the dimensions of the root system and parameters associated with the permeability of the endodermis for solutes and water, and with the flow of solutes through the root. In the model the whole root system is represented as a single root with average diameter \bar{d} and length l . In longitudinal direction, no different zones are distinguished: radial water and solute flow densities are assumed to be equal over the whole root length. A cross-sectional slice of the root is considered to be the composite of concentric layers of different tissues in series (Figure 5.2.6): the epidermis, several cortex layers and the xylem of the root in the stele. Between stele and cortex layer a semi-permeable membrane is located (the endodermis). In all tissues, only the apoplast is considered: radial water volume flow via the symplast is assumed to be negligible compared to flow via the apoplast, due to a much higher hydraulic resistance in the symplast (Nobel, 1985). Therefore, water is assumed to flow via the apoplasts of epidermis and cortex to the endodermis, where further apoplastic transport is blocked by the Casparian strips. At the endodermis it enters the symplast, crosses the endodermis

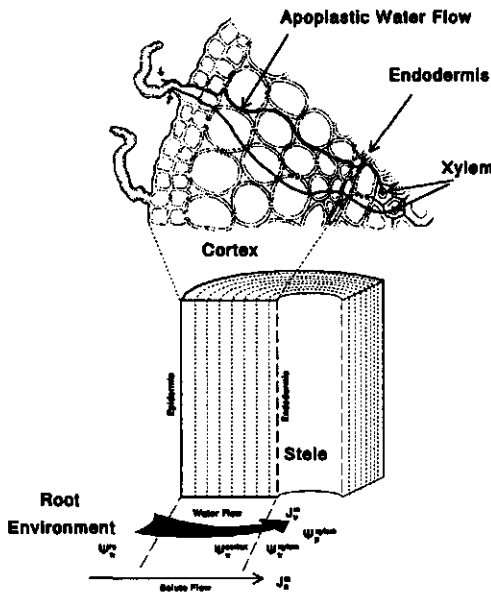


Figure 5.2.6: Schematic representation of radial solute and water flow through a cross sectional slice of a root

and enters the apoplast of the stele. In the model the endodermis is not included as a compartment, but only as a single semi-permeable membrane. Xylem vessels and apoplast of the stele are considered as one compartment. Solute transport in the apoplast of epidermis and cortex results of convection (mass flow with the water stream) and diffusion. The effect of solute exchange between symplast and apoplast on the solute mass balance of the apoplast in the cortex, is assumed to be negligible compared to the effect of radial apoplastic solute transport (Bouma, 1995). For each compartment solute mass balances are formulated and used to calculate solute concentrations and osmotic potentials.

5.2.3b Flow of water and solutes across endodermis

Radial water flow through a root is driven by a combination of a gradient in hydrostatic pressure potential and a gradient in osmotic potential. The rate equation for water uptake (per m root length) is given by:

$$J_v = -L_p A_s^{root} (\Delta\psi_p + \sigma\Delta\psi_\pi) \quad (5.2.14)$$

where:

J_v	radial volumetric water flow per m root length	$\text{m}^3 \text{s}^{-1} \text{m}^{-1}$
A_s^{root}	conversion factor root surface area/ root length where $A_s^{root} = \pi \bar{d}^{root}$ and \bar{d}^{root} = root diameter	$\text{m}^2 \text{m}^{-1}$ m
L_p	hydraulic conductance of the root system ($1/R^{root}$)	$\text{m}^3 \text{s}^{-1} \text{MPa}^{-1} \text{m}^{-2}$
$\Delta\psi_p$	pressure potential difference across the endodermis	MPa
σ	reflection coefficient for solutes of the endodermis	-
$\Delta\psi_\pi$	osmotic potential difference across the endodermis	MPa

The volumetric water flow J_v is assumed to be the same in all compartments. Osmotic gradients influence water flow when membranes are involved, and thus in the presented model specifically at the endodermis level. Consequently, $\Delta\psi_\pi$ in Eq. 5.2.14 represents the difference in apoplastic osmotic potential between the inner cortex layer and root xylem in the stele: $(\psi_\pi^{x(\text{root})} - \psi_\pi^{\text{cor}})$. The main hydrostatic pressure gradient is also found at the endodermis level, because the membranes have a high hydraulic resistance compared to the rest of the apoplastic path for water transport (Nobel, 1983). In the model the pressure potential in the cortex is assumed to be equal to the pressure potential in the root medium ($\psi_p^{\text{re}}=0$), and the pressure potential in the stele is assumed to be equal to the pressure potential in the root xylem ($\psi_p^{x(\text{root})}$).

The radial solute flow per m root length across the endodermis is given by Eq.5.2.15, which is based on the rate of solute flux across a single membrane (Katchalski and Curran, 1965). It includes, respectively, convective, diffusive and active components of solute transport:

$$J_s^{\text{end}} = C_s^{\text{cor}} (1 - \sigma) J_v + \omega A_f^{\text{end}} \Delta\psi_\pi + J_s^* A_f^{\text{end}} \quad (5.2.15)$$

where:

J_s^{end}	solute flow rate over endodermis per m root length	$\text{mol.s}^{-1}.\text{m}^{-1}$
C_s^{cor}	solute concentration in apoplast inner cortex layer	mol.m^{-3}
ω	solute mobility coefficient per m root length	$\text{mol.s}^{-1}.\text{MPa}^{-1}.\text{m}^{-2}$
A_f^{end}	conversion factor endodermis area/root length	$\text{m}^2.\text{m}^{-1}$
	where $A_f^{\text{end}} = \pi \bar{d}^{\text{stele}}$, and \bar{d}^{stele} = diameter stele	m
J_s^*	active solute flow rate across endodermis	$\text{mol.s}^{-1}.\text{m}^{-2}$

It has to be mentioned that this equation is only valid when there is net inflow of water. The water and solute transport equations used in this study, and by others before (Dalton *et al.*, 1975; Fiscus, 1975) are not a detailed physiological description of the root system, but are meant to be operational. For instance, transport across one membrane is considered, while at least two membranes are involved in water and solute transport. In a steady state situation Eq. 5.2.14 and 5.2.15 may be rewritten to give the standard quadratic form for J_v , which can be solved analytically. The volumetric flow J_v is then a function of $\Delta\psi_p$, ψ_π^{re} , and the parameters σ , ω and J_s^* . The osmotic potential in the xylem in the stele of the root $\psi_\pi^{x(\text{root})}$ is given by:

$$\psi_\pi^{x(\text{root})} = -RT \frac{J_s^{\text{end}}}{J_v} \quad (5.2.16)$$

Using Eq. 5.2.16 in Eq 5.2.15 gives:

$$J_s^{\text{end}} = \frac{C_s^{\text{cor}}(1-\sigma)J_v^2 + (J_s^*A_f^{\text{end}} + \omega A_f^{\text{end}}RT C_s^{\text{cor}})J_v}{J_v + \omega A_f^{\text{end}}RT} \quad (5.2.17)$$

In turn using Eq. 5.2.17 into 5.2.16 gives:

$$\psi_{\pi}^{\text{X(root)}} = \frac{\psi_{\pi}^{\text{cor}}(1-\sigma)J_v + \omega A_f^{\text{end}}RT\psi_{\pi}^{\text{cor}} - RTJ_s^*A_f^{\text{end}}}{J_v + \omega A_f^{\text{end}}RT} \quad (5.2.18)$$

Substitution of Eq. 5.2.18 in Eq. 5.2.14 gives:

$$J_v = Lp_r A_f^{\text{root}} (\Delta\psi_p + \sigma\psi_{\pi}^{\text{cor}}) - \dots \\ \dots Lp_r A_f^{\text{root}} \left(\frac{\psi_{\pi}^{\text{cor}}(1-\sigma)J_v + \omega A_f^{\text{end}}RT\psi_{\pi}^{\text{cor}} - RTJ_s^*A_f^{\text{end}}}{J_v + \omega A_f^{\text{end}}RT} \right) \quad (5.2.19)$$

Eq. 5.2.19 can be rewritten into the standard quadratic form:

$$J_v^2 + J_v (\omega A_f^{\text{end}}RT - Lp_r A_f^{\text{root}} [\Delta\psi_p + \sigma^2\psi_{\pi}^{\text{cor}}]) \dots \\ \dots - Lp_r A_f^{\text{root}} RT (\omega A_f^{\text{end}}\Delta\psi_p + \sigma A_f^{\text{end}}J_s^*) = 0 \quad (5.2.20)$$

Eq. 5.2.20 may be used to solve Eq. 5.2.14 and 5.2.15 analytically. J_v may be calculated for valid combinations of the variables $\Delta\psi_p$ and ψ_{π}^{cor} , and the parameters σ , ω and Lp_r , and the root dimensions. Fiscus (1975) also derived Eq 5.2.18 from the water and solute transport equations.

$$J_v = Lp_r A_f^{\text{root}} \left(\Delta\psi_p + \frac{2\sigma^2\psi_{\pi}^{\text{cor}}}{(1+\sigma)} \right) + \left(\frac{2\sigma Lp_r A_f^{\text{root}} RT J_s^* A_f^{\text{end}}}{J_v(1+\sigma)} \right) \quad (5.2.21)$$

This equation is especially useful in determining characteristics of J_v - $\Delta\psi_p$ relationships: When J_v increases, the last part of Eq. 5.2.21 approaches zero, and the equation becomes linear relating J_v to $\Delta\psi_p$. This linear equation equals the equation of the regression line of the (J_v - $\Delta\psi_p$)-curve at high J_v . Therefore, the slope of the regression line equals $Lp_r A_f^{\text{root}}$ (or Lp_r when J_v is expressed per m^2 root area), while the intercept at the pressure-axis equals $2\sigma^2\psi_{\pi}^{\text{cor}}/(1+\sigma)$. In the previous equations the solute concentration and related osmotic potential in the root cortex are used (C_s^{cor} and ψ_{π}^{cor}). When the solute concentration in the cortex at the endodermis is assumed to be equal to the solute concentration in the root environment C_s^{cor} equals C_s^{re} , and the superscript cor in each equation may be replaced by the superscript re . To describe a possible difference in sol-

ute concentration between root environment and cortex at the endodermis the solute mass balance in the cortex is incorporated.

5.2.3c Solute distribution cortex

Outside the endodermis (root medium, epidermis and cortex layers), radial solute transport is driven by diffusion (Eq. 5.2.22) or mass flow (Eq. 5.2.23), or by both:

$$J_{sd}^{(i-1) \rightarrow i} = D_s A_f^{(i-1) \rightarrow i} \left(\frac{\Delta C}{\Delta x} \right) \quad (5.2.22)$$

where:

- $J_{sd}^{(i-1) \rightarrow i}$ diffusional solute flow between two compartments $\text{mol.s}^{-1}.\text{m}$
- $A_f^{(i-1) \rightarrow i}$ conv. factor boundary area / root length $\text{m}^2.\text{m}^{-1}$
- D_s solute diffusion coeff. in the apoplast of the root cortex $\text{m}^2.\text{s}^{-1}$
- ΔC solute conc. difference between two compartments mol.m^{-3}
- Δx diffusion distance between the compartments (i-1) and i m^{-1}

$$J_{sc}^{(i-1) \rightarrow i} = J_v \times C_s^{(i-1)} \quad (5.2.23)$$

where:

- $J_{sd}^{(i-1) \rightarrow i}$ solute mass flow between the compartments (i-1) and i $\text{mol.s}^{-1}.\text{m}^{-1}$
- J_v water flow per m root length $\text{m}^3.\text{s}^{-1}.\text{m}^{-1}$
- $C_s^{(i-1)}$ solute concentration in the upstream compartment mol.m^{-3}

Solute mass balance equations for the epidermis layer and all cortex layers except the most inner one are given by:

$$\frac{dS^i}{dt} = \left(J_{sc}^{(i-1) \rightarrow i} + J_{sd}^{(i-1) \rightarrow i} \right) - \left(J_{sc}^{i \rightarrow (i+1)} + J_{sd}^{i \rightarrow (i+1)} \right) \quad (5.2.24a)$$

where:

- $\frac{dS^i}{dt}$ net solute flow into compartment i mol.s^{-1}

The solute mass balance equation for the cortex layer at the endodermis is given by:

$$\frac{dS^i}{dt} = \left(J_{sc}^{(i-1) \rightarrow i} + J_{sd}^{(i-1) \rightarrow i} \right) - J_s^{end} \quad (5.2.24b)$$

and for the xylem of the root by:

$$\frac{dS^{x(\text{root})}}{dt} = J_s^{end} - J_v C_s^{x(\text{root})} \quad (5.2.24c)$$

The solute mass balance equations were used to calculate the solute concentrations per compartment:

$$C^i = \frac{S^i}{\left(0.25\pi \left(d_{out}^i{}^2 - d_{in}^i{}^2 \right) \times f_{apo} \right)} \quad (5.2.25)$$

where:

C^i	solute conc in apoplast compartment i	mol.m^{-3}
S^i	amount of solutes in compartment i per m root	mol.m^{-1}
d_{out}^i	outer diameter circular compartment i	m
d_{in}^i	inner diameter circular compartment i	m
f_{apo}	fraction apoplast of total volume compart. i	-

Using Van 't Hoffs law osmotic potentials per compartment could be calculated. The osmotic potentials of root xylem and cortex layer at the outer side of the endodermis were used to calculate the gradient in osmotic pressure ($\Delta\psi_\pi$) which influences J_v (Eq. 5.2.14).

5.3 Parameters of the model

The parameters in the model may be divided into parameters associated with the xylem network (hydraulic xylem resistances; $R^{x(n)}$), parameters associated with the tissues adjacent to the xylem ($C_p^{(n)}$, $R_{eff}^{(n)}$, $f_{sym}^{(n)}$, $\psi_n^{(n, sat)}$) and parameters associated with the water and solute uptake of the roots. Values for the xylem resistances in the model are based on values derived from literature. Values for the parameters associated with the adjacent tissues are determined experimentally. Values for the parameters concerning water and solute uptake by the roots are derived from literature.

5.3.1 Parameters concerning the xylem network in the sub-model WRTomSim

Many researchers quantified xylem resistances: A proportion of 2.5:1:1 is often mentioned for the absolute hydraulic resistances of roots, stems and leaves (Cowan and Milthorpe, 1968; Milthorpe and Moorby, 1979). In literature, hydraulic xylem resistances are often given as absolute values which depend on the characteristics (size, age) of the plant considered. To compare xylem between organs and species, they are sometimes expressed per volume or length unit. The latter because it is generally assumed that resistances are proportional with the length of the transport path (see Eq. 2.18). In the present model the resistances in the xylem network are based on values obtained by Dimond (1966). He presented an extensive study on xylem resistances of individual leaves and stem segments of a tomato plant (Table 5.3.1).

Table 5.3.1: Specific hydraulic xylem resistances of stem internodia and absolute hydraulic xylem resistances of leaves of tomato at different plant heights (after Dimond, 1966)^a.

Internode No. ^b	$R^{x(stem)}$	$R^{x(leaf)}$
[-]	($m^{-3} s MPa$) m^{-1}	$m^{-3} s MPa$
2	7.6×10^7	9.6×10^8
4	6.0×10^6	2.7×10^8
8	6.1×10^6	1.3×10^8
12	1.4×10^7	5.0×10^7
15	7.3×10^8	1.3×10^8

^a obtained on a 16 internodia "tall" plant

^b counted from bottom upwards

Dimond's observations were roughly in agreement with values of xylem resistances in tomato reported by Jensen *et al.*, (1961). He observed that xylem resistances of petioles and stem segments changed with position on the plant: in the base of the plant the

resistance of the xylem in the stem was somewhat higher than in the middle of the plant while it increased again in the top of the plant. The resistance of the xylem in the petiole on leaf initially decreased with plant height but increased in the quick growing region at the top of the plant. Values for the absolute hydraulic resistances of the stem segments between two layers in the model ($R^{x(\text{stem } 1)}$, $R^{x(\text{stem } 2)}$ and $R^{x(\text{stem } 3)}$; Figure 5.2.1) are estimated from the specific hydraulic resistances of the stem internodia observed by Dimond and the length of the stem segments between two layers in the model. The substitute hydraulic resistance for the leaf xylem per layer (e.g. $R^{x(\text{leaf } 3)}$; Figure 5.2.1) depends on the position of the leaves on the plant and the number of leaves per layer: all leaves per layer are assumed in parallel and connected to the stem xylem in the middle of a layer.

5.3.2. Determination of tissue related parameters in WRShoot

Values for the tissue-related parameters (C_p^t , $R_{\text{eff}}^{1(n)}$, f_{sym} and $\psi_n^{1(\text{sat})}$) are determined experimentally on leaves of mature tomato plants. Comparable determinations were done on root systems and stem segments of tomato. However, no reliable parameter values were obtained on the latter due to experimental problems. In the model values of the root and stem parameters were assumed to be equal to values of the corresponding leaf parameters.

Determination of the parameters C_p^t , f_{sym} and $\psi_n^{1(\text{sat})}$

C_p^t , f_{sym} and $\psi_n^{1(\text{sat})}$ were determined on mature leaves of tomato plants (*Lycopersicon esculentum* Mill. cv Counter), which were grown on water culture in a greenhouse at 5 mS cm⁻¹ salinity level (Van Ieperen, 1996). The parameters f_{sym} and $\psi_n^{1(\text{sat})}$ were derived from so-called pressure-volume (PV) curves (Turner, 1987), which relate the inverse of ψ_w^t and RWC^t (Figure 5.3.1). The parameters f_{sym} and $\psi_n^{1(\text{sat})}$, and the measured combinations of ψ_w^t and RWC^t were used to construct so-called Höfler diagrams (Figure 5.3.2). The inverse of the slope of the ψ_w^t - RWC^t relationship in this curve equals the parameter C_p^t . For accurate determination of PV-curves an automated version of a Scholander-type pressure bomb (Figure 5.3.3) was used. To find out whether the parameter values were independent of leaf size and light conditions during growth, determinations were done on leaves of different sizes (1.5-3.5 g) and grown in summer and autumn.

PV-relationships were determined using the following procedure: leaves were cut in dark under water and allowed to rehydrate to full turgidity during 12 hours in dark. After measuring the initial (saturated) weight of the leaf, it was sealed in a plastic bag (to prevent leaf transpiration) and placed in the pressure bomb. Pressure was increased with pressure steps of 0.2 MPa from 0 MPa to 1 MPa followed by pressure

steps of 0.5 MPa until 2 MPa was reached. Rates of pressure change in the bomb never exceeded 6 MPa h⁻¹. Each pressure level (± 0.01 MPa) was maintained for about 1 h. Expressed sap was collected in a plastic container filled with tissue paper, which was placed on the cut end of the leaf outside the pressure bomb. The volume of expressed sap was measured by weighing the plastic container. Leaf water potential was measured after each pressure step. After finishing the measurements in the pressure bomb all leaves were dried in a ventilated oven (7 d, at 65 °C) and leaf dry weight was determined. From the weight measurements RWC^t was calculated and related to $1/\psi_w^t$ in PV-curves.

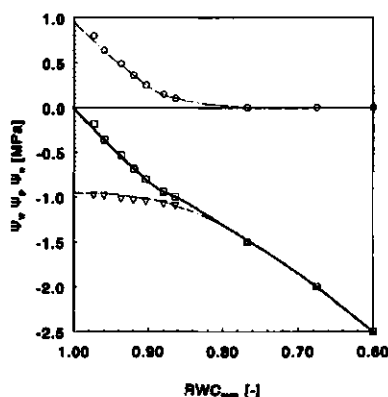
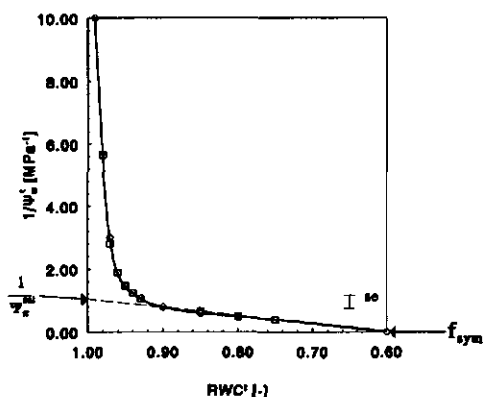


Figure 5.3.1: Pressure-Volume relationship measured on a representative tomato leaf.

Figure 5.3.2: Höfler-diagram constructed from the PV-relationship in Figure 5.3.1. $\psi_p(\circ)$, $\psi_w^t(\square)$ and $\psi_w(\nabla)$.

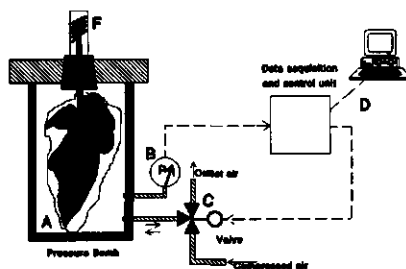


Figure 5.3.3: Automated version of a Scholander type pressure bomb. Pressure level and rates of pressure increase and decrease in the bomb were measured and controlled using a pressure transducer (Valedine, UK) (B) and an adjustable valve (C). Data acquisition and control of the valve were conducted by a datalogger (Datataker DT100, Australia) in combination with a personal computer (HP-Vectra, Hewlett Packard, US) (D). Expressed sap from the leaf (A) was collected in a plastic container filled with tissue paper (F) outside the pressure bomb.

The parameters $\psi_x^{(sat)}$ and f_{sym} were obtained from the measured PV-relationships according to Turner (1987) (Figure 5.3.1). $\psi_x^{(sat)}$, f_{sym} and the measured combinations of ψ_w^i and RWC^i were used to calculate RWC_{sym}^i and to construct a Höfler diagram (Figure 5.3.2). The inverse of the slope of the (ψ_p^i - RWC_{sym}^i)-relationship in the Höfler diagram provides the relative pressure-based hydraulic capacitance (C_p^i) of the leaf tissue.

Determination of the time constant of leaf tissue (τ^i) and the parameter R_{eff}^i :

To determine τ^i time response curves of changes in average leaf water potential and leaf water content were measured on excised leaves of tomato after a change in external pressure. Measured data were fitted on Eq. 5.2.13 to obtain τ^i . The parameter R_{eff}^i was calculated from τ^i and C_p^i according to Eq. 5.2.12. The time-response curves were determined using the automated version of the pressure bomb and leaves grown in summer and autumn on a constant salinity level (5 mS cm⁻¹; Van Ieperen, 1996):

After measuring its initial (saturated) weight, the leaf was placed in the pressure bomb. Its average water potential was measured and pressure in the bomb was increased to 1.0 MPa at a rate of about 30 MPa h⁻¹. Expressed sap was collected in a plastic container which was filled with tissue paper. After 60-90 seconds at a constant pressure level (1.0 MPa), pressure was decreased to a level just below the last measured average water potential. Volume of the expressed sap was measured by weighting the plastic container. Average water potential in the leaf was determined by slowly increasing

the pressure (at a rate of ± 6 MPa h⁻¹) until sap began to appear at the cut surface. This pressure was taken as the average water potential in the tissue. Pressure was increased to 1.0 MPa again and was kept constant for another 60-90 seconds. The duration of the period at 1.0 MPa, weight of expressed sap and average water potential were recorded per period. This procedure was repeated until the average water potential in the leaf reached 1.0 MPa. Final fresh weight was measured. Dry weight was measured after at least 5 d of drying in a ventilated oven (65 °C). ψ_w^i was plotted against time (Figure 5.3.4) and τ^i estimated by fitting the measured data on Eq. 5.2.13.

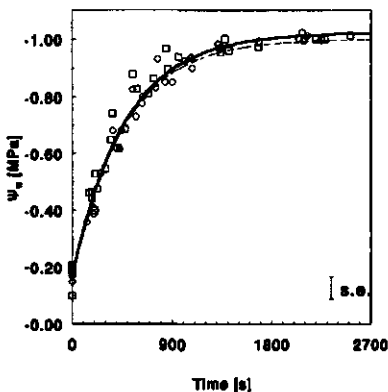


Figure 5.3.4: Time response curve of the leaf water potential after a change in pressure potential outside the leaf. Measured on leaves grown in summer (\square) and autumn (\circ). The pressure potential was altered from atmospheric pressure to 1.0 MPa at $t=0$ s.

RWC^t at each average water potential was calculated using the initial saturated fresh weight, leaf dry weight and measured weight loss per period. The RWC^t- ψ_w^t combinations, determined in this way, were used to construct the PV-relationships and related Höfler-diagrams. f_{sym} , $\psi_x^{(sat)}$ and C_p^t were calculated as described above. The determination of C_p^t differed from the method described above by its relative short equilibrium time per water potential/RWC^t measurement. Finally, R_{eff}^t was calculated as τ^t/C_p^t (Eq. 5.2.12).

Results and Discussion

Results of the parameter determinations using the long equilibrium time on leaves grown in summer and autumn are summarised in Table 5.3.2. Results of the determinations of τ^t , and of C_p^t and R_{eff}^t using the short equilibrium time on leaves grown in summer and autumn are summarised in Table 5.3.3. Observed parameter values were independent of leaf size (results not shown) and season.

Table 5.3.2: Osmotic potential at saturation ($\psi_x^{(sat)}$), fraction symplastic volume (f_{sym}) and the normalised pressure-based capacitance of leaf tissue (C_p^t) derived from pressure-volume curves. Averages and standard errors.

Season	Tissue	$\psi_x^{(sat)}$ [MPa]	f_{sym} [-]	C_p^t [(m ³ MPa ⁻¹).m ³]	n
Summer	leaf	-0.95 ± 0.012	0.60 ± 0.032	0.117 ± 0.0031	10
Autumn	leaf	-0.93 ± 0.024	0.58 ± 0.018	0.135 ± 0.0071	10

¹ Relative: per m³ symplastic water content at full turgor; ² Relative: × m³ symplastic water content at full turgor; ³ Averages ± standard error

Table 5.3.3: Time constants (τ^t), relative pressure-based hydraulic capacitance's (C_p^t) and relative effective hydraulic resistances (R_{eff}^t) determined on leaves of mature tomato plants. Averages and standard errors.

Season	τ^t	C_p^t	R_{eff}^t	n
[-]	[s]	[m ³ MPa ⁻¹ m ³]	[m ³ s MPa m ³]	[-]
Summer	471 ± 28.3	0.127 ± 0.0421	3283 ± 721.8	10
Autumn	465 ± 26.1	0.139 ± 0.0162	3345 ± 149.6	10

All values for C_p^t obtained in present determinations are comparable. Values for C_p^t in literature differ between species and organs, and roughly range between 0.07 and 0.35 m³.MPa⁻¹.m³ (e.g. Jordan and Nobel, 1983; Turner, 1987). The observed values for C_p^t (Table 5.3.2 and Table 5.3.3) are considerably lower than the values which follow from

PV-relationships reported on tomato by Slatyer (1962) and Behboudian (1977): $0.12 \text{ m}^3 \cdot \text{MPa}^{-1} \cdot \text{m}^{-3}$ versus 0.20 and $0.23 \text{ m}^3 \cdot \text{MPa}^{-1} \cdot \text{m}^{-3}$, respectively. This indicates a higher drought resistance of the plants in our experiments because the ability to maintain a high relative water content at conditions of water stress is higher. Although the observed value of C_p^i is within the normally observed range, some remarks have to be made about this parameter:

C_p^i is closely related to the inverse of the bulk modulus of elasticity ($\bar{\epsilon}$) of a multicellular tissue (see Eq. 2.15). It is well known that $\bar{\epsilon}$ is pressure and volume dependent and not a constant (Tyree and Jarvis, 1986). $\bar{\epsilon}$ may change on a relative short time. Schultz and Matthews (1993) for example observed that $\bar{\epsilon}$ of leaves of wine grape (*Vitis vinifera* L.) increased almost twofold within several days after withholding water from the plant roots. From ϵ measurements on single cells using the pressure probe, it may be expected that C_p^i also changes with cell volume on the very short-term (within min-hours) (Steudle *et al.*, 1977). Therefore, it has to be noted that the assumption that C_p^i is a constant on the short-term, as is done in present and many other plant water relation models (e.g. Bruggink *et al.*, 1988; Nobel and Jordan, 1983) could be false, and may cause errors in the simulation results.

The observed time constants for changes in leaf water content and leaf water potential are rather short (Table 5.3.3), which indicates a close relation between water potentials in the conducting vessels of the xylem and in the surrounding tissue. The calculated values for R_{eff}^i are of the same order as values for the hydraulic resistance of cells or tissues of higher plants as reported by e.g. Cosgrove (1985) and Nonami and Boyer (1990).

Standard values for all xylem and tissue related parameters in the sub-model WRTomSim are summarised in Table 5.3.4.

Table 5.3.4: Standard values for hydraulic xylem resistances, and tissue related parameters in present model study^a.

$R^{x(\text{root-stem1})}$	7.5×10^6	$\text{m}^{-3} \cdot \text{s} \cdot \text{MPa}$	$R^{x(\text{leaf1})}$	4.5×10^7	$\text{m}^{-3} \cdot \text{s} \cdot \text{MPa}^{-1}$
$R^{x(\text{stem1-stem2})}$	4.0×10^6	$\text{m}^{-3} \cdot \text{s} \cdot \text{MPa}$	$R^{x(\text{leaf2})}$	1.5×10^7	$\text{m}^{-3} \cdot \text{s} \cdot \text{MPa}^{-1}$
$R^{x(\text{stem2-stem3})}$	6.6×10^6	$\text{m}^{-3} \cdot \text{s} \cdot \text{MPa}$	$R^{x(\text{leaf3})}$	1.0×10^7	$\text{m}^{-3} \cdot \text{s} \cdot \text{MPa}^{-1}$
C_p^i	0.12	$\text{m}^3 \text{MPa}^{-1} \text{m}^{-3}$	f_{sym}	0.4	-
R_{eff}^i	3300	$\text{m}^{-3} \cdot \text{s} \cdot \text{MPa} \cdot \text{m}^3$	$\psi_{\text{r}}^{\text{sat}}$	-0.95	MPa

^a concerning a 2 m height, 30 leaves, 1250 g fresh weight tomato plant.

5.3.3 Parameters in the sub-model 'WURoot'

Most of the parameters used in the sub-model 'WURoot' were derived from literature. Only the parameters concerning the dimensions of the root system were derived from measurements. All parameters are summarised in Table 5.3.5.

Table 5.3.5: Standard values of the model parameters used in present study. Values are for tomato (unless indicated different).

Name	Description	Value	Units	
L_{pr}	Hydraulic Conductivity Root System	6.1×10^{-8}	$m^3 \cdot s^{-1} \cdot MPa^{-1} \cdot m^{-2}$	^{a,b}
σ	Reflection Coefficient	0.9	-	^c
J_s^*	Active Solute Transport Rate	1×10^{-7}	$mol \cdot s^{-1} \cdot m^{-2}$	^g
ω	Diffusional Solute Mobility Coefficient	1×10^{-7}	$mol \cdot s^{-1} \cdot MPa^{-1} \cdot m^{-2}$	^g
d_r	Average Root Diameter	0.40×10^{-3}	m	^{b,e}
d_s	Average Diameter Stele of the Root	0.13×10^{-3}	m	^e
D_s	Diffusion Coefficient	1×10^{-9}	$m^2 \cdot s^{-1}$	^d
F_{apo}	Apoplastic Volume Fraction in Root	0.05	-	^f
A_f	Root Surface Area / length Ratio	πd_r	$m^2 \cdot m^{-1}$	-

^a Salim and Pitman (1984); ^b Shalhevet *et al.* (1976); ^c Mees and Weatherley (1957); ^d Weast (1981); ^e Esau (1960); ^f Newman (1974);

^g values of soybean: *Fiscus* (1977, 1986)

The parameter values in Table 5.3.4 and Table 5.3.5 are the standard values for the parameters in the model used during simulations. The dimensions of the plant in the model are the dimensions of plant 1 given in Table IA in Chapter 3.4.

5.4 Simulations

5.4.1 Simulation results root part of the model: "WURoot"

It is assumed that salinity mainly influences plant water status via an effect on the water uptake by the roots. Therefore special attention was given to the root part of the model simulating the water uptake. Simulations were done to investigate the differences between the models for water uptake based on: a) the simple Ohm's law analogue (simple model); b) the Ohm's law analogue including coupled solute and water uptake (extended model); c) the extended model including the solute mass balance in the cortex of the root. Sensitivity analysis were done on parameters in the models. The latter model (c) was used to investigate whether the solute accumulation at the endodermis could occur and whether it influences the water uptake and water status in the plant significantly.

Steady State Simulations

In the simulations the pressure potential in the root xylem was varied between 0 and -1 MPa. The simulation results are presented in $(\Delta\psi_p - J_v)$ - and $(\Delta\psi_p - \psi_\pi)$ -relationships.

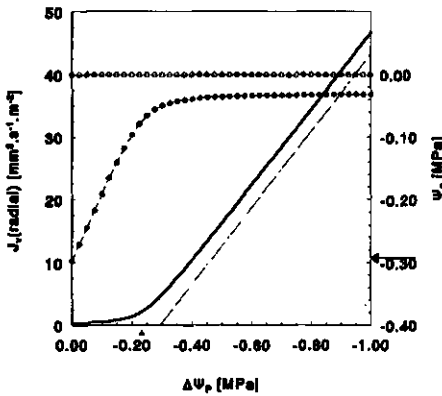


Figure 5.4.1: Simulated $(\Delta\psi_p - J_v)$ - and $(\Delta\psi_p - \psi_\pi^x)$ -relationships. J_v : simple Ohm's Law analogue (—) and model including coupled solute and water flow (---) (extended model). $\psi_\pi^{x(\text{root})}$ simple model (o o o) and extended model (• • •) The horizontal arrow on the ψ_π -axis indicates the osmotic potential of the root medium. Root surface area was 1 m^2 , all other parameter values see Table 5.3.5.

The surface area of the simulated root was 1 m^2 , which corresponded with a root system of $\pm 100 \text{ g}$ (Shalhevet *et al.*, 1976), the other parameters were as given in Table 5.3.5. The solute concentration in the root medium was 120 mmol.m^{-3} , which corresponded with an osmotic potential of $\pm -0.29 \text{ MPa}$. The results of the extended model were calculated with different computer programs: one using the analytical solution of Eq. 5.2.21, and the other using an iterative algorithm program based on Eq. 5.2.14 and 5.2.15. Simulations results obtained with the two computer programs were equal. The iterative algorithm was further used as the basis for a simulation model including the solute mass balance in the cortex of the root.

Contrary to the results of the simple model, simulated $(\Delta\psi_p-J_v)$ and $(\Delta\psi_p-\psi_\pi^{x(\text{root})})$ -relationships (Figure 5.4.1) from the extended model were qualitatively in good agreement with the commonly observed non-linear relationships obtained by experiments on excised root systems (Figure 5.2.5B; Mees and Weatherley, 1957; Lopuchinsky, 1964; Fiscus, 1977). The simulated $(\Delta\psi_p-J_v)$ -relationship was about linear above a J_v of $10 \text{ mm}^3 \cdot \text{s}^{-1} \cdot \text{m}^{-2}$ ($\Delta\psi_p < -0.35 \text{ MPa}$), where the curve approached a straight line with a slope of $6.1 \times 10^{-8} \text{ m}^3 \cdot \text{s}^{-1} \cdot \text{MPa}^{-1} \cdot \text{m}^{-2}$, which was equal to L_p , ($= 1/R^{\text{root}}$). The intercept on the pressure-axis was equal to $(2\sigma^2/(1+\sigma))\psi_\pi^{\text{cor}}$. ($= 0.85\psi_\pi^{\text{cor}}$; see Eq. 5.2.21). Below a J_v of about $10 \text{ mm}^3 \cdot \text{s}^{-1} \cdot \text{m}^{-2}$ the $(\Delta\psi_p-J_v)$ and $(\Delta\psi_p-\psi_\pi^{x(\text{root})})$ -relationships were not linear: $\psi_\pi^{x(\text{root})}$ strongly increased with decreasing $\Delta\psi_p$, due to dilution of the solute concentration in the xylem sap by increasing water flow. Consequently, the absolute value of $\Delta\psi_\pi$ over the endodermis increased, which, due to the direction of the potential difference, increasingly opposed J_v . Above a J_v of $10 \text{ mm}^3 \cdot \text{s}^{-1} \cdot \text{m}^{-2}$, $\psi_\pi^{x(\text{root})}$ was about constant. From then on, further dilution of the xylem sap by an increasing J_v was counterbalanced by an increasing solute flow across the endodermis, since the convective term of the solute flow (Eq. 5.2.15) prevailed and depended upon J_v . Consequently, the osmotic gradient in Eq. 5.2.14 became a constant and J_v was linearly related to $\Delta\psi_p$.

To investigate the sensitivity of the extended model for important parameters, the parameters were altered and changes in the curvature of the simulated $(\Delta\psi_p-J_v)$ -relationships were investigated:

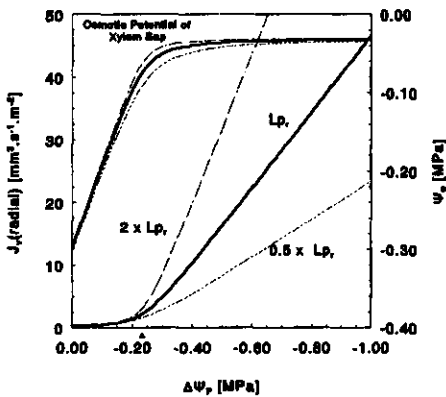


Figure 5.4.2A: Sensitivity of simulated $(\Delta\psi_p-J_v)$ and $(\Delta\psi_p-\psi_\pi^{x(\text{root})})$ -relationships for changes in L_p , ($= 1/R^{\text{root}}$). All other parameter values see Table 5.3.5.

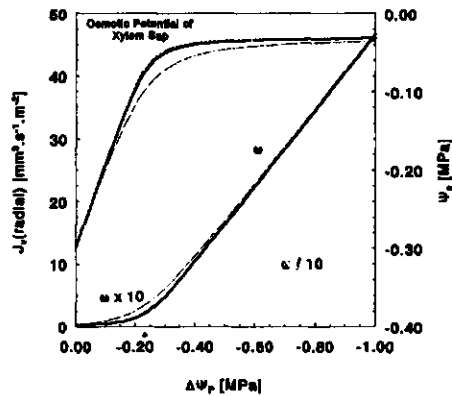


Figure 5.4.2B: Sensitivity of simulated $(\Delta\psi_p-J_v)$ and $(\Delta\psi_p-\psi_\pi^{x(\text{root})})$ -relationships for changes in ω . All other parameter values see Table 5.3.5.

As expected, the parameter L_p influenced the slope at high J_v (Figure 5.4.2A). Increasing ω and J_s^* increased the net solute uptake rate across the endodermis (Eq. 5.2.15). As a result $\psi_n^{x(\text{root})}$ increased slower with increasing J_v , which influenced the curvature of the $(\Delta\psi_p-J_v)$ -relationship at low J_v (Figure 5.4.2B and C).

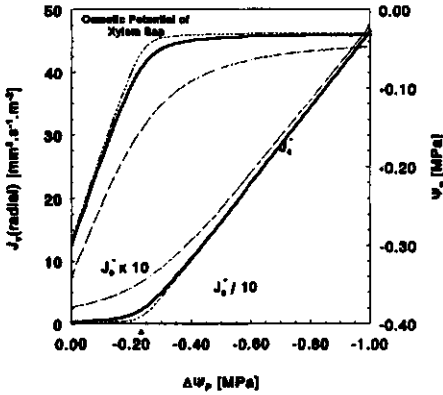


Figure 5.4.2C: Sensitivity of simulated $(\Delta\psi_p-J_v)$ and $(\Delta\psi_p-\psi_n^{x(\text{root})})$ -relationships for changes in J_s^* . All other parameter values see Table 5.3.5.

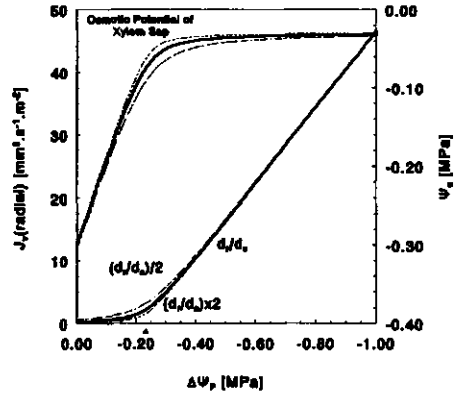


Figure 5.4.2D: Sensitivity of simulated $(\Delta\psi_p-J_v)$ and $(\Delta\psi_p-\psi_n^{x(\text{root})})$ -relationships for changes in the position of the endodermis in the root. All other parameter values see Table 5.3.5.

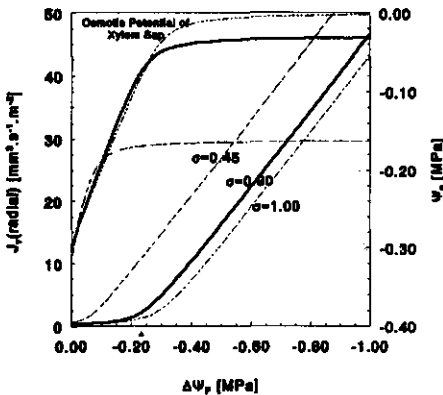


Figure 5.4.2E: Sensitivity of simulated $(\Delta\psi_p-J_v)$ and $(\Delta\psi_p-\psi_n^{x(\text{root})})$ -relationships for changes in σ . All other parameter values see Table 5.3.5.

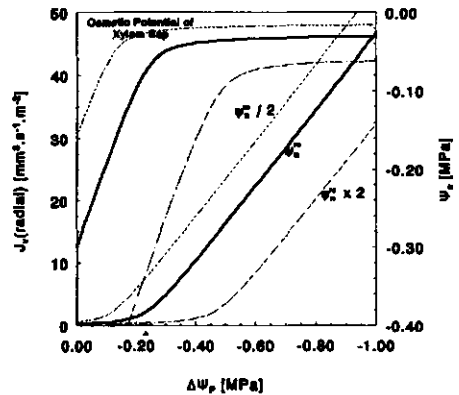


Figure 5.4.2F: The effect of different osmotic potentials in the root medium (ψ_n^{ic}) on simulated $(\Delta\psi_p-J_v)$ and $(\Delta\psi_p-\psi_n^{x(\text{root})})$ -relationships. ($\psi_n^{ic} = -0.18$ MPa). Parameter values see Table 5.3.5.

Decreasing ω and J_s^* did not influence the $(\Delta\psi_p-J_v)$ -relationship significantly, probably because the effect of the osmotic component in the driving force of the water uptake rate was low at high J_v . Changing the position of the endodermis in the root (d_r/d_s) in the model hardly influenced the $(\Delta\psi_p-J_v)$ -relationship (Figure 5.4.2D).

Increasing σ (Figure 5.4.2E) shifted the $(\Delta\psi_p-J_v)$ -relationship as a whole along the $\Delta\psi_p$ axis to the right. This improved the simulation results because the simulated $(\Delta\psi_p-J_v)$ -relationship shifted in the direction of the measured $(\Delta\psi_p-J_v)$ -relationship (see 5.2.3; Figure 5.2.5B). However, even at maximal σ ($\sigma=1$) the $(\Delta\psi_p-J_v)$ -relationship was not shifted far enough along the $\Delta\psi_p$ -axis to meet the measured data of e.g. Lopuchinsky (1964). According to Eq. 5.2.21 the other parameters in the model will not influence the simulated $(\Delta\psi_p-J_v)$ -relationship at high J_v , because the last part of Eq. 5.2.21 can be neglected at high J_v . Therefore it can be concluded that the measured $(\Delta\psi_p-J_v)$ -relationship cannot entirely be described by the model based on Eq. 5.2.14 and 5.2.15. Decreasing the boundary variable ψ_n^{cor} (equals ψ_n^{ro} in the simple model) shifted the $(\Delta\psi_p-J_v)$ -relationship as a whole to the right (Figure 5.4.2F) and thus in the direction of the measured data (Figure 5.2.5B). In order to explain the difference between simulated and measured data, Fiscus (1977) suggested that the effective ψ_n^{cor} might have been lower than the applied ψ_n^{ro} . Although this idea seems in agreement with the model output presented in Figure 5.4.2F, it has to be mentioned that ψ_n^{cor} is probably not a constant but a variable, which depends on several parameters and variables (e.g. J_v).

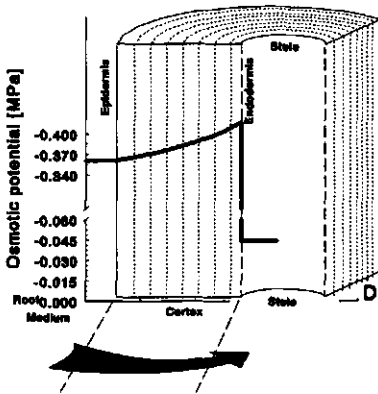


Figure 5.4.3: Radial distribution of the osmotic potential in the root, when the solute mass balance in the cortex is incorporated in the model. $\psi_n^{ro} = -0.36$ MPa; $J_v = 40$ mg.s⁻¹; other parameters see Table 5.3.5.

To show the effect of the incorporation of the cortex solute mass balance in the model, comparisons were made between the extended model without and the extended model with this solute mass balance incorporated. Iterative computer programs were used to calculate the solute concentration distribution in the cortex and $(\Delta\psi_p-J_v)$ and $(\Delta\psi_p-\psi_n^{x(root)})$ -relationships.

Adding the solute mass balance in the cortex to the model changed the simulation output clearly: without the solute mass balance incorporated the osmotic potential at the cortex side of the endodermis (ψ_n^{cor}) was equal to ψ_n^{ro} . With the

solute mass balance incorporated ψ_n^{cor} decreased below ψ_n^{e} due to a higher solute concentration at the cortex side of the endodermis than in the root medium (Figure 5.4.3).

The radial distribution of the solute concentration in the root mainly depends on the solute concentration in the root medium and the rate of water uptake (Table 5.4.1): The accumulation of solutes at the endodermis increased (ψ_n^{cor} decreased) with increasing rate of water uptake (J_v) and with increasing solute concentration in the root medium (C^{re}). At the combination of a low C^{re} and a low J_v , $\psi_n^{\text{x(root)}}$ was lower than ψ_n^{cor} , mainly due to the active uptake of solutes in combination with a low uptake of water (low dilution of the xylem sap). Consequently, $\Delta\psi_n$ favoured water uptake instead of opposing it. The osmotic part of the driving force for water uptake (Eq. 5.2.14) was relative high compared with the pressure part ($\Delta\psi_p$): This type of osmotic driven water uptake is known as root pressure.

At low C^{re} and high J_v , a small decrease in ψ_n^{cor} was simulated due to accumulation of solutes at the endodermis. The influence of this decrease on J_v was low because the relative importance of $\Delta\psi_n$ in the driving force for water uptake was low. Only at high C^{re} and high J_v , ψ_n^{cor} was significantly decreased with a clear effect on the rate of water uptake.

Table 5.4.1: Radial distribution of osmotic potentials in the root, simulated at different combinations of solute concentrations in the root environment (C^{re}) and rates of water uptake (J_v).

C^{re} mmol.m ⁻³	J_v mg.s ⁻¹	$\psi_n^{\text{re a}}$ MPa	$\psi_n^{\text{cor b}}$ MPa	$\psi_n^{\text{x(root) c}}$ MPa	$\Delta\psi_n^{\text{d}}$ MPa	$\Delta\psi_p^{\text{e}}$ MPa
10	2.0	-0.024	-0.024	-0.042	-0.018	-0.017
10	40.0	-0.024	-0.026	-0.005	0.021	-0.675
120	2.0	-0.292	-0.293	-0.078	0.215	-0.226
120	40.0	-0.292	-0.320	-0.035	0.285	-0.913

^a osmotic potential in root medium; ^b osmotic potential at cortex side of endodermis; ^c osmotic potential at stele (xylem) side of endodermis; ^d $\Delta\psi_n = \psi_n^{\text{x(root)}} - \psi_n^{\text{cor}}$; ^e pressure potential difference between root xylem and root environment.

In none of the simulations ψ_n^{cor} increased above ψ_n^{e} , which means that the import of solutes by diffusion and mass flow was sufficient to meet the solute uptake across the endodermis. As soon as $\psi_p^{\text{x(root)}}$ decreases due to transpiration, ψ_n^{cor} decreases due to solute accumulation, and $\psi_p^{\text{x(root)}}$ increases due to dilution of the xylem sap.

Incorporation of the cortex solute mass balance in the model changed the simulated ($\Delta\psi_p$ - J_v)-relationship clearly (Figure 5.4.4): It remained approximately linear

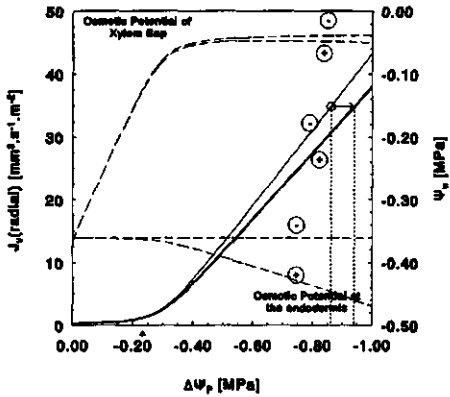


Figure 5.4.4: Effect of including the solute mass balance in the model on simulated $(\Delta\psi_p-J_v)$, and $(\Delta\psi_p-\psi_\pi^{x(\text{root})})$ and $(\Delta\psi_p-\psi_\pi^{\text{cor}})$ -relationships. Simulations extended model without (-), and with the solute mass balance incorporated (+). $\psi_\pi^{\text{re}} = -0.36$ MPa, other parameter values see Table 5.3.5.

at high J_v , but the slope of the regression line was lower. Consequently, this slope did not reflect the input parameter L_p , anymore.

The lower values for J_v with increasing $|\Delta\psi_p|$, compared to simulations without solute mass balance incorporated, were due to an increasing osmotic gradient across the endodermis, mainly due to a decreasing ψ_π^{cor} with increasing J_v .

The high linearity of the simulated $(\Delta\psi_p-J_v)$ -curve at high J_v is not in agreement with the expected shape (Figure 5.2.5B) proposed by Passioura (1984). Passioura assumed a stronger build-up of solutes at the endodermis with increasing J_v , probably because he did not account for solute uptake across the endodermis.

Passioura's assumption that $\sigma = 1$ causes overestimation of the effect of the osmotic gradient upon J_v . Ignoring solute flow across the endodermis influences the solute mass balances at both sides of the endodermis, thus ignoring a lowering effect upon the osmotic gradient. A lower osmotic gradient increases J_v , because J_v proceeds against the osmotic gradient. In these simulations the increase in $\Delta\psi_\pi$ with increasing J_v is small compared to the required increase in pressure difference necessary to obtain the increase in J_v . As a result the $(\Delta\psi_p-J_v)$ -relationship still seems linear, although with a smaller slope.

A sensitivity analysis on the comprehensive model showed that the solute concentration in the root medium as well as σ and the diffusion coefficient for solutes in the cortex (D_s) influence the slope greatly (Table 5.4.2). The model is very sensitive for D_s . The standard value for D_s (Table 5.3.5) equals the diffusion coefficient for small solutes in free water, and could be much lower due to interactions between solutes and wall material (Newman, 1971). The length of the diffusion path is also uncertain and could be larger than is assumed in the model. For tomato values for σ between 0.76 and 0.98 were reported (Table 5.3.5). For other species this range was much smaller: σ was seldom lower than 0.85. Therefore we choose a standard value of 0.90 for the σ of tomato roots (Shalhevet *et al.*, 1976). σ also influenced the slope of the $(\Delta\psi_p-J_v)$ -

relationship at high J_v (Table 5.4.2). The solute concentration in the root environment influences the slope of the $(\Delta\psi_p-J_v)$ -relationship greatly (Table 5.4.2).

Table 5.4.2: Change in slope^a of the simulated $(J_v-\Delta\psi_p)$ curve at high J_v , due to changes in solute concentration in the root environment (C^r) at different values of the diffusion coefficient for solutes in the apoplast of the cortex and epidermis (D_s) and at different values of the reflection coefficient of the endodermis (σ).

C^r [mol.m ⁻³]	Slope [m ³ .s ⁻¹ .MPa ⁻¹ .m ⁻²]			
	$D_s = 1 \times 10^{-9} \text{ m}^2.\text{s}^{-1}$	$D_s = 5 \times 10^{-10} \text{ m}^2.\text{s}^{-1}$	$D_s = 1 \times 10^{-10} \text{ m}^2.\text{s}^{-1}$	
60	6.01×10^{-8}	5.92×10^{-8}	5.01×10^{-8}	
120	5.90×10^{-8}	5.70×10^{-8}	4.19×10^{-8}	
240	5.68×10^{-8}	5.28×10^{-8}	3.35×10^{-8}	
C^r [mol.m ⁻³]	$\sigma=0$	$\sigma=0.7$	$\sigma=0.9$	$\sigma=1.0$
60	6.10×10^{-8}	6.06×10^{-8}	6.01×10^{-8}	5.96×10^{-8}
120	6.10×10^{-8}	6.02×10^{-8}	5.90×10^{-8}	5.80×10^{-8}
240	6.10×10^{-8}	5.94×10^{-8}	5.68×10^{-8}	5.47×10^{-8}

^a Slope of the regression line on the simulated $(J_v-\Delta\psi_p)$ curve between -0.6 and -1.0 MPa. $Lp_r = 6.1 \times 10^{-8} \text{ m}^3.\text{s}^{-1}.\text{MPa}^{-1}.\text{m}^{-2}$. The other parameters used in the model were those in Table 5.3.5

From these steady state simulation results three important conclusions can be drawn.

1. Assuming that solutes accumulate in the cortex, data obtained in experiments to determine Lp_r have to be interpreted carefully: Curves similar to Fig. 5.2.5B may be obtained, while the slope of these curves at high J_v and low ψ_x^r do not represent Lp_r . Instead this slope is a complex function of several parameters and variables (Table 5.3.5).
2. Not taking into account the cortex solute mass balance in models concerning water transport through plants may lead to underestimated pressure potentials in the xylem of the plant. Solute accumulation leads to an apparent increase in R^{root} . The magnitude of this apparent change of R^{root} depends on the solute concentration in the root environment and on the water uptake rate of the plant.
3. Adding the solute distribution in the cortex to the model did not shift the simulated $(\Delta\psi_p-J_v)$ -relationship in the direction of measured data presented in literature (Fig. 5.2.5B). Differences between measured and simulated data still exist: the model with solute distribution incorporated does not entirely explain the measured $(\Delta\psi_p-J_v)$ -relationship.

Dynamic flow

An important aspect of solute accumulation in the cortex is the dynamics of the process: It takes some time to build up or break down the solute concentration gradient between root environment and endodermis. The time constant of these processes influences the dynamic behaviour of the water uptake and thus of the water balance of the whole plant. To find out on what time scale J_v reaches a new equilibrium value after changes in solute concentration in the root environment (C^{re}) or after a change in transpiration rate by the shoot (simulated by a step upon $\Delta\psi_p$), a dynamic version of the model was used.

When C^{re} versus time follows a step function ($60 - 120 \text{ mol.m}^{-3}$) the resulting J_v follows with a phase lag. This phase lag was about similar when C^{re} was changed from low to high and from high to low (Figure 5.4.1A-B).

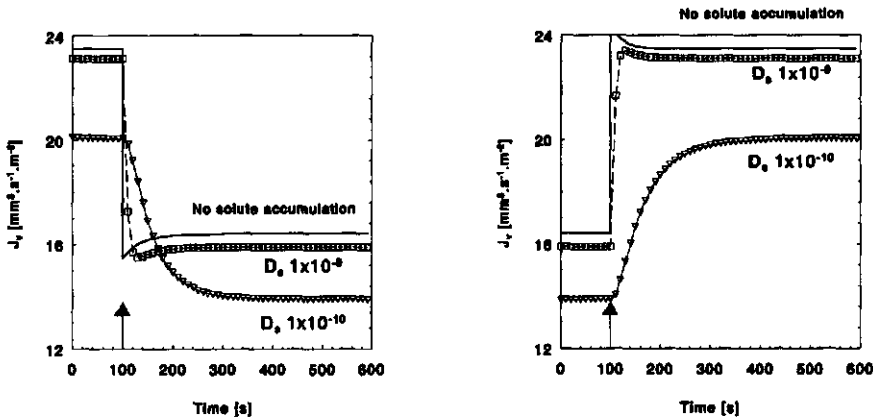


Figure 5.4.1A: Simulated rate of water uptake (J_v) after a change in solute concentration in the root medium from 60 to 120 mol m^{-3} . Simulated with the model without (—) and with the solute mass balance incorporated: $D_s = 1 \times 10^{-9} \text{ m}^2 \text{ s}^{-1}$ (\square) and $D_s = 1 \times 10^{-10} \text{ m}^2 \text{ s}^{-1}$ (∇). $\Delta\psi_p = -0.5 \text{ MPa}$. Other parameters root see Table 5.3.5.

Figure 5.4.1B: Simulated rate of water uptake (J_v) after a change in solute concentration in the root medium from 120 to 60 mol m^{-3} . See further Figure 5.4.1A.

The parameters σ , J^s , and ω did not change the simulated delay time (results not shown). D_s , on the other hand, influenced the length of the delay time considerably. This illustrates the relative importance of solute diffusion in the cortex on the solute concentration at endodermis level: In the first situation (60 to 120 mol.m^{-3}) the directions of solute flow by mass flow and diffusion are in the same direction, in the second situation (120 to 60 mol.m^{-3}) the directions are opposite. Diffusion in the cortex has a much larger impact on the solute mass balance at endodermis level than solute transport by mass flow, or the solute uptake across the endodermis. Simple calculations also

point into that direction: The diffusion flux density at the moment C^{ro} is changed, equals $D_s \times (\Delta C / \Delta x)$ (Eq. 5.2.22) and therefore, with a cortex thickness of 0.13 mm and a D_s of $1 \times 10^{-9} \text{ m}^2 \cdot \text{s}^{-1}$, $0.46 \times 10^{-4} \text{ mol} \cdot \text{s}^{-1} \cdot \text{m}^{-2}$. The solute flux density by mass flow is much lower: $J_v \times C^{\text{ro}} = 23 \times 10^{-9} \times 60 = 0.14 \times 10^{-6} \text{ mol} \cdot \text{s}^{-1} \cdot \text{m}^{-2}$ (Eq. 5.2.23) The total solute flux density over the endodermis was in the order of $10^{-7} \text{ mol} \cdot \text{s}^{-1} \cdot \text{m}^{-2}$. Consequently, the time to reach a new equilibrium value depends largely upon D_s : the lower D_s , the larger the delay time.

The course of J_v after a step upon $\Delta \psi_p$ is characterised by an immediate response with some overshoot, followed by a period of adjustment to the new equilibrium situation (Fig. 5.3.4C-D).

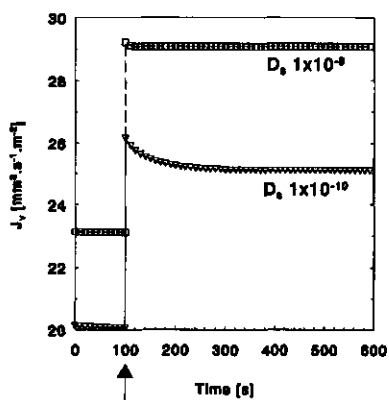


Figure 5.4.1C: Simulated rate of water uptake (J_v) after a change in pressure potential in the xylem of the root from $-0,5$ to $-0,6$ MPa. $C^{\text{ro}} = 60 \text{ mol m}^{-3}$. See further Figure 5.4.1A.

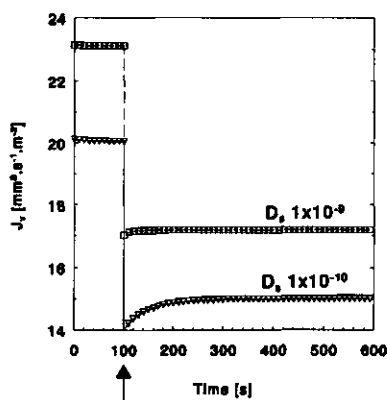


Figure 5.4.1D: Simulated rate of water uptake (J_v) after a change in pressure potential in the xylem of the root from $-0,5$ to $-0,4$ MPa. $C^{\text{ro}} = 60 \text{ mol m}^{-3}$. See further Figure 5.4.1A.

D_s influences the time of adjustment considerably. These responses look similar to the ones described above, but have a different background. Changes in J_v induced by the shoot environment are immediate because $\Delta \psi_p$ is changed in the first place and $\Delta \psi_x$ afterwards. Changes in solute concentration in the root medium do not influence J_v immediately, because it takes some time to build up the solute concentration at the endodermis due to the time-dependence of solute transport processes. With D_s in the range 10^{-9} - 10^{-10} the simulated delay time never exceeded 400 s, which is still a relative short time.

Conclusions:

The described non-linearity in the $(\Delta\psi_p-J_v)$ -relationship is important in modeling water relations of greenhouse grown tomato plants: during large parts of the day and the whole night, transpiration rates are below $10 \text{ mm}^3 \cdot \text{s}^{-1} \cdot \text{m}^{-2}$ (van Ieperen, 1996), and therefore not within the linear range of the $(\Delta\psi_p-J_v)$ -relationship (Figure 5.4.1). Consequently, the simple Ohm's law analogue is not sufficient to describe water uptake during large parts of the day. Ignoring the non-linearity at low J_v results in a serious over-estimation of pressure- and water potentials (less negative) in the shoot of the plant during large parts of the day. This may effect simulations of water potential dependent processes (transport, growth) seriously.

Incorporation of the radial solute distribution in the model introduces a change in the $(\Delta\psi_p-J_v)$ -relationship at high J_v , which is influenced by C^{sc} (Figure 5.4.4; Table 5.4.1). These simulation results quantitatively agree with the measurements presented in Figure 7A (chapter 3.), where a change in slope of the (plant water deficit - J_v) curve was observed with C^{sc} . (assuming plant water deficit linearly related to the pressure potential in the root system).

Dynamic courses as well as steady-state equilibrium situations depend largely upon the value for the diffusion coefficient for solutes in the apoplast of the root cortex (D_s). Due to the relative short distance for diffusion in the root cortex, new equilibrium situations are established within a relative short time ($< 400 \text{ s}$) after changes in the shoot or the root environment. Consequently, hysteresis effects found on the root conductivity or plant water potentials over a day (van Ieperen, 1996a) are most likely not the result of slowly changing solute concentrations in cortex of the root.

5.4.2 Simulation results of the complete model

5.4.2a Validation of the simulated water uptake at low and high salinity

To investigate the performance of the complete simulation model (including the solute mass balance in the cortex of the root), simulated and observed rates of water uptake were compared. Observed diurnal courses of transpiration of a single tomato plant, grown at daily alternating high ($\psi_{\pi}^{\text{re}} = -0.36$ MPa; $C^{\text{re}} = 145$ mol.m⁻³) and low ($\psi_{\pi}^{\text{re}} = -0.01$ MPa; $C^{\text{re}} = 5$ mol.m⁻³) salinity (Chapter 3.4) were used as input for the model. From the experimental data, days with fluctuating courses of transpiration were chosen as input to investigate the short-term dynamic performance of the model. The dimensions of the plant together with the parameter values in Table 5.3.4 and 5.3.5 were used to calculate the parameters in this simulation study. Simulated and observed courses of the rate of water uptake (J_v) at high and low salinity are presented in Figure 5.4.7A and B respectively, together with the main driving force for water uptake: the observed rate of transpiration.

Simulated J_v was generally in reasonable agreement with measured J_v . Short-term fluctuations after sudden changes in transpiration rate were simulated well. At low salinity (Figure 5.4.7B), simulated J_v was underestimated during almost the whole day. At high salinity this was not the case. The underestimation of J_v at low salinity was most likely the result of growth not being incorporated in the model: in the experiments considerable growth occurred at low salinity, whilst growth was almost absent at high salinity (Chapter 3.4). According to Nonami and Boyer (1993) water fluxes

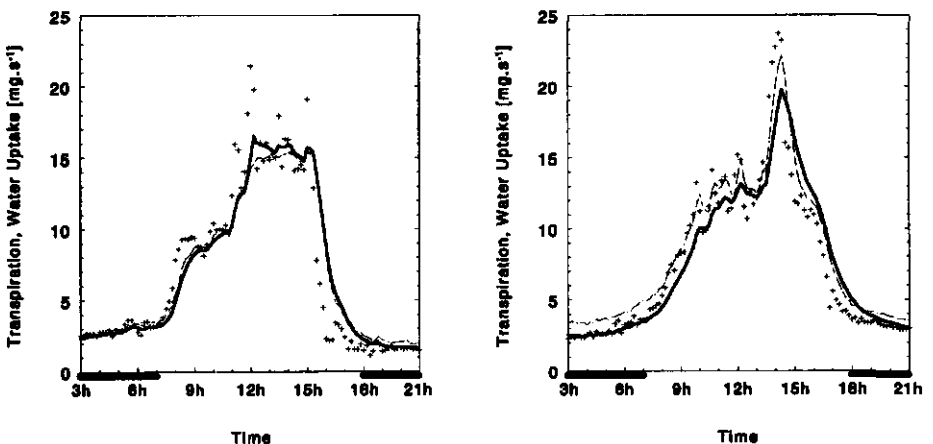


Figure 5.4.7: Simulated (—) and observed (---) diurnal courses of water uptake and observed diurnal course of transpiration rate (+) at high salinity (A; $\psi_{\pi}^{\text{re}} = -0.36$ MPa) and low salinity (B; $\psi_{\pi}^{\text{re}} = -0.36$ MPa).

caused by growth and transpiration are additive. Growth therefore increased the observed rate of water uptake, but was ignored by the model.

5.4.2b Observed and simulated changes in amount of water in the plant.

Observed transpiration and simulated water uptake were used to calculate the simulated diurnal courses of amount of water in the plant (Water Content Plant or WC^P) at high and low salinity (Figure 5.4.8A and B, respectively). These simulated courses were compared with the observed courses calculated from the observed courses of transpiration and water uptake in Figure 5.4.7A and B.

Deviations between simulated and observed courses of WC^P differed considerably between high and low salinity: At high salinity almost no structural increase in WC^P was

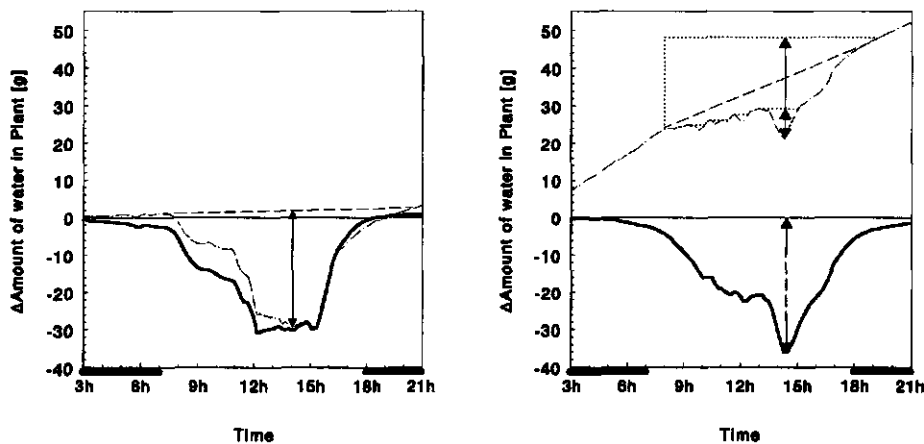


Figure 5.4.8: Simulated (—) and observed (---) diurnal courses of variations in the amount of water in a tomato plant (WC^P) at high salinity (A) and low salinity (B), calculated from the diurnal courses of transpiration and water uptake as given in Figure 5.4.7A and B respectively. The stable dark situation at midnight was chosen as point of reference. The arrows indicate the maximal reversible decline in amount of water in the plant. The dotted lines in (B) indicate the theoretical constraints of the course of the amount of water in the plant (determined by growth rate being greater or equal to zero).

observed. At low salinity, on the other hand, the observed course of WC^P clearly increased due to growth (ca. 45 g over 18 h). The simulated overall changes in WC^P were approximately zero at high and low salinity because the model only simulated temporary changes in WC^P , and the stable dark situation was chosen as point of reference.

Comparison of simulated and observed courses of WC^P at low salinity is possible by accounting for the theoretical limitations of the WC^P curve corrected for variations due to reversible changes in WC^P (see Chapter 3.4). The observed decline in WC^P was between ca. 5 and 25 g (indicated by the arrows; Figure 5.4.8B). The simulated

decline in WC^p during the day was larger (ca. 35 g): the simulation model overestimated the reversible decline in WC^p during the day at low salinity.

Simulated Relative Water Content of the vegetative parts of the plant (RWC^p) differed clearly between low and high salinity (Figure 5.4.9). Variations in RWC^p with

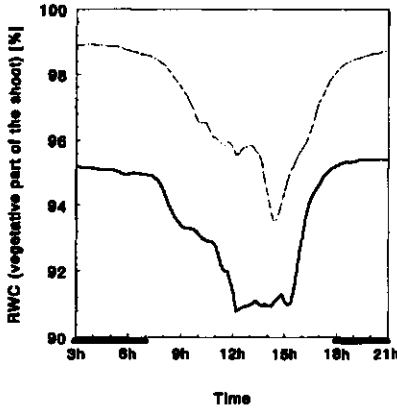


Figure 5.4.9: Simulated courses of the relative water content of the plant (RWC^p) at high (—, see Figure 5.4.7A and Figure 5.4.8A) and low salinity (- - -, see Figure 5.4.7B and Figure 5.4.8B).

The observed hysteresis effect in the relationship between plant water deficit and transpiration over a day was simulated by the model (Figure 5.4.10). In contrary to the observations, the model simulated approximately similar changes in plant water deficit (declines in WC^p relative to the stable dark situations) with increasing transpiration (Figure 5.4.10): in the observations the slope of this relationship changed with salinity (Chapter 3.4; Figure 7B). Decreasing the parameter D_e in the model increased the solute accumulation at the endodermis and changed the slope of the simulated relationship in Figure 5.4.10 at high salinity. However, the decline in WC^p decreased too and be-

changing transpiration over a day were about similar at low and high salinity level. Including the weights of the fruits in the calculations of RWC^p would have decreased calculated variations in RWC^p considerably, because fruits hardly add to reversible changes in WC^p due to the poor xylem connection between fruits and the rest of the plant (Lee, 1989).

To enable better comparison between simulations at low and high salinity, additional simulations were done using the diurnal course of transpiration at low salinity (Figure 5.4.7B) as input for simulations at high salinity ($C^{**} = 145 \text{ mol.m}^{-3}$).

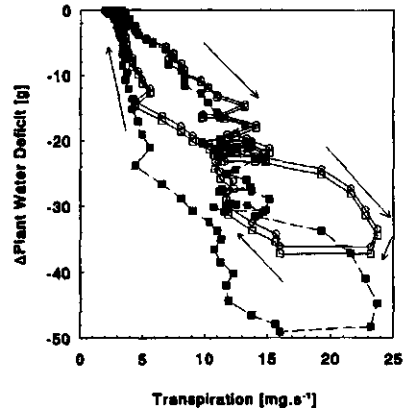


Figure 5.4.10: Simulated relationships between diurnal courses of WC^p (relative to the stable mid-night situation) versus transpiration at low (\circ) and high salinity (\square , $D_e = 1 \times 10^9 \text{ m}^2 \cdot \text{s}^{-1}$; \blacksquare , $D_e = 1 \times 10^{11} \text{ m}^2 \cdot \text{s}^{-1}$). The arrows indicate the sequence of data points in time.

came considerably larger than the observed decline in WC^p .

Solute concentrations in the xylem and cortex of the root, as well as water potentials, turgor pressures and osmotic potentials in the xylem and tissues in the whole plant are influenced by the salinity level. High salinity increased the simulated solute concentration in the xylem of the root (Figure 5.4.11) compared to at low salinity. High salinity also increased the simulated solute concentration in the cortex of the root during the day (Figure 5.4.12). At low salinity this increase was almost negligible.

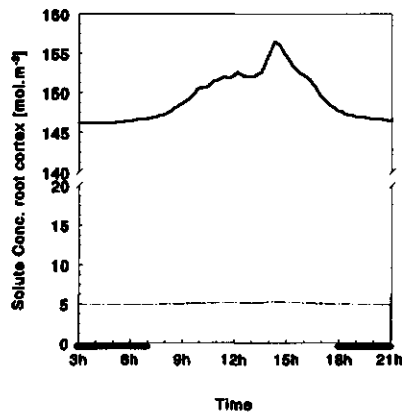
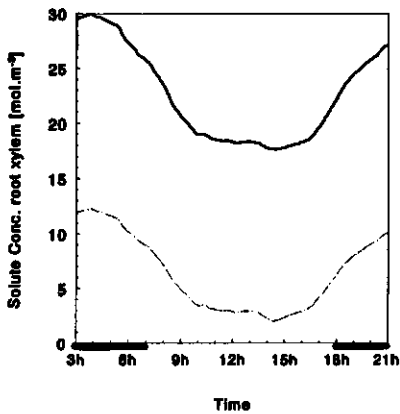


Figure 5.4.11: Simulated diurnal courses of the solute concentration in the xylem of the root at low (-----) and high salinity (—). **Figure 5.4.12:** Simulated diurnal courses of the solute concentration in the cortex of the root at low (-----) and high salinity (—).

The impact of the solute accumulation in the cortex on simulated water uptake and water status variables was rather low because serious solute accumulation occurred only at a relative high rate of water flow through the root. Such a high flow rate only occurred when the pressure potential difference dominated the driving force for water uptake across the endodermis during the day. At low salinity and low water flow rates (in the night) the solute concentration gradient favoured water uptake: the active solute transport across the endodermis (see Eq. 5.2.15) caused a higher solute concentration in the xylem than in the cortex of the root (results not shown). This phenomenon is known as root pressure.

High salinity decreased water potentials (not shown), turgor (Figure 5.4.13) and osmotic potentials (not shown). The alterations in osmotic potentials due to salinity and diurnal changes in transpiration resulted from the changes in tissue volume. Active regulation of the solute concentration in tissues was not included in the model. No relation was modelled between the solute concentration in the xylem and solute uptake by the symplastic tissues.

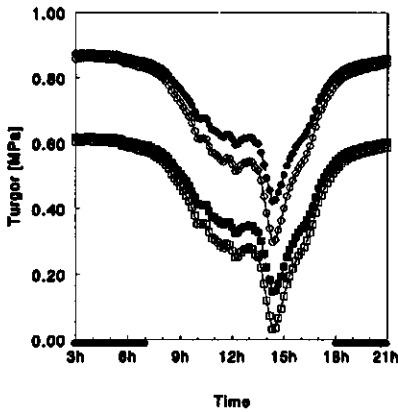


Figure 5.4.13: Simulated diurnal courses of the pressure potentials (turgor) in the bottom (open symbols) and top leaf layer (closed symbols) of the model at low (o) and high salinity (\square). See further Figure 5.4.8B.

In contrary to the stem xylem water potentials (not shown), leaf tissue water potentials and pressure potentials (turgor) were lower in the bottom leaf layer than in the top leaf layer. Simulated turgor in the plant was influenced by salinity, transpiration rate and the position on the plant. The position effect was caused by the hydraulic resistance distribution in the xylem of the plant (Dimond, 1966) together with the distribution of transpiration over the leaf layers: the hydraulic xylem resistance's in the petioles and leaves are lower in the top leaf layer than in the bottom leaf layer. During the day turgor was higher in the top leaf layer than in the bottom leaf layer. Salinity decreased simulated turgor during the day approximately as much as during the night.

Alterations in solute concentration in the root environment.

The objective of following simulations was to investigate the kinetics of the complete model at changes in salinity in the root environment. Simulations were done

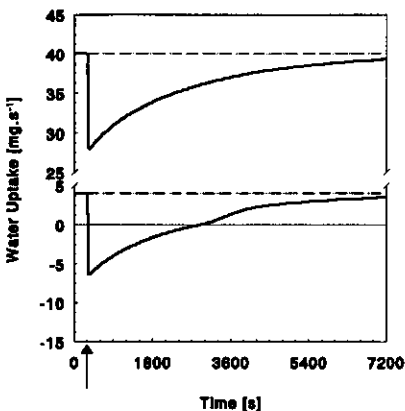


Figure 5.4.14: Simulated water uptake after a change in salinity at $t=300$ s from 5 to 145 mol.m^{-3} . At high transpiration (—, upper part) and low transpiration (—, lower part)

over a period of 2 h. Constant low and high transpiration rates (4 mg.s^{-1} and 40 mg.s^{-1}) were used as input. The solute concentration in the root environment (C^{re}) was changed at $t=300$ s from 5 to 145 mol.m^{-3} . Dimensions of the simulation plant and parameters were as described above. Simulated water uptake after a change from low to high salinity at low transpiration (Figure 5.4.14 lower part) became negative during ca. 2500 s after the change in salinity. Comparable measurements showed no negative water uptake, although it has to be mentioned that the measurements were halted during 600

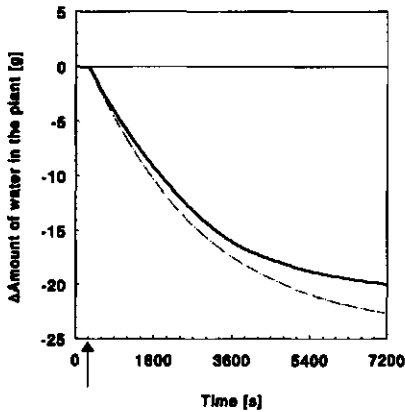


Figure 5.4.15: Simulated decline in WC^p after a change in salinity 5 to 145 mol.m^{-3} at low (—, 4 mg.s^{-1}) and high transpiration rate (---, 40 mg.s^{-1}).

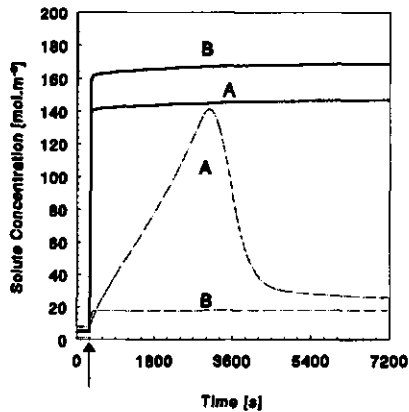


Figure 5.4.16: Simulated solute concentrations at the cortex side of the endodermis (---) and in the xylem of the root (—) after a change in salinity from 5 to 145 mol.m^{-3} at low (A) and high (B) transpiration rate.

to 1200 s after the change in salinity (Chapter 3.4; Figure 6A). The decline in WC^p after the change in salinity from 5 to 145 mol.m^{-3} depended on the rate of transpiration (Figure 5.4.15). The simulated decline in WC^p was rather high compared to the observed decline in WC^p (Chapter 3.4; Figure 6A). The associated courses of solute concentration in the cortex and the xylem of the root are given in Figure 5.4.16. The transpiration influenced the dynamics of these courses considerably.

5.4.2c Effects of different day- and night salinity levels on simulated water uptake and plant water status.

Greenhouse experiments showed that different day and night salinity levels changed vegetative and generative growth considerably (Chapter 4). Relationships between salinity, water uptake, internal plant water relations and these effects were assumed. However, clear experimental results were lacking due to shortcomings of present measurement techniques and the complexity of the relationships. Therefore, the simulation model was used to simulate diurnal courses of internal plant water relations at different salinity treatments. As simulation input an artificial diurnal course of transpiration was applied which combined an overall diurnal pattern with short-term fluctuations. Plant dimensions and parameters used in present simulations were the same as described in the simulations above. Intervals of three consecutive days with the same transpiration and salinity patterns were simulated. Results are presented from the third day to be sure that eventual long-term effects are presented in a correct way. There were three salinity treatments: 1. A constant salinity level ($C^{nc}=70 \text{ mol.m}^{-3}$) during day

and night (intermediate salinity treatment). 2. A low salinity ($C^{re} = 5 \text{ mol.m}^{-3}$) during the day (6 h to 18 h) combined with a high salinity ($C^{re} = 145 \text{ mol.m}^{-3}$) during the night (18 h to 6 h) (intuitive treatment). 3. A low salinity ($C^{re} = 5 \text{ mol.m}^{-3}$) during the night combined with a high salinity ($C^{re} = 145 \text{ mol.m}^{-3}$) during the day (anti-intuitive treatment).

In the model salinity influences plant water relations in the first place via the water uptake. The simulated diurnal course of water uptake (J_v) was clearly influenced by the salinity treatments (Figure 5.4.17A-C).

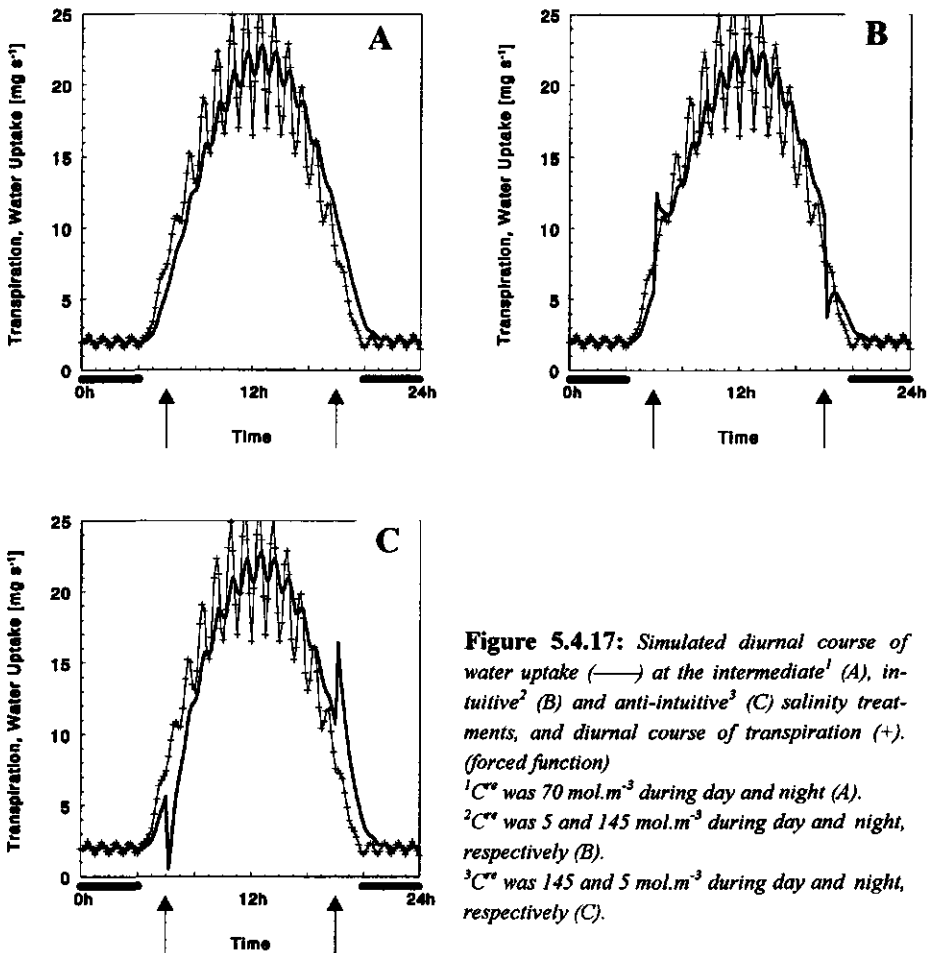


Figure 5.4.17: Simulated diurnal course of water uptake (—) at the intermediate¹ (A), intuitive² (B) and anti-intuitive³ (C) salinity treatments, and diurnal course of transpiration (+). (forced function)

¹ C^{re} was 70 mol.m^{-3} during day and night (A).

² C^{re} was 5 and 145 mol.m^{-3} during day and night, respectively (B).

³ C^{re} was 145 and 5 mol.m^{-3} during day and night, respectively (C).

In the intuitive and anti-intuitive salinity treatments simulated J_v responded rapidly at 6 h and 18 h (indicated by the arrows in Figure 5.4.17B and C). The simulated changes in J_v at these salinity transitions are rather large: observed changes in

water uptake at changes in salinity during the day were less pronounced (Chapter 3.4; Figure 2 and 3).

Relative Water Contents (RWC) of tissues and the pressure potentials (turgor) in tissues are often mentioned as important variables influencing physiological functions in the plant (Hsiao, 1973). The simulated diurnal courses of RWC^p (Figure 5.4.18A) and turgor in the top leaf layer of the plant (Figure 5.4.18B) were used as indicators for the diurnal changes in plant water status.

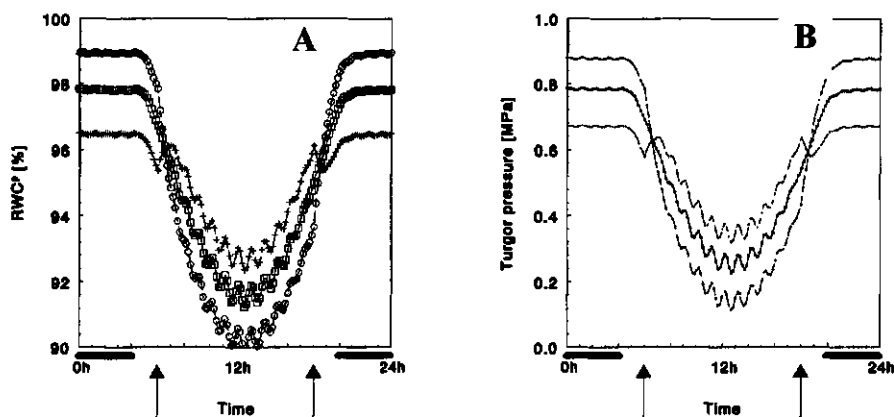


Figure 5.4.18: Simulated Relative Water Content (A) of the whole plant (RWC^p), and Turgor in the top leaf layer (B) at the intuitive (+), intermediate (\square) and anti-intuitive (O) salinity treatments¹.

¹see Figure 5.4.17

The salinity treatments changed the diurnal courses of RWC^p and turgor considerably. The intuitive treatment (low salinity during the day and high salinity during the night) decreased the variation in RWC^p and in turgor over a day. RWC^p and turgor pressure during the day were higher than at the other treatments. The anti-intuitive treatment caused the opposite reaction: RWC^p and turgor were increased during the night (when they were already relative high) and decreased during the day. Simulated differences in turgor between day and night were approximately 0.75, 0.55 and 0.35 MPa for the anti-intuitive, intermediate and intuitive treatments, respectively

5.5 Discussion

Results of the present model showed that salinity clearly influenced the internal water relations of a plant: water uptake, relative water content in the plant (RWC^p) and turgor changed with salinity level. It is generally assumed that these changes in RWC^p and turgor are closely related to changes in physiological functioning of the plant (e.g. regulation of stomatal conduction and expansion growth, see Hsiao, 1973). In the pre-

sent model, however, relationships between RWC^p and/or turgor and physiological functioning were not simulated because especially on the long term these relationships are rather unclear and literature is contradictory (e.g. Kramer, 1988b; Passioura, 1988; Boyer, 1989). Furthermore, the relative simple thermodynamic approach for internal water relations in the plant, used in the present model, is insufficient to describe a complex process such as expansion growth of (a part of) a plant, which undoubtedly also depends on metabolic factors. This does not mean that present model is useless. In contrary, it may be very useful in analysing the possible role of water relations in experimental results obtained in complex situations (e.g. plants grown in greenhouses at changing environmental conditions such as salinity in the root environment and transpiration in the shoot environment).

One of the main assumptions in the present model is the thermodynamic approach of plant water relations. Biochemical and/or metabolic properties are not considered. The rate of transpiration was an input of the model. However, simulation of the rate of transpiration is also desirable. Consequently, stomatal behaviour has to be incorporated in the model. However, in many experiments no consistent pattern was found relating salinity in the root environment, leaf water potential (or one of its components) and stomatal conductance (see review Davies and Zhang, 1991). In contrary, there are physiological arguments to doubt this relationship: it has been observed that plants closed their stomata in response to water stress in their root environment, while leaf water potential was not affected (yet) (Gollan *et al.*, 1986; Zhang and Davies, 1990). It has been stated that other 'messages' than hydraulic ones were transmitted by the roots which the shoot detected. Plant hormones or altered solute concentrations in the xylem are often mentioned as possible messengers (Davies and Jeffcoat, 1990; Johnson, 1991). The present model has the ability to incorporate 'message' control easily because 'messages' are most likely transported via the xylem, and water flow in the xylem system is included in the model.

The simple pressure-flow relation to describe long distance water transport in the xylem part of the model was questioned by Zimmerman and co-workers on experimental grounds. They used a pressure probe to measure negative xylem pressures in very high trees and found relative high values (less negative than expected) which did not agree with the present theories for water flow in the xylem. In an interesting article Zimmerman *et al.* (1993) critically commented on most of the commonly used methods of measuring water potentials, thus questioning experimental results in the past. They used data of their own direct negative pressure measurements and data obtained by nuclear magnetic resonance (NMR)-imaging to argue that several forces may

be responsible for long distance water flow including pressure, osmotic pressure, capillary and air-water interfacial forces (see further, Passioura, 1991; Zimmerman *et al.* 1991). In the present model, however, water flow in the xylem is modelled in the usually way (Ohm's law analogue). New insights may require to reconsider the concept of pressure-flow for xylem water transport in the present model.

Simulated and observed (E- ΔWC^p)-relationships (Figure 5.4.10 and Chapter 3.4; Figure 7B, respectively) are different in several aspects. The slope of the observed relationships differs between salinity-levels, while this is hardly the case in the simulation results. At low salinity the simulated decline in WC^p is greater than the observed one, and the hysteresis effect over a day is approximately similar at low and high salinity, while in the observations it is more pronounced at high salinity.

First of all it has to be mentioned that the presented observed and simulated (E- ΔWC^p)-relationships at low and high salinity reflect changes in amount of water in the plant *relative to the stable night WC^p* . This WC^p at night was different at low and high salinity, as could be concluded from observed WC^p -transients after changes in salinity in dark (Chapter 3.4; Figure 6A and B). According to these transients the difference in WC^p between low and high salinity at night is 4-8 g, which corresponds with a change in RWC^p (plant minus fruits) of approximately 0,5 - 1,5 %. This is already considerably lower than the simulated difference in RWC^p of 4 % between low and high salinity in dark (Figure 5.4.9). Due to the difference in WC^p between low and high salinity the observed (E- WC^p)-curve at high salinity should be shifted downwards along the y-axis relative to the (E- WC^p)-curve at low salinity.

According to simulation results, solute accumulation at the endodermis could not have caused the different slopes of the (E- WC^p)-relationships at low and high salinity, although at high salinity some accumulation of solutes at the cortex side was simulated (Figure 5.4.12). However, the associated decline in osmotic potential in the cortex of the root at high salinity was low (up to ca. 15% at high J_v) and the maximum decline occurred when the relative importance of the gradient in osmotic potential across the endodermis was low (at high J_v).

In the present model the capacitances for water storage in the tissues adjacent to the xylem were constants, following Nobel (1983). The above described conflict between slopes of the simulated and observed (E- WC^p)-relationships and some theoretical considerations raise the question whether this was correct: the pressure-volume relationships of tissues in the model, of which the slope provides the capacitance parameters, are probably not linear. Instead the slope may vary with pressure potential: variable capacitance's are well possible because the capacitance is closely related to the bulk modulus of elasticity of tissues ($\bar{\epsilon}$), and pressure dependence of $\bar{\epsilon}$ was confirmed

by measurements in bulk tissues in various plants (Zimmerman, 1978; Cheung *et al.*, 1976). The determinations of capacitance parameters using Höfler diagrams (e.g. Figure 5.3.2) showed that the (RWC- ψ_p)-relationships were about linear between RWC = 1 to 0.9 but not below 0.9. Therefore, it probably would have been better to use pressure potential dependent capacitances in the model. In that case, the analysis of the dynamic properties, as described by the equations 5.2.11-5.2.13 should be reconsidered too. The small difference in RWC^p between low and high salinity in dark, compared with the more pronounced alterations in RWC^p at low and high salinity during the light raise the question whether pressure dependent capacitances would solve the whole slope problem: lowering the observed (E-WC^p)-curve at high salinity with 8 g to put the curves at low and high salinity on the same absolute y-axis, results in two (E-WC^p)-relationships between WC^p = 8-15 g with salinity dependent slopes.

The parameter for the hydraulic resistance of the root (R_r , or root conductivity ($L_p=1/R_r$)) in present model was a constant. It is well known that this parameter may vary with temperature (Passioura, 1984). In present simulations a temperature effect on L_p was neglected because root temperature in the greenhouse was approximately constant on the short-term. Others observed a direct dependency of L_p from salinity (e.g. Leary, 1969). Simulations showed that solute accumulation in the cortex of the root apparently change L_p (Figure 5.4.4). However, this apparent change is not enough to account for the observed differences in slopes of the (E-WC^p)-relationships at low and high salinity. Perhaps salinity did change L_p directly.

One of the objectives of present study was to develop a model in which growth could be easily included (see 5.1.3). In present model expansion growth was not integrated yet, but the framework was developed to incorporate growth in the model. However, which (state) variable or combination of variables in present model should be used to drive expansion growth is not clear. Recently, several researchers presented models which contained expansion growth in some way (e.g. Alm *et al.*, 1994; Arkebauer, 1995abc; Johnson, 1991). Often a relationship between turgor and cell expansion is assumed. Expansion growth is usually simulated using the Lockhart Equation which describes the relative growth rate of the symplast as a function of the growth effective turgor (the pressure potential (ψ_p) minus a threshold pressure potential (p')) and a constant m , known as the cell wall extensibility (Eq. 2.16).

However, consistent knowledge about the nature of the relationship is lacking. It is uncertain which parameter controls cell expansion in a growing tissue in response to water stress: Some researchers argued that the cell wall extensibility was the primary factor limiting growth (e.g. Cosgrove 1985; Volkenburgh *et al.*, 1985) others found that it was the water uptake of the expanding cell that limited growth (Boyer,

1985), or both factors may be important (see review of Dale (1988); Nonami and Boyer, 1990). Cell wall extensibility (m) includes two phenomena: besides the wall material properties the processes cell wall loosening and hardening are important. These latter two processes are under metabolic control (see reviews of Taiz, 1984 and Cosgrove, 1986). Dynamic measurements of turgor and growth rates in roots (Frensch and Hsiao, 1994) and leaves (Shackel *et al.*, 1987; Serpe and Matthews, 1992) showed that the parameters m and p' are not constants but may change on the short-term (minutes) in response to water stress. Moreover, Zhu and Boyer, 1992) stated that growth was not regulated by turgor. They found from direct measurements on growth and turgor in internode cells of *Chara corallina* that a certain threshold turgor was necessary for growth to occur, but that above the threshold turgor growth rate was independent of turgor and metabolic reactions determined growth rate, probably by influencing the synthesis and/or extension of cell wall polymers.

A water potential gradient associated with growth (growth-induced-water potential) was directly demonstrated by measurements in actively growing soybean seedlings (Nonami and Boyer, 1993). Measurements on tomato plants and citrus trees showed that growth rates in leaves and stems are controlled by the size of the growth-induced water potential (Okatani *et al.*, 1995). It was stated (Nonami and Boyer, 1989; 1990; Nonami, 1993;) that when plant growth is inhibited by water stress, the primary cause of a decrease in expansion growth is to be the change in growth-induced-water potential. Secondly, changes in cell wall permeability and cell wall extensibility may take place (Boyer and Nonami, 1993). At low water potentials due to water stress conditions, growth was not directly related to turgor. In some experiments the relation between turgor and expansion growth was even reversed. Consequently, turgor may not play a critical role in controlling extension growth in transpiring conditions (Nonami and Boyer, 1989; Okatani *et al.*, 1995).

Summarising: The structure of the model allows the integration of growth-induced water potentials and/or the Lockhart Equation to describe growth. However, actual incorporation of growth in the model will be a difficult task. Although the theory of Lockhart (1965) provides an attractive concept for the use in models, recent experimental data contradict a clear relationship between turgor and expansion growth. Moreover, parameters in this concept are not constants but may vary with water stress conditions and metabolic mediated processes. A first predictive model for m and p' (of a single cell on molecular basis) was developed by Passioura and Fry (1992). Incorporation of this model in models for plant water relations is still far away, because the authors qualified their model in many respects rather naive. Still a first attempt was made. The concept of the growth-induced water potential field, controlling expansion growth by its size, is another possibility to include expansion growth in the model.

However, it needs a description of the lowering of the water potential in the growing tissue which again depends largely on the wall extensibility. Perhaps a combination with metabolic oriented models is needed.

Simulation of different day and night salinity treatments during a day showed that the intuitive treatment (high salinity during the night and low salinity during the day) decreased the variation in RWC^p (Figure 5.4.18A), water potentials and turgor (Figure 5.4.18B) in a plant within a day. RWC^p and turgor were decreased during the night and increased during the day. It is possible that the lower variation in these variables on the long term caused the positive effect on expansion growth of the plant as observed (Chapter 4). The differences in variation in RWC^p and turgor within a day between the salinity treatments would have been even greater when the model had accounted for the different declines in WC^p with increasing transpiration at different salinity-levels (see Chapter 3.4; Figure 7B).

Although the model still has some serious deficiencies, it could be well used to check parts of the theoretical framework concerning effects of salinity on internal plant water relations. Its structure easily allows extension with for example transport of solutes and hormones through the xylem network and/or expansion growth.

6. General Discussion

6.1 General

It was clearly shown that variation of the EC within a day (24 h) during a whole growth season influences fruit production of tomato grown on water culture (Chapter 4). Fruit yield increased considerably when a low EC was supplied during the day in combination with a high EC during the night, compared to a constant intermediate EC-level. Blossom-end-rot almost disappeared at the same EC-treatment. Most important effects of changing EC-levels on growth and production of tomato are summarised in Table 6.1. It is generally assumed that the effects of EC are comparable with effects of salinity. Based on preliminary experiments on young tomato plants (Bruggink *et al.*, 1987) positive effects of the "intuitive" treatment on production were expected. The decrease in salinity level during the day was expected to support maintenance of turgor, whilst at the usual salinity level a reduction in cell turgor during the

Table 6.1: Important effects of different day and night EC-treatments (intuitive¹, anti-intuitive² and high³ treatments) on growth and production of tomato, compared with a constant intermediate⁴ EC.

Treatments:	intuitive ¹	anti-intuitive ²	high ³
Fruit Yield	++	-	--
Average Fresh Weight	+	-	--
Average Dry Weight	0+	0-	-
No of Fruits on Plant	0+	-	--
Dry Matter Percentage	0-	0+	+
Blossom-End-Rot	--	0+	++
Vegetative Part of the Plant			
Fresh weight	0+	0-	0
Dry weight	0	-	--
Leaf Area	0	-	-
Dry Matter Distribution			
To Generative Part	0+	0	-
<i>Within vegetative parts</i>			
To the Roots	0	+	++
To the Stem	0	0	0
To the Leaves	0	-	--

¹low EC during the day (12 h) and high EC during the night (12 h); ²high EC during the day and low EC during the night; ³high EC during day and night; ⁴intermediate between low and high EC during day and night.

+ more/higher (compared with the intermediate treatment; - less/lower; 0 no effect; 0+/0- small, not in all experiments statistical significant effect.

day would be expected due to the higher rate of transpiration by day. It has been argued (e.g. Turner and Jones, 1980) that small changes in turgor are the most likely means by which the water status in higher plants affects transpiration, expansion growth and metabolism. In this chapter the effects of (changing) salinity on growth and production mediated by plant water relations are discussed within the theoretical framework of Figure 1.1 in the introduction of this thesis. Relationships between EC, transpiration, water uptake, plant water deficit, plant expansion growth, fruit yield and fruit quality are discussed, integrating the results obtained in the long-term greenhouse experiments (Chapter 4) with short-term measurements of plant water relations (Chapter 3), predictions of the simulation model and relevant literature. Initial assumptions and working methods are critically evaluated. Finally, the impact of presented results and possibilities of short-term EC-control in horticultural practice are evaluated.

6.2 Integration of experimental results obtained by short- and long-term experiments using the theoretical framework and its model representation

Water uptake & transpiration

Water uptake depends on the combination of a difference in osmotic potential ($\Delta\psi_{\pi}$) and a difference in pressure potential ($\Delta\psi_p$) across the endodermis in the root on the one hand, and on the hydraulic conductivity of the root (L_p) on the other hand. $\Delta\psi_{\pi}$ and $\Delta\psi_p$ are known as the driving force for water uptake. Some reports suggest that salinity reduces L_p , (e.g. Leary, 1969), others claim that salinity does not influence L_p , (e.g. Munns and Passioura, 1984). One important problem is that L_p is usually determined on excised root systems which influences the obtained values considerably (Salim and Pitman, 1984). Our short-term measurements on intact plants showed that the relation between plant water deficit and water flow rate through the plant was clearly influenced by salinity, which could indicate a salinity mediated decrease in L_p . Simulations, on the other hand, demonstrated (Chapter 5.4.1) that observed L_p may change with salinity level, while in fact L_p was constant but the driving force for water uptake decreased because of solute accumulation at the cortex side of the endodermis. It is uncertain whether solutes do accumulate since experimental proof is lacking. Although the concept of a variable solute concentration in the root cortex improves the simulation results at different salinity levels, it does not explain the whole effect of different salinity levels on the water status of the plant. Measurements and simulations proved that the straightforward approach of water uptake being dependent on an undivided water potential difference and a constant hydraulic root resistance does not satisfy and may lead to misunderstandings concerning the relation between salinity and plant water content. Based on the simulation results it may be concluded that the prin-

ciple of solute accumulation at the endodermis is probable. Its effect on the internal plant water relations, however, depends highly on the salinity level and transpiration rate. Solute accumulation at the endodermis should therefore receive attention in future research.

Water uptake transients showed an almost immediate response to changes in salinity level (Chapter 3.4; Figure 6): Within several minutes after a change from low to high salinity in darkness (at approximately constant transpiration rate) water uptake initially decreased severely, followed by a slow recovery to a constant yet lower new value. After the opposite change in salinity, however, the adaptation of water uptake required much more time while the water uptake transient followed a complete different pattern. Changes in water deficit and growth rate of the shoot and probably in solute concentration in the cortex of the root may add to this transient.

Plant transpiration normally depends on leaf area, leaf conductance, the boundary layer conductance and the water vapour concentration gradient between leaf interior and ambient air (Monteith and Unsworth, 1990). Leaf conductance depends on stomatal density, stomatal opening, and the cuticular conductance. On the short-term salinity is supposed to influence plant transpiration via the plant water status: it was assumed that high salinity induces a low leaf turgor pressure which causes stomata to close during the day (Hsiao, 1973). It should be mentioned, however, that recent literature on this subject is contradictory: in the absence of measurable changes in leaf water status often another mechanism for stomatal control, based on hormone signals originating from the roots, is reported (Davies and Zhang, 1991). In growth chamber experiments at a constant climate, an increase in salinity level caused the expected decrease in transpiration rate during the light (Chapter 3.3). The clear effect of salinity on the transpiration rate in dark, however, was surprising because it is usually assumed that stomata are closed in the dark (Kramer, 1983; Schulze and Hall, 1982). Some reports, however, suggest that stomata of tomato may not completely close in darkness (Kuiper, 1961; Bakker, 1991) and because the growth chamber climate was constant in present experiments it was argued that changes in stomatal conductance caused the differences in night-time transpiration rate between low and high salinity (Chapter 3.3). In the growth chamber the driving force for transpiration was constant within a dark or light period for as far as it depended on outside properties. Salinity mediated differences in transpiration rate may have caused small differences in leaf temperature and associated water vapour concentration in the leaf between salinity levels. Experiments in the greenhouse showed a small tendency for a lower transpiration rate in darkness after the salinity level was increased. The absolute change in transpiration rate, however, was marginal (Chapter 3.4; Figure 6). In the greenhouse no clear effect of salinity on transpiration rate during the light was observed, while the simultaneously deter-

mined effect of salinity on plant water deficit was obvious. These results suggest that there was no effect of leaf turgor pressure on stomatal conductance during the light. The relationship between stomatal conductance and transpiration in a greenhouse is complex: a change in stomatal conductance does not necessarily change the rate of transpiration significantly. First of all, feed-back mechanisms exist: in a greenhouse a rise in stomatal conductance may increase crop transpiration, and subsequently the vapour concentration in the ambient air. As a result the driving force for transpiration is reduced which decreases the initial positive effect on plant transpiration (hydraulic feed-back). The positive effect of a rise in stomatal conductance on the rate of transpiration is tempered even more by a thermal feed-back mechanism: due to a higher transpiration rate leaf temperature decreases which decreases the saturated vapour pressure inside the leaf and thus the driving force for transpiration (Jarvis and McNaughton, 1986). It is not very likely that in the greenhouse experiments (Chapter 3.4) the hydraulic feedback was important because the greenhouse was not completely filled with tomato plants. Secondly, at high stomatal conductance the conductance of the boundary layer may become predominant and may prevail changes in stomatal opening. Concluding, salinity may have influenced stomatal opening during the light in the greenhouse whilst transpiration rate was not or hardly changed. Therefore, changes in transpiration rate have to be used carefully in interpreting the effect of salinity on stomatal conductance. The different results concerning the effect of salinity on plant transpiration between growth chamber and greenhouse experiments show once more that extrapolation of results from growth chambers experiments to horticultural practise should be done carefully.

Changes in amount of water in the plant

Water uptake lagged behind transpiration with a lag time in the order of minutes rather than hours. Measured rates of transpiration and water uptake were used to calculate plant water content transients. These transients were very clearly affected by changes in salinity (Chapter 3) and were discussed in terms of irreversible growth and reversible changes in plant water content associated with changes in plant water deficit (RWC^p or plant water potential). Therefore, a method which was used to interpret transients of elongation of single cells and separated organs in terms of growth and plant water deficit, was scaled up to a whole plant: transients with comparable characteristics and responses to changes in salinity were shown with elongation measurements on single cells (e.g. Zhu and Boyer, 1992), excised roots (e.g. Frensch and Hsiao, 1994) and leaves on intact plants (e.g. Serpe and Mathews, 1992). Although scaling-up to the whole plant level provided valuable information of whole plant responses to salinity, caution is necessary with applying the obtained results on separated

parts of the plant: It is likely that at a lower integration level (organs, tissues or cells) transients of changes in water content differed among organs and tissues, and that some organs may initially have reacted faster than the whole plant and others slower. Position on the plant and characteristics of the tissues involved may have influenced the behaviour of a specific tissue or organ.

Plant water deficits

Simultaneous measurements of transpiration and water uptake with a high resolution in time permit an estimation of the plant water deficit during the day. Plant water deficit during the day was clearly influenced by salinity (Chapter 3), but the effect was generally small. It is well known from destructive measurements that the relative water content and water potential in tomato decrease in response to salinity (e.g. Bruggink *et al.*, 1987). However, increasing salinity from low to high in dark (decreasing ψ_n from -0.01 to -0.36 MPa) decreased the water content of a shoot in the non-destructive measurements only 4-8 g: The accompanying decline in relative water content (RWC^P) was less than 0.6%. The estimated declines in plant water content and RWC^P due to transpiration during the day were 25 g (2.5%), and 15 g (1.1%) at high and low salinity respectively. These declines in RWC^P are extraordinary low: From literature it is known that leaf water potential of tomato declines 0.5 to 1 MPa during the day, dependent on transpiration rate and salinity level (Bruggink *et al.*, 1987; 1988; Batta, 1989) and that the associated RWC^{leaf} (measured using a destructive method) decreases 10-20% (Slatyer, 1969; Behboudian, 1977). However, the overall "plant capacitance" obtained from the alteration in plant water deficit during a change in salinity in dark was only 0.8-1.6% per MPa (assuming a constant L_p and constant transpiration rate in dark). This contradiction may be attributed to a part of the plant not being involved in the hydraulic plant capacitance. Tomato fruits probably hardly act as dynamic water storage organs and are hardly able to deliver water back to the xylem system at water stress because the hydraulic resistance in the xylem of the pedicel of a tomato fruit is very high (Lee, 1989).

Expansion growth

Growth of a tissue or whole plant is defined as the irreversible increase in volume resulting from cell division and cell expansion. Knowledge concerning the relation between plant water status and growth is still under development (e.g. Kramer, 1988b; Passioura, 1988; Boyer, 1989). The often assumed (Fig. 1.1) direct relation between turgor pressure and growth (Lockhart, 1965) has been challenged recently on the basis of dynamic measurements of turgor pressure and growth rates of single cells (Zhu and

Boyer, 1992), roots (Frensch and Hsiao, 1994) and leaves (Chazen and Neuman, 1994). They concluded that a certain minimum turgor is required for growth, but that growth rate was not determined by the growth-effective-turgor (turgor minus a threshold turgor). Moreover, important constants in the often used Lockhart relationship for the relation between turgor and growth, were not constant but varied with water stress conditions. Therefore, it has been concluded that simple turgor related expansion growth is conceptually disputable.

Nonami and Boyer (1990) introduced the growth-induced water potential field as a factor that relates plant water status to expansion growth: They found that after applying water stress to a plant the rate of expansion growth was primarily influenced by the difference in water potential between the xylem and the growing cells (growth-induced-water potential-field), and that secondly a metabolic mediated change in cell wall extensibility occurred, which also altered the expansion growth. Growth induced water potential gradients were demonstrated by direct measurements in soybean seedlings (Nonami and Boyer, 1993) and stems and leaves of tomato plants and citrus trees (Okatani, *et al.*, 1995). Growth induced water potential gradients were not confirmed in enlarging tissues of castor bean (Meshcheryakov, *et al.*, 1992) and pea (Malone and Tomos, 1992). In our short-term experiments on tomato plants in a greenhouse (Chapter 3.4) a change in salinity influenced the growth rate of the plant almost immediately. Adaptation of the growth rate to a certain salinity level occurred only in light and was only partial, which was possibly the result of a metabolic mediated feed-back effect on the cell wall extensibility of the growing tissues. However, although these results seem to point into the direction of the growth-induced-water potential concept the experimental evidence is weak. It can be concluded that expansion growth is influenced by water potentials in the plant and metabolic factors. Therefore, for a reliable prediction of expansion growth on the long-term (days), integration between biophysical and metabolic oriented models is necessary. The relation between plant water relations, metabolic factors and expansion growth should therefore receive more attention in future experimental and modelling research.

In the long term experiments it was shown that especially leaf area and fruit growth were influenced by different day and night salinity treatments. High salinity during the day decreased total leaf area by 25 %. High salinity during the night did not influence leaf area. Total leaf area depends on the rates of leaf formation and leaf expansion. Fluctuating salinity did not influence the leaf formation rate. Therefore it was concluded that day-time salinity level mainly influenced the leaf expansion rate.

Dry matter production and distribution

It was anticipated that a systematic decrease in leaf turgor pressure by salinity would change stomatal conductance and thus dry matter production (Fig. 1.1). In the long-term greenhouse experiments total dry matter was indeed increased by the intuitive treatment, compared to the anti-intuitive treatment. The overall response, however, was small. In principle the small positive effect could have been the result of the assumed positive effect of low salinity during the day on leaf turgor pressure. However, it should be noted that total dry matter production not only depends on stomatal conductance but also on leaf area, leaf temperature, and stomatal density. Stomatal density was not measured. Leaf area clearly differed between the salinity treatments, which could account for a large part of the dry matter differences. Consequently no firm conclusions concerning stomatal conductance could be drawn from the long-term greenhouse experiments. The effect on CO₂-absorption must have been low, probably because the assumed effect on stomata conductance was negligible. This was in accordance with the short-term transpiration measurements on single plants in greenhouses during the day in which no statistical significant difference in transpiration rate was measured at low and high EC (Chapter 3.4). Transpiration measured in the growth chamber experiments, on the other hand, was influenced by the EC (Chapter 3.3). This effect in the growth chamber, however, was measured at a rather low light level. In a greenhouse transpiration was slightly influenced by changes in EC during the night. However, this did not influence dry matter production directly.

The distribution of dry matter was slightly influenced by short-term changes in salinity level. A tendency for a lower shoot/root ratio was observed at the anti-intuitive treatment. Such a lower shoot/root ratio is a general phenomena at constant high salinity level (Chapter 4) or in general when water is a limiting factor for plant growth (Wilson, 1988). The lower shoot/root ratio might have influenced fruit yield on the long term by lowering leaf area and subsequent dry matter production.

In the long-term greenhouse experiments (Chapter 4), with the intuitive treatment a tendency for a higher distribution towards the fruits was observed. It is questionable whether this effect is mediated directly via plant water relations. De Koning and Hurd (1983) observed that a slight water stress in tomato increased dry matter partitioning into the fruits, while Ehret and Ho (1986a) and Ho and Adams (1994) observed that high salinity had no effect on the fraction of dry matter partitioned to tomato fruits. Ho (1988) concluded that the supply of assimilates to the fruit is not generally affected by the water relations in the plant. Air humidity did not influence dry matter partitioning into tomato fruits (Bakker, 1991). Dry matter distribution towards the fruits is influenced by the amount of fruits on the plant (Heuvelink and Buiskool, 1995). It is therefore well possible that the differences in dry matter partitioning to-

wards the fruits were caused by the reducing effect of salinity on the amount of fruits on the plant (Chapter 4.1; Table VI).

The incidence of Blossom-End-Rot (BER)

One of the unexpected results in the long-term experiments of present research (Chapter 4) was the clear effect of different day and night EC-levels on the incidence of BER: with the intuitive treatment (a low EC during the day and a high EC during the night) BER almost disappeared. It is well known that continuous high salinity increases the incidence of BER in tomato fruits (e.g. Ho and Adams, 1989). Because it is well known that BER in tomato fruits is due to local Ca^{2+} deficiency in the distal end of the fruits (Van Goor, 1968) an explanation could be found in the effect of fluctuating salinity on the Ca^{2+} import in the fruits. The mobility of Ca^{2+} within the plant is low: distribution of free Ca^{2+} within a plant is only by mass flow in the xylem stream (Clarkson, 1984), and free Ca^{2+} is readily fixed in cell walls, cell membranes and vacuoles. The rate of Ca^{2+} import in the distal-end of the fruit depends on the Ca^{2+} -concentration in the xylem sap and the direction and flow rate of the xylem sap between stem and distal-end of the fruits. The flow rate of the xylem sap is influenced by the water potential gradient between stem and fruit and by the hydraulic resistance in the xylem of pedicel and fruit. Thus, Ca^{2+} -import into the fruits is determined by: 1. water potentials in stem and fruit xylem. 2 the hydraulic resistance of the xylem transport path between stem and distal-end of the fruit, and 3. Ca^{2+} concentration in the xylem sap. In theory, diffusion of Ca^{2+} from the stem via the xylem towards the distal-end of the fruits may also play a role. However, due to the long diffusion pathway diffusion is assumed to be negligible and further ignored.

According to Ho and Adams (1989) salinity has an immediate effect on the uptake of Ca^{2+} by the roots and distribution of Ca^{2+} within a plant, and a long-term effect on the development of the xylem tissue in the fruit and thus on the hydraulic resistance. On the long-term high salinity causes poor xylem development in tomato fruits (Ehret and Ho, 1986b). Ho *et al.*, (1993) reported that salinity hardly influenced the number of vascular bundles in the fruit, but the number of bundles containing lignified vessels was substantially reduced by high salinity, which could have influenced the ion exchange capacity of the xylem vessels (Ferguson and Bollard, 1976) and therefore the Ca^{2+} supply to the distal-end of the fruits. In present research, the long-term effect of different day and night salinity treatments on the hydraulic xylem resistance in the fruit and pedicel was not investigated.

The uptake of Ca^{2+} and water by the roots are equally reduced by high salinity (Ho and Adams, 1989). As a result the concentration of Ca^{2+} in the xylem sap is not affected by salinity, even when the volume of the xylem sap is greatly reduced (Ehret

and Ho, 1986b). Therefore it is concluded that salinity does not influence the Ca^{2+} -import in the fruits by varying the Ca^{2+} -concentration of the xylem sap in the stem, but by varying the volume flow of water towards the fruit. Not only the uptake of Ca^{2+} by the roots is reduced by high salinity but also the proportional distribution towards the fruits (Ehret and Ho, 1986b; Ho and Adams, 1989). Although generally less Ca^{2+} is taken up by the roots at night than during the day, more Ca^{2+} is distributed to the fruits during the night than during the day (Ho, 1989), probably because the xylem stream towards the transpiring leaves is greatly reduced at night. Because low humidity (causing high transpiration) caused comparable responses as high salinity on the distribution of Ca^{2+} within the plant, and because it is known that high transpiration and high salinity both influence water potentials in the xylem of the stem significantly, an important role is assumed for the water relations of the plant. It is possible that diurnal dynamics of the water potential gradient between stem and fruit influenced water and Ca^{2+} -import through the xylem in the fruits: during the day at high transpiration, the water potential in the xylem of the stem may decrease and become lower than the water potential in the fruit. In that case the direction of the flow of water reverses and water loss through the xylem may occur. As a result Ca^{2+} -import into the fruit is blocked. Reversed water potential gradients between stem and fruit are observed at high radiation by Johnson *et al.* (1992) during large parts of the day. During the night and at low plant transpiration observed water potential gradients favoured import of water and thus of Ca^{2+} via the xylem. Since the hydraulic resistance of the xylem between stem and fruits is high due to a poor xylem connection in the pedicel (Lee, 1989), the volume flow through the xylem and accompanied change in water potential in the fruit is assumed to be low. The observations of Johnson *et al.* (1992) showed that the variation in water potential in the fruit was much lower than the variation in water potential in the stem. According to our own short-term measurements on plant water deficit during the day (Chapter 3.3 and 3.4) substantial net back-delivering of water from the fruits to the rest of the shoot at water stress situations is unlikely: only small variations in plant water content were measured while a considerable volume of water was stored in the fruits on that plant. On theoretical basis, it is possible that little reversed water flow in the xylem (which blocks Ca^{2+} import) occurs while at the same time water enters the fruit via the phloem and the fruit volume increases. The volume flow of water between stem and fruit via the phloem is usually much larger than the volume flow via the xylem: Based on accumulation ratios of ions Ho *et al.* (1987) calculated that ca. 90% of the water entering the fruit enters through the phloem. The driving force for phloem water flow is the turgor pressure gradient in the sieve tubes. Although it is influenced by the apoplastic water potential gradient it may be opposite to the apoplastic water potential gradient (for instance: when photosynthates are ex-

ported from a transpiring mature leaf). Ehret and Ho (1986c) suggested that phloem and xylem water transport into the fruits work on opposite diurnal cycles: Significant water transport via the xylem into the fruit only occurred during the night when phloem water import was at its minimum. This agrees with reported relative high amount of Ca^{2+} distributed to the fruits during the night (Ho, 1989). It is possible that our 'intuitive' salinity treatment decreased the incidence of BER by extending the total period during the day that water and Ca^{2+} import to the fruits is favoured.

Final conclusions concerning the underlying causes of the clear effect of the intuitive salinity treatment on the incidence of BER are hard to make because experimental evidence is lacking. The present simulation model (Chapter 5) is not suitable for simulations of xylem water flow between the stem xylem and fruits because fruits are not incorporated in the model. It is very well possible, however, to add fruits to the model and simulate the dynamic behaviour of xylem water flow between stem and fruits in response to changes in salinity level in the root environment.

6.3 Consequences

Present study show that short-term control of the EC (variation of the EC within a day) has the potency to become an additional tool to control yield and quality of tomato in greenhouses. Long-term control of the EC to influence growth and development of tomato plants has been used for years in Dutch tomato culture: it is common practise to force the plants to enter the reproductive stage by supplying a restricted amount of nutrient solution with a constant high EC during the first weeks of a growth season. Last decade, the long-term EC-level has been also used to influence the dry matter percentage of harvestable fruits, while it is accepted that this increase in quality is accompanied with a decrease in yield, and sometimes with an increase in the incidence of blossom-end-rot. Measurements in present study showed that changes in EC influenced plant water status and expansion growth of a plant within minutes. Adaptation to a EC-level occurred only partially and slowly (Chapter 3.3). These results suggest that short-term control of the EC could be probably well used as a tool to choose between yield and quality in producing tomatoes.

Useful application of short-term control of the EC is also determined by the growing system. In the Netherlands most of the tomatoes are grown on rockwool. Short-term changes of the EC at the root surface such as applied in this study are difficult to achieve in rockwool due to its buffering capacity. In rockwool growth systems the supply of nutrient solution is mostly restricted to the day time period. Variation between day and night salinity level would therefore be useless. Still, lowering the EC during parts of the day with high transpiration might be well profitable: decreasing the EC of the water supply will decrease the EC in the region of the rockwool slab where

the water is supplied, and it is known from split-root experiments that plants may use only a part of their roots to account for their water uptake when the conditions around this part of the roots favour water uptake.

The restriction of (macro) nutrient supply to the dark (as in the intuitive treatment) did not influence plant growth negatively. Instead an overall positive effect was measured on plant and fruit growth and on the incidence of BER. This demonstrates that the uptake of macro-nutrients during a limited period of the day could fulfil the need for macro-nutrients by the plant. This fact should be used in future research to investigate the possibility for reduction of the use and waste of nutrients in soilless culture.

The system for simultaneous measurements of transpiration and water uptake, which was developed within the framework of present study, provided lots of interesting data concerning short-term effects of shoot and root environment conditions on plant water relationships. Besides its positive characteristics, which made it appropriate for use in in situ situations (such as greenhouses), it has the 'disadvantage' of measuring changes in plant water content, which has to be converted into a thermodynamic property (water potential) to fit in the thermodynamic approach of plant water relations. However, due to its high accuracy and the possibility to measure transpiration, water uptake and changes in plant water content at a high resolution in time on the same plant, it promises to be a valuable tool in the research field of interaction between plant and environment.

Summary

More than 95 percent of the tomatoes produced in the Netherlands are grown in greenhouses on artificial substrates. Intensive control of the greenhouse climate and water supply, mainly by computers, are important tools in establishing the high fruit production of more than 40 kg m⁻² per year (1994). Since approximately a decade more and more is emphasised on an efficient production and on quality of the produced tomatoes, forced by the increasing competition from South European countries.

Recognition of the importance and possibilities of integration of climate control and control of the water and nutrient supply to the plants was the reason to start the research described in this thesis. This study concentrates on the possibilities of short-term control of the total nutrient concentration (salinity level) in the root environment in relation to the greenhouse climate. In horticultural practise the salinity level of the nutrient solution is generally characterised by its Electric Conductivity (EC; mS cm⁻¹). This EC is closely related to the osmotic potential of the nutrient solution. Except for a short period during the start of a growth season, usually an empirically determined long-term optimal nutrient solution with a constant EC of $\pm 2\text{-}3$ mS cm⁻¹ is supplied to roots of the plants.

A general assumption in this study is that the EC mainly influences plant functioning via its effect on the water relations of the plant: A high EC decreases the availability of water to the roots of the plant osmotically, and influences therefore the water uptake directly. In combination with a high demand for water caused by transpiration, it may lower water potentials in the plant significantly which negatively effects important physiological processes such as expansion growth and opening and closing of stomata. Although this concept is widely accepted, experimental results concerning effects of salinity on expansion growth and stomata opening are contradictory. This is partially due to a lack of reliable techniques to measure plant water relations in situ, and partially due to a poor understanding of the generally accepted thermodynamic approach of plant water relations. Therefore in this thesis a chapter is included which deals with the current concepts, measures and methods related to the thermodynamic approach of plant water relations and the associated term water potential (Chapter 2).

The experimental part of this study concentrates on short- and long-term responses of (changes in the) EC on plant growth and functioning. Short-term experiments were done to investigate short-term plant responses (changes in expansion growth, water status and transpiration within a day) upon changes in EC. Long-term experiments were done following a previous study concerning the effect of different day and night EC levels on the growth of young tomato plants. In this previous study growth of the plants was improved by a low EC during the day in combination with a high EC during the night. In the long-term experiments this previous study was ex-

tended to the production phase of the tomato plants during a whole growth season to check whether the positive effect on plant growth was followed by a positive effect on fruit production.

To analyse and integrate the short- and long-term experimental results (Chapter 3 and 4, respectively) in a theoretical concept based on the thermodynamic approach of plant water relations (Chapter 2) a model is developed which describes internal plant water relations and in particular dynamics of changes in water uptake by the roots and in plant water content in response to changes in salinity and transpiration (Chapter 5).

Although the history of plant water research goes back to at least 300-400 BC (Aristotle), and the introduction of thermodynamics into plant physiology took place around 80 years ago, measures of plant water status (Relative Water Content and Water Potential) and related methods to measure are still a source for discussion. The techniques to obtain values of RWC or water potentials in situ (greenhouses) are mostly destructive. Measured values depend highly on the technique used and on other trivial circumstances. Monitoring short-term changes in plant water status is therefore difficult and susceptible to errors. To be able to obtain reliable measurements of short-term changes in transpiration, water uptake and changes in plant water content (the total amount of water stored in the plant) a new method for simultaneous measurements of water uptake and transpiration on the same plant was developed (Chapter 3.2). From the accurately measured rates of transpiration and water uptake the momentaneous change in plant water content was obtained, which was used to construct plant water content transients in time. The method was described and tested thoroughly and used to investigate the short-term effects of changes in salinity on tomato plants in a growth chamber and in a greenhouse.

Short-term experiments were done in a growth-chamber at stable climate conditions and a 12 h dark 12 h light schedule, and in a greenhouse under normal growth conditions in spring/summer. Changes in EC (between 0.2 and 10 mS cm⁻¹) were applied in dark and in light, while transpiration, water uptake and plant water content were measured. In the growth chamber, salinity clearly influenced expansion growth and transpiration. In the greenhouse the effect on expansion growth was clearly apparent while the effect on transpiration was not significant: Directly after a change from low to high salinity in dark, expansion growth was completely ceased. In the following light period expansion growth partially recovered. When a similar change in salinity was done in the light, expansion growth recovered already during the same light period (within several hours). After the opposite change in salinity in dark (high to low salinity), expansion growth initially increased enormously and partially reduced during the

following light period. When this change was done in the light no overshoot on expansion growth was measured. These results point to a bipartite response of expansion growth to a change in salinity: a direct hydraulic response followed by some adaptation (probably under metabolic control).

Sudden changes in plant water content at transitions between light and dark in the growth chamber were attributed to changes in RWC of the plant (RWC^p). These changes in RWC^p clearly increased with increasing salinity. No simple quantitative relationships were found between the changes in RWC^p and simultaneously measured changes in transpiration rate (and estimated stomatal conductance) and expansion growth rate.

In the greenhouse experiments transpiration fluctuated with global radiation outside the greenhouse, while the water uptake followed with a short delay time of several minutes. As a result the water content of the plant (WC^p) fluctuated with global radiation while increasing (at low salinity). These fluctuations in WC^p as well as the transient changes in WC^p immediately after a change in salinity in dark, were attributed to changes in plant water deficit. Changes in plant water deficit after changes in salinity were low: approximately 8 g on a total plant weight of ca. 1250 g. The decline in plant water content (relative to the stable dark value) due to transpiration during the day varied between 0 and 15 g at low salinity, and between 0 and 35 g at high salinity (at about similar transpiration rates). These variations in plant water deficit were very low. The effect on expansion growth rate, on the other hand, was large.

Relating the measured transpiration to the estimated plant water deficits during a day resulted in different curves at low and high salinity. At both salinity levels the relationship showed a hysteresis effect over the day. At low salinity the average slope of the curve was lower than at high salinity and the hysteresis effect was less pronounced. Solute accumulation at the endodermis in the root was raised as a possible explanation for the hysteresis effect and the different slopes at low and high salinity. However, simulations showed that, although solute accumulation changed the transpiration-plant water deficit relationship clearly with increasing salinity, this was not the only cause for the different slopes at low and high salinity. Changes in capacities of cells for water storage with cell volume, or a direct effect of salinity on the root resistance were mentioned as possible other causes for the different slopes at low and high salinity. The hysteresis effect over a day was clearly simulated by the model.

Based on these results it may be concluded that the short-term effects of salinity on plant water relations, expansion growth and transpiration are rather complex. Probably other than hydraulic responses may play an important role. It was concluded that present simulation model needs some adaptation and should probably be combined with metabolic oriented models to describe expansion growth.

Different day and night salinity levels changed vegetative growth, yield and quality of tomato significantly. In the long-term experiments clear positive effects were measured of the intuitive treatment (low salinity during the day and high salinity during the night) on the yield of tomato: yield was increased greatly, mainly by a positive effect on average fruit size. After 12 weeks of harvesting a not statistically significant tendency for a higher number of harvested fruits was observed. Dry-matter distribution towards the fruits was increased and a small positive effect on fruit dry weight was measured. In contrary to a previous study on young tomato plants, vegetative growth of the plants was hardly influenced by the intuitive salinity treatment. Several aspects of fruit quality were influenced by the intuitive salinity treatment: A clear negative effect was measured on the dry matter percentage of the harvested fruits. The incidence of Blossom-End-Rot on the other hand was decreased greatly by the intuitive salinity treatment. Applying a low salinity during the night and a high salinity during the day caused in many aspects opposite responses as compared to the intuitive salinity-treatment.

In Chapter 6 the observed effects of changes in salinity on short-term expansion growth and transpiration and long-term yield and quality of the fruits are discussed within the theoretical framework of plant water relations. It is concluded that the daytime salinity level mainly influenced expansion growth of tomato fruits, and that the restriction of (macro) nutrient supply to the dark did not influence plant growth and production negatively. It is also mentioned that extrapolation of results obtained in a growth chamber to horticultural practise should be done with care, as was shown by the different effects of salinity on the transpiration rate in growth-chamber and greenhouse experiments.

It is concluded that short-term control of the EC could probably be well used as a tool to choose between yield and quality in tomato culture. It is also mentioned that in present growth systems (rockwool and glaswool) short-term control is probably less useful, due to the large nutrient solution buffer in the substrate which frustrates a quick change in salinity level at the root surface.

Samenvatting

Meer dan 95 % van de tomatenproductie in Nederland vindt plaats in kassen op kunstmatige bodemvervangers zoals steen- en glaswol. De huidige productie van veel bedrijven ligt boven de 40 kg tomaten per m² per jaar (peil 1994). Geautomatiseerde regelingen van zowel het kasklimaat als de water- en nutriëntengiften spelen bij het bereiken van deze hoge productie een belangrijke rol. Gedwongen door de stijgende concurrentie vanuit enkele landen aan de middellandse zee, is de nadruk bij de tomatenteelt steeds meer verschoven van het streven naar maximale productie naar het streven naar een efficiënte productie van een kwalitatief hoogwaardig produkt.

In het kader daarvan deed de vraag zich voor of integratie van de regelingen van het kasklimaat en van de water- en nutriëntengiften zou kunnen bijdragen aan het tot stand komen van een optimale productie. Dit vormde de aanleiding tot het onderzoek dat is beschreven in dit proefschrift.

Door toevoeging van nutriënten aan het water dat aan planten op substraat wordt gegeven, wordt voorzien in de behoefte aan voedingsstoffen, maar stijgt eveneens de zoutconcentratie van dat water. In de tuinbouwpraktijk wordt als grootheid voor de zoutconcentratie de EC (Electric Conductivity; mS cm⁻¹) gebruikt. Deze EC is direct gerelateerd aan de osmotische potentiaal van de voedingsoplossing. Gewoonlijk wordt de EC gedurende bijna het hele teeltseizoen op een constant niveau van ca. 2-3 mS cm⁻¹ gehouden. Momenteel wordt de EC nog niet gebruikt als een faktor om de plantengroei op de kort termijn te beïnvloeden. In dit onderzoek zijn de mogelijkheden van een korte termijn regeling van de EC in relatie tot het kasklimaat onderzocht.

Een belangrijk uitgangspunt van dit onderzoek is dat de EC het functioneren van de plant vooral beïnvloedt via een osmotisch effect op de waterhuishouding van de plant: een hoge EC verlaagt op osmotische wijze de beschikbaarheid van water aan het worteloppervlak, en bemoeilijkt daardoor de wateropname van de plant. Vooral in combinatie met een hoge transpiratiesnelheid kan een hoge EC daardoor de waterpotentialen in de plant aanzienlijk laten dalen. Lage waterpotentialen kunnen een aantal fysiologische processen in de plant, waaronder celstrekking en fotosynthese, negatief beïnvloeden.

Alhoewel deze gedachtengang algemeen geaccepteerd is, is de experimentele onderbouwing niet sterk. Metingen leverden vaak tegenstrijdige resultaten op, waarschijnlijk voor een groot deel door het gebruik van gebrekkige meettechnieken. Om een goede en duidelijke theoretische basis aan dit proefschrift te geven is er een hoofdstuk toegevoegd dat de huidige inzichten en theorieën m.b.t. de waterhuishouding van planten behandelt.

Het experimentele gedeelte van dit proefschrift concentreert zich op korte en lange termijn effecten van de EC op de groei en het functioneren van de plant. Er zijn

enkele experimenten uitgevoerd om snelle reacties van de plant (groei, veranderingen in water status en veranderingen in verdampingssnelheid) op veranderingen van de EC te onderzoeken. Ook werden er enkele lange termijn experimenten uitgevoerd (kasproeven gedurende enkele hele teeltseizoenen) waarin het effect van verschillende dag en nacht EC's op groei, productie en kwaliteit van de tomaten werd onderzocht.

Om de resultaten van deze korte en lange termijn experimenten goed te kunnen analyseren en integreren is een simulatie model ontwikkeld. Dit model beschrijft de interne waterhuishouding van de plant, en in het bijzonder de dynamiek van de wateropname en het watergehalte in de plant, als functie van veranderingen in EC en verdamping van de plant (Hoofdstuk 5).

Het model is gebaseerd op de thermodynamische benadering van de waterhuishouding van een plant. Hoewel deze benadering al zo'n 80 jaar geleden werd geïntroduceerd, is de grootheid (Relatief Water Gehalte of Water Potentiaal) die de water status van de plant moet beschrijven nog steeds een bron van discussie. De grootheden worden vaak gemeten met gebrekkige technieken, en gemeten waarden blijken vaak af te hangen van de gebruikte techniek en omgevingsafhankelijke omstandigheden. Het volgen van veranderingen in de water status van een plant op de korte termijn is met de huidige meettechnieken zeer moeilijk uitvoerbaar en gevoelig voor fouten. Om toch op de korte termijn in situ metingen te kunnen uitvoeren, is er een nieuwe methodiek ontwikkeld om verdamping en wateropname gelijktijdig te meten aan één plant met een hoge resolutie in de tijd. Deze gemeten grootheden werden vervolgens gebruikt om het verloop van de hoeveelheid water in de plant in de tijd te volgen. De meetmethode is uitgebreid getest en vervolgens gebruikt om korte termijn effecten van EC-veranderingen op groei, water status en verdamping van planten te meten.

Korte termijn experimenten werden uitgevoerd in een geconditioneerde omgeving met vaste licht/donker perioden (fytotron), en in een kas onder normale groeiomstandigheden (variabel licht). Veranderingen in de EC werden uitgevoerd in licht en donker, terwijl verdamping en wateropname werden gemeten. De veranderingen in hoeveelheid water in de plant waren gedeeltelijk structureel (het gevolg van groei) en gedeeltelijk van tijdelijk aard (veranderingen in plant water status). In het fyto-tron beïnvloedde de EC zowel de verdampings- als de groeisnelheid van de plant duidelijk. In de kas werd alleen het effect op de groeisnelheid zeer duidelijk gevonden: onmiddellijk na een verandering van een lage naar een hoge EC in het donker stagneerde de groei. Gedurende de daarop volgende licht periode trad een gedeeltelijk herstel op. Bij eenzelfde EC-verandering, maar dan uitgevoerd in het licht, trad het herstel eerder, namelijk in dezelfde lichtperiode, op. Bij een omgekeerde EC-verandering (van hoog naar laag) uitgevoerd in het donker, steeg de groeisnelheid in eerste instantie sterk, maar

vlakke vervolgens weer af in de daarop volgende licht periode. Wanneer eenzelfde EC-verandering werd uitgevoerd in licht werd er geen overreactie op de groeisnelheid gemeten. Deze meetresultaten wijzen op een tweeledig reactie van de plant op een verandering in EC: een directe, hydraulisch bepaalde reactie, gevolgd door een tweede, kleinere, en meer geleidelijke tegenreactie waarschijnlijk onder invloed van metabolische processen.

Plotselinge veranderingen in de hoeveelheid water in de plant bij overgangen tussen licht en donker (fytotron) werden toegeschreven aan veranderingen in water status (RWC^p) van de plant. Er is geen eenvoudige quantitative relatie gevonden tussen veranderingen in RWC^p en veranderingen in verdamping en groeisnelheid van de plant.

In de kasexperimenten was de verdamping vooral afhankelijk van de instraling. De wateropname volgde de verdamping met een vertragingstijd van enkele minuten. Als gevolg daarvan fluctueerde de hoeveelheid water in de plant met de instraling, terwijl de hoeveelheid water in de plant op de lange termijn toenam als gevolg van groei. Veranderingen in hoeveelheid water in de plant, gemeten direct na veranderingen in EC, waren laag: ca. 8 g op een totaal plant gewicht van ca. 1250 g. De daling in hoeveelheid water in de plant als gevolg van verdamping tijdens de dag varieerde tussen 0 en 15 g bij een lage EC, en tussen 0 en 35 g bij een hoge EC. Hoewel deze variaties in watergehalte in de plant erg laag waren, was het effect op de groeisnelheid groot.

De relatie tussen verdamping en water status in de plant over een dag, verschilde tussen een hoge en een lage EC. Het watergehalte in de plant zakte bij olopende instraling sneller bij een hoge EC dan bij een lage EC. Zowel bij een lage als ook bij een hoge EC werd over de dag heen een hysteresis effect gemeten op de relatie tussen watergehalte en instraling. Dit effect het duidelijkst bij een hoge EC. Als mogelijke verklaring voor dit verschil tussen een hoge en lage EC werd de ophoping van zouten aan de endodermis in de wortel gegeven. Echter, simulaties wezen uit dat deze zoutaccumulatie niet sterk genoeg kan zijn om het hele effect te verklaren. Veranderingen in de capaciteit voor wateropslag in de plant als gevolg van veranderende cel volumina, en een direct effect van de EC op de weerstand voor water transport in de wortels, werden geopperd als mogelijke andere verklaringen voor de als gevolg van EC veranderde relatie tussen water status en verdamping. Het hysteresis effect over een dag werd wel gesimuleerd door het model.

Deze resultaten laten zien dat de effecten van EC-veranderingen op de waterhuishouding, verdamping en groei van de plant complex zijn. Waarschijnlijk spelen ook andere effecten dan die op de waterhuishouding een rol. Om te komen tot een goed model van groei lijkt het noodzakelijk om waterhuishoudingsmodellen te combineren met meer metabolisch georiënteerde modellen.

Het toepassen van verschillende dag en nacht EC's tijdens lange termijn proeven in een kas (heel groei seizoen), veranderde de groei, produktie en kwaliteit van tomaten aanzienlijk. Duidelijke positieve effecten werden gemeten van een behandeling waarbij een lage EC gedurende de dag werd gecombineerd met een hoge EC gedurende de nacht (intuïtieve behandeling): De produktie steeg aanzienlijk, vooral door een positief effect op de gemiddelde vruchtengrootte. Ook steeg het aantal geoogste vruchten licht. De drogestof verdeling naar de vruchten was enigszins verhoogd en een klein positief effect werd gemeten op het droog gewicht per vrucht. In tegenstelling tot wat was gemeten aan jonge planten in een voorgaand experiment, bleek dat de vegetatieve groei nauwelijks was beïnvloed. De kwaliteit van de vruchten was wel beïnvloed door de intuïtieve EC-behandeling: het droge stof gehalte in de vruchten nam af terwijl neusrot vrijwel niet meer voorkwam. Een tegengestelde EC-behandeling (laag gedurende de nacht en hoog gedurende de dag) bleek in veel opzichten een omgekeerd effect te veroorzaken.

In het laatste hoofdstuk van het proefschrift zijn de gemeten korte termijn effecten van veranderingen in de EC op groei en verdamping en lange termijn effecten op produktie en kwaliteit van de vruchten bediscussieerd binnen het theoretische kader van de waterhuishouding. Er werd geconcludeerd dat vooral de EC tijdens de dag de groei van de vruchten beïnvloedde, en dat restrictie van de gift van macro-nutrienten tot de nacht geen negatieve effecten had op groei en produktie. Verder werd opgemerkt dat uit het huidige onderzoek wederom is gebleken dat extrapolatie van resultaten gemeten in een fytotron naar de tuinbouwpraktijk zeer voorzichtig moet gebeuren.

Regeling van de EC op de korte termijn zou een goede mogelijkheid kunnen zijn om te sturen op produktie of kwaliteit. In de huidige teeltsystemen zal het effect ervan waarschijnlijk beperkt zijn door het grote bufferende vermogen van de substraten m. b. t. water en nutrienten.

References

- ACEVEDO, E., HSIAO, T.C. and HENDERSON, D.W. (1971). Immediate and subsequent growth responses of Maize leaves to changes in water status. *Plant Physiology*, **48**, 631-36.
- ACOCK, B. (1987). Characterizing Physiological factors in water relations. In: *Plant growth modeling for resource management*. Volume II (Eds.)
- ACOCK, B., CHARLES EDWARDS, D.A., FITTER, D.J., HAND, D.W., LUDWIG, L.J., WARREN WILSON, J., WITHERS, A.C. (1978). The contribution of leaves from different levels within a tomato crop to canopy net photosynthesis: an experimental examination of two canopy models. *Journal of Experimental Botany* **29**, 815-27.
- ADAMS, P. (1991). Effects of increasing the salinity of the nutrient solution with major nutrients or sodium chloride on the yield, quality and composition of tomatoes grown in rockwool. *Journal of Horticultural Science*, **66**, 201-7.
- ADAMS, P. And EL-GIZAWY, A.M. (1988). Effect of calcium stress on the calcium status of tomatoes grown in NFT. *Acta Horticulturae*, **222**, 15-22.
- ADAMS, P. and HO, L.C. (1989). Effects of constant and fluctuating salinity on the yield, quality and calcium status of tomatoes. *Journal of Horticultural Science*, **64**, 725-32.
- ADAMS, P. and HO, L.C. (1992). The susceptibility of modern tomato cultivars to blossom-end rot in relation to salinity. *Journal of Horticultural Science*, **67**, 827-839.
- AIKMAN, D.P. and HOUTER, G. (1990). Influence of radiation and humidity on transpiration: Implications for calcium levels in tomato leaves. *Journal of Horticultural Science*, **65**, 245-53.
- ALM, D.M., HESKETH, J.D. STOLLER, E.W. and WAX, L.M. (1994). A model of water flow through growing plants. *Biotronics*, **23**, 11-34.
- ANONYMOUS (1995). *Kwantitatieve informatie voor de glastuinbouw 1995-1996*. Informatie en Kennis Centrum Landbouw, Afdeling Glasgroente en Bloemisterij, Aalsmeer/Naaldwijk.
- ARKEBAUER, T.J. and NORMAN J.M. (1995a). From cell growth to leaf growth: I. Coupling cell division and cell expansion. *Agronomy Journal*, **87**, 99-105.
- ARKEBAUER, T.J. and NORMAN J.M. (1995b). From cell growth to leaf growth: I. Simulation of a file of cells. *Agronomy Journal*, **87**, 106-112.
- ARKEBAUER, T.J., NORMAN J.M. and SULLIVAN, C.Y. (1995c). From cell growth to leaf growth: I. Kinetics of leaf expansion. *Agronomy Journal*, **87**, 112-121.
- ASTON, M.J. and LAWLOR, D.W. (1979). The relationship between transpiration, root water uptake and leaf water potential. *Journal of Experimental Botany*, **30**, 169-81.
- BAKER, D.A. (1985). Water relations. In: *Advanced Plant Physiology*. (Wilkins, W.M., Ed.). Longman, London, UK, 295-318.
- BAKKER, J.C. (1991). Analysis of humidity effects on growth and production of glasshouse fruit vegetables. Dissertation Agricultural University Wageningen, 155 pp.
- BATES, L.M. and HALL, A.E. (1981). Stomatal closure with soil water depletion not associated with changes in bulk leaf water status. *Oecologia*, **50**, 62-65.
- BATTA, L.G.G. (1989). Modelling of water potential and water uptake rate of greenhouse tomato plants. *Acta Horticulturae*, **248**, 356-60.
- BEHBOUDIAN, M.H. (1977). Responses of eggplant to drought. I. Plant water balance. *Scientia Horticulturae*, **7**, 303-10.
- BENSEN, R., BOYER, J.S. and MULLET, J.E. (1988). Water deficit-induced changes in abscisic acid content, growth, polysomes, and translatable RNA in soybean hypocotyls. *Plant Physiology*, **88**, 289-94.

- BERNSTEIN, L. (1963). Osmotic adjustment of plants to saline media. II. Dynamic phase. *American Journal of Botany*, **50**, 360-70.
- BLACKMAN, P.G., DAVIES, W.J. (1985). Root to shoot communication in maize plants of the effects of soil drying. *Journal of Experimental Botany*, **36**, 39-48.
- BOT, G.P.A. (1983). Greenhouse climate: from physical process to a dynamic model. Dissertation Agricultural University, Wageningen, 240 pp.
- BOUMA, T.J. (1995). Utilization of respiratory energy in higher plants: requirements for 'maintenance' and transport processes. Dissertation Agricultural University, Wageningen. 143 pp.
- BOYER, J.S. (1985). Water transport. *Annual Review of Plant Physiology*, **36**, 473-516.
- BOYER, J.S. (1989). Water potential and plant metabolism: comments on Dr P. J. Kramer's article, 'Changing concepts regarding plant water relations', Volume 11, Number 7, pp. 565-568, and Dr J. B. Passioura's Response, pp. 569-571 *Plant Cell and Environment*, **12**, 213-216.
- BOYER, J.S. and NONAMI, H. (1993). Direct demonstration of a growth induced water potential gradient. *Plant Physiology*, **102**, 13-19.
- BRADFIELD, E.G. and GUTTRIDGE, C.G. (1984). Effects of night-time humidity and nutrient solution concentration on the calcium content of tomato fruit. *Scientia Horticulturae*, **22**, 207-17.
- BRADFORD, K.J. and HSIAO, T.C. (1982). Physiological responses to moderate water stress. In: *Encyclopaedia of Plant Physiology: Physiological Plant Ecology II, Water relations and Carbon Assimilation (NS)*, 12B. (Lange, O.L., Nobel, P.S., Osmond, C.B. and Ziegler, H., Eds). Springer Verlag, Berlin/New York, 263-323.
- BRUGGINK, G.T., SCHOUWINK, H.E. and COOLEN, E.A.J.M. (1987). Effects of different day and night osmotic potentials of the nutrient solution on growth, waterpotentials and osmotic potentials of young tomato plants, *Soiless Culture*, **3**, 9-19.
- BRUGGINK, G.T., SCHOUWINK, H.E. and GIELING, Th.H. (1988). Modelling of water potential and water uptake rate of tomato plants in the greenhouse: preliminary results. *Acta Horticulturae*, **229**, 177-85.
- BURROWS, F.J. and MILTHORPE, F.L. (1976). Stomatal conductance in the control of gas exchange. In: *Water deficits and plant growth. Vol. IV: Soil water measurement, plant responses and breeding for drought resistance*. (Kozłowski, T.T., Ed.). Academic Press, New York, 103-52.
- CANNY, M.J. (1985). Translocation of nutrients and hormones. In: *Advanced Plant Physiology*, (Wilkins, M.B., Ed.), Longman, London, UK, 295-318.
- CHALLA, H. and SCHAPEDONK, A.H.C.M. (1986). Dynamic optimisation of the CO₂-concentration in relation to climate control in greenhouse crops. In: *Carbon dioxide enrichment of greenhouse crops. Volume I, Status and CO₂ sources* (Enoch, H.Z. and Kimball, B.A., Eds.), CRC Press Inc., Boca Raton, Florida, 147-60.
- CHALLA, H., (1990). Crop growth models for greenhouse climate control. In: *Theoretical production ecology: reflections and prospects*. (Rabbinge, R., Goudriaan, J., Van Keulen, H., Penning de Vries, F.W.T. and Van Laar, H.H., Eds.), Simulation monographs, 34, PUDOC, Wageningen, 125-145.
- CHALLA, H., (1993). Optimal diurnal climate control in greenhouses as related to greenhouse management and crop requirements. In: *The Computerized Greenhouse: automatic control application in plant production*. (Hashimoto, Y., Bot, G.P.A., and Day, W., Eds.) Academic Press, San Diego, 340 pp.
- CHALLA, H., BOT, G.P.A., NEDERHOFF, E.M. and VAN DE BRAAK, N.J. (1988). Greenhouse climate control in the nineties. *Acta Horticulturae*, **230**, 459-470.

- CHARBONNEAU, J., GOSSELIN, A. and TRUDEL, M.J. (1988). Influence of electric conductivity and intermittent flow of the nutrient solution on growth and yield of greenhouse tomato in NFT. *Soilless Culture*, **4**, 19-30.
- CHAZEN, O., and NEUMANN, P.M. (1994). Hydraulic signals from the roots and rapid cell-wall hardening in growing Maize (*Zea mays* L.) leaves are primary responses to polyethylene glycol-induced water deficits. *Plant Physiology*, **104**, 1385-92.
- CHEUNG, Y.N.S., TYREE, M.T. AND DAINTY, J. (1976). Some possible sources of error in determining bulk elastic moduli and other parameters from pressure-volume curves of shoots and leaves. *Canadian Journal of Botany* **54**, 758-65.
- CHRIST, R.A. (1978). The elongation of wheat leaves. I. Elongation rates during day and night. *Journal of Experimental Botany*, **29**, 603-10.
- CLARKSON, D.T. (1984). Calcium transport between tissues and its distribution in the plant. *Plant, Cell and Environment*, **7**, 207-17.
- COSGROVE, D.J. (1985). Cell wall yield properties of growing tissue. *Plant Physiology*, **78**, 347-356.
- COSGROVE, D.J. (1986a). Biophysical control of plant cell growth. *Annual Review of Plant Physiology*, **37**, 377-405.
- COSGROVE, D.J. (1986b). Update on cell walls: How do plant cell walls extend? *Plant Physiology*, **102**, 1-6.
- COSGROVE, D.J. (1993). How do plant cell walls extend? *Plant Physiology*, **102**, 1-6.
- COWAN, I.R. (1965). Transport of water in the soil-plant-atmosphere system, *Journal of Applied Ecology*, **2**, 221-39.
- COWAN, I.R. and MILTHORPE, F.L. (1968). Plant factors influencing the water status of plant tissues. In: *Water deficits and plant growth*. (KOZLOWSKI, T.T., Ed.), Volume 1. Academic Press New York/London, 23-47.
- CRAMER, G.R. and BOWMAN, D.C. (1991). Kinetics of Maize leaf elongation. *Journal of Experimental Botany*, **42**, 1417-26.
- DAINTY, J. (1976). Water relations of plant cells. In: U Löttge, MG Pitman, Eds, Transport in plants II. *Encyclopedia of plant physiology*, Vol IIA, Springer Berlin, Heidelberg, New York. pp 12-35.
- DALE, J.E. (1988). The control of leaf expansion. *Annual Review of Plant Physiology*, **39**, 267-295.
- DALE, J.E. and SUTCLIFFE, J.F. (1986). Water relations of plant cells. In: FC Steward, ed. *Plant Physiology*, Volume IX, Water and solutes in plants, Academic press, London. pp 1-48.
- DALTON, F.N., RAATS, P.A.C. and GARDNER, W.R. (1975). Simultaneous uptake of water and solutes by plant roots. *Agronomy Journal*, **67**, 334-9.
- DAVIES, W.J. and JEFFCOAT, B. (1990). Eds: *Importance of root to shoot communication in the response to environmental stress*. Monogr. 21. Bristol: Br. Society. Plant Growth Regul. 398 pp.
- DAVIES, W.J. and ZHANG, J. (1991). Root signals and the regulation of growth and development of plants in drying soil. *Annual Review of Plant Physiology and Plant Molecular Biology*, **42**, 55-76.
- DIMOND, A.E. (1966). Pressure and flow relations in vascular bundles of the tomato plant. *Plant Physiology*, **41**, 119-131.
- EHRET, D.L. and HO, L.C. (1986a). The effect of salinity on dry matter partitioning and fruit growth in tomatoes grown in nutrient film culture. *Journal of Horticultural Science*, **61**, 361-7.
- EHRET, D.L. and HO, L.C. (1986b). Translocation of calcium in relation to tomato fruit growth. *Annals of Botany*, **58**, 679-88.

- EHRET, D.L. and HO, L.C. (1986c). Effects of osmotic potential in nutrient solution on diurnal growth of tomato. *Journal of Experimental Botany*, **37**, 1294-302.
- ESAU, K. (1960). *Anatomy of seed plants*. New York: J. Wiley and sons.
- FERGUSON, I.B. and BOLLARD, E.G. (1976). The movement of calcium in woody stems. *Annals of Botany*, **40**, 1057-65.
- FISCUS, E.L. (1975). The interaction between osmotic- and pressure induced water flow in plant roots. *Plant Physiology* **55**, 917-22
- FISCUS, E.L. (1977). Determination of hydraulic and osmotic properties of soybean root systems. *Plant Physiology*, **59**, 1013-20
- FISCUS, E.L. (1986). Diurnal changes in volume and solute transport coefficients of Phaseolus roots. *Plant Physiology*, **80**, 752-59.
- FISCUS, E.L., KLUTE, A. and KAUFMANN, M.R. (1983). An interpretation of some whole plant water transport phenomena. *Plant Physiology*, **71**, 810-17.
- FRENSCH, J. and HSIAO, T.C. (1994). Hydraulic propagation of pressure along immature and mature xylem vessels of Zea Mays measured by pressure-probe techniques. *Planta*, **190**, 263-70.
- FRENSCH, J. and HSIAO, T.C. (1994). Transient responses of cell turgor and growth of maize roots as affected by changes in water potential. *Plant Physiology*, **104**, 247-54.
- GARDNER, W.R. (1965). Movement of Nitrogen in soil. In: *Soil Nitrogen* (Bartholomev, W.V. and Clark, F.E., Eds). American Society of Agronomy, Madison, 550-72.
- GOLLAN, T., PASSIOURA, J.B. and MUNNS, R. (1986). Soil water status affects the stomatal conductance of fully turgid wheat and sunflower leaves. *Australian Journal of Plant Physiology*, **13**, 495-464.
- GOLLAN, T., SCHURR, U. and SCHULZE, E.D., (1992). Stomatal response to drying soil in relation to changes in the xylem sap composition of *Helianthus annuus*. I. The concentration of cations, anions, amino acids in, and pH of, the xylem sap. *Plant Cell and Environment*, **15**, 551-559.
- GOOR, B.J. VAN, (1968). The role of calcium and cell permeability in the disease blossom-end rot of tomatoes. *Physiologia Plantarum*, **21**, 1110-1121.
- GOUDRIAAN, J. (1977). *Crop Meteorology: a simulation study*. Pudoc, Wageningen, 257 pp.
- GOUGH, C. and HOBSON, G.E. (1990). A comparison of the productivity, quality, shelf-life characteristics and consumer reaction to the crop from cherry tomato plants grown at different levels of salinity. *Journal of Horticultural Science*, **65**, 431-39.
- GRAAF, R. DE, and ENDE, J. VAN DEN (1981). Transpiration and evapotranspiration of glasshouse crops. *Acta Horticulturae* **119**, 147-58.
- GRAVES, C.J. (1983). The Nutrient Film Technique. In: *Horticultural Reviews* (Janick, J. Ed.). AVI Publishing Company INC, West Port, Connecticut, volume 5, 1-44.
- HALES, S. (1727) In: *Vegetable statistics* (Innys, W., Innys, J. and Woodward, T. Eds.). London (Reprinted by Scientific Book Guild, London, 1961).
- HAYWARD, H.E. and LONG, E.M. (1943). Some effects of sodium salts on the growth of tomato. *Plant Physiology*, **18**, 556-69.
- HEUVELINK, E. (1996). Tomato growth and yield: quantitative analysis and synthesis. Dissertation Agricultural University, Wageningen. 319 pp.
- HEUVELINK, E. (1996a). Dry matter partitioning in tomato: validation of a dynamic simulation model. *Annals of Botany*, **77**, 71-80.
- HEUVELINK, E. and BUISSKOOL, R.P.M. (1995). Influence of sink-source interaction on dry matter production in tomato. *Annals of Botany*, **75**, 381-9.

- HICKLENTON, P.R. and JOLLIFFE, P.A. (1980). Alterations in the physiology of CO₂ exchange in tomato plants grown in CO₂ enriched atmospheres. *Canadian Journal of Botany*, **58**, 2181-89.
- HILLEL, D. (1971). In: *Soil and Water: Physical Principles and Processes*, Academic Press, New York, 288 pp.
- HO, L.C. (1988). The physiological basis for improving dry matter content and calcium status in tomato fruit. *Applied Agricultural Research*, **3**, 275-81.
- HO, L.C. (1989). Environmental effects on the diurnal accumulation of ⁴⁵Ca by young fruit and leaves of tomato plants. *Annals of Botany*, **63**, 281-8.
- HO, L.C. and ADAMS, P. (1989). Effects of diurnal changes in salinity of the nutrient solution on the accumulation of calcium in the tomato fruit. *Annals of Botany*, **64**, 373-82.
- HO, L.C. and ADAMS, P. (1994). The physiological basis for high fruit yield and susceptibility to calcium deficiency in tomato and cucumber. *Journal of Horticultural Science*, **69**, 377-83.
- HO, L.C. and EHRET, D.L., (1984). Effects of salinity on dry matter partitioning, fruit growth and calcium accumulation in tomatoes grown in nutrient-film culture. *Glasshouse Crops Research Institute, Annual Report*, 49-50.
- HO, L.C., BELDA, R., BROWN, M., ANDREWS, J. and ADAMS, P. (1993). Uptake and transport of calcium and the possible causes of blossom-end rot in tomato. *Journal of Experimental Botany*, **44**, 509-518.
- HO, L.C., GRANGE, R.I., and PICKEN, A.J. (1987). An analysis of the accumulation of water and dry matter in tomato fruit. *Plant, Cell and Environment* (1987) **10**, 157-62.
- HÖFLER, K. (1920). Ein schema für die osmotische leistung de Pflanzenzelle. *Berichte der Deutschen Botanischen Gesellschaft*, **38**, 288-98.
- HONERT, T.H. VAN DEN (1948). Water transport in plants as a catenary process. *Discussion Faraday Society* **3**, 146-53.
- HSIAO, T.C. (1973). Plant responses to water stress. *Annual Review of Plant Physiology*, **24**, 519-70.
- IEPEREN, W. VAN and MADERY, H. (1994). A new method to measure plant water uptake and transpiration simultaneously. *Journal of Experimental Botany*, **45**, 51-60.
- IEPEREN, W. VAN. (1996). Effects of different day and night salinity levels on vegetative growth, yield and quality of tomato. *Journal of Horticultural Science*, **70**, in press.
- IEPEREN, W. VAN. (1996a). Dynamic effects of changes in electric conductivity on transpiration and growth of greenhouse grown tomato plants. *Journal of Horticultural Science*, **71**, 481-96.
- JARVIS, P.G. and McNAUGHTON, K.G. (1986). Stomatal control of transpiration: scaling up from leaf to region. *Advances in Ecological Research*, **15**, 1-49.
- JARVIS, P.G., EDWARDS, W.R.N. and TALBOT, H. (1981). Models of plant and crop water use. In: *Mathematics and Plant Physiology*. (Rose, D.A. and Charles-Edwards, D.A. Eds). Academic Press, London, UK, 151-94.
- JENSEN, C.R., HENSON, I.E. and TURNER, N.C. (1989). Leaf gas exchange and water relations of Lupins and Wheat II. Root and shoot water relations of Lupin during drought-induced stomatal closure. *Australian Journal of Plant Physiology*, **16**, 401-13.
- JENSEN, R.D., TAYLOR, S.A. and Wiebe, H.H. (1961). Negative transport and resistance to water flow through plants. *Plant Physiology*, **36**, 633-8.
- JOHNSON, I.R. (1991). A model of water flow through plants incorporating shoot/root 'message' control of stomatal conductance. *Plant, Cell and Environment*, **14**, 531-44.
- JOHNSON, R.W., DIXON, M.A. and LEE, D.R. (1992). Water relations of the tomato during fruit growth. *Plant, Cell and Environment*, **15**, 947-53.

- KAMOTO, F. and NAITA, Y. (1975). Studies of photosynthesis and transpiration of vegetable crops. II. A linear electronic device for continuous measurements of stem and fruit enlargement in relation to water stress. *Bulletin of the Vegetable and Ornamental Research Station, Japan series A2*, 33-47.
- KATCHALSKY, A. and CURRAN, P.F. (1965). *Nonequilibrium thermodynamics in biophysics*. Cambridge: Harvard University Press.
- KLEPPER, B. (1971). Stem diameter in relation to plant water status. *Plant physiology*, **48**, 683-85.
- KONING, A.N.M. DE. (1994). Development and dry matter distribution in glasshouse tomato: a quantitative approach. Dissertation Agricultural University, Wageningen, 240 pp.
- KONING, A.N.M. de. and HURD, R.G. (1983). A comparison of winter sown tomato plants grown with restricted and unlimited water supply. *The Journal of Horticultural Science*, **58**, 575-81.
- KRAMER, P.J. (1983). *Water relations of plants*. Academic Press, New York, 489 pp.
- KRAMER, P.J. (1988a). Plant relative water content and related methods: Historical perspectives and current concerns, *Irrigation Science*, **9**, 275-87.
- KRAMER, P.J. (1988b). Changing concepts regarding plant water relations. *Plant Cell and Environment*, **11**, 565-68.
- KUIPER, P.J.C. (1961). The effects of environmental factors on the transpiration of leaves with special reference to stomatal light response. *Med. Agricultural University Wageningen*, **61**, 1-49.
- LANDSBERG, J., BLANCHARD, T.W. and WARRIT, B. (1976). Studies on the movement of water through apple trees. *Journal of Experimental Botany*, **99**, 579-96.
- LEARY, J.W. (1969). The effect of salinity in permeability of roots to water. *Israeli Journal of Botany* **18**, 1-9.
- LEE, D.R. (1989). Vasculature of the abscission zone of tomato fruit: implications for transport. *Canadian Journal of Botany*, **67**, 1898-02.
- LOCKHART, J.A. (1965). An analysis of irreversible plant cell elongation. *Journal of Theoretical Biology*, **8**, 264-75.
- LOPUSHINSKY, W. (1961). Effect of water movement on salt movement through tomato roots. *Nature*, **192**, 994-5.
- LOPUSHINSKY, W. (1964). Effect of Water Movement on Ion Movement into the Xylem of Tomato Roots. *Plant Physiology*, **39**, 494-501.
- MALONE, M. and TOMOS, A.D. (1992). Measurements of gradients of water potential in elongating pea stem by pressure probe and picolitre osmometry. *Journal of Experimental Botany*, **43**, 1325-31.
- MANSFIELD, T.A. and SNAITH, P.J. (1989). Circadian rhythms. In: *Advanced Plant Physiology*. (Wilkins, M.B., Ed). Longman Scientific & Technical, Harlow, UK, 201-18.
- MARCELIS, L.F.M. (1989). Simulation of plant-water relations and photosynthesis of greenhouse crops. *Scientia Horticulturae*, **41**, 9-18.
- MARTIN, E.S. and MEIDNER, H. (1971). Endogeneous stomatal movements in *Tradescantia virginiana*. *New Phytologist*, **70**, 923-28.
- MARTIN, E.S. and MEIDNER, H. (1972). The phase response of the dark stomatal rhythm in *Tradescantia virginiana*. *New Phytologist*, **71**, 1045-54.
- MASSEY, D.M., HAYWARD, A.C. and WINSOR, G.W. (1984). Some responses of tomatoes to salinity in nutrient-film culture. *Glasshouse Crops Research Institute, Annual Report*, 60-62.
- MCDONALD, A.J.S., JORDAN, J.R. and FORD, E.D. (1981). An automated potometer. *Journal of Experimental Botany*, **32**, 581-89.

- MEES, G.C. and WEATHERLEY, P.E. (1957). The mechanism of water absorption by roots I. Preliminary studies on the effects of hydrostatic pressure gradients. *Proceedings Royal Society London, B*, **147**, 367-80.
- MEIDNER, H. and SHERRIF, D.W. (1976). *Water and plants*. Blackie and Son Limited, Glasgow/London, UK 147 pp.
- MESHCHERYAKOV, A., STEUDLE, E. and KOMOR, E. (1992). Gradients of turgor, osmotic pressure, and water potential in the cortex of the hypocotyl of growing *Ricinus* seedlings. *Plant Physiology*, **98**, 840-52.
- MILTHORPE, F.L. and MOORBY, (1979). *An introduction to crop physiology*. Cambridge University Press, London, New York, New Rochelle, Melbourne, Sydney, 244 pp.
- MONTEITH, J.L. and UNSWORTH, M.H. (1990). *Principles of environmental physics*. Edward Arnold, Hodder & Stoughton, London, UK, 291.
- MORGAN, J.M. (1984). Osmoregulation and water stress in higher plants. *Annual Review of Plant Physiology*, **35**, 299-319.
- MUNNS, R. (1993). Physiological processes limiting plant growth in saline soils: some dogmas and hypotheses. *Plant Cell and Environment*, **16**, 15-24.
- MUNNS, R. and KING, R.W. (1988). Abscisic acid is not the only stomatal inhibitor in the transpiration stream of wheat plants. *Plant Physiology*, **88**, 703-8.
- MUNNS, R. and PASSIOURA, J.B. (1984). Effect of prolonged exposure to NaCl on the osmotic pressure of leaf xylem sap of intact transpiring Barley plants. *Australian Journal of Plant Physiology*, **11**, 497-507.
- NAGAYAMA, F.S. and EHRLER, W.L. (1964). Beta-ray gauging technique for measuring leaf water content changes and water status of plants. *Plant Physiology*, **39**, 95-98.
- NEDERHOF, E.M. (1994). Effects of CO₂ concentration on photosynthesis, transpiration and production of greenhouse fruit vegetable crops. Dissertation Agricultural University, Wageningen, 213 pp.
- NEWMAN, E.I. (1971). Root-Soil water relations. In: *The plant root and its environment*. (Carson, E.W. Ed.). University press of Virginia, Charlottesville.
- NEWMAN, E.I. (1976). Interaction between osmotic and pressure-induced water flow in plants. *Plant Physiology*, **57**, 738-39.
- NOBEL, P.S. (1983). *Biophysical plant physiology and ecology*, Freeman and Company, New York, USA, 608 pp.
- NOBEL, P.S. and JORDAN, P.W. (1983). Transpiration stream of desert species: resistances and capacitances for a C₃, a C₄, and a CAM plant. *Journal of Experimental Botany*, **34**, 1379-91.
- NONAMI, H. (1993). Growth regulation in plant factories and greenhouses from physiological viewpoint. In: *The Computerized Greenhouse: automatic control application in plant production*. (Hashimoto, Y., Bot, G.P.A., and Day, W., Eds.) Academic Press, San Diego, 340 pp.
- NONAMI, H. and BOYER, J.S. (1990). Primary events regulating stem growth at low water potentials. *Plant Physiology*, **93**, 1601-19.
- OKATANI, M., NONAMI, H., FUKUYAMA, T. and HASHIMOTO, Y. (1995). Growth-induced water potential in leaves and stems of tomato plants and citrus trees grown in hydroponic culture. *Acta Horticulturae*, **396**, 99-106.
- PAPADOPOULOS, I., and RENDIG, V.V. (1984). Interactive effects of salinity and nitrogen on growth and yield of tomato plants. *Plant and Soil*, **73**, 47-57.
- PASSIOURA, J.B. (1980). The meaning of matric potential. *Journal of Experimental Botany*, **31**, 1161-69.
- PASSIOURA, J.B. (1984). Hydraulic Resistance of Plants. I. *Australian Journal of Plant Physiology* **11**, 333-9.

- PASSIOURA, J.B. (1988). Response to Dr P. J. Kramers's article, 'Changing concepts regarding plant water relations', Volume 11, Number 7, pp. 565-568, *Plant Cell and Environment*, **11**, 569-71.
- PASSIOURA, J.B. (1988a). Water transport in and to roots. *Annual Review of Plant Physiology*, **39**, 245-65.
- PASSIOURA, J.B. (1991). An impasse in Plant Water Relations? *Acta Botanica*, **104**, 405-9.
- PASSIOURA, J.B. and FRY, S.C. (1992). Turgor and cell expansion: beyond the Lockhart equation. *Australian Journal of Plant Physiology*, **19**, 565-76.
- PASSIOURA, J.B. and GARDNER, A. (1990). Control of leaf expansion in wheat seedlings growing in drying soil. *Australian Journal of Plant Physiology*, **17**, 149-57.
- PEARCE, B.D., GRANGE, R.I. and HARDWICK, K. (1993a). The growth of young tomato fruit. I. Effects of temperature and irradiance on fruit grown in controlled environments. *Journal of Horticultural Science*, **68**, 1-11.
- PEARCE, B.D., GRANGE, R.I. and HARDWICK, K. (1993b). The growth of young tomato fruit. II. Environmental influences on glasshouse crops grown in rockwool or nutrient film. *Journal of Horticultural Science*, **68**, 13-23.
- PLODOWSKA, J.W., JONGEBLOED, P.H.J., VAN DE SANDEN, P.A.C.M. and STRUIK, P.C. (1989). Effects of a short period of drought on changes in tuber volume and specific leaf weight. II. Diurnal changes. *Potato Research*, **32**, 255-66.
- RASCHKE, K. (1975). Stomatal action. *Annual Review of Plant Physiology*, **26**, 309-40.
- REINDERS, J.E.A. (1987). A nuclear magnetic resonance study of plant-water relationships. Dissertation. Agricultural University, Wageningen. 148 pp.
- RENNER, O., (1912). Versuche zur mechanik der wasserversorgung. 2. Über Wurzelatigkeit. *Berichte der Deutschen Botanischen Gesellschaft*, **30**, 642-48.
- RUDICH, J., KALMAR, D., GEIZENBERG, C. and HAREL, S. (1977). Low water tensions in defined growth stages of processing tomato plants and their effects on yield and quality. *Journal of Horticultural Science*, **52**, 391-99.
- SALIM, M. and PITMAN, M.G. (1984). Pressure-induced water and solute flow through plant roots. *Journal of Experimental Botany*, **35**, 869-81.
- SÁNCHEZ CONDE, M.P. and AZUARA, P. (1979). Effect of balanced solutions with different osmotic pressure on tomato plant. *Journal of Plant Nutrition*, **1**, 295-307.
- SANDEN, P.A.C.M. VAN DEN, and VEEN, B.W. (1992). Effects of air humidity and nutrient solution concentration on growth, water potential and stomatal conductance of cucumber seedlings. *Scientia Horticulturae*, **50**, 173-186.
- SCHOLANDER, P.F., HAMMEL, H.T., BRADSTREET, D.E. and HEMMINGSEN, E.A. (1965). Sap pressure in vascular plants. *Science*, **148**, 339-46.
- SCHULTE, P.J. (1992). The units of currency for plant water status. *Plant Cell and Environment*, **15**, 7-10.
- SCHULTZ, H.R. and MATTHEWS, M.A. (1993). Growth, osmotic adjustment and cell wall mechanics of expanding grape leaves during water deficits. *Crop Science*, **33**, 287-94.
- SCHULTZE, E.D. and HALL, A.E. (1982). Stomatal responses, water loss and CO₂ assimilation rate in contrasting environments. In: *Encyclopaedia of Plant Physiology: Physiological Plant Ecology II, Water relations and Carbon Assimilation (NS)*, 12B. (Lange, O.L., Nobel, P.S., Osmond, C.B. and Ziegler, H., Eds). Springer Verlag, Berlin/New York. 181-230.
- SCHULZE, E.D. (1986). Carbon dioxide and water vapour exchange in response to drought in the soil. *Annual Review of Plant Physiology*, **37**, 247-74.

- SCHULZE, E.D., STEUDLE, E., GOLLAN, T. and SCHURR, U. (1988). Response to Dr P. J. Kramers's article, 'Changing concepts regarding plant water relations', Volume 11, Number 7, pp. 565-568, *Plant Cell and Environment*, **11**, 573-76.
- SERPE, M.D. and MATTHEWS, M.A. (1992). Rapid changes in cell wall yielding of elongating *Begonia argento-guttata* L. leaves in response to changes in plant water status. *Plant Physiology*, **100**, 1852-57.
- SHACKEL, K.A. (1984). Theoretical and experimental errors for in situ measurements of plant water potential. *Plant Physiology*, **75**, 766-72.
- SHACKEL, K.A., MATTHEWS, M.A. and MORRISON, J.C. (1987). Dynamic relation between expansion and cellular turgor in growing grape (*Vitis vinifera* L.) leaves. *Plant Physiology*, **84**, 1166-71.
- SHALHEVET, J., MAAS, E.V., HOFFMAN, G.J. and OGATA, G. (1976). Salinity and the hydraulic conductance of roots. *Physiology Plantarum* **38**, 224-32.
- SHANNON, M. C., GRONWALD, J. W. and TAL, M. (1987). Effects of salinity on growth and accumulation of organic and inorganic ions in cultivated and wild tomato species. *Journal of the American Society for Horticultural Science*, **112**, 416-23.
- SINCLAIR, T.R. and LUDLOW, M.M. (1985). Who taught plant thermodynamics? The unfulfilled potential of plant water potential. *Australian Journal of Plant Physiology*, **12**, 213-17.
- SLATYER, R.O. (1961). Plant-Water Relations in Osmotic Substrates. *Australian Journal of Biological Science*, **14**, 519-41.
- SLATYER, R.O. (1962). Effects of several osmotic substrates on the water relationships of tomato. *Australian Journal of Biological Science*, **14**, 519-40.
- SLATYER, R.O. (1967). *Plant-Water relations*. Academic Press, London/New York.
- SLATYER, R.O. and TAYLOR, S.A. (1960). Terminology in plant and soil-water relations. *Nature*, **187**, 992-24.
- SLAVIK, B. (1974). *Methods of studying plant water relations*. Springer Verlag, Berlin.
- SONNEVELD, C., (1991). Rockwool as a substrate for greenhouse crops. In: *Biotechnology in agriculture and forestry*. (Y.P.S. Bajaj, Ed.) Vol 17, Springer Verlag, Berlin, 285-312.
- SONNEVELD, C., (1993). Watervoorziening, bemesting en waterkwaliteit bij teelten onder glas. In: *Watervoorziening en gewasproductie*. (Van Keulen, H., Penning de Vries, F.W.T., Eds.), Agrobiologische thema's 8, CABO-DLO, Wageningen, 41-48.
- SPANNER, D.C. (1951). The Peltier effect and its use in the measurement of suction pressure. *Journal of experimental Botany*, **11**, 145-68.
- SPITTERS, C.J.T., VAN KEULEN, H., and VAN KRAALINGEN, D.W.G. (1989). A simple and universal crop growth simulation: SUCROS87. In: *Simulation and system management in crop protection*. (Rabbinge, R., Ward, S.A., and Van Laar, H.H. Eds.), Simulation Monographs, 32, PUDOC, Wageningen, 147-181.
- STANGHELLINI, C. (1987). Transpiration of greenhouse crops. An aid to climate management. Dissertation Agricultural University, Wageningen, 150 pp.
- STEUDLE, E. and ZIMMERMANN, U. (1974). Determination of the hydraulic conductivity and of the reflection coefficients in *Nitella flexilis* by means of direct cell-turgor pressure measurements. *Biochem. Biophys. Acta*, **332**, 399-412.
- STEUDLE, E., ZIMMERMANN, U. and LÜTTGE, U. (1977). Effect of turgor pressure and cell size on the wall elasticity of plant cells. *Plant Physiology*, **59**, 285-89.
- TAIZ, L. (1984). Plant cell expansion: Regulation of cell wall mechanical properties. *Annual Review of Plant Physiology*, **35**, 585-657.

- TARDIEU, F. and DAVIES, W.J. (1993). Integration of hydraulic and chemical signalling in the control of stomatal conductance and water status of droughted plants. *Plant Cell and Environment*, **16**, 341-49.
- TARDIEU, F., ZHANG, J. and GOWING, D.J.G. (1993). Stomatal control by both [ABA] in the xylem sap and leaf water status: a test of a model for droughted or ABA-fed field-grown maize. *Plant Cell and Environment*, **16**, 413-20.
- TARDIEU, F., ZHANG, J., KATERJI, N., BETHENOD, O., PALMER, S. and DAVIES, W.J. (1992). Xylem ABA controls the stomatal conductance of field grown maize subjected to soil compaction or soil drying. *Plant Cell and Environment*, **15**, 193-97.
- TAYLOR, S.A. (1968). Terminology in plant and soil water relations. In: TT Kozlowski, ed, *Water deficits and plant growth*. Academic Press, New York, 49-72.
- THODAY, D. (1918). On turgescence and the absorption of water by the cells of plants. *New Phytol* **17**: 108-113 (from) The use of the pressure chamber in studies of plant water status. In: *International conference on measurement of soil and plant water status*. Vol. 2. 13-24.
- TURNER, N.C. (1987). The use of the pressure chamber in studies of plant water relations. *International conference on measurement of soil and plant water status*. Volume 2.
- TYREE, M.T. and JARVIS, M.G. (1986). Water in tissues and cells. In: *Encyclopaedia of Plant Physiology: Physiological Plant Ecology II, Water relations and Carbon Assimilation (NS)*, 12B. (Lange, O.L., Nobel, P.S., Osmond, C.B. and Ziegler, H., Eds). Springer Verlag, Berlin/New York, 36-77.
- TYREE, M.T., YANG, S., CRUIZIAT, P. and SINCLAIR, B. (1994). Novel methods of measuring hydraulic conductivity of tree root systems and interpreting using AMAIZED. *Plant Physiology*, **104**, 189-99.
- UDINK TEN CATE, A.J., BOT, G.P.A. and VAN DIXHOORN, J.J. (1978). Computer control of greenhouse climates. *Acta Horticulturae*, **87**, 265-72.
- URSPRUNG, A. and BLUM, G. (1916). Zur methode der Saugkraftmessung. *Berichte der Deutschen Botanischen Gesellschaft*, **34**, 525-39.
- VOOREN, J. VAN DE, WELLES, G.W.H. and HAYMAN, G. (1986). Glasshouse crop production. In: *The tomato crop. A scientific basis for improvement*. (Atherton, J. G. and Rudich, J., Eds). Chapman and Hall. London. 581-623.
- WALKER, A.J. and HO, L.C. (1977). Carbon translocation in the tomato: carbon import and fruit growth. *Annals of botany*, **41**, 813-23.
- WEAST, R.C. (1981). *Handbook of Chemistry and Physics*. Chemical Rubber. Cleveland
- WINSOR, G. and ADAMS, P. (1987). *Mineral disorders in plants*. Volume 3. Glasshouse Crops (Robinson, J. B. D., Ed.), Crown. London. UK.
- WIT, C.T. DE. (1978). Simulation of assimilation, respiration and transpiration of crops. PUDOC Wageningen. 141 pp.
- WOLTERBEEK, H.T. (1986). Physico-chemical aspects of ion transport in the xylem. Dissertation. State University Utrecht, Utrecht, The Netherlands. 237 pp.
- ZHANG, J. and DAVIES, W.J. (1990). Changes in concentration of ABA in xylem sap as a function of changing soil water status can account for changes in leaf conductance and growth. *Plant Cell and Environment*, **13**, 277-85.
- ZHU, G.L. and BOYER, J.S. (1992). Enlargement in Chara studied with a turgor clamp. Growth rate is not determined by turgor. *Plant Physiology*, **100**, 2071-80.
- ZIMMERMANN, U. (1984). *Xylem structure and Ascend of Sap*. Springer-Verlag. Berlin and New York
- ZIMMERMANN, U. and STEUDLE, E. (1974). Hydraulic conductivity and volumetric elastic modulus in giant algal cells: Pressure and volume dependence. In: *Membrane transport in*

- plants.* (Zimmermann, U. and Dainty, J., Eds) Springer-Verlag, Berlin and New York, 64-71.
- ZIMMERMANN, U., HAASE, A., LANGBEIN, D. and MEINZER, F. (1993). Mechanisms of long-distance water transport in plants: a re-examination of some paradigms in the light of new evidence. *Philosophical Transactions of the Royal Society of London, Series B*, **341**, 19-31.

Curriculum vitae

Wim (Willem) van Ieperen was born on 2 November 1965 at Haarlem (The Netherlands). In 1984 he passed the final exams for gymnasium- β at the Marnix Gymnasium te Rotterdam. In the same year he started to study horticulture at Wageningen Agricultural University. The main subjects of his study were Horticulture, Physics and Plant physiology, while Theoretical Production Ecology and Computer Science were studied too. In June 1989 he received the MSc degree (cum laude).

After a short temporary appointment as assistant at the department of Horticulture of the Wageningen Agricultural University, he started at the same department the research which is described in this thesis.

Wim (Willem) van Ieperen werd geboren op 2 november 1965 te Haarlem. In 1984 behaalde hij zijn gymnasium- β diploma aan het Marnix Gymnasium te Rotterdam. In datzelfde jaar begon hij aan de studie Tuinbouwplantenteelt aan de Landbouwhogeschool (thans Landbouw Universiteit) te Wageningen. Tijdens de doctoraal fase werden de afstudeervakken Tuinbouw, Natuurkunde en Plantenfysiologie gekozen. Tevens werd er de nodige aandacht gegeven aan de vakken Theoretische teeltkunde en Informatica. In juni 1989 werd de studie afgerond met het behalen van het doctoraal examen (met lof).

Na een korte periode als tijdelijk medewerker bij de Vakgroep Tuinbouwplantenteelt te hebben gewerkt, werd hij in november 1989 aangesteld als assistent in opleiding aan dezelfde vakgroep. Een belangrijk deel van het onderzoek dat is uitgevoerd in het kader van deze aanstelling is beschreven in dit proefschrift.